43592

National Library
of Canada

Bibliothèque nationale
du Canada

Canadian Theses Division

Division des thèses canadiennes

Ottawa, Canada
K1A 0N4

PERMISSION TO MICROFILM — AUTORISATION DE MICROFILMER

- Please print or type — Écrire en lettres moulées ou dactylographier

Full Name of Author — Nom complet de l'auteur

WITHERS, ROBERT LOUIS

Date of Birth — Date de naissance

MARCH 5, 1953

Country of Birth — Lieu de naissance

CANADA

Permanent Address — Résidence fixe

APT 212 - BLDG B - 3615 - 49TH ST. N.W.
CALGARY ALBERTA T3A 2L8

Title of Thesis — Titre de la thèse

Mineral Deposits of the Northrim Mine and a Brief Enquiry into the Genesis of Veins of the (Ag, Bi, Ni, Co, As) Type

University — Université

Alberta (U of)

Degree for which thesis was presented — Grade pour lequel cette thèse fut présentée

MSc GEOLOGY

Year this degree conferred — Année d'obtention de ce grade

1975

Name of Supervisor — Nom du directeur de thèse

Dr. ROBERT FOLINSBEE

Permission is hereby granted to the NATIONAL LIBRARY OF CANADA to microfilm this thesis and to lend or sell copies of the film.

The author reserves other publication rights, and neither the thesis nor extensive extracts from it may be printed or otherwise reproduced without the author's written permission.

L'autorisation est, par la présente, accordée à la BIBLIOTHÈQUE NATIONALE DU CANADA de microfilmer cette thèse et de prêter ou de vendre des exemplaires du film.

L'auteur se réserve les autres droits de publication; ni la thèse ni de longs extraits de celle-ci ne doivent être imprimés ou autrement reproduits sans l'autorisation écrite de l'auteur.

Date

Aug 15 / 1975

Signature

Robert L. Withers

NL-91 (4/77)

National Library of Canada

Cataloguing Branch
Canadian Theses Division

Ottawa, Canada
K1A 0N4

Bibliothèque nationale du Canada

Direction du catalogage
Division des thèses canadiennes

NOTICE

The quality of this microfiche is heavily dependent upon the quality of the original thesis submitted for microfilming. Every effort has been made to ensure the highest quality of reproduction possible.

If pages are missing, contact the university which granted the degree.

Some pages may have indistinct print especially if the original pages were typed with a poor typewriter ribbon or if the university sent us a poor photocopy.

Previously copyrighted materials (journal articles, published tests, etc.) are not filmed.

Reproduction in full or in part of this film is governed by the Canadian Copyright Act, R.S.C. 1970, c. C-30. Please read the authorization forms which accompany this thesis.

THIS DISSERTATION
HAS BEEN MICROFILMED
EXACTLY AS RECEIVED

AVIS

La qualité de cette microfiche dépend grandement de la qualité de la thèse soumise au microfilmage. Nous avons tout fait pour assurer une qualité supérieure de reproduction.

S'il manque des pages, veuillez communiquer avec l'université qui a conféré le grade.

La qualité d'impression de certaines pages peut laisser à désirer, surtout si les pages originales ont été dactylographiées à l'aide d'un ruban usé ou si l'université nous a fait parvenir une photocopie de mauvaise qualité.

Les documents qui font déjà l'objet d'un droit d'auteur (articles de revue, examens publiés, etc.) ne sont pas microfilmés.

La reproduction, même partielle, de ce microfilm est soumise à la Loi canadienne sur le droit d'auteur, SRC 1970, c. C-30. Veuillez prendre connaissance des formules d'autorisation qui accompagnent cette thèse.

LA THÈSE A ÉTÉ
MICROFILMÉE TELLE QUE
NOUS L'AVONS REÇUE

NL-339 (3/77)

THE UNIVERSITY OF ALBERTA

MINERAL DEPOSITS OF THE NORTHRIM MINE AND A BRIEF ENQUIRY INTO THE GENESIS OF VEINS OF THE (Ag, Bi, Ni, Co, As) TYPE

BY

© ROBERT LOUIS WITHERS

A THESIS
SUBMITTED TO THE FACULTY OF GRADUATE STUDIES AND
RESEARCH IN PARTIAL FULFILMENT OF THE
REQUIREMENTS FOR THE DEGREE OF
MASTER OF SCIENCE

DEPARTMENT OF GEOLOGY

EDMONTON, ALBERTA
WINTER, 1979

THE UNIVERSITY OF ALBERTA

FACULTY OF GRADUATE STUDIES AND RESEARCH

The undersigned certify that they have read, and recommend to the Faculty of Graduate Studies and Research, for acceptance, a thesis entitled MINERAL DEPOSITS OF THE NORTHRIM MINE AND A BRIEF ENQUIRY INTO THE GENESIS OF VEINS OF THE (Ag, Bi, Ni, Co, As) TYPE, submitted by ROBERT LOUIS WITHERS in partial fulfilment of the requirements for the degree of Master of Science in Geology.

R E Folinsbee
Supervisor

R. S. Lambert

L.B. Halferdahl
External Examiner

Date July 24, 1979

DEDICATION

To my wife, Monique, who has patiently aided this work's completion.

ABSTRACT

Veins of the (Ag, Bi, Ni, Co, As) association are the products of retrograde greenschist facies metamorphism involving brine-mineral exchange in geothermally-heated fluids. This has been determined on the basis of all mineralogical, petrographical, geochemical, stratigraphical, structural and tectonic evidence either studied directly by the writer at the Northrim Mine or gained through interpretation of the available literature. Areas studied intensively from the literature include the Camsell River, Echo Bay (Port Radium) and Cobalt-Gowganda districts. Brief references to the Erzegebirge, Kongsberg and Broken Hill districts have also been made.

The 'lateral secretion' hypothesis of Robinson (1971) and Robinson et al. (1972), and the metahydrothermal hypothesis of Halls and Stumpfl (1969, 1972) appear to be consistent with all the available geological evidence gathered by the writer. The Cobalt-Gowganda deposits, previously considered to be genetically distinct from other (Ag, Bi, Ni, Co, As) deposits, are also products of retrograde greenschist facies metamorphism involving brine-mineral exchange of elements.

The genesis of (Ag, Bi, Ni, Co, As) vein deposits

involves the coincidence of several geological conditions. At minimum, these conditions include the presence of partially confined aquifer systems, high geothermal gradients, restricted surface water influx, waning geothermal activity and fracture generation. All of these conditions were almost certainly present during vein and wall rock mineralization in all the districts studied. Magmatic conditions, resulting in plutonic intrusion of one kind or another, are insignificant with respect to hydrothermal fluid provenance, but not with respect to hydrothermal fluid migration. Fluid-mineral exchange would occur in plutonic rocks in the same manner as in the volcanic and sedimentary rocks. The Salton Sea is a modern geothermal system with brine fluids similar to the ones which were almost certainly responsible for (Ag, Bi, Ni, Co, As) deposit and greenschist facies mineralization.

The Northrim deposits, including host rock volcanogenic massive sulfide deposits, have been studied in detail and the following points may be of interest. A possibly new mineral, "brederite" (formula: PbAs) was observed in the veins. A mineral of the aikinite-rezbanyite series is a common component of the Northrim veins. The Northrim vein paragenesis is remarkably similar to the ones of the Norex and Terra veins in the Camsell River district and of the Eldorado and Echo Bay veins in the Port Radium district. The Northrim, Camsell River and Port Radium veins are remarkably similar in details of mineralogy, composition, morphology and paragenesis to the veins of the Cobalt-Gowganda region.

ACKNOWLEDGMENTS

The work is a dissertation submitted to the University of Alberta in partial fulfillment of the requirements for the M. Sc. degree. I thank Professor R. E. Folinsbee, who supervised the thesis research, for his guidance and encouragement, and the members of the dissertation committee, Professors R. St. J. Lambert, R. D. Morton and for their assistance. Dr. D. G. W. Smith helped with the electron microprobe analyses and the writer has benefitted immensely from discussions with Doctors R. St. J. Lambert, R. Houghton, K. Hattori and H. Baadsgaard regarding some aspects of the dissertation. Electron microprobe analyses and oscilloscope radiation images were taken with the assistance of Messrs. D. Tomlinson and S. Launspach and O isotope analyses were performed by Dr. K. Hattori. Dr. R. D. Morton contributed the geochemical data incorporated within the thesis and Mr. F. Dimitrov gave pertinent advice concerning photographic techniques.

The writer is indebted to Northrim Mines Limited for access to and for permission to perform the necessary field work at the Northrim Mine. Assistance was rendered by Messrs. Al Farrel, W. Timmins and Dr. R. Morton in these endeavors.

Financial support was provided by the Boreal Institute for Northern Studies of the University of

Alberta, National Research Council grants to Dr. R. Folinsbee and by the private funds of the writer.

The writer accepts full responsibility for the facts and opinions expressed in this dissertation since all information has been crosschecked and verified several times during periods of active research and the writer has performed most of the editing.

TABLE OF CONTENTS

Page

Chapter 1. INTRODUCTION 1

The Northrim Mine 1

Previous Work 8

The Bear Province 9

Great Bear Lake Stratigraphy . . . 11

Great Bear Lake Plutonism 12

Great Bear Lake Structure 16

Age Relationships 18

Chapter 2. HOST ROCK GEOLOGY 21

Lithology 21

(a) Flows 21

(b) Pyroclastic Breccias 27

(c) Plutonic and Hydrothermal Units 29

(d) Volcanogenic Massive Sulfides 35

Depositional Conditions 48

Chapter 3. HOST ROCK GEOCHEMISTRY, MAGMATISM AND METAMORPHISM 54

Introduction 54

Geochemical Results 56

(a) Major Oxide Distribution . . 56

(b) Trace Element Distribution . 64

Page

(c) Geochemical Exploration 69

Magmatic Characteristics 74

(a) Northrim Basalts 74

(b) Camsell River Rocks 85

Metamorphic Conditions 87

Spilitization, Diagenesis and Metamorphism 94

Summary Statement 95

Chapter 4. REGIONAL STRUCTURE AND VEIN CONTROL 97

Structural Features 97

Structural Relationships 99

Great Bear Structural Features . . . 111

Structural Vein Control 115

Chapter 5. NORTHRIM MINERALIZED VEINS 120

Introduction 120

Vein Alteration 123

Paragenesis 125

Mineralogy 130

(a) Carbonates and Quartz 130

(b) Native Elements 135

(c) Arsenides and Sulfarsenides 151

(d) Oxides 175

(e) Sulfides 179

(f) Sulfosalts 187

Page

(g) Other Minerals 192

Depositional Conditions 193

Chapter 6. THE NORTHRIM, GREAT BEAR AND COBALT-GOWGANDA VEINS 205

Mineralization 205

Depositional Conditions 210

Cobalt-Gowganda Regional Metamorphism 213

Nipissing "Contact" Metamorphism . . 218

Temporal Relationships 222

Genesis 226

Chapter 7. CONCLUSIONS 232

Mineralogical Summary 232

Geothermal-Metamorphic Model of (Ag, Bi, Ni, Co, As) Vein Formation 238

Summary Statement 254

APPENDIX 257

BIBLIOGRAPHY 262

LIST OF TABLES

		Page
Table 1	Concentrate Components of the Northrim Mine	7
Table 2	Major Oxide and Sulfide Contents of Volcanic Host Rocks	57
Table 3	Trace Element Contents of Volcanic Host Rocks	65
Table 4	Comparison of Camsell River Basalt Composition with Varietal Basalt Averages	86
Table 5	Arsenide Mineral Composition	167
Table 6	Sphalerite Composition	182
Table 7	Sulfosalt Mineral Composition	189
Table 8	Cobalt-Gowganda and Great Bear Ore Minerals	207
Table 9	Cobalt-Gowganda Precambrian Geological Column	214
Table 10	Gowganda Formation Alkaline and Water Analyses	216
Table 11	Radiometric Dates of Huronian Units	223
Table A-1	Table of Volcanic Rock Analyses: Major Oxides and Sulfur	258
Table A-2	Table of Volcanic Rock Analyses: Minor Elements	259
Table A-3	Petrochemical Functions of Volcanic Host Rocks	260
Table A-4	Normative Minerals and Petrochemical Functions of Volcanic Host Rocks	261

LIST OF FIGURES

		Page
Fig. 1	Northrim Mine Location	2
Fig. 2	Northrim Mine Workings	4
Fig. 3	Northrim Mill Flow Chart	6
Fig. 4	Camsell River District Regional Geology	13
Fig. 5	Northrim Geochemical Sample Location	55
Fig. 6	Northrim Harker Diagram (1)	59
Fig. 7	Northrim Harker Diagram (2)	62
Fig. 8	Northrim Indicators of Vein Mineralization (1)	70
Fig. 9	Northrim Indicators of Vein Mineralization (2)	72
Fig. 10	Northrim (Na_2O+K_2O)-FeO-MgO Ternary	75
Fig. 11	Total Alkali-Silicon Oxide Plot	76
Fig. 12	Normative Alumina Oxide Plagioclase Plot	78
Fig. 13	Alkaline-Tholeiitic Basalt Discriminants	80
Fig. 14	TiO_2-Zr-Y Ternary for Altered Basalts	82
Fig. 15	TiO_2-Sr-Y Ternary for Fresh Basalts	84
Fig. 16	Granitic and Dioritic Dyke Orientation	101
Fig. 17	Major Strike-slip Fault Orientation	103

		Page
Fig. 18	Mineralized and "Giant Quartz" Vein Orientation	107
Fig. 19	Diabase Dyke Orientation	110
Fig. 20	Tectonic Elements of the Great Bear Batholith	112
Fig. 21	Depositional and Tectonic History of the Great Bear Batholith	114
Fig. 22	Northrim Mine Vein Mineral Paragenesis	126
Fig. 23	Vein Element Paragenesis of the Northrim Mine	196
Fig. 24	Hydrothermal Silicate and Sulfide Mineral Stabilities	199
Fig. 25	Geothermal-metamorphic Model of (Ag, Bi, Ni, Co, As) Vein Formation	253

LIST OF PHOTOGRAPHIC PLATES

		Page
Plate 1	Major Rock Units	23
Plate 2	Minor Rock Units	32
Plate 3	Suflide Pyroclastic Breccia	41
Plate 4	Sulfide Mineralization	43
Plate 5	Wall Rock and Vein Mineralization	91
Plate 6	Ag-As Mineralization	137
Plate 7	Ag-As Mineralization (con't.)	139
Plate 8	Bi-Ag-As Mineralization	143
Plate 9	Bi-Ag-As Mineralization (con't.)	145
Plate 10	Bi-Ag-As Mineralization (con't.)	147
Plate 11	As-Bi-S Mineralization	153
Plate 12	PbAs Mineralization	156
Plate 13	Ag-As Mineralization	159
Plate 14	Ag-As Mineralization (con't.)	162
Plate 15	Ag-As Mineralization (con't.)	165
Plate 16	U-As-S Mineralization	170

CHAPTER 1

INTRODUCTION

The Northrim Mine

The Northrim Mine is situated on the north shore of the Rainy Lake reach of the Camsell River 250 miles north northwest of Yellowknife, Northwest Territories (Fig. 1). The mine is entered via a portal into the side of a 50 foot high hill which drops steeply into the Camsell River. The underground workings consist of a haulage ramp, exploratory crosscuts and subdrifts, compressor, mill, machine shop and shipment rooms, a winze which drops to the 125 foot level, a decline which curls around once in a 10% descent to the 250 foot level, and several drifts which follow major complex vein structures (Fig. 2).

Ore has been mined out of the 000 composite vein structure between the land surface and the 210 foot level, out of the 014 composite vein structure between the land surface and the 210 foot level, and the 056 vein on the 056 level. Two four-wheel drive scoop trams deliver the ore up the haulage ramp where it is fed directly through a grizzly and into a 75 ton per day (t.p.d.) jaw crusher on the east wall of the mill room.

The jaw crusher comminutes the ore to gravel-sized fragments which are then fed into a 75 t.p.d.

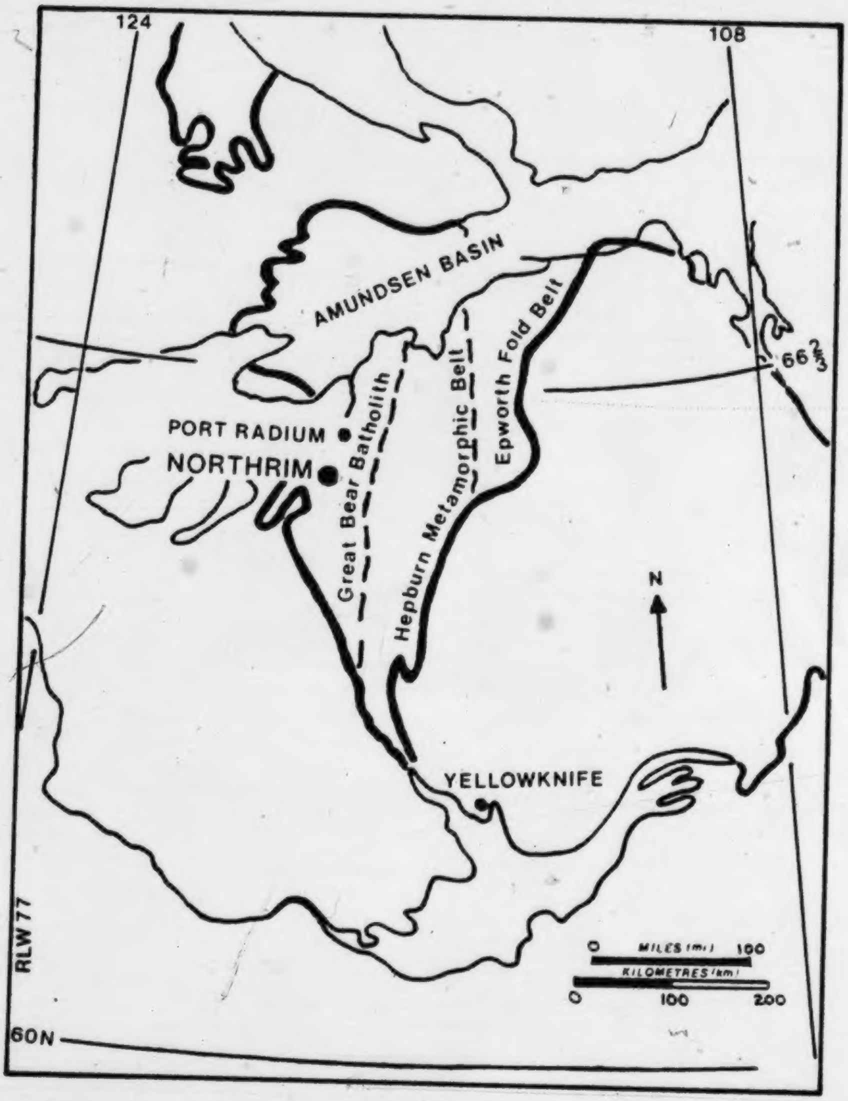

Figure 1: Northrim Mine location map.

ball mill. The ground product is then passed onto a coarse jig from which the heaviest granules are bagged. The remaining product is then recycled through a classifier and ball mill until sufficiently ground to sand-size for the gravity table. The heavy separate off the table is bagged; the lighter separate is dumped into one of 9 small flotation cells with a total 75 t.p.d. capacity. The sulfide-rich float is bagged and like the jig and table concentrates is stored in an adjacent room to await shipment. The tailings are pumped above the hill and into a small land-locked slough. The concentrates are then trucked out (winter) or barged out (summer) to be smelted at the Cominco-owned complex at Trail, British Columbia. A flow chart displaying the milling process in greater detail is shown in Figure 3.

The concentrates contain abundant Ag, Cu, Pb, Zn, Fe, Sb, As and Bi but very little Au (Table 1). Not included in the concentrate assays given but also found in abundance are U, Ni and Co. Minerals identifiable in the concentrates include native silver, native bismuth, acanthite[1], galena, sphalerite, chalcopyrite, uraninite, various arsenides and some sulfosalts. Pyrite, marcasite, magnetite, dolomite, calcite,

---

[1] Low temperature polymorph of argentite.

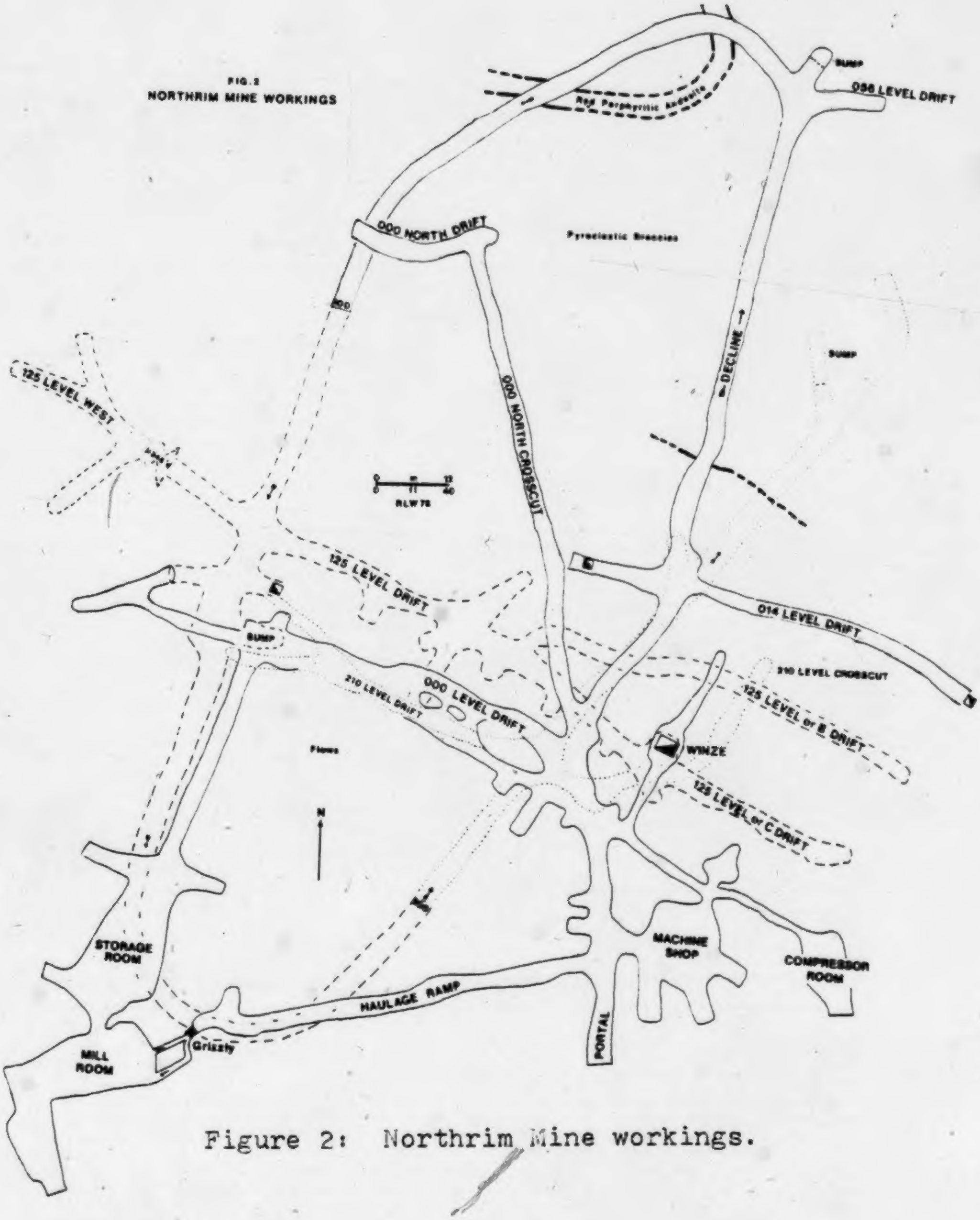

Figure 2: Northrim Mine workings.

plagioclase, quartz and several ferromagnesian minerals are the identifiable impurities in these concentrates. All concentrate impurities save the first three are abundant in the tailings which contain little of the heavier metal-bearing minerals[2].

The Northrim concentrates and ores thus contain the elements and minerals characteristic of the ores referred to as the "Cobalt-type" (Stanton, 1972), the "(Ag, Bi, Co, Ni, As) veins" (Hall and Stumpfl, 1972) or as the "Ni-Co-Ag ore type" (Bastin, 1939). Concentrates and ores similar to the ones at Northrim have been or are being produced in the Norex Mine 1½ kilometres south, the Terra Mine 6 kilometres west and the Eldorado, Echo Bay and Contact Lake Mines 50 kilometres north of the Northrim minesite. The purpose of this dissertation is to describe the minerals, structure and geological environment of the ores which contain the rare elements produced from the mines, particularly with reference to the ones at Northrim. In addition, suggestions will be made concerning the genesis of these ores.

---

[2] On a trial mill-run, millheads assayed 13 ounces Ag/ton, jig concentrates 660 ounces Ag/ton, table concentrates 84 ounces Ag/ton, float concentrates 175 ounces Ag/ton but tailings less than 1 ounce Ag/ton. All were from fire-assays performed by Dr. D. Robertson on January 24, 1977.

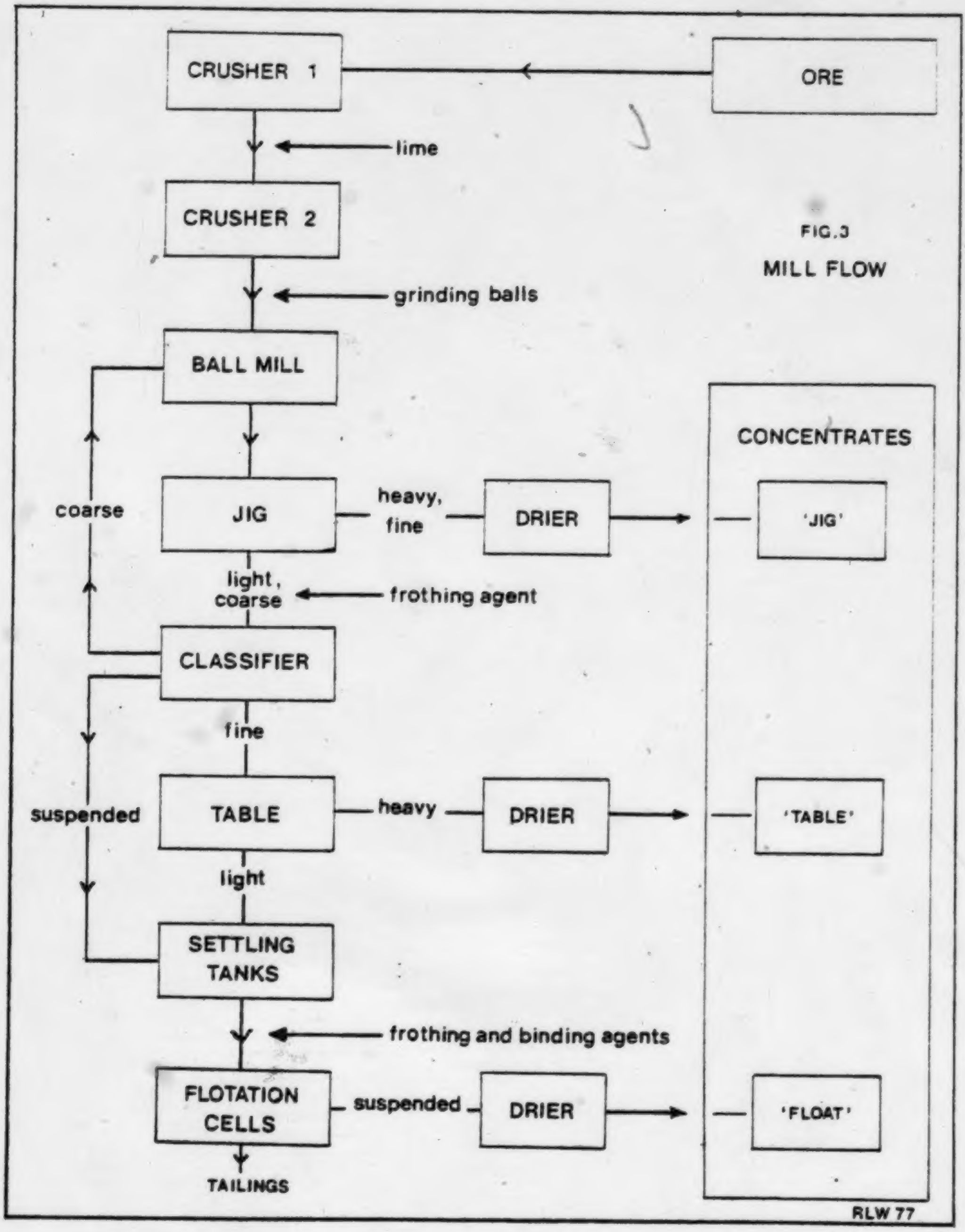

Figure 3: Northrim Mine mill flow chart.

TABLE 1

CONCENTRATE COMPONENTS

Component (wt. %)	Concentrate Jig	 Table	 Float
Au (oz/ton)	0.01	0.04	0.02
Ag (oz/ton)	2733.0	502.1	295.5
Cu	0.95	1.1	5.2
Pb	13.7	18.9	22.3
Zn	1.8	2.3	19.4
S	-	-	25.7, 25.8*
SiO_2	2.0	2.3	3.3
Al_2O_3	1.2	1.4	1.5
Fe	33.0	29.0	17.7
$CaCO_3$	0.3	0.5	0.2
Sb	0.1	0.1	0.1
As	8.5	11.9	3.4
Bi	2.55	2.5	0.94
Proportion of total concentrate	23%	42%	33%

All assays performed by Cominco Ltd. on a dry 10 pound sample concentrate. Values given are those for an assay settlement (Cominco - Northrim Mines Ltd.) dated May 16, 1972, save those values marked * which were from a similar settlement dated November 11, 1975. Co and Ni were not assayed.

Previous Work

The first scientific expedition to the Great Bear Lake discovered erythrite and annabergite in altered veins which were to become the mines in the Port Radium vicinity, some 50 kilometres north of the present Northrim Mine (Bell, 1900). Staking at Port Radium in 1929 drew prospectors to the area and similar deposits were found in the Camsell River area. Among them were veins discovered by E. B. McLellan and W. S. Workman at the site of the current Northrim Mine and veins discovered by John Borthwick one-half mile to the northeast. In 1934, White Eagle Silver Mines Limited excavated the presently employed adit, winze and 000 drift at the mine. A 1,365 pound bulk sample from the 000 drift was sent to the Mines Branch in Ottawa--it assayed 988 ounces Ag/ton, 0.01 ounce Au/ton, 5.27% Pb, 0.55% Co and 1.10% Ni (Assessment files, Dept. Ind. Aff. North. Dev.). At the same time, a 60 foot shaft was sunk on the Borthwick property.

Following discovery of gold at Yellowknife, work was discontinued until Camsell River Silver Mines took over both properties. Drilling commenced in 1947, and 26 holes totalling 1,750 feet in length outlined an ore shoot averaging 34 ounces Ag/ton across 46 inches for 260 feet west of the adit (op. cit.). Two radioactive highs were discovered on the 100 level and samples of the highs assayed 7.38 ounces Ag/ton and 0.226% U_3O_8.

The workings lay idle until Fred Lypka restaked the property in 1967. Silver Bay Mines Limited took over mining operations the following year and Federated Mining Corporation three years later. The present owners, Northrim Mines Limited, took over in 1972 (Assessment files, Dept. Ind. Aff. North. Dev.). Most of the mine development has occurred since then.

Except for mining assessment and engineering reports, only J. P. N. Badham (1973b, 1975) and D. F. Kidd (1936) have described parts of the Northrim occurrences. The nearby Terra and Norex deposits have been studied in detail by Badham (1973b) but much of the academic literature only concerns the ore deposits near Port Radium (e.g. Robinson and Ohmoto, 1971). There have been, however, many attempts at proposing geneses for one or all of the vein deposits in the Great Bear Lake area. Among them are the geneses of Robinson (1971), Robinson et al. (1972), Thorpe (1974), Shegelski and Scott (1975), Badham (1976) and Gandhi (1978).

The Bear Province

The east shore of Great Bear Lake lies within the Bear Province defined by Jolliffe (1948) and characterized by K-Ar ages at 1700 to 1850 m.y. in the Wopmay

Orogen and 700 to 850 m.y. in the stratigraphically younger Amundsen Basin (Wanless et al., 1968). The Wopmay Orogen has been subdivided into three parts: the eastern Epworth fold belt, the central Hepburn plutono-metamorphic belt and the belt of the Great Bear Batholith (Fraser et al., 1972). The younger belt of the Great Bear Batholith is separated from the older Hepburn plutono-metamorphic belt by the Wopmay Fault.

The Great Bear Batholith consists of three north-trending volcano-sedimentary belts which have been partially separated by epizonal plutons and which have been offset by major northeast-trending dextral faults (Hoffman et al., 1976). The westernmost volcano-sedimentary belt, bordering the eastern shore of Great Bear Lake, comprises the geographically separated Echo Bay and Camsell River "blocks", two volcano-sedimentary roof pendants draped over the Great Bear Batholith. Their geographical separation has been attributed to displacement along major northeast-trending dextral faults (Hoffman and Bell, 1975).

All occurrences of (Ag, Bi, Co, Ni, As) veins in the Bear Province known to the writer have been found within or adjacent to the Camsell River - Echo Bay volcano-sedimentary belt.

Great Bear Lake Stratigraphy

The Camsell River - Echo Bay volcano-sedimentary belt has been divided into 7 sequences by P. Hoffman and J. McGlynn (1977). The lowermost Hottah Lake sequence (2500 m.) begins with interbedded quartzite and siltstone (Unit 1, Fig. 4) which is riddled with basalt dykes that act as feeders to overlying basalt flows (Unit 2) containing thin interbeds of mudstone laminated air-fall tuff and quartz pebble conglomerate. The overlying Camsell River sequence (4500 m.) begins with welded rhyolitic ignimbrite (Unit 3) which contains small, discontinuous horizons of basalt flows, air-fall tuff and volcanoclastic sandstone. Rhyolitic plug domes (Unit 4) intrude the ignimbrite and are flanked by wedges of rhyolite pebble conglomerate within the ignimbrite. The ignimbrite is overlain by orthoquartzite (Unit 5) which is in turn succeeded by volcanoclastic sandstones and tuffaceous mudstones interfingered with rhyolite flows (Unit 6). The mudstones are the hosts to the ores at the Terra Mine (Badham, 1973b).

Host rocks at the Norex and the Northrim Mines are the intercalated porphyritic andesite and basalt flows and tuffs (Unit 7) of the overlying Echo Bay sequence which varies in thickness from 1500 metres near the Camsell River to 2600 metres near Port Radium (op. cit., 1977). Similar flows and tuffs are the host rocks for the ores of the Eldorado and Echo Bay Mines at Port Radium (Robinson et al., 1971; Robinson, 1971). These rocks are in turn succeeded by andesite pebble conglomerate (Unit 8) and dacitic ignimbrite (Unit 9, Fig. 4) of the Conjuror Bay sequence (0-2200 m.). A few porphyritic andesite and basalt flows are found in the ignimbrite (Hoffman et al., 1976).

The next three sequences of the Camsell River - Echo Bay volcano-sedimentary belt: the Lindsley Bay (0-1160 m. of rhyolitic ignimbrites intercalated with alluvial sediments), the Achook Island (110 m. - 810 m. of andesite flows) and the Doghead Point (400 m. of dacitic ignimbrite); resemble the previous three sequences (Hoffman and McGlynn, 1977) but do not occur in the Camsell River area nor do they host any (Ag, Bi, Ni, Co, As) veins known to the writer. These same two conditions also apply to the uppermost Elizabeth Lake sequence (1200 m.) of rhyolitic ignimbrites which resemble ignimbrites of the Lindsley Bay sequence.

Great Bear Lake Plutonism

The plutonic basement of the Camsell River - Echo Bay volcano-sedimentary belt includes members of three suites: a monzonite-syenite suite, an adamellite suite and a granitic suite (Hoffmann and McGlynn, 1977). Members of the monzonite-syenite suite include the Rainy

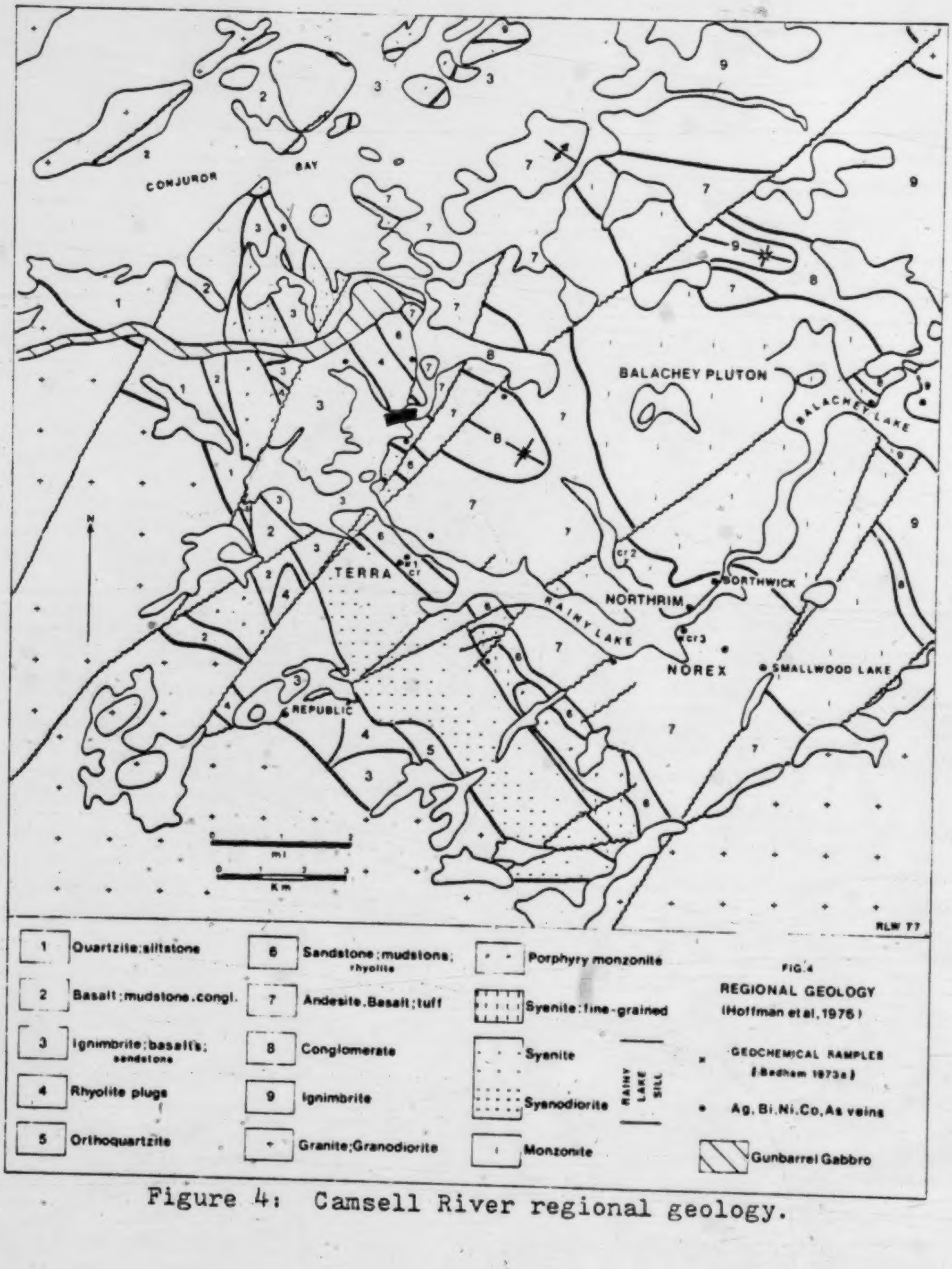

Figure 4: Camsell River regional geology.

Lake and Balachey Lake plutons in the Camsell River area (Fig. 4) and the Contact Lake and Glacier Lake plutons in the Echo Bay area. The (Ag, Bi, Ni, Co, As) veins of the Contact Lake Mine are found inside and the veins of the El Bonanza Mine beside the Contact Lake monzonite (Furnival, 1939; op. cit., 1977).

The Rainy Lake pluton is a differentiated sill whose lower part consists of coarsely prophyritic syenodiorite which grades into an upper part composed of finely crystalline syenite (Fig. 4). There is a narrow chill zone of porphyritic monzonite and there are satellite intrusions of finely crystalline hornblende syenodiorite (Hoffman et al., 1976). The other plutons of the syenite-monzonite suite are less differentiated but Badham (1973b) notes borders and dykes of aplite and porphyry related to these plutons. The dioritic intrusions and dykes in the Camsell River volcano-sedimentary sequence mapped by Shegelski and Murphy (1972) also belong to this suite.

The plutons of the syenite-monzonite suite have sharp contacts, are generally concordant with the volcano-sedimentary pile and are demonstrably synvolcanic (op. cit., 1977). Conglomerates in ignimbrite (Unit 3, Fig. 4) contain pebbles of quartz monzonite; the conglomerate (Unit 8) near Balachey Lake contains plutonic clasts of syenitic and monzonitic composition (op. cit., 1976) and pyroclastic breccias at the Northrim Mine contain fragments of plutonic lithology (this study). The conglomerate near Balachey Lake rests unconformably on the Balachey Lake pluton which intrudes the lavas and flows north of the Northrim Mine (Badham, 1973b).

Plutons of the biotite-hornblends adamellite suite include the Hogarth pluton but even this pluton occurs north of the (Ag, Bi, Ni, Co, As) occurrences near Port Radium. Plutons of this suite are also demonstrably synvolcanic (op. cit., 1977). They are slightly discordant with the volcano-sedimentary pile and are surrounded by contact metamorphic aureoles wider than those of the plutons of the syenite-monzonite and granite suites (ibid., 1977).

Plutons of the biotite granite suite, often porphyritic, include the Richardson Island pluton. They are very coarsely crystalline but unlike plutons of the other two suites, they have chilled borders, are highly discordant and postdate folding of the volcano-sedimentary pile (ibid., 1977). The granite plutons in the north are preceded by northeast trending alkaline porphyritic dykes. The porphyritic dykes described by Badham (1973a; b) and mapped as granite dykes by Shegelski and Murphy (1972) are most likely their counterparts in the south. The porphyritic granite dykes truncate the Balachey Lake pluton.

It should be stressed that some members of the granite suite may not intrude the volcano-sedimentary pile. In one instance, the lowermost Hottah Lake sequence rests unconformably on a granite which has not been known to intrude any member of the volcano-sedimentary pile. The unconformity may represent the paleotopographical surface of a pre-volcanic granite (Hoffman and McGlynn, 1977).

Great Bear Lake Structure

The Camsell River - Echo Bay volcano-sedimentary belt has been broadly folded. Fold axial planes strike northwest and fold axes plunge towards the northwest. Northeast dipping limbs are the more prominent (Hoffman and Bell, 1975) and folding increases in intensity but decreases in amplitude towards some plutonic margins (Badham, 1973a, b). Thus plutonic intrusion may have accompanied folding, and folding may have accompanied volcanism since most plutons, for example the one which helped produce ptygmatic folding in tuff beds near the Echo Bay Mine (Robinson, 1971), are synvolcanic. Folding was probably accompanied by faulting which in at least two instances is known to be synvolcanic.[3]

---

[3] Evidence cited includes minor northeast trending faults of small displacement (Hoffman et al., 1976) and a tectonically brecciated limestone immediately overlain

The dominant faults of the Camsell River - Echo Bay belt, and of the whole of the Great Bear Batholith, are dextral northeast trending faults which generally splay towards the Wopmay Fault in the east. Movements of up to several kilometres occurred along them and their splays but only far lesser movements occurred along faults of different orientation. Several kilometre displacements of all plutonic, sedimentary and volcanic lithologies suggest that the major dextral movement of the northeast trending faults occurred after all felsic and intermediate igneous activity had ceased.

Faults are key features in the Camsell River and Echo Bay areas for they are the loci of porphyritic dykes, "giant quartz" veins, mineralized (Ag, Bi, Ni, Co, As) veins and diabasic dykes. Porphyritic dykes antedate major dextral movements along northeast faults but "giant quartz" veins, which often occupy major northeast fault systems (Badham, 1973b), must have been formed contemporaneously during major fault movements since they have been repetitively brecciated and infilled by later generations of quartz (ibid., 1973b). Mineralized (Ag, Bi, Ni, Co, As) veins truncate porphyritic dykes north of the Northrim Mine (Dollery-Pardy,

---

by a non-brecciated conglomerate containing angular fragments of that same limestone near the Terra Mine (Badham, 1973b).

unpub.) and at the Norex Mine but the Norex veins are truncated in turn by a diabase dyke (op. cit., 1973b). The mineralized veins of the Echo Bay and Eldorado Mines have also been truncated by a diabase dyke (Robinson, 1971).and diabase dykes truncate both "giant quartz" veins and major northeast faults in the Camsell River area (op. cit., 1973b). Thus both the "giant quartz" veins and the mineralized (Ag, Bi, Ni, Co, As) veins were emplaced synchronously with major movements on the northeast faults, after the intrusion of porphyritic dykes but before the intrusion of diabase dykes.

Age Relationships

Relative age relationships have been established for the Camsell River - Echo Bay volcano-sedimentary belt and associated intrusive rocks. However, absolute ages may only be inferred from radiometric dating of the rocks concerned. Dating of Echo Bay volcanic and plutonic rocks yields a cluster of dates within Aphebian times. A Rb-Sr whole rock isochron date of 1770±30 m.y. is accompanied by K-Ar hornblende dates of 1580±60 and 1650±40 m.y. (Robinson, 1971; Robinson and Morton, 1972). Other radiometric dates from the same authors include K-Ar hornblende dates of 1630 and 1690±40 m.y. and

K-Ar biotite dates of 1650 and 1700±20 m.y. on a granodiorite of the Glacier Lake pluton and similar K-Ar dates on a granite along the shore of Great Bear Lake. U-Pb zircon dating of the same granite at Echo Bay yields an age of 1820±30 m.y. (Thorpe, 1974). A K-Ar biotite date of 1785 m.y. (GSC 61-55) has been obtained on a granodiorite in the Camsell River area (Lowdon, 1961).

Radiometric dates of Proterozoic age have also been obtained from diabase dykes and mineralized veins. A Rb-Sr whole rock isochron date of 1425±48 m.y. on the diabase sheet at Port Radium, is accompanied by a K-Ar biotite-hornblende date of 1400±75 m.y. on a diabase sheet 25 kilometres northeast of Port Radium (Thorpe, 1974). U-Pb pitchblende dates averaging 1445±20 m.y. have been determined in the mineralized veins at the Eldorado Mine but the model Pb age obtained from ordinary vein galenas from the Eldorado, Echo Bay and Norex Mines is 1633±34 m.y. (ibid., 1974). Thus the diabase dykes at Port Radium, and probably throughout the Camsell River - Echo Bay volcano-sedimentary belt, appears to be younger than the mineralized veins or any other lithological feature. An exception would be the magnetite-actinolite veins dated at 1420±60 m.y. applying the K-Ar method to actinolite (Robinson, 1971). The "skarn" at the

Terra Mine and a galena vein on Clut Island, share a model Pb date of about 1780 m.y. (op. cit., 1974).

The radiometric dates are consistent with field evidence as to the synvolcanic nature of the plutons, the Aphebian age of the rocks, and the succession of depositional and tectonic events. The dates also indicate that there has not been any intense regional scale thermal metamorphism since the Aphebian. More specifically, regional rock temperatures have not exceeded 150-200° C. since 1600 m.y., the inferred maximum temperature at which biotite loses ^{40}Ar (Hart et al., 1968; Moorbath, 1971).

CHAPTER 2

HOST ROCK GEOLOGY

Lithology

(a) Flows

The dominant host rock for the silver-bearing veins of the Northrim Mine is basalt. The basalt is generally massive, does not appear porphyritic and contains few vesicles (Plate I-1). It varies in color depending on the predominant mineral: gray and grayish pink basalts contain more albite, yellow green basalts more epidote, dark green basalts more chlorite and black basalts more magnetite than the more standard intermediate green variety. The basalt is composed of a non-aligned albite microlite (0.05-0.5 mm.) matrix with interstitial and intersertal chlorite, magnetite, calcite, dolomite, biotite, amphiboles, apatite, pyrite, ilmenite and sphene. Labradorite and pyroxene phenocrysts were present but the labradorite has been altered to epidote, albite, sericite, quartz and/or carbonate and the pyroxene has been altered to actinolite, biotite, chlorite, sphene, pyrite, ilmenite and/or magnetite. Phenocryst outlines may still be observed in most specimens (Plate I-2) and phenocryst replacement minerals are identical to those in the few vesicles found in the common Northrim basalt.

PLATE I. Major Rock Units.

I-1. Non-porphyritic basalts. The core at the top of the image represents a dark green, chloritic lava which has been brecciated. The light rims adjacent to the chlorite interfragmental spaces are carbonate-rich. Two examples of calcite-mineralized vesicular basalts are also shown. The one which grades into mottled non-vesicular material of the same flow contains chalcopyrite (cp) mineralization, and the other which is by far the most vesicular lava found at the Northrim Mine contains pyrite (py) mineralization. 0.7x actual size.

I-2. Porphyritic latite. Transmitted light image. x nicols. Albite microlites with interstitial magnetite, biotite and chlorite. Area: 2.7 x 2.0 mm.

I-3. Porphyritic latites. The core at the top represents the common green andesine-porphyritic variety and the core at the bottom represents the marker brick-red anorthoclase(?)-porphyritic variety found in the Northrim sequence. Phenocrysts of the latter unit are cloudy in thin section and contain appreciable quantities of K. 0.7 x actual size.

I-4. Porphyritic latite. Transmitted light. X nicols. Two andesine phenocrysts, whose boundaries have been corroded by matrix solutions, occur in an albite-chlorite matrix. Area: 2.7 x 2.0 mm.

I-5. Pyroclastic breccias. Three examples, one of them a magmato-pyroclastic breccia with large plutonic clasts, another a winnowed (cf. reworked) pyroclastic breccia with small basaltic and plutonic clasts and a sulfide pyroclastic breccia are shown on the image. Sulfide pyroclast boundaries have been altered slightly by sulfide mineral flowage.

I-6. Trachybasalt fragments. Transmitted light. Plagioclase phenocrysts have been replaced pseudomorphously by carbonate (white). The hexagonal mineral may have once been apatite. The black mineral is magnetite. Area 2.7 x 2.0 mm.

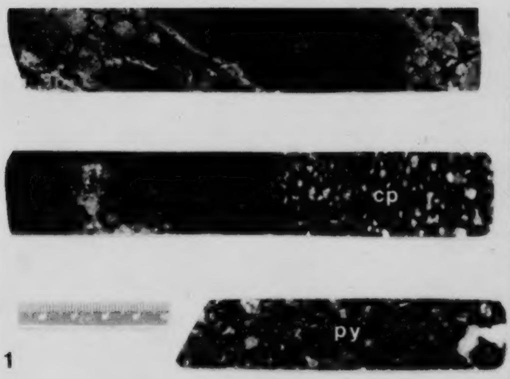

1

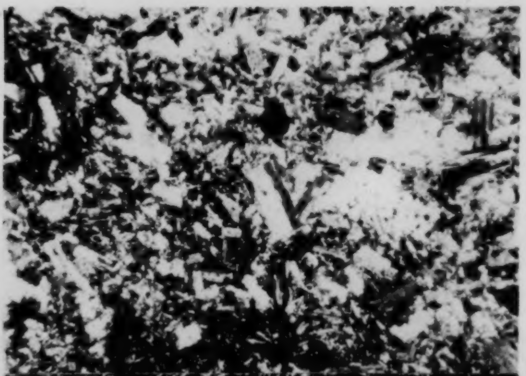

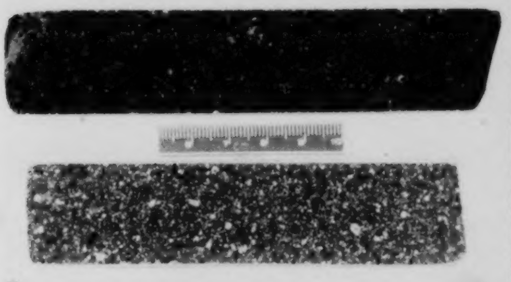

3

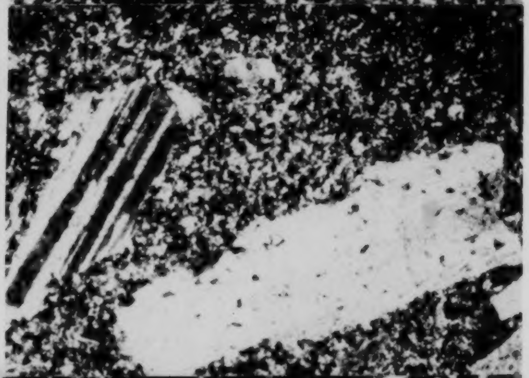

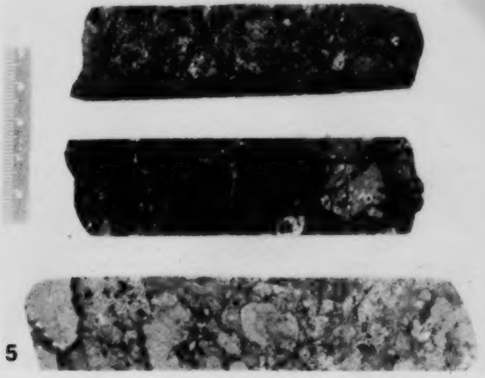

5

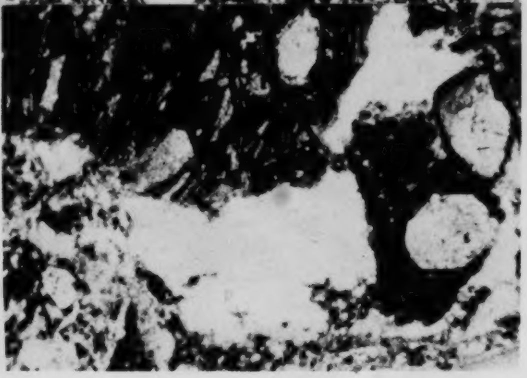

PLATE I

Tremolite-actinolite is the common amphibole and there are blue to colorless Na^+ and Fe^{+3} rich amphibole needles whose composition and optics change during crystal growth off vesicle walls and inside former phenocrysts (R. Lambert, pers. comm.). Biotite is pleochroic in deep greens and replaces both amphiboles and is in return replaced by chlorite. Much of the chlorite is a penninite variety with mauve and Berlin blue interference colors, but there are chlorites with normal interference colors. Chlorite and biotite appear dark brown next to pyrite but not to sphene, magnetite, ilmenite, and other mafic minerals.

Vesicular basalts, seemingly non-porphyritic and resembling the previous basalts in all other characteristics (Plate I-1) have been found in the southern half of the mine. Vesicles (1 mm. - 2 cm.) are filled with calcite, chlorite, a sodic amphibole, epidote, pyrite, chalcopyrite, pyrrhotite, magnetite, ilmenite, sphene, apatite quartz and/or albite. Albite microlites and quartz anhedra occur most often along vesicle walls; apatite is a sporadic constituent; ilmenite and magnetite sometimes rimmed by sphene, occur both as skeletal and euhedral masses with calcite, chlorite, epidote and/or amphibole needles; pyrrhotite, chalcopyrite and pyrite may fill vesicles completely, but they may also occur with other vesicle minerals and in such instances they often overgrow vesicle-matrix boundaries; epidote has only been observed with calcite, chlorite and quartz in some vesicles from the southern half of the mine; the sodic amphibole occurs as needles growing off vesicle walls; chlorite and calcite are by far the most abundant vesicle filling minerals, and either may rim vesicle walls even when other vesicle filling minerals are present. All basalts and tuffs have a few vesicles and the specific vesicle minerals present are those which replace phenocrysts and matrices in their respective hosts.

Dark green, generally non-vesicular, porphyritic, andesites and latites (Plate I-3), conformable with other rocks in the Northrim sequence, are found throughout the mine. Broken, non-oriented, relict andesine-labradorite phenocrysts (0.5-5 mm.) are characteristically enveloped by an albite microlite (0.05-1 mm.) matrix containing intersertal and interstitial chlorite, amphiboles, biotite, magnetite, ilmenite, pyrite, sphene apatite, dolomite and calcite. Phenocryst centers are sometimes altered to calcite, biotite and epidote and phenocryst-microlite boundaries have been corroded (Plate I-4). A sodic alteration rim representing albite replacement of labradorite phenocrysts is common. Phenocryst-microlite boundaries are also overgrown by chlorite, amphibole, biotite, calcite, magnetite, ilmenite and pyrite crystals and patches but all these minerals except calcite may be found as skeletal masses replaced by another generation of albite microlites. One such skeletal mass consisted of alternating pyrite and magnetite.

A curious brick-red variety of porphyritic latite (Plate I-3) occurs on the north end of the decline at the 060 level. Texturally it resembles the dark green porphyritic andesite but there are two important differences. Andesine phenocrysts (0.5-3 mm.) are more highly altered to epidote, biotite and calcite. Magnetite is rare and where present has been replaced by hematite; a fine hematite dust also permeates the whole rock. Hematite accounts for the brick-red color of the rock but both the hematite and the red color is restricted to this unit. The lithic lapilli pyroclastic breccia below and the non-porphyritic basalt above are green and magnetic. The porphyritic latite is locally magnetic and gray-green only within 0.5 metres of the lower and within 2 centimetres of the upper contacts. Both contacts are sharp and the red color does not occur with high K-feldspar content, unlike the brick-red altered rocks adjacent to some vein structures. Therefore, the brick-red coloration of the latite is an original magmatic characteristic representing high oxygen fugacity. Red lavas and tuffs of this nature are found in island arc volcanic rocks of New Zealand (Coombs in Amstutz, 1974).

(b) Pyroclastic Breccias

Lithic lapilli and agglomeratic pyroclastic breccias (Plate I-5) are most common in the northern half of the mine. The breccias are composed of angular, blocky, non-oriented and poorly-sorted fragments set in a matrix of non-oriented, non-clastic biotite, chlorite, magnetite, pyrite and albite. The coarser agglomerates contain numerous clasts of finely crystalline and coarsely crystalline, light-colored and dark-colored porphyritic and non-porphyritic, syenites, syenodiorites and monzonites of various textures, with or without andesine/labradorite phenocrysts (0.5-3 mm.). The finer lapilli pyroclastic breccias contain more clasts of basalt, especially a highly magnetic variety particularly common at the base of the pyroclastic breccia-dominated sequence at the Northrim Mine. Lapilli breccia matrices are more variable than agglomerate matrices: some lapilli matrices are composed almost completely of crystal and lithic fragments but others resemble basalt lavas, for the fragments are often completely separated by non-clastic secondary minerals. Plutonic fragments of the granite-granodiorite suite are conspicuously absent in the breccias.

Pyroclastic breccias are altered in the same manner as the other Northrim rocks. Magnetite patches, prominent in the interfragmental matrix, transect pyroclast-matrix boundaries as do biotite-chlorite patches, pyrite cubes, chlorite veinlets, epidote needles and calcite-chlorite-dolomite- etc. masses and stringers. Some pyroclast plagioclases have been irregularly replaced by epidote, albite. quartz and carbonate; all hornblendes (?) have been replaced by biotite, chlorite, sphene, pyrite, ilmenite, and magnetite. The latter three minerals also overgrow plagioclase.

Volcanoclastic sediments are found within the pyroclastic breccias of the northern half of the mine. They are of three kinds: a poorly sorted and poorly graded variety with oriented, lapilli-sized, subangular to subround and varied-colored volcanic and plutonic clasts (cf. reworked pyroclastic breccia); a moderately well-sorted but poorly-graded variety with many angular plagioclase (to 2 mm.) and a few subround magnetic basalt (to 3 mm.) fragments set in a chloritic-fragmental matrix (cf. reworked crystal tuff); and a moderately well-sorted, non-graded variety with round granules, mostly of volcanic provenance (cf.

volcanoclastic sandstone). The reworked pyroclastic breccia (Plate I-5) is particularly abundant in the mine; the reworked crystal tuff occurs 5 metres north of the 056 level sump; and the volcanoclastic sandstone is found only as two bands less than 1 centimetre wide apiece and less than 5 centimetres apart within the reworked pyroclastic breccia.

Trachybasalts are uncommon host rocks of the Northrim mine but they are common elsewhere in the Camsell River area (Badham, 1973a,b). Trachybasalt fragments occur in volcanic flow and pyroclastic breccias and in such instances are recognized by their high magnetite content. One example, a pyroclastic breccia fragment (Plate I-6) contains relict plagioclase phenocrysts completely replaced by carbonate and set in a matrix almost completely replaced by magnetite and ilmenite. Another example, a trachybasalt flow, has been intensively carbonatized and its phenocrysts and matrix are composed of the alteration assemblages and textures characteristic of the non-trachytic basalts.

(c) Plutonic and Hydrothermal Units

Magnetite-apatite-actinolite±hematite bodies have not been found in the Northrim Mine but there are several lenses a few kilometres north (Fig. 4).

All are located in brick-red, hematite-dusted, potassic volcanic rocks. In one, pegmatitic magnetite octahedra, orthoclase laths and apatite columns intrude a feldspathized andesite. In another, specular hematite is disseminated throughout a sericitic and chloritic matrix. In another, magnetite fills fractures within a brecciated andesite which has been highly metamorphosed. The breccia fragments contain chlorite with bronze-yellow interference colors, feldspars, epidote, actinolite, ilmenite, magnetite and pyrite. The latter minerals have been partially altered to sphene and hematite. There were no contact textures (e.g. chilled borders) observed save for local centimetre scale hematitic alteration of the host rock matrix. Contact metamorphic minerals such as scapolite and tourmaline were not observed although the occurrences are situated close to the Balachey Lake pluton and well within that pluton's feldspathized contact aureole (Dollery-Pardy, unpublished mine reports).

Feldspathized volcanic rocks also occur at the Northrim Mine. They occur erratically along vein structures and xenoliths of these rocks occur within the veins themselves, especially amongst the earlier phases of mineralization. These rocks are identified by their deep brick-red color along vein margins and their gray green color further away (Plate II-1).

PLATE II. Minor Rock Units.

II-1. Feldspathized and hematized lava sequence. The most intense feldspathization and hematization occurs adjacent to the mineralized dolomite-quartz veins. The lighter gray areas are the ones where feldspathization and hematization occur: the core taken furthest from the vein is only albitized along three stringers.

II-2. Porphyritic syenite dyke. Transmitted light image. A relict feldspar crystal has been replaced pseudomorphously by quartz crystals. Area: 2.7 x 2.0 mm.

II-3. Porphyritic syenite dyke. Transmitted light. Relict hornblende phenocrysts have been replaced pseudomorphously by green biotite (gray), sphene (dark gray) and pyrite (black). The smaller dark gray crystals are sericitized orthoclases. Other orthoclases in the same thin section have hardly been altered. Area: 2.7 x 2.0 mm.

II-4. Porphyritic monzonite dyke. Transmitted light. Quartz (white) and carbonate (gray) have pseudomorphously replaced a relict plagioclase crystal. Epidote needles surround the pseudomorphs. Some other plagioclases in the same section have hardly been altered. Area: 2.7 x 2.0 mm.

II-5. Sulfide-oxide lens. Reflected light image. Magnetite (dark gray) and chalcopyrite (light gray) crystals are present in this section. The magnetite crystals have been fractured. Area: 1.9 x 1.4 mm.

II-6. Brecciated sulfide mass. Reflected light. Pyrite (gray) has been tectonically brecciated. Some of the fractures have been filled by sphalerite. Area: 2.4 x 1.9 mm.

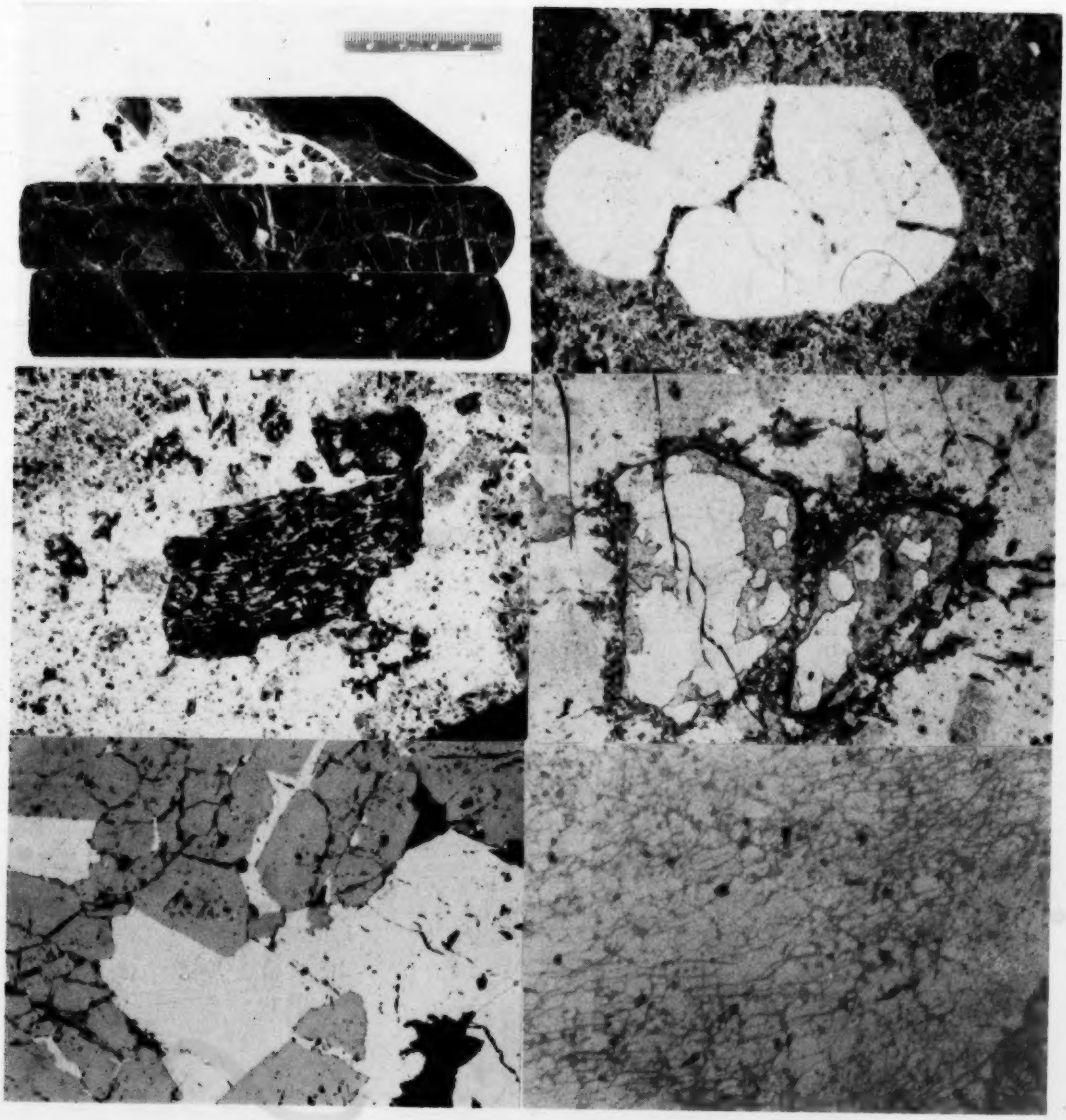

PLATE II

The red color is imparted by fine grained hematite (<1μ); the gray-green color is imparted by K-feldspar and/or albite. In both the brick-red and gray-green altered lavas, K-feldspar laths (1μ - 5μ) are dominant but albite becomes dominant towards the outside edges of these altered rocks. Relict pyroxene phenocrysts have been completely altered to biotite, chlorite, sphene, ilmenite and/or magnetite; relict plagioclase phenocrysts have been completely altered to epidote, sericite (?) and K-feldspar. The ground mass is composed of K-feldspar, quartz, albite and the alteration minerals just mentioned. Magnetite and to a lesser extent, ilmenite, may be completely absent from the most intensely altered rocks and replacement textures are more regular towards the outside edges of the feldspathized volcanic rocks. The feldspathized rocks have the relict textures of the other wall rocks that they grade into but they are characterized by their more altered nature and by the presence of abundant K-feldspar and/or albite. Carbonate may replace all alteration minerals locally in the feldspathized rocks adjacent to mineralized veins and stringers but only carbonate stringers are abundant throughout these rocks.

Porphyritic dyke rocks of the granite-granodiorite suite are numerous 1 kilometre north of the mine and two samples were available for study. The first, a granite, contains non-oriented megacrysts of sericitized and silicified orthoclase (2-10 mm.+), sericitized and epidotized oligoclase (3-15 mm.+) and chloritized and titanitized hornblende (1-5 m.), set in an aphanitic matrix of quartz, orthoclase and albite. Quartz porphyroblasts (3-15 mm.+) may assume the shapes of feldspar laths (Plate II-2) but replacement of feldspar by quartz is variable in intensity: the feldspars may have been replaced completely or hardly at all. Orthoclase megacrysts have been replaced by chlorite and albite along fractures; oligoclase megacrysts by biotite, orthoclase and chlorite along fractures; and hornblende megacrysts have been replaced directly by ilmenite, pyrite sphene, biotite and chlorite (Plate II-3). Sphene may also rim ilmenite and overgrow feldspar. The quartz porphyroblasts show smooth regular outlines with the matrix; the oligoclase and orthoclase megacrysts corroded outlines. The relict feldspar and hornblende megacrysts are remarkably fresh compared to those of the volcanic rocks.

The second sample, a porphyritic granodiorite (cf. quartz monzonite) is somewhat similar. It consists of non-oriented epidotized oligoclase (0.5-6 mm.) and chloritized hornblende (0.5-3 mm.) phenocrysts set in an aphanitic matrix of quartz and albite. Pseudomorphous replacement of oligoclase phenocrysts first by quartz, then by calcite, has been beautifully preserved (Plate II-4). Once again, replacement of plagioclase phenocrysts by quartz (and in this instance, calcite) is a variable process. Oligoclase fractures are occupied by chlorite, calcite and epidote; hornblende phenocrysts are replaced by ilmenite, sphene, chlorite and calcite. Calcite and chlorite patches overgrow phenocryst and matrix minerals.

Alteration of porphyritic granite-granodiorite dyke rocks resembles alteration of volcanic rocks since the secondary mineral assemblages and their respective replacement features are nearly identical. Differences are few: quartz is an uncommon secondary mineral in the highly aluminous but silica-poor volcanic rocks and tremolite-actinolite and other secondary amphiboles have not yet been found in the more felsic dyke rocks.

(d) Volcanogenic Massive Sulfides

Sulfide minerals are abundant throughout the Northrim Mine and they occur as disseminated crystals, irregular masses, vesicle fillings, fracture fillings, vein mineralization and discrete lenses throughout the Northrim Mine. Pyrite is by far the most common sulfide and it, chalcopyrite, sphalerite, galena and pyrrhotite, occur in wall rocks far removed from mineralized veins.

Discrete sulfide lenses have been found in the Northrim Mine. These lenses are thin (0.2-1 m.), narrow (0.5-2 m.) and short (1-5 m.) and they are numerous, especially near the major flow to breccia transition and the 000 and 014 vein structures. Their long and intermediate axes lie on planes oriented parallel to flow and bedding contacts and therefore these lenses may be magmatic deposits related to their host lavas, tuffs and breccias in the Northrim Mine.

One small lens, a magnetite-pyrite-chalcopyrite-silicate mass (Plate II-5), occurs on the decline north of the 210 level drift. Chalcopyrite and pyrite blebs (0.5-3 cm.) are intruded by elongated idiomorphic magnetite crystals (0.2-2.5 mm.). Magnetite-sulfide contacts are idiomorphic and magnetite inclusions (1-10μ) are abundant inside non-brecciated pyrite crystals and hence magnetite and the two sulfide minerals are thought to be coeval. No exsolution lamellae were observed in the magnetite and this magnetite most likely contains low Ti^{+4}, Fe^{+3}, V^{+4} and Mn^{+4} in solid solution. Two vesicles (0.5, 1.0 cm. dia.) composed of calcite, quartz, actinolite and chalcopyrite embay the magnetite-sulfide mass. Vesicle actinolite and quartz intrude the host sulfides but not magnetite and neither host magnetite nor pyrite enter the vesicles. One vesicle assumes a shape which pseudomorphs an isometric mineral, perhaps a zeolite and hence the host lens is demonstrably premetamorphic and most likely syngenetic with the associated silicate rocks. Both mineralogy and texture are similar to samples of the metamorphosed sulfide-magnetite ore body at Balmat, New York seen by the writer at the University of Western Ontario.

Most lenses contain no magnetite and are numerous near the 000 vein structure. Minerals observed include pyrite, marcasite, chalcopyrite, sphalerite, galena and ilmenite. All primary and secondary sulfide minerals and lenses are transected by mineralized quartz-carbonate stringers and veins representing all stages of vein mineralization. In massive varieties, i. e. lenses almost completely composed of sulfides and having sharp contacts with all host rocks, pyrite and sphalerite porphyroblasts (0.1-4 mm. and up) stand out from their finer crystalline marcasite-pyrite-chalcopyrite matrices. In tectono-brecciated varieties (Plate II-6), by far the more common, brittle pyrite and/or marcasite crystals have been broken into smaller fragments (0.01-1 mm.), morphologically parallel to ESE rock cleavages. Interfragmental spaces may then be filled by sphalerite, chalcopyrite, tremolite, chlorite, quartz, feldspar and/or carbonate and fractures may be filled by later quartz-carbonate vein mineralization. Marcasite, a low temperature polymorph of pyrite, often occurs as masses replaced by pyrite. Galena and ilmenite are only accessory minerals of the sulfide lenses.

Two sulfide pyroclastic breccias were found and both occur in horizons conformable to other beds of the Northrim Mine. The first, a lapilli pyroclastic breccia at the 000 north drift, consists of slightly broken, non-oriented, subangular pyrite fragments (1-8 mm.) set in a matrix of smaller silicate fragments. The second, a pyroclastic breccia of subround to subangular pyrite-chalcopyrite lapilli and bombs, was found in core drilled 70 metres south of the 125 level drift along the decline. It is described below.

The bottom contact of the second pyroclastic breccia is sharp and conformable with other contacts observed in core sections from the same hole. Sulfide pyroclasts decrease in size upwards from the bottom, and at 0.4 m. above the bottom contact, all traces of fragment outlines disappear. Larger pyroclasts are more regular than smaller ones and smaller ones become less regular and less discernible than the larger ones towards the top of the unit. Chalcopyritic and pyritic pyroclasts are more easily discerned; sphaleritic pyroclasts less so. Galena is a constant but less abundant member of some pyroclasts. The top of the pyroclastic breccia is truncated by a 4 centimetre thick quartz-carbonate vein and several quartz-carbonate stringers truncate sulfide pyroclasts and masses below. Some of the pyroclasts and masses have been rimmed by carbonate (Plate III-1) and intruded upon by idioblastic quartz (Plate III-2).

The larger (0.5-3.5 cm.), more easily discerned pyroclasts near the bottom of the unit, consist of non-oriented pyrite fragments (0.05-1 mm.) set in a chalcopyrite matrix (Plate III-1). The pyrite fragments occur as random clusters which form regular crystals/fragments upon reconstruction fragment by fragment. The chalcopyrite matrix and pyrite fragments nevertheless form a pyroclast with subangular outlines despite any matrix replacements (Plates III-1, III-2),and despite possible sulfide flowage. The pyrite-chalcopyrite pyroclasts themselves are variable in size and orientation and hence they were emplaced under free-fall conditions. The pyrite fragment - chalcopyrite matrix texture is similar to some breccia textures found in the massive sulfide ores of Outukumpu, Finland (Ramdohr, 1969). The texture at Northrim is thought to be the result of two phreatic explosions: the first, a contained explosion which brecciated pyrite in place, an event followed by chalcopyrite infilling in place; and the second, a non-contained explosion, which broke and scattered the sulfide pyroclasts which subsequently settled into their present positions. The pyrite fragments

PLATE III. Sulfide Pyroclastic Breccia

III-1. Reflected light image. A sulfide pyroclast, consisting of pyrite fragments (white) and a chalcopyrite matrix (light gray) is enveloped by a carbonate (black) rim. The pyrite fragments occur in clusters, each of which may be rearranged into idiomorphic crystals. Chalcopyrite has filled the interstitial space between pyrite fragments and some chalcopyrite has filled interstitial spaces between carbonate rhombs. A relict sphalerite (gray)-chalcopyrite (light gray) pyroclast occurs in the upper left corner.

III-2. Reflected light. Another pyroclast, similar to the one before, has been extensively replaced by quartz (qz) and chlorite (ch). Quartz, a mineral uncommon in the Northrim rocks, may have formed during exhalative activity. Chalcopyrite and sphalerite fill the spaces between pyrite fragments.

III-3, III-4. Reflected light. Chalcopyrite-sphalerite-pyrite flow structure. Pyrite fragments (white) and sphalerite (dark gray) lamellae align parallel to one another in a chalcopyrite-dominated field. Note the changes in alignment: these may correspond to differences in present individual chalcopyrite crystal orientations and may indicate relict, melded pyroclasts. Pyrite fragments maintain their brecciated outlines, the sphalerite and chalcopyrite material does not.

III-5. Reflected light. Relict sphalerite pyroclast with exsolved chalcopyrite inclusions (white). Numerous galena inclusions of this size (not photographed) also occur in this relict sphalerite pyroclast. The dark gray mineral is calcite and it rims numerous pyroclasts.

III-6. Reflected light. Galena (white)-chalcopyrite (light gray) eutectoid intergrowth. Sphalerite (gray) and quartz (black) also occur in the image. This texture results from sulfide recrystallization and triple junctions are discernible within the chalcopyrite on the original photograph. The sulfide recrystallization almost certainly occurred during regional metamorphism.

The white bars of this plate and the ones of succeeding plates represent 50 μ sample distance.

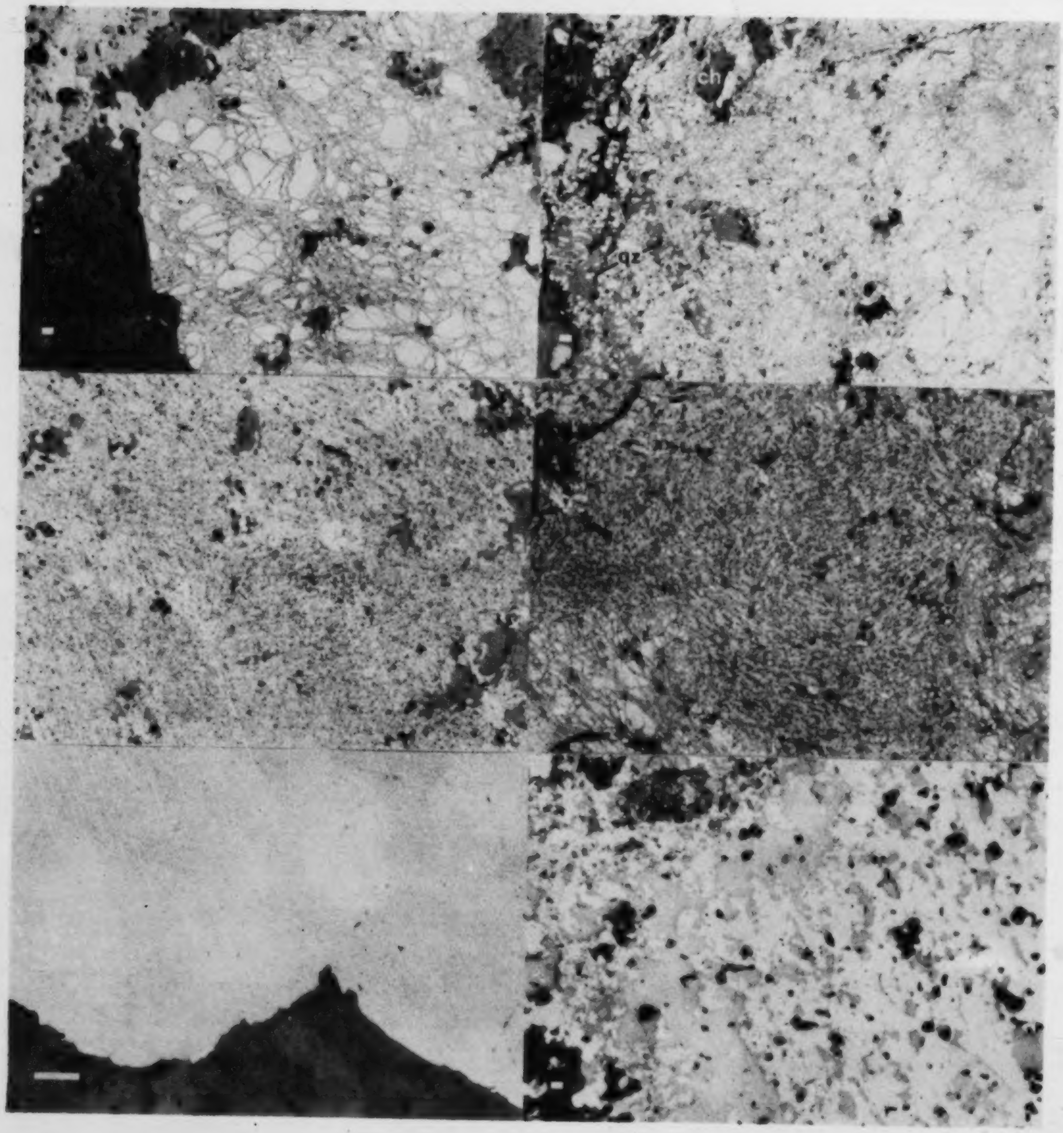

PLATE III

PLATE IV. Sulfide Mineralization.

IV-1. Reflected light image. Chalcopyrite (white) and sphalerite (light gray) has been partially replaced by felty biotite, fibrous actinolite and by clear feldspar. A quartz stringer containing chalcopyrite and sphalerite occurs within the left side of the image.

IV-2. Reflected light. Pyrite (white) and sphalerite (light gray) has been enveloped by biotite (felted gray). The matrix mineral is feldspar.

IV-3. Reflected light. Pyrite-chalocpyrite pyroclastic mass veined by sphalerite (dark gray). Galena veins may also occur and both galena and sphalerite veins are spatially continuous with sulfide mineralization interstitially emplaced between carbonate rhombs. Quartz veins (black) occur towards the edges of host pyroclasts.

IV-4. Reflected light. Galena (white) and chalcopyrite (light gray) mineralization in vein quartz which truncates the sulfide pyroclastic breccia of previous images. Idiomorphic hexagonal crystals of quartz (gray) and a matrix of dolomite (mottled gray) are also present.

IV-5. Reflected light. Pyrite cube (white) whose fractures have been filled by chalcopyrite (light gray) occurs as a xenolith in vein dolomite (black).

IV-6. Reflected light. Black sphalerite (white) vein crosses brown sphalerite (white)-rich wall rock. A few chalcopyrite (light gray) blebs also occur in the wall rock. The sphalerite vein has been truncated by a felted mass of biotite (bi). The vein sphalerite (v) has a slightly different composition than the host exhalative (?) sphalerite (h)--element concentrations of these two varieties have been included in Table 7. One grain of cobaltite (w) occurs in this image.

The white bars of this plate represent 50μ sample distance.

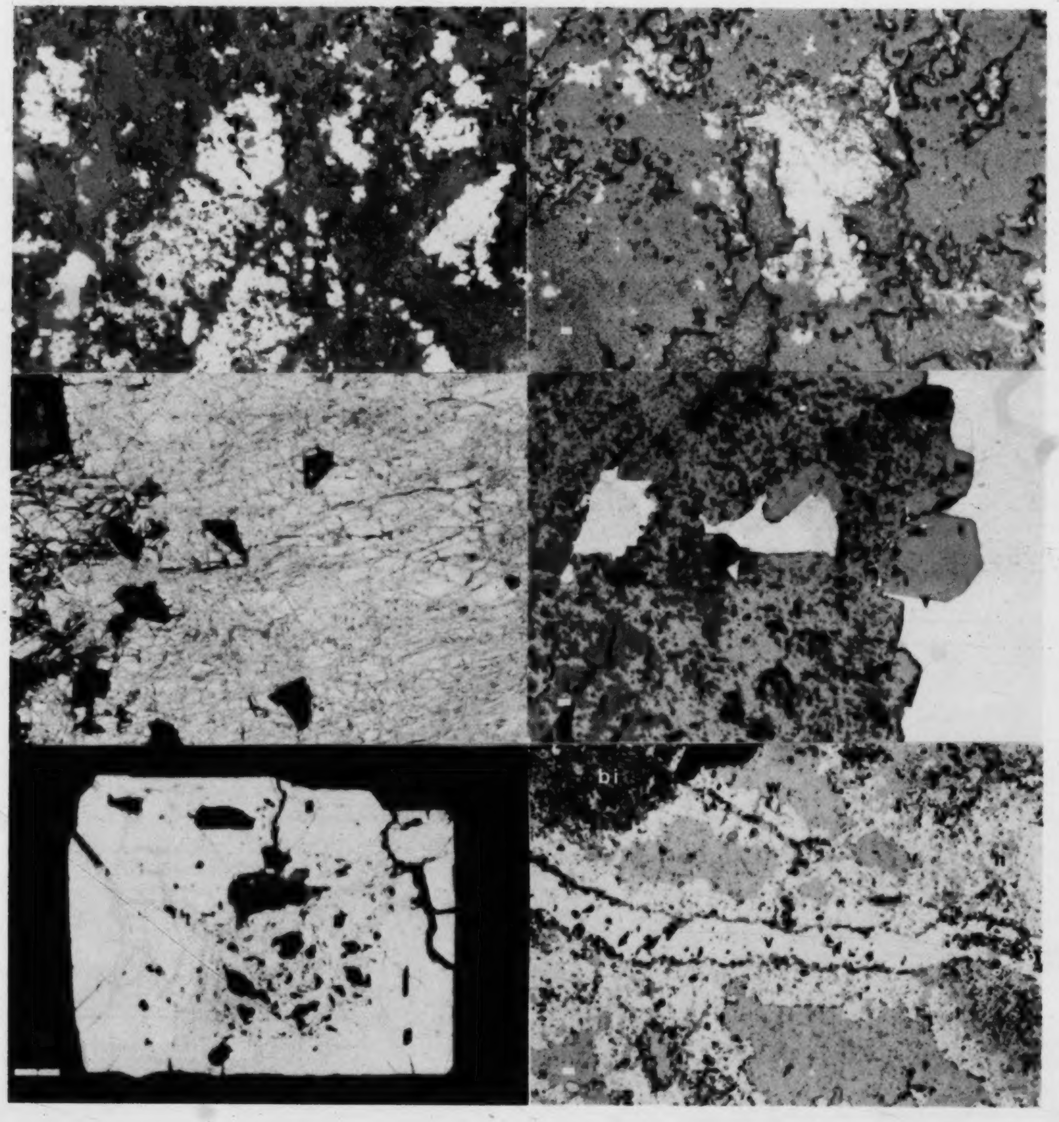

PLATE IV

were broken in place and their interfragmental spaces were filled by chalcopyrite before and not after the second explosive event since chalcopyrite and pyrite together formed the pyroclasts and the pyroclast surfaces were neither broken nor separated in the same manner as the pyrite fragments. The same observation precludes a post-depositional, tectonic fragmentation of pyrite as does the spheroidal shape of the pyrite fragment clusters themselves. The large size of some heavy sulfide clasts (1-3 cm.) suggest that the explosion occurred in a vent well within 2 kilometres of the present mine, a suggestion confirmed by the presence of even larger (up to 18 cm.) monzonitic pyroclasts in the agglomeratic pyroclast breccias elsewhere in the Northrim Mine.

Smaller pyroclasts are discernible near the bottom of the unit but become more irregular towards the top. Chalcopyrite-sphalerite intergrowths, some of which resemble pyroclasts in shape, may also contain pyrite fragments (Plate III-3). Pyrite "rafts" (i.e. fragments) and sphalerite "islands" have been aligned parallel to one another and this alignment may change direction but not form, within fractions of a millimetre. This alignment cannot be an exsolution feature since the pyrite still retains its fragmental outlines and the proportion of sphalerite to chalcopyrite is too high. The present alignment does not coincide with pyroclast outlines and can only be accounted for by recrystallization and "plastic" flowage of chalcopyrite and sphalerite. Some chalcopyrite-sphalerite intergrowths and pyrite fragments are found together in parallel alignments (Plate IV-4) and this indicates some sulfide flowage occurred under directional stress. This stress is thought to be tectonic since any sulfide mineral alignment displayed is parallel throughout the breccia but is not parallel to the pyroclastic breccia contact.

Sphalerite masses (1-5 mm.) with numerous random chalcopyrite (5-50μ) and a few random galena (10-50μ) inclusions (Plate III-5), characteristic of higher temperature sphalerites in massive sulfide deposits in general, and Kuroko deposits in particular (K. Hattori, pers. comm.), appear to have clastic outlines. Eutectoid intergrowths of galena and chalcopyrite are common (Plate IV-6) and are far more irregular than intergrowths of other sulfides. Pyrite fragments are few in chalcopyrite-galena and sphalerite±galena± chalcopyrite pyroclasts and masses and this probably reflects an original bottom (Cu, Fe sulfides) to top (Zn, Cu and then Pb and Zn sulfides) segregation of minerals of the original non-brecciated source deposit.

All pyroclastic sulfides have been partially replaced by matrix carbonate (Plate III-1), quartz (Plate III-2) and tremolite (Plates IV-1, IV-2). If the space now occupied by the replacing minerals was once occupied by the replaced sulfides without a corresponding displacement of the sulfide minerals upon replacement, an extremely likely event indicated by interpolation of sulfide mineral boundaries, then some portion of the sulfide minerals must have been broken down to soluble components and these components must have been taken away by solutions similar to those which contributed to the growth of the replacing minerals. The presence of corroded and embayed sulfides on sulfide-quartz and sulfide-carbonate boundaries is also highly suggestive of metal and sulfur loss and the presence of sphalerite and galena-rich stringers truncating brecciated mineral structures (Plate IV-3) indicates that some of this metal and sulfur may have precipitated close to the breccia source. Such stringers are associated within pyroclasts rimmed by carbonate and chalcopyrite, galena and sphalerite may fill the interstitial spaces between individual rim carbonate and quartz crystals (Plate IV-4). The writer regards the presence of interstitial chalcopyrite, galena and sphalerite in carbonate stringers and the 4 centimetre wide vein which crosscut the sulfide pyroclastic breccia textures as no coincidence: these minerals were precipitated from the hydrothermal vein solutions, most likely the very ones responsible for the corrosion and mobilization of the nearby sulfide minerals found in the wall rock. The interstitial sulfide minerals are not to be confused with the occasional xenoliths of brecciated pyrite-chalcopyrite matrix pyroclasts and sphalerite crystal - chalcopyrite inclusion masses (Plate IV-5) found in a mineralized stringer of the 000 vein structure. These xenoliths represent physical, rather than chemical addition of sulfides to the mineralized veins.

The continuum between sulfide bodies having primary characteristics and those having secondary characteristics is not restricted to the example above. Sulfide laminae, now recrystallized to euhedral pyrite (0.1-3 mm.) and/or euhedral arsenopyrite and cobaltite (0.1-2 mm.), may be completely conformable with bedding contacts or sometimes with the dominant ESE cleavage, like the more massive, tectono-brecciated lenses above. Sulfide flow bands, consisting mainly of chalcopyrite, sphalerite and galena, are conformable with the dominant ESE fracture cleavage in the same manner as these same sulfides in the more massive bodies. Vesicles may be completely filled with calcite and/or sulfide minerals, particularly pyrite, chalcopyrite and pyrrhotite. Sulfide porphyroblasts and sulfide-dominated stringers are abundant wherever host rock sulfide mineralization is found next to fracture systems hosting mineralized veins. In one instance, black sphalerite-dominated stringers truncate a brown sphalerite-dominated host rock (Plate IV-6). A fibrous mafic silicate (probably actinolite) and K-feldspar replace the sulfides in the same host rock and stringers. All secondary sulfide textures, except for the sulfide-rich stringers have been truncated by mineralized quartz-carbonate veins. The mineralized quartz-carbonate veins are clearly a late-stage post-sulfide mineralization feature.

The primary and secondary minerals and textures observed in volcanogenic massive sulfides at the Northrim Mine are common to all Precambrian and most Phanerozoic volcanogenic massive sulfide deposits (Sangster, 1972).

Depositional Conditions

The Northrim wall rocks are volcanogenic. They consist of pyroxene-porphyritic and labradorite-porphyritic basalt flows, andesine-lapilli crystal tuffs, magmato-pyroclastic flow breccias and lithic lapilli and agglomeratic breccias. Volcanoclastic sedimentary rocks are few and the only common variety, a reworked pyroclastic breccia, is very poorly graded and sorted.

The Northrim rocks were emplaced in a high relief, high energy surface environment where sediments did not accumulate.

The great size of lithic fragments in the pyroclastic breccias indicate that the Northrim rocks were emplaced within 1 kilometre of a volcanic center. Their extremely poorly sorted, non-graded, disordered and non-laminated nature suggest not only gaseous, confined and explosive conditions within the magma chamber during volcanic activity but also subaerial, free-fall deposition. Even the crystal tuffs have been poorly sorted and graded and this also indicates a high energy subaerial accumulation of the volcanic pile.

The basaltic flows are 2-5 metres in thickness and have been chilled only at their margins. Pillowed and other distinctive chill textures (e.g. ropey, spinifex structures) have not been observed at the Northrim Mine and again, subaerial conditions are indicated. Phreatic breccias (Plate I-1) occur locally in the basalts and explosive volcanicity was present during deposition of the volcanic pile. The great thickness of some basalt flows and some free-fall pyroclastic breccias (up to 2 m.) and the general lack of visible weathered horizons near their contacts indicate that accumulation of the volcanic pile was rapid.

The occurrence of quartz-poor plutonic clasts in the agglomerates and tuffs suggest not only that members of the syenite-monzonite (but not the granite-granodiorite) plutonic suite of the Camsell River area are synvolcanic, but also that the plutonic rocks themselves existed at shallow depths (approx. 3 km.) at time of eruption. Thus members of both the Balachey Lake pluton and the Rainy Lake differentiated sill may be represented in the Northrim breccias, a relationship suggested by pyroclast mineralogical and textural similarity to the descriptions of the various plutonic lithologies found in Hoffman and Bell (1975), Hoffman et al. (1976) and Hoffman and McGlynn (1977). Plutonic lithologies apparently present in the Northrim agglomerates are those of the differentiated sill and not the low quartz hornblende porphyritic monzonite of the Balachey Lake pluton. Unfortunately samples of the pluton and the sill were not available to the writer for comparison.

Alkaline plutonic pyroclasts are accompanied by basalt pyroclasts in the same breccias and cumulo(?) porphyritic varieties of the two look much alike. Andesine euhedra are of similar size (0.5-5 mm.) and shape (laths) to the labradorite phenocrysts of the basalt, and both may be aligned. The distinguishing characteristic between the two porphyritic lithologies, is the variable but great concentration of magnetite in the matrix of the latter, occasionally up to 100 volume %. The plutonic matrices do contain magnetite and other mafic minerals, but in far lesser concentrations. Magnetite is also abundant in the matrices of both porphyritic and non-porphyritic basalt flows underlying the pyroclastic breccia sequence. The high magnetite content of some breccia matrices, most basaltic fragments and all neighboring basalts suggest a close magmatic affinity between magnetite-rich lavas, pyroclastic flow breccias and pyroclastic free-fall breccias. The abundance of andesine-labradorite phenocrysts (0.5-5 mm.) in some weakly magnetic monzonite and some highly magnetic basalt fragments provides not only direct evidence for the calcalkaline affinity and similar origin of both Camsell River plutonic and volcanic rocks, but also indirect evidence for the separation of an Fe-rich magnetite magma from an Fe-poor monzonite magma, alluded to by Badham and Morton (1976) in reference to magnetite-actinolite-apatite±sulfide lenses of the Camsell River area.

The magnetite-actinolite-apatite lenses may have been emplaced in the volcanic sequence at depths sufficient for actinolite formation at the same time as magnetite-rich lavas were being deposited at the top of the volcanic pile. One sample, a probable phreatically-brecciated, magnetite-filled body may occupy a breccia pipe similar in texture to the breccia pipes underlying some stratabound volcanogenic sulfide deposits. There are a couple of magnetite-apatite (?) bands/xenoliths in the pyroclastic breccias of the Northrim Mine and preliminary electron dispersive reconnaissance of general Northrim magnetites indicate that they have the low concentrations of Ti and V reported for magnetite in magnetite-actinolite-apatite lenses (Badham and Morton, 1976). The proposed physical and implied magmatic relationship between magnetite-rich lavas and magnetite-rich intrusions is analogous to that between intrusive and extrusive stratabound sulfide deposits.

The high magnetite and low quartz content of the Northrim rocks suggest an alkaline association of the parent volcanic magma. The sporadic distribution and the oblong but not elongated shape of vesicles implies quick cooling of and low vapor pressure conditions within most Northrim basalts at time of eruption. The vesicles have been subsequently filled with the secondary mineral assemblages characteristic of phenocryst and matrix replacements and of greenschist metamorphism. The dominance of labradorite and not olivine, amphibole nor orthopyroxene phenocrysts and lapilli of most Northrim rocks indicate that the volcanic magma was of calcalkaline affinity.

The depositional conditions implied by petrological and field studies of the Northrim rocks are similar to those of other workers in the Great Bear Lake area and only two important differences will be mentioned here. Firstly, there is a volcanic center within the Camsell River belt, a feature not reported by Hoffmann et al. (1975, 1976, 1977). Secondly, the presence of relict pyroxene, not amphibole, phenocrysts in the Northrim lavas counters Badham's (1973a, 1973b) interpretation of hornblende relicts in Camsell River basalts but supports Hoffman and McGlynn's (1977) observations of pyroxene phenocrysts in the wall rocks at the Northrim and Norex Mines. Hence this writer does not consider the Camsell River basalts to be the products of unduly hydrous magmas, since all the H_2O present in the basalts has been incorporated into minerals characteristic of secondary, metamorphic assemblages and not of the relict, non-hydrous, volcanogenic assemblages. Replacement textures indicate that H_2O must have been added after rock formation. Primary hornblende occurs in the more siliceous plutons, but has not been observed by the writer in the Northrim volcanic rocks, even as relicts.

The Northrim basalts, tuffs and breccias form but a small part of the subaerial, calcalkaline Great Bear volcanic pile.

CHAPTER 3

HOST ROCK GEOCHEMISTRY, MAGMATISM AND METAMORPHISM

Introduction

A geochemical study of the volcanic rocks hosting the Northrim mineralization was started by R. D. Morton to (1) evaluate various elements as host rock indicators to the presence of vein mineralization and (2) the thesis writer has used the geochemical data to describe and define the magmatic affinities and metamorphic nature of the Northrim host rocks, a task only partially performed by the petrological study of the previous chapter. Samples were taken at 25 foot intervals along traverses which approach the 000 and 014 vein complexes from both the hanging wall and foot wall sides. In addition, several samples were taken from the 000 vein complex on the footwall side (Fig. 5). Sample traverses perpendicular to the vein structures transect the volcanic sequence.

The 29 samples were analyzed for major oxides and trace elements by Dr. J. G. Holland of the University of Durham using X-ray fluorescence techniques. Major oxide analyses were corrected using a computer technique developed from Holland and Brindle (1966). Corrected values were then returned to the computer under the Normcal program of Dr. R. C. O. Gill, formerly of the

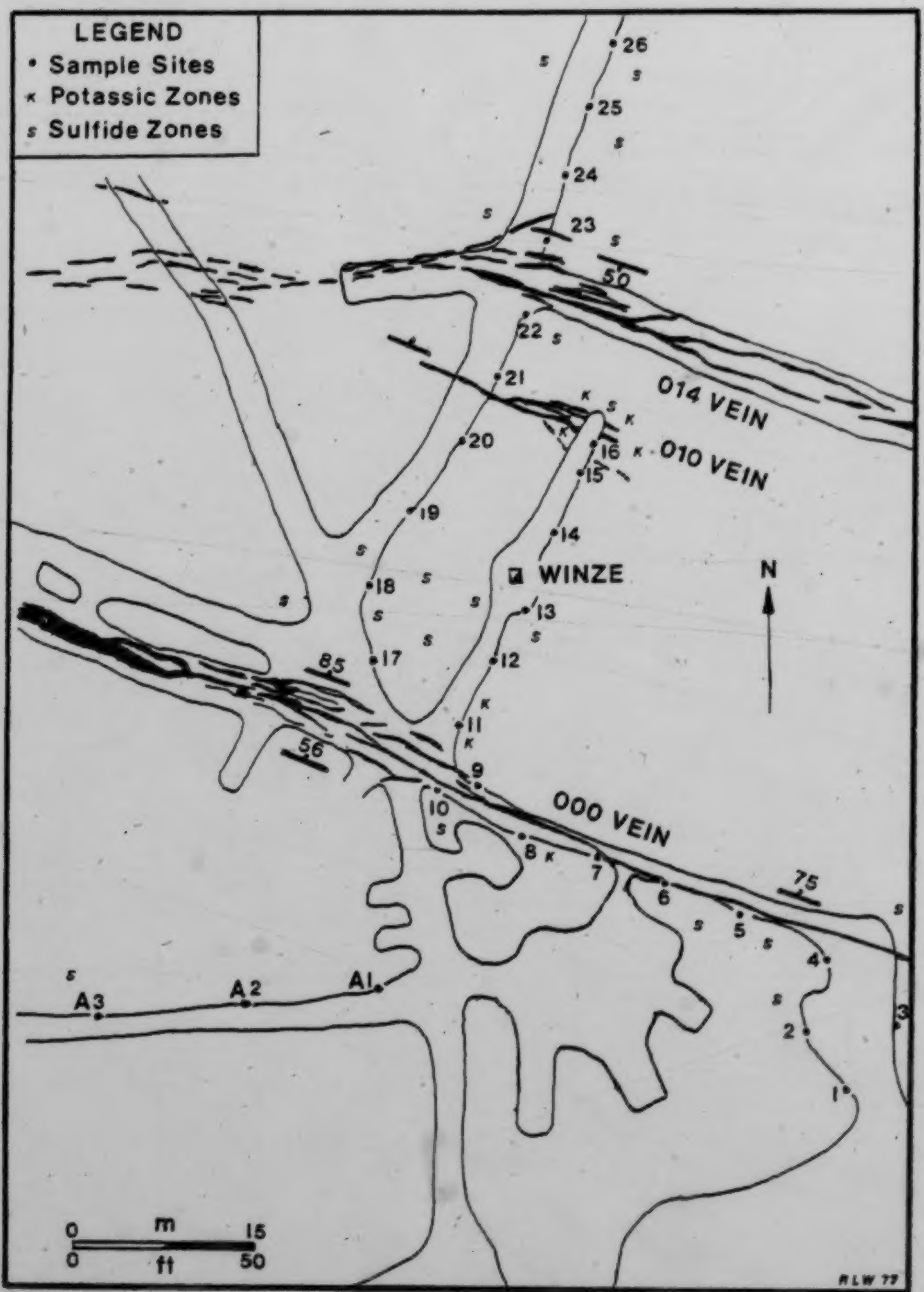

Figure 5: Northrim Mine geochemical sample locations.

State University of New York at Binghamton. This program generates tables of atomic cation, normative mineral, and residual oxide percentages; coordinates of the normative Ab-Qz-Ol-Cpx system; and values for several petrochemical functions. The program does this on a CO_2-free and H_2O-free basis.

The analytical data gained in the manner stated above are incorporated into this chapter of the thesis and analytical results for individual samples are tabulated in the appendices.

(a) Major Oxide Distribution

The average Northrim volcanic rock is a basalt (Table 2), although individual samples may appear more mafic or more felsic in composition (Table A-1, Appendix I). SiO_2 concentration tends to be highest in the feldspathized lavas between the 000 and 010 vein structures, the only Northrim rocks which generally contain matrix quartz. Quartz is only a minor constituent of the average norm (Table A-4) and the Northrim rock is very slightly undersaturated with respect to SiO_2. SiO_2 is the differentiation index standard employed in the Harker diagrams (Fig. 6, 7).

The Northrim basalts are highly aluminous and sample Al_2O_3 concentrations decrease slightly with

TABLE 2

MAJOR OXIDE AND SULFIDE CONTENTS OF VOLCANIC HOST ROCKS

Major Oxide	Average Composition		Average (Revised) Composition			
	Mean	Standard Deviation	Mean	Standard Deviation	Rejection Level	No. Used
SiO_2	49.07	4.50	50.02	4.55	-	29
Al_2O_3	17.98	1.52	18.30	1.53	-	29
Fe_2O_3	3.83	0.82	3.91	0.83	-	29
FeO	10.36	2.27	10.56	2.29	-	29
MgO	7.08	3.01	7.22	3.01	-	29
MnO	0.16	0.09	0.16	0.09	-	29
TiO_2	0.90	0.12	0.91	0.12	-	29
CaO	2.42	2.17	1.40	0.68	> 3.00%	22
Na_2O	4.77	1.77	5.15	1.47	< 2.00%	27
K_2O	2.12	2.17	1.69	1.32	> 5.00%	27
P_2O_5	0.37	0,06	0.38	0,06	-	29
Excess S_2	0.71	0.81	0.10	0.03	> 0.25%	12
Total	99.77		99.80			

All entries are weight percentages. Average composition refers to the average of individual oxide and sulfur values for the 29 samples collected from the mine. Revised composition pertains to the same samples but anomalous concentrations of CaO, Na_2O, K_2O and S have been discarded in the manner stated in the appendix. The "number used" subheading refers to the number of analyses included in the derivation of revised individual oxide values and the revised compositional average. Major oxide analyses of all 29 samples are tabulated in Table A-1.

increasing SiO_2 sample concentrations. The Northrim basalts are also highly ferroan but sample ΣFeO concentrations decrease rapidly with increasing SiO_2 concentrations. The Northrim rocks are not particularly rich in MgO but MgO concentrations may be significantly high in the more mafic samples. Sample concentrations of the three oxides are highly dependant on the relative abundances of the major minerals albite, magnetite, pyrite, biotite, chlorite, and dolomite: samples with extremely low Al_2O_3/SiO_2 ratios are rich in carbonate; samples with extremely low $MgO/\Sigma FeO$ ratios are highly pyritic or highly magnetic pyroclastic breccias; samples with extremely low $\Sigma FeO/Al_2O_3$ ratios are either carbonate-rich (sample 1) or feldspathic (samples 15, 16, 19) rocks.

MnO_2, TiO_2 and P_2O_5 concentrations in Northrim basalts are relatively constant. The former two oxides may decrease slightly and the latter may increase slightly with greater SiO_2 content (Fig. 7). The P_2O_5 trend is expected for calcalkaline and/or tholeiitic differentiation (Pearce and Cann, 1973; Floyd and Winchester, 1975). Mn-bearing minerals include calcite, dolomite, magnetite and tremolite; Ti-bearing minerals include anatase, rutile, ilmenite, sphene and magnetite; the P_2O_5-bearing mineral is apatite. The TiO_2 concentrations of the Northrim basalts are quite low; the P_2O_5 concentrations somewhat high. The TiO_2 concentrations

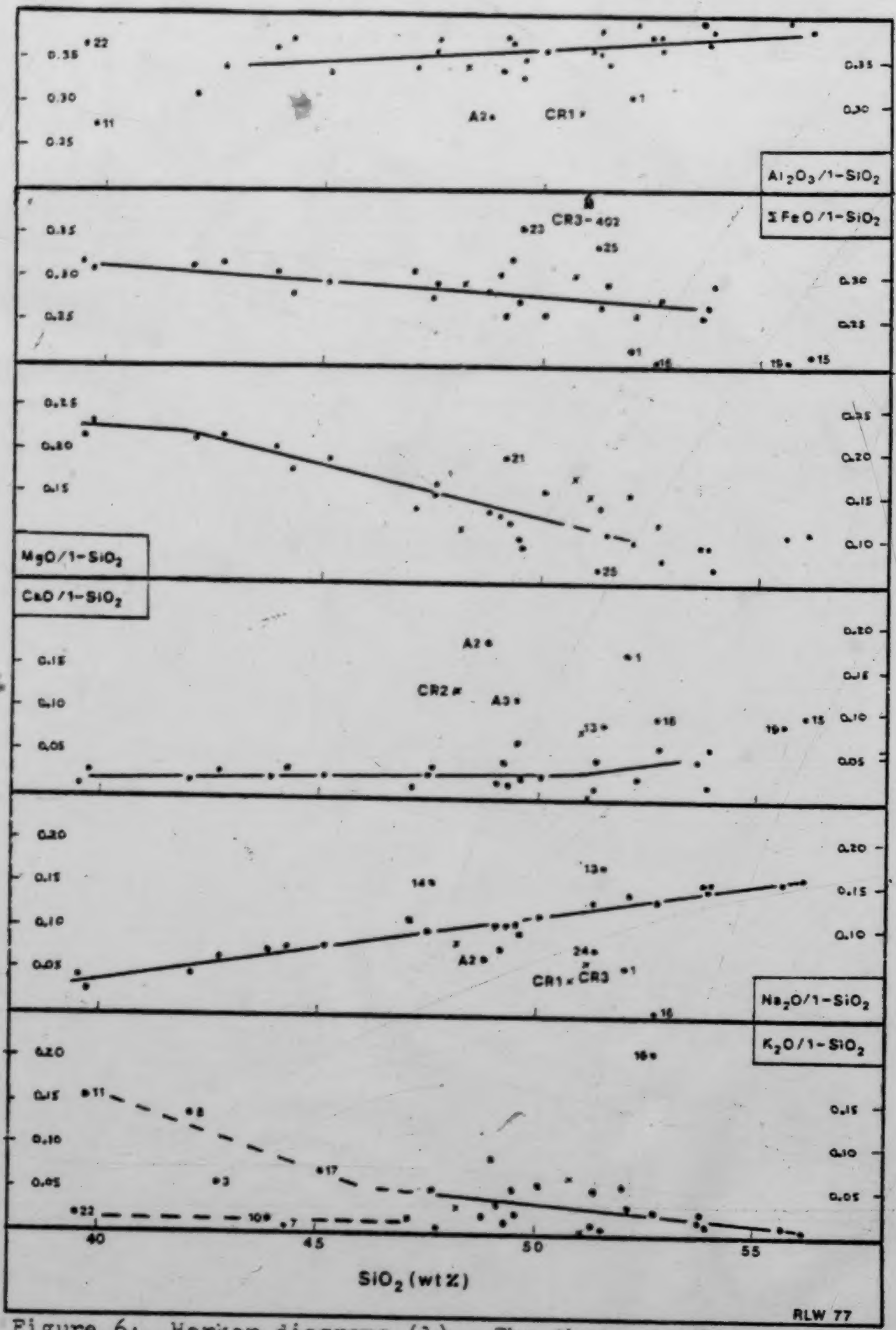

Figure 6: Harker diagrams (1). The three samples marked by crosses and labelled CR-1, CR-2, CR-3 are the basalts analyzed by Badham (1973a). Northrim sample points are marked by dots.

suggest a general primitive condition and the P_2O_5 concentrations a slight alkaline affinity of the parent basaltic magma.

The Northrim rocks contain variable but abnormally low CaO concentrations. Sample CaO values do increase with increasing SiO_2 as expected for the SiO_2 48 wt. % range but CaO values are almost totally dependant on the highly variable secondary carbonate content for the SiO_2 48 wt. % range. All samples contain some carbonate, mostly in small stringers, but samples with higher CaO content also contain carbonate as fillings within vesicles, as replacements of plagioclase and pyroxene phenocrysts, or as fillings between primary breccia fragments. Anomalously low CaO values suggest metamorphic CaO depletion as does the low CaO concentration of the Northrim basalts in general. The apparent breakdown in the general ΣFeO and MgO differentiation trends in the SiO_2 48 wt. % range (Fig. 6) are attributed partly to variability of secondary carbonate content and partly to variability in secondary feldspar abundance between individual samples.

The Northrim basalts are highly sodic and sample Na_2O concentrations increase regularly with increasing SiO_2 concentration. Samples low in Na_2O concentration include two carbonate-rich samples (1, A-2), one pyroclastic breccia (24) and one highly potassic rock (16).

The potassic rock is a brick red feldspathized andesite, a rock almost completely composed of K-feldspar and almost devoid of mafic minerals.

Some Northrim rocks are highly potassic but sample K_2O concentration is extremely variable. Sample K_2O concentrations vary inversely with Na_2O concentrations (Table A-1). The highly potassic rock of the previous paragraph has extraordinarily low Na_2O/K_2O ratios unlike the anomalously high ones found in the adjacent samples (15, 14, 13, 19), also feldspathized rocks. The high but variable K_2O and Na_2O concentrations, coupled with corresponding low but variable ΣFeO concentrations in such rocks indicate that metamorphic and not weathering conditions were responsible for their present chemical and mineral composition.

The sample Al_2O_3, MgO, MnO, TiO_2 and ΣFeO (in part) concentrations are thought to represent the concentrations of the primary Northrim basalts despite their dependance on secondary mineral abundances. Firstly, sample concentrations of these oxides form magmatic trends on the Harker diagrams. Secondly, sample concentrations are remarkably similar to the ones found in fresh, subalkaline basalts. Primary minerals and textures may still be discerned. Furthermore, secondary minerals replacing primary minerals both contain the same elements. This is almost invariably

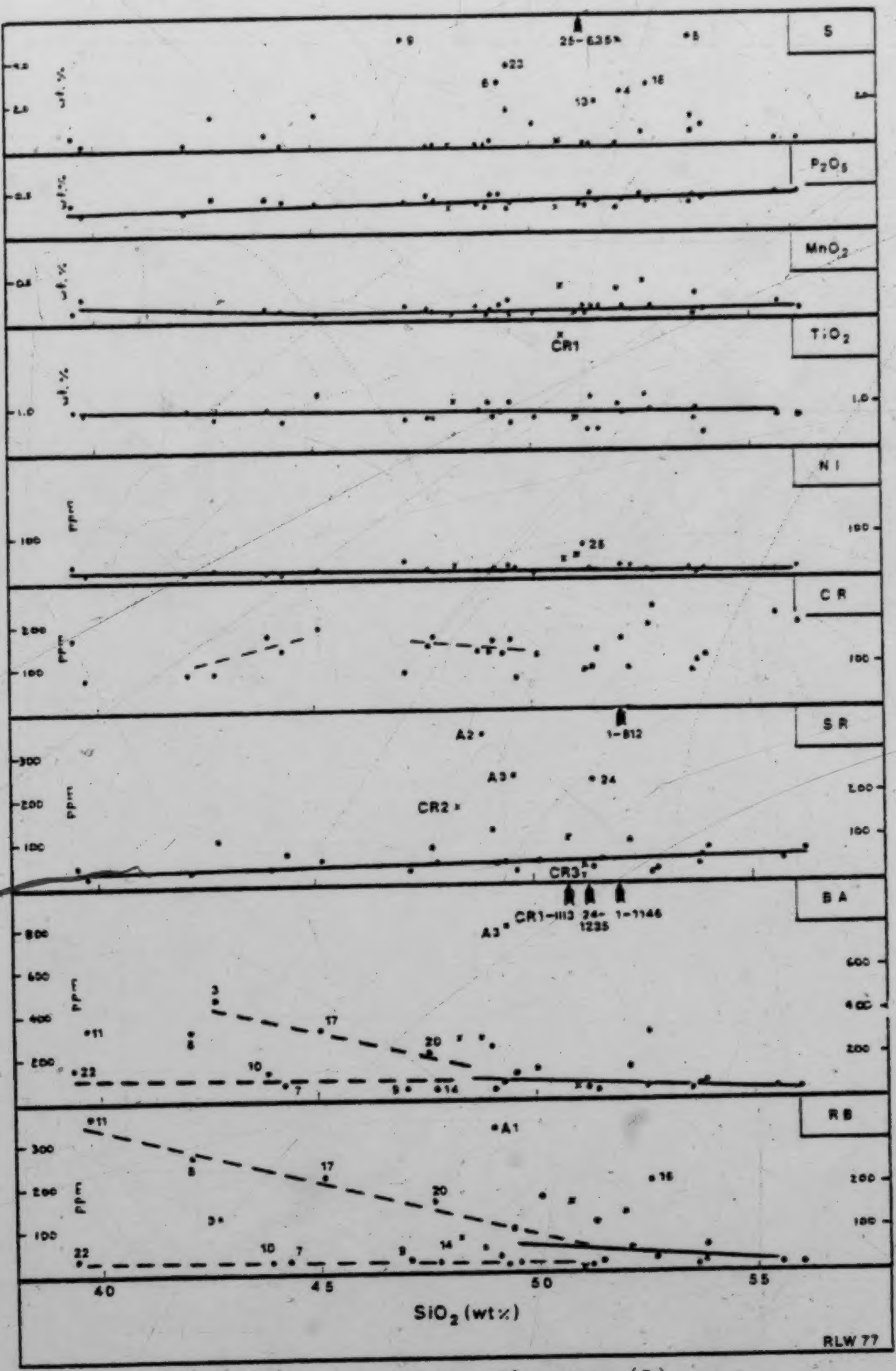

Figure 7: Harker diagrams (2).

true of TiO_2-bearing minerals: ilmenite and rutile are replaced by anatase and sphene; clinopyroxenes and amphiboles are replaced by sphene on site. Similar replacements occur with respect to aluminous, magnesian, manganiferous and ferrous primary minerals, but to a lesser extent. In extremely feldspathized rocks, sample ΣFeO concentrations may be particularly low. Migration of ΣFeO must have occurred in such rocks since relict clinopyroxene outlines may be observed.

The sample K_2O, Na_2O and CaO concentrations are not representative of the primary concentrations of the fresh Northrim basalts. Sample concentrations of these oxides do not form the expected magmatic trends in the Harker diagrams. K_2O/Na_2O ratios do not increase during magmatic differentiation. Na_2O concentrations are much too high, K_2O concentrations much too variable and CaO concentrations are much too low for fresh, unaltered basalts of any kind. The distribution of alkaline-bearing minerals is erratic including the all-pervasive secondary albite. Na_2O concentrations vary systematically with SiO_2 concentrations but this relationship only represents the alteration and eventual replacement of labradorite (higher Ca^{+2}, Al^{+3}) by albite (higher Na^{+}, Si^{+4}). Al^{+3} probably did not migrate since the Northrim basalts are still highly aluminous but the Ca^{+2} must have since the Northrim basalts contain remarkably low concentrations of the element.

(b) Trace Element Distribution

S, usually an accessory element in volcanic rocks, is present in major quantities in some Northrim samples. S values do not correlate with any other major oxide nor trace element values and this is attributed to the often irregular distribution of sulfide minerals in the wall rocks. S concentrations are unusually high in samples 4, 5, 6, 9, 13, 18, 23 and 25 but the locations of these samples are related more to sulfide-bearing horizons than to mineralized veins (Fig. 5). Wall rock S-bearing minerals, in order of decreasing occurrence are pyrite, chalcopyrite, marcasite, sphalerite, galena and pyrrhotite.

Individual Rb sample concentrations and Rb distribution correlate almost perfectly with individual K_2O sample concentrations and K_2O distribution (Fig. 6). This is to be expected for Rb easily substitutes for K in feldspar, biotite and other K-bearing minerals and K/Rb values are known to remain constant up to granulite facies metamorphism (Heier and Billings in Wedephol, 1972). Individual Sr sample concentrations and Sr distribution correlate with individual CaO sample concentrations and

TABLE 3

TRACE ELEMENT CONTENTS OF VOLCANIC HOST ROCKS

Element	Average Composition		Average (Revised) Composition			
	Mean	Standard Deviation	Mean	Standard Deviation	Rejection Level	No. Used
Rb	94	102	28	14	> 60	18
Sr	91	110	52	28	> 90	25
Ba	248	309	83	44	< 200	18
Cr	132	45	132	45	-	29
Ni	18	14	18	14	-	29
Cu	790	1618	41	45	> 175	13
Zn	3286	10919	107	33	> 200	13
Pb	314	692	7	5	> 14	14
Σ Cu, Zn, Pb	2837	8983	273	187	> 400	14
As	76	129	< 5	-	< 5	18
Y	20	5	20	5	-	29
Zr	104	10	104	10	-	29
Nb	4	2	4	2	-	29

All entries are parts per million. Average composition refers to the average of individual element values for the 29 samples collected. Revised composition pertains to the same samples but anomalous concentrations have been discarded for reasons given in the appendix. The "number used" subheading refers to the number of analyses included in the derivation of revised trace element averages. Trace element analyses of all 29 samples are tabulated in Table A-2.

CaO distribution but this correlation is not perfect. Individual Ba sample concentrations and Ba distribution generally correlate with K_2O and Rb sample concentrations and distributions but anomonously high Ba values are found in carbonate-rich samples. Ba is thought to be concentrated in microcline and carbonate but perhaps barite is a constituent of some carbonate-rich wall rocks. Anomalously high Sr values also correlate with high carbonate content. Individual Rb, Sr and Ba concentrations are not affected by proximity to mineralized veins.

Ni content is low except in sample 25 which contains abundant sulfide mineralization. Cr content is highly variable in individual samples and Cr distribution is puzzling since the expected Cr decrease with SiO_2 increase does not occur on the Harker diagram (Fig. 7). There is a possibility that Cr migrated upon the breakdown of olivine, clinopyroxene and magnetite during metamorphism. Present Ni distribution may coincide with the distribution of sulfides but the postulated sulfide Ni content may have originated from the dissolution of primary clinopyroxene and olivine.

Cu, Pb, and Zn contents (not plotted) are related to S content and all high values are found in samples from sulfide-bearing horizons, both near and far from mineralized veins. Arsenic values also correlate with

S values but all high As values are found in samples adjacent to mineralized vein structures, regardless of S content in the respective samples.

Zr, Nb and Y concentrations (not plotted) are relatively constant and increase but slightly with greater SiO_2 content. This is to be expected for subalkaline magmatic differentiation. Slight departures of individual sample values from the average are attributed to analytical uncertainties (up to 20%) due to the low concentrations of these elements present.

Trace element concentrations and distributions differ from one another. The alkaline trace elements Rb, Sr and Ba, are distributed in the same irregular manner as two major alkaline elements, K and Ca. Cr distribution is also irregular but in a non-correlative manner with respect to other elements. Zr, Nb and Y concentrations are nearly constant. Ni, Cu, Pb, Zn and As concentrations and distributions coincide with those of S but As distribution is more closely related to proximity of major mineralized vein structures than to S distribution.

Trace element data are consistent with major oxide data for geochemically similar elements and only one problem with interpretation of the data was encountered. TiO_2 and P_2O_5, immobile elements like Zr, Nb and Y under low grade metamorphic conditions

(Pearce and Cann, 1973; Pearce, 1975), were found to vary in concentration in a manner not expected from magmatic differentiation. This variation was greater than variation from analytic uncertainty (±5%). There are two possibilities: either the TiO_2 and P_2O_5 concentration or the SiO_2 concentration which was used as the reference index for magmatic differentiation on the Harker diagrams has changed during metamorphism. The latter interpretation is preferred with respect to TiO_2 since SiO_2 concentration is known to change during weathering and metamorphism of basalts (op. cit., 1973; 1975) and SiO_2 redistribution would also account for some of the irregularities of other element distributions with respect to the magmatic hypothesis presented. The former interpretation is preferred for sample P_2O_5 concentration, since P_2O_5 concentrations have been known to increase during weathering and greenschist metamorphism (R. Houghton, pers. comm). Apatite commonly appears as idiomorphic crystals in the Northrim quartz-carbonate veins and stringers.

The interpretation problem generated by using the SiO_2 concentration as the index of magmatic differentiation could not have been circumvented by using the differentiation index based on the total of combined normative quartz, orthoclase and albite percentages (Table A-3) since normative feldspar abundances depend on the highly variable alkaline element analyses.

(c) Geochemical Exploration

The Northrim host rock major oxide and trace elements were examined as possible host rock indicators to vein mineralization. It was found that host rock concentrations of most elements do not vary with sample proximity to mineralized veins and only the sample concentrations of some elements which appear to vary towards known mineralized veins are plotted with respect to sample-vein distances in Figures 8 and 9.

The alkaline elements were found to be poor host rock indicators. Host rock CaO concentrations are rather low near mineralized veins except for the high concentrations of the carbonate impregnated, potassic rocks associated with the poorly-mineralized 010 vein structure. Low host rock CaO concentrations exist near the well-mineralized 000 and two other vein structures but these concentrations are indistinguishable from those of some wall rocks at greater distances from the veins. K_2O concentrations and K_2O/K_2O+Na_2O ratios are highly variable near some vein structures but they are not useful indicators since their values are similar to those of most wall rocks further away from mineralized veins. The sample alkaline element concentrations and ratios also appear to vary with

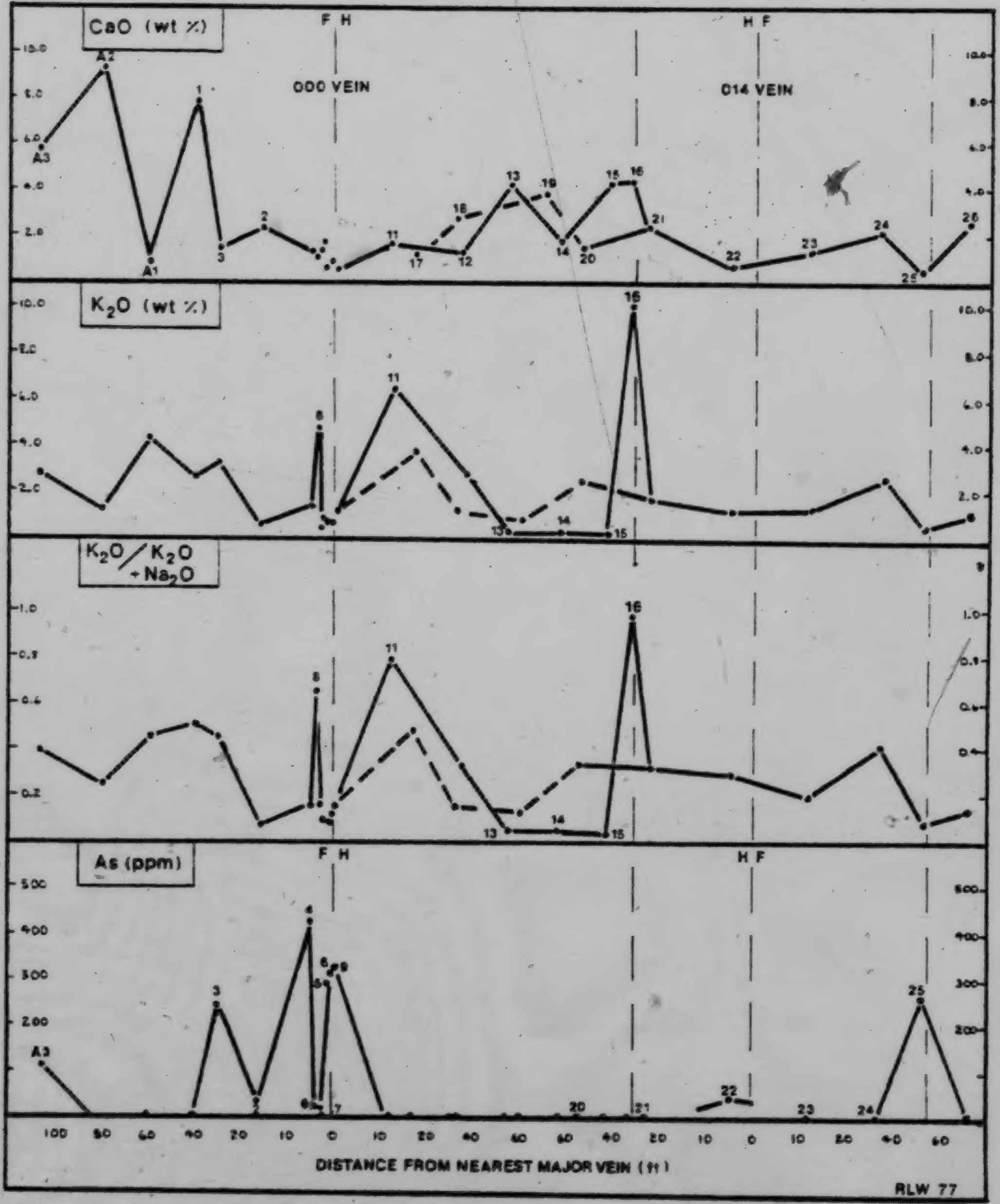

Figure 8: Host rock indicators of vein mineralization (1). The 010 vein structure occurs between the 000 and 014 vein structures and is marked by long dashes. H refers to hanging wall side; F to footwall side of the 000 and 014 vein structure.

rock type and stratigraphical position (sample value couplets 11-17, 12-18, 13-19, 1-A2).

Pb, Zn and Cu concentrations (Fig. 9) are unreliable host rock indicators of vein mineralization. High concentrations do occur in samples next to mineralized veins but these concentrations are extremely variable. The combined Pb, Zn, Cu total indicates the position of the 000 vein structure but for the one sample with high base metal content, there are 6 samples also within 3 metres of the 000 vein with base metal content no higher than those measured in some surrounding rocks. The Pb, Zn, Cu content may be a useful host rock indicator of base metal deposits but a poor indicator of Ag, Bi, Ni, Co, As etc. veins.

As is the only reliable host rock indicator. As concentrations are high near all mineralized veins in the sample area and moreover, the poorly mineralized 010 vein structure does not coincide with high wall rock As concentrations. A threshold concentration of 5 ppm seems to be most useful, but unfortunately reliable vein detection is limited to distances of 3 metres from vein structures. The high As concentration of sample 25 indicates mineralization previously unsuspected in a small carbonate vein and the high As concentration of sample A-3 may be related to mill dust generated by the crusher nearby.

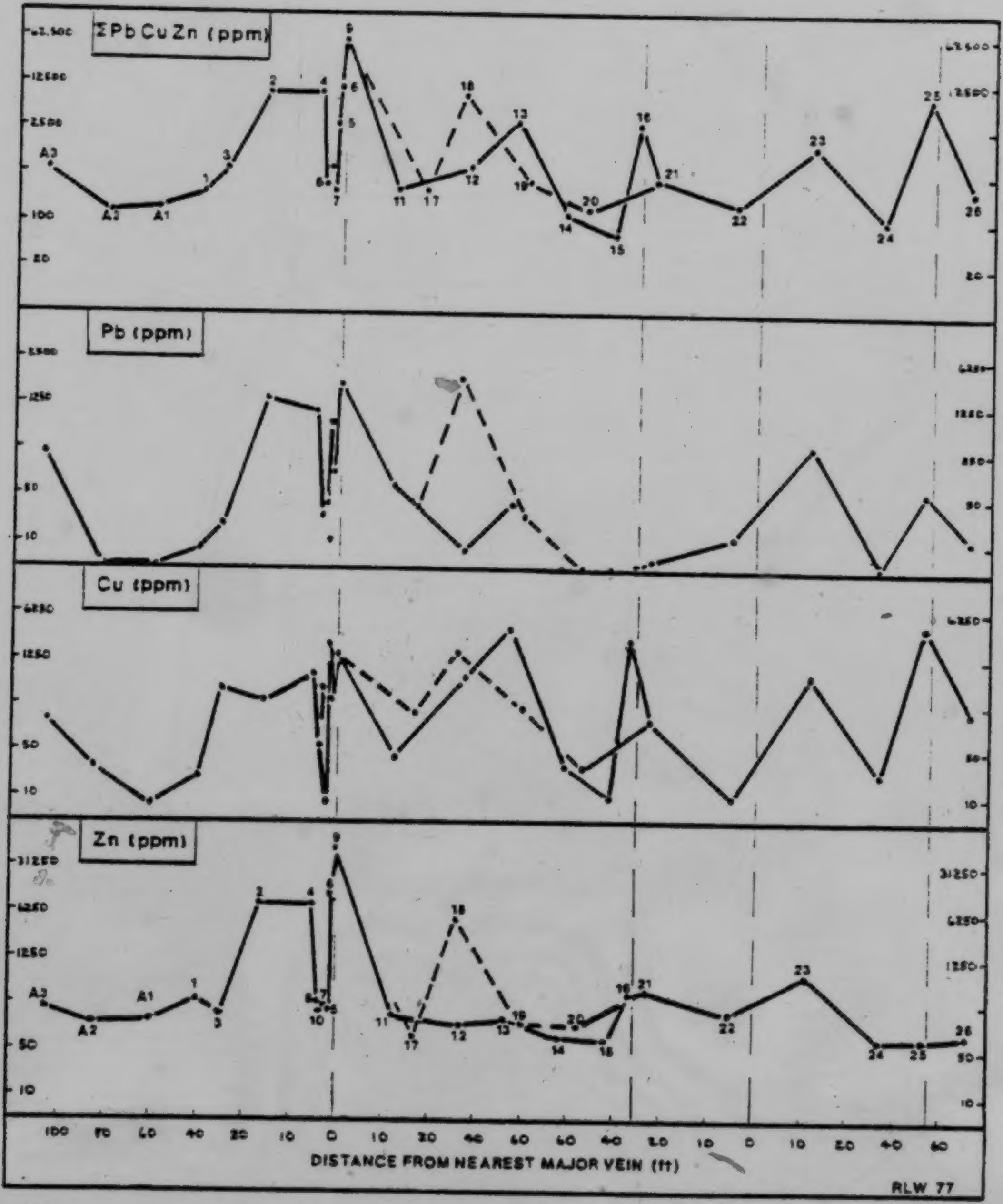

Figure 9: Host rock indicators of vein mineralization (2).

The geochemical results confirm textural evidence relating to mineral emplacement in the wall rocks but are of little use in geochemical prospecting for mineralized veins. The only reliable host rock indicator of vein mineralization, As, is fully dependable only in samples located within 3 metres (10 ft.) of mineralized vein structures. Rock sampling on a 3 metre (10 ft.) interval is prohibitively expensive for reconnaissance exploration purposes but it is practical in predicting undiscovered or extending known ore shoots in existing mines and prospects. The writer suggests soil and water geochemical, not rock geochemical surveys, in areas with little outcrop and the application of more direct prospecting techniques to areas with abundant outcrop.

The variable but generally low K_2O, CaO, Pb, Zn and Cu concentrations in the wall rocks immediately adjacent to mineralized veins suggest that these elements may have been locally extracted from the wall rocks by hydrothermal fluids immediately preceding vein mineralization in the major fracture systems. The feldspathization adjacent to the poorly-mineralized 010 vein structure does not appear to be genetically related to any alteration which may have occurred next to the mineralized vein structures during vein mineralization.

Co and Hg were not analyzed in the geochemical survey. The former is expected to be as useless an indicator as Ni but the latter may be extremely useful in vein detection.

Magmatic Characteristics

(a) Northrim Basalts.

The Northrim basalts are considered comagmatic for several reasons. These include the general similarity of the chemical analyses, mineral norms, mineral modes and petrochemical functions; the existence of magmatic trends for some elements on variation diagrams; and the uninterrupted nature of the basalt sequence sampled. In addition, sample values plot into homogenous groups within the SiO_2-Al_2O_3-(Na_2O+K_2O) ternary and the (Na_2O+K_2O)-FeO-MgO ternary diagram (Fig. 10).

At first glance the basalts may be dismissed as "alkaline" (Fig. 11). However there is doubt that the high Na_2O and K_2O content of Northrim basalts is an original magmatic and not a metamorphic feature. The Northrim basalts appear "alkaline" with respect to total alkali content but if the Opx-Ol-Cpx discriminant of Chayes (1966) is employed, the basalt values plot within and beside the "subalkaline" but not the "alkaline" field. Irvine and Baragar (1971)

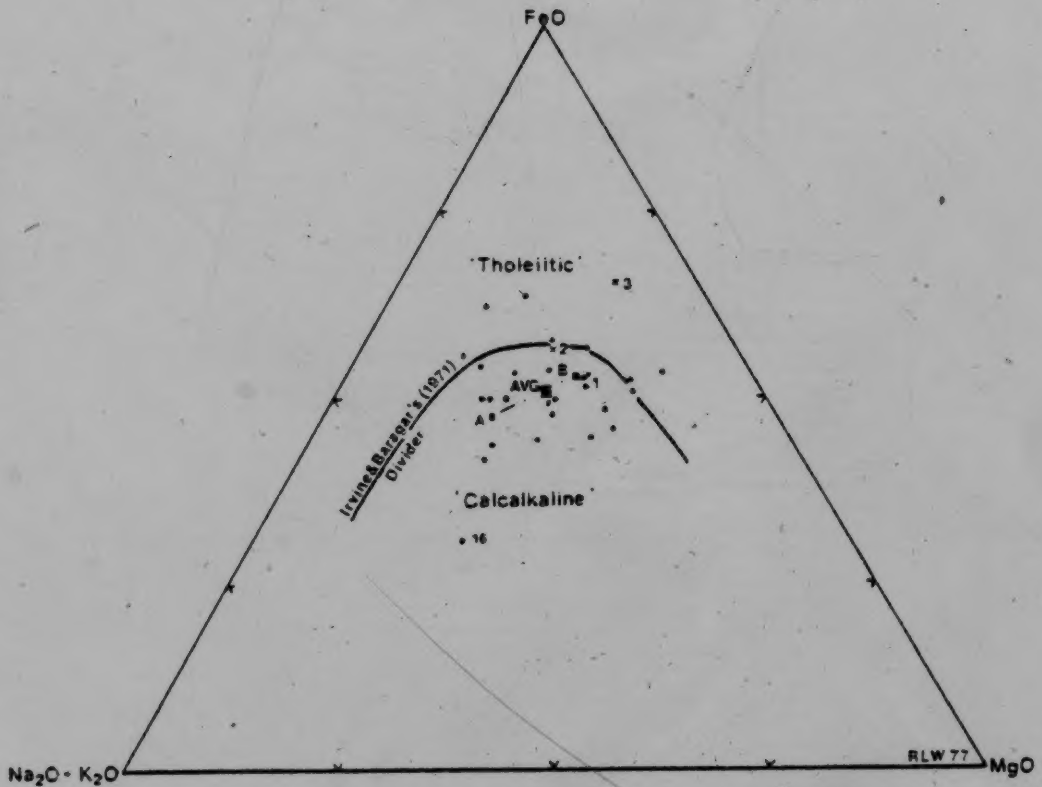

Figure 10: Total alkaline element-FeO-MgO ternary diagram. Northrim sample points are marked by dots; sample points of Camsell River basalts analyzed by Badham (1973a) are marked by crosses. The Northrim general average (avg), basaltic average (B) and andesitic average (A) points have also been plotted on the diagram.

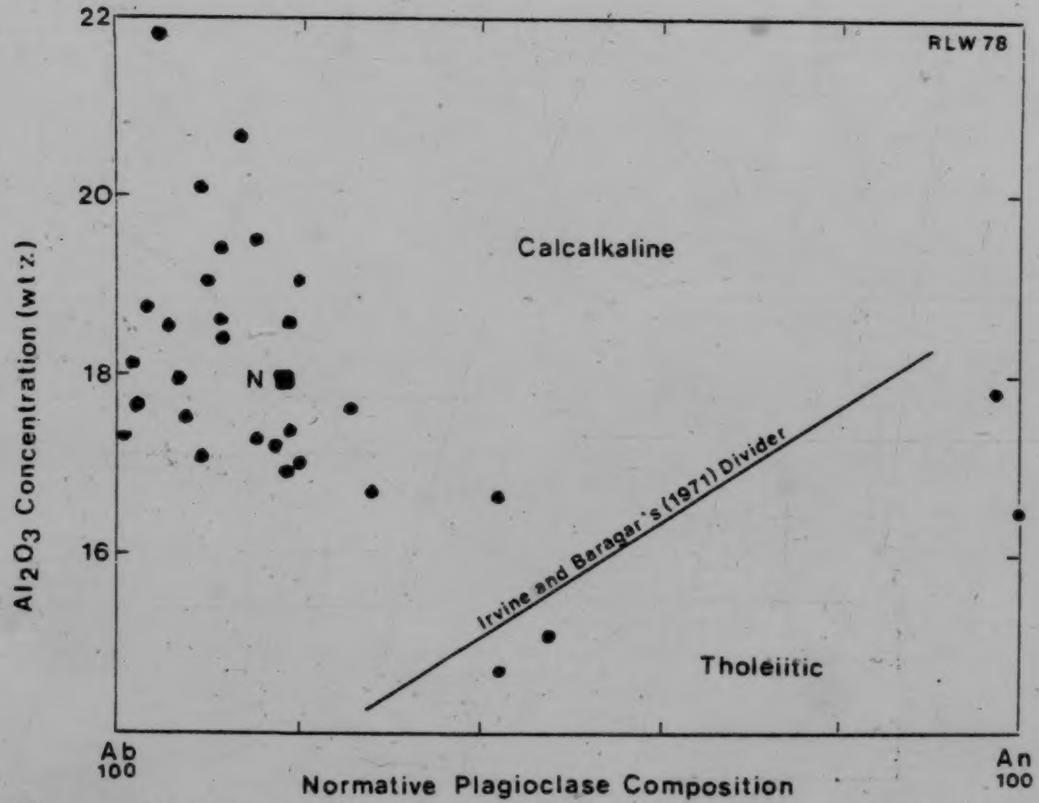

Figure 11: Alumina vs. normative plagioclase plot. The average Northrim sample point has been indicated by a square labelled "N".

mention a similar example: a subalkaline tholeiitic Coppermine basalt sequence is alkaline with respect to total alkali content but subalkaline with respect to normative Opx-Ol-Cpx proportions. It seems that magmatic discriminants based on major oxides, especially alkaline ones, are subject to vagarities but the Opx-Ol-Cpx ternary seems to be most suitable since it does not incorporate Na_2O and K_2O analyses. The subalkaline Northrim rocks may be termed calcalkaline on the basis of their alkaline element concentrations, $MgO/\Sigma FeO$ ratios and the normative plagioclase compositions (Fig. 11, 12).

The major oxides implied to have migrated during the metamorphism of the Northrim basalts are the migratory ones compiled by Pearce (1975):

Seafloor Weathering

very mobile: $+K_2O - CaO - MgO$
mobile: $-Na_2O - SiO_2$
slightly mobile: $+FeO + TiO_2$
immobile: Al_2O_3

Greenschist Metamorphism

very mobile: $-CaO - Al_2O_3$
mobile: $+Na_2O + SiO_2 + (MgO + FeO) - K_2O$
immobile: TiO_2

The writer thus doubts that major oxide data, with the exception of TiO_2 and possibly MnO_2 for unweathered

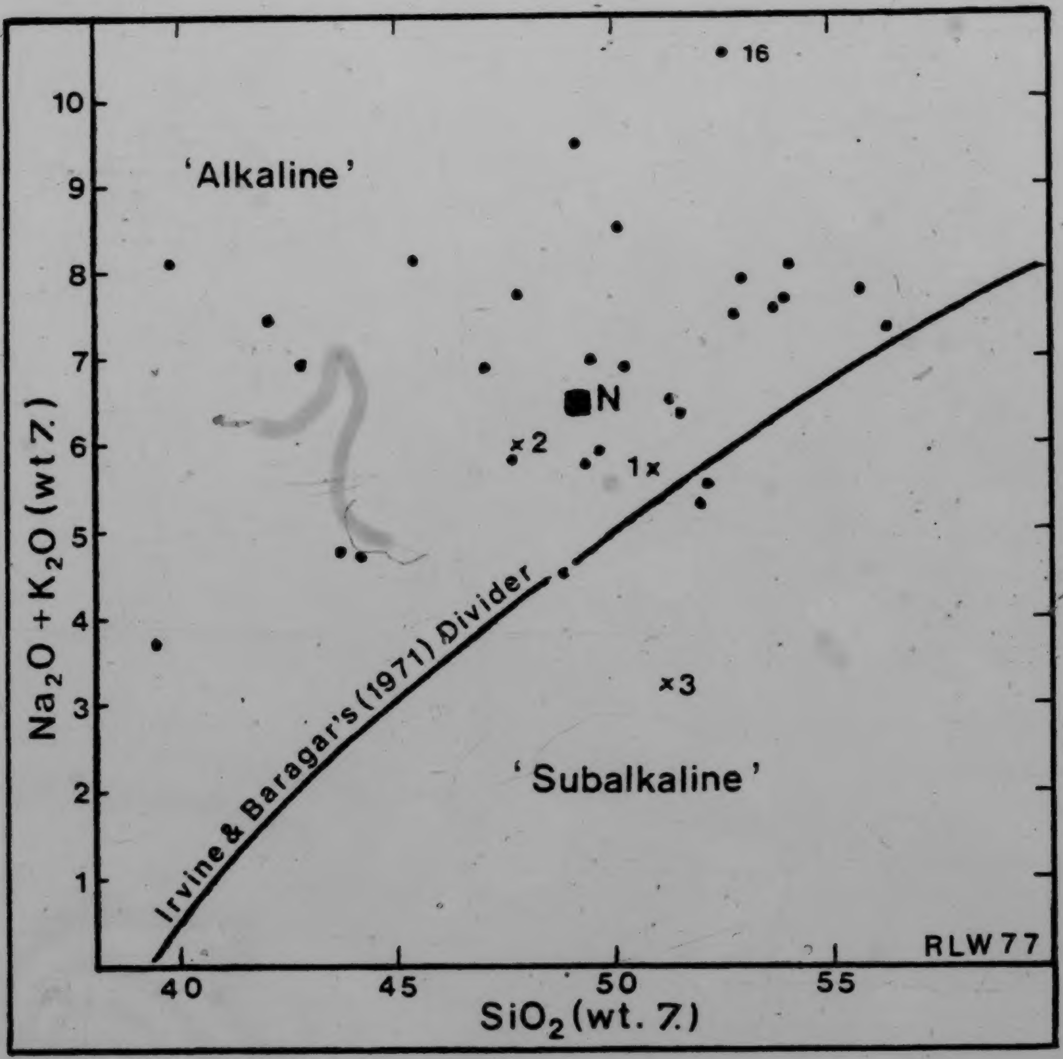

Figure 12: Total alkaline element vs. SiO_2 plot. The Northrim Mine sample points have been represented by dots; the sample points of 3 other Camsell River basalts (Badham, 1973a) have been represented by crosses. The average sample point for Northrim analyses is labelled "N".

basalts, conclusively defines the original magmatic condition of any greenschist facies basalt although it does account for the wide-spread SiO_2 and some other oxide values for Northrim samples. Instead, the writer agrees that the relatively immobile major oxide TiO_2 and the relatively immobile trace elements Y, Zr and Nb are more reliable geochemical indicators of original magmatic conditions and primary rock compositions.

The Northrim rocks have been termed basalts on the basis of SiO_2 concentration, a concentration which may not be that of the primary rocks. The SiO_2 concentration may not have changed very much since the Northrim rocks resemble modern high-alumina (calcalkaline) basalts with respect to TiO_2, Y, Zr and Nb concentrations and ratios. The average Northrim Zr/TiO_2 ratio of 0.012 and Nb/Y ratio of 0.22 are nearly identical to Winchester and Floyd's (1977) ratios of 0.011 and 0.22 for modern high-alumina basalts.

According to Floyd and Winchester (1975) tholeiitic basalts contain less TiO_2, P_2O_5, Y, Zr and Nb than alkaline basalts. They exclude island arc tholeiites and calcalkaline basalts as more complex in their deliberations but for every discrimination parameter they provide but one, a P_2O_5 parameter, the Northrim basalts are discretely tholeiitic (Fig. 13).

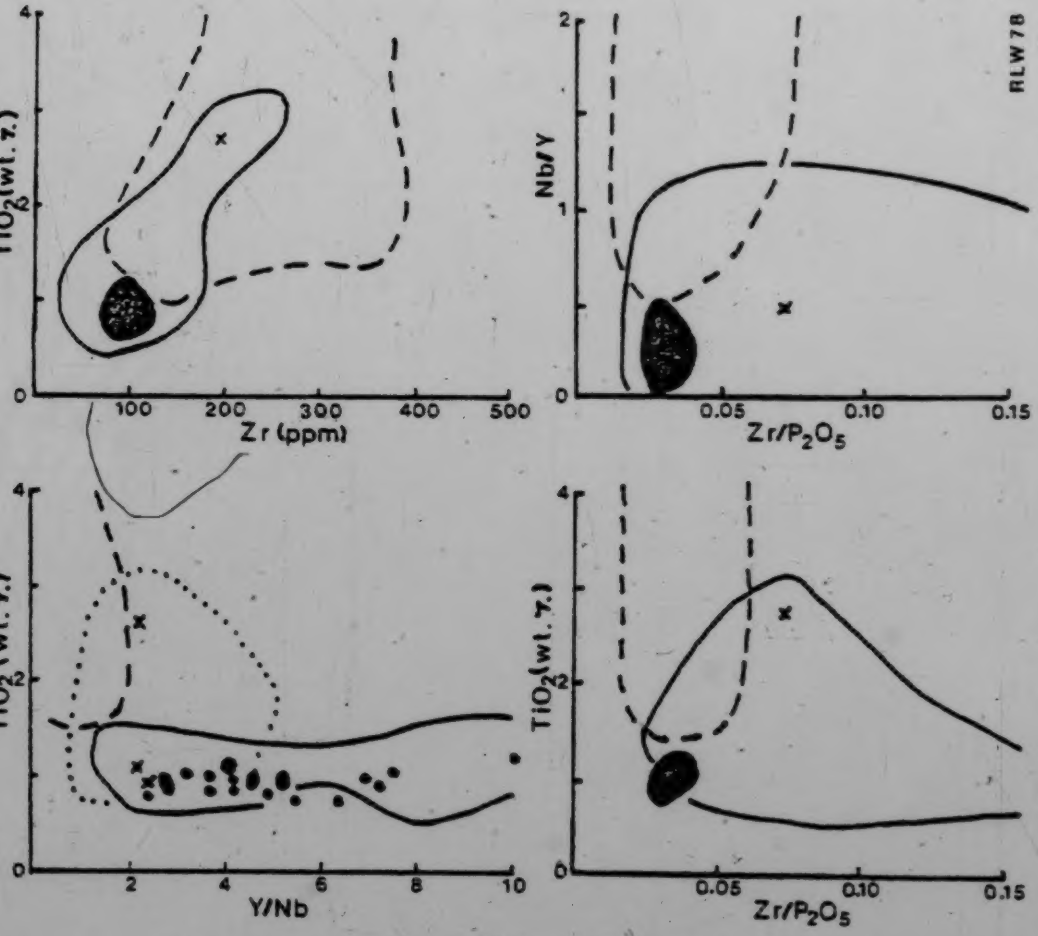

Figure 13: Tholeiitic-alkaline basalt discrimination diagrams (after Pearce and Cann, 1972). The Northrim and/or Camsell River sample points occur in the areas blacked in or as dots and crosses. Solid lines circumscribe sample point fields commonly obtained from modern oceanic and continental 'tholeiitic' basalts; dashed lines circumscribe sample point fields obtained from modern alkaline basalts. The dotted line represents a sample point field of continental and the solid line sample point field of oceanic 'tholeiitic' basalts in the TiO_2-Y/Nb plot. The wayward sample points were obtained from Camsell River 1.

Northrim sample Y/Nb ratios vary between 2 and 10+ at relatively constant TiO_2 concentrations, indicated by Floyd and Winchester (1975) to differentiate oceanic from continental "tholeiites" (subalkaline basalts) but also indicated to be characteristic of calcalkaline basalts (Pearce and Cann, 1973).

Pearce and Cann (1973) differentiate tholeiitic from calcalkaline basalts and subdivide on the basis of tectonic setting. "Within plate" basalts including ocean island and continental varieties contain higher TiO_2 and Zr but less Y than "plate margin" basalts[4]. "Plate margin" basalts include ocean floor i. e. spreading center tholeiitic (higher Ti and Zr), island arc tholeiitic (lower Ti and Zr) and calcalkaline (lower Ti and higher Zr) varieties. The Northrim basalts are plate margin calcalkaline basalts for both discriminatory parameters employed (Fig. 14, 15). Therefore, Northrim basalts could only be termed "subalkaline" on the basis of immobile trace element and major oxide data.

Several features emerge from the discourse above. Firstly, Northrim basalts are alkaline only

---

[4] The difference between the two is presumed to be the same as that between "recycled" and/or "contaminated" (cf. within plate) and "primitive" (cf. plate magmas.

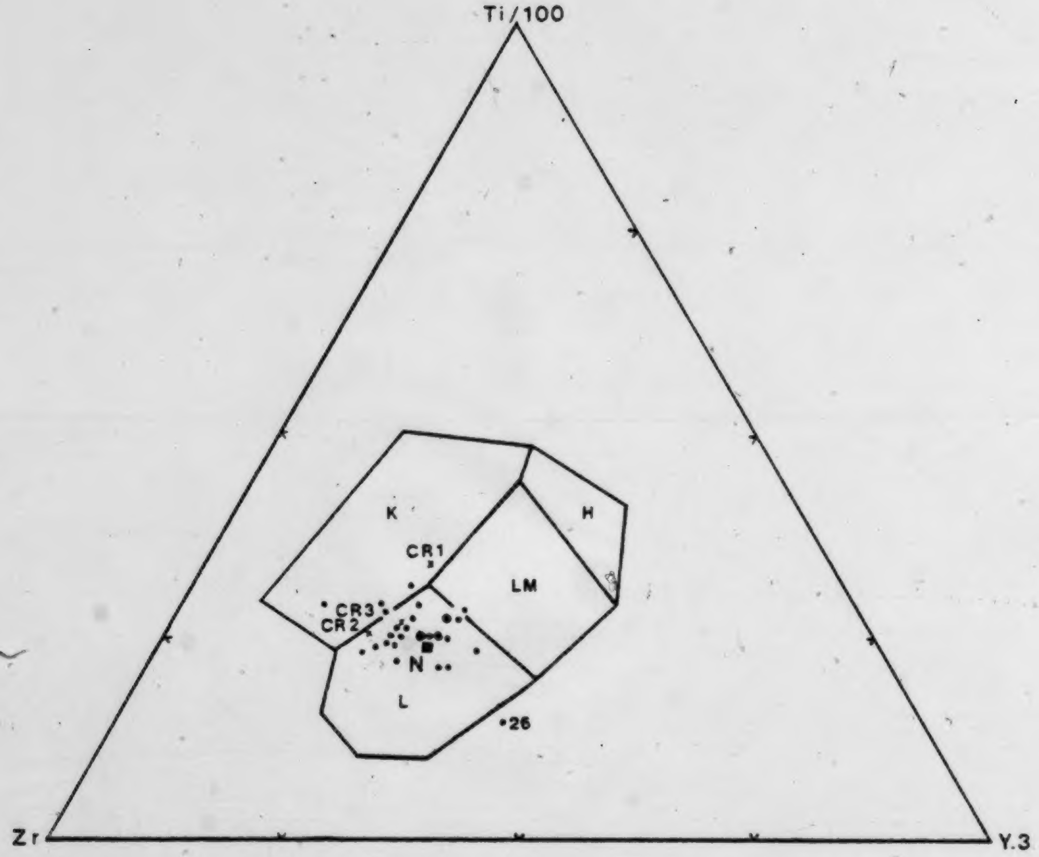

Figure 14: Discrimination diagram for altered basalts (after Pearce and Cann, 1972). "Within plate" basalt values plot in field K; ocean floor basalt values in field H; low K tholeiite values in fields H and LM; and calcalkaline vasalt values plot in fields L and LM. Northrim basalt and 3 Camsell River basalt values are plotted on the diagram. The square labelled "N" marks the average position for Northrim Mine basalts.

with respect to total alkali content--otherwise they are subalkaline. Secondly, TiO_2, Y, Zr and Nb, regarded as immobile components during diagenesis and low grade metamorphism are present in concentrations and proportions uniformly characteristic of calcalkaline basalts. Thirdly, Al_2O_3, MgO, FeO, ($Na_2O + K_2O$) and normative plagioclase concentrations and proportions are more characteristic of calcalkaline basalts than they are of tholeiitic basalts. Furthermore TiO_2, Y, Zr, Nb and P_2O_5 contents change but slightly with magmatic differentiation. The low TiO_2, Y, Zr, and Nb concentrations are features of "primitive" plate margin basalts.

The inevitable conclusion is that the Northrim basalts were primitive, calcalkaline volcanic rocks at time of effusion but have since been altered with respect to the alkaline elements and to a lesser extent, most other elements, all noted to be prone to migration under greenschist metamorphic conditions. The Northrim basalts differ from most other calcalkaline rocks only with respect to high P_2O_5 concentration, a distinction which is irrelevant because of the most probably metamorphic P_2O_5 migration. The geochemical evidence suggests that the Northrim basalts are related to subduction zone magmatism in either an island arc or cordilleran setting. The migration of alkaline

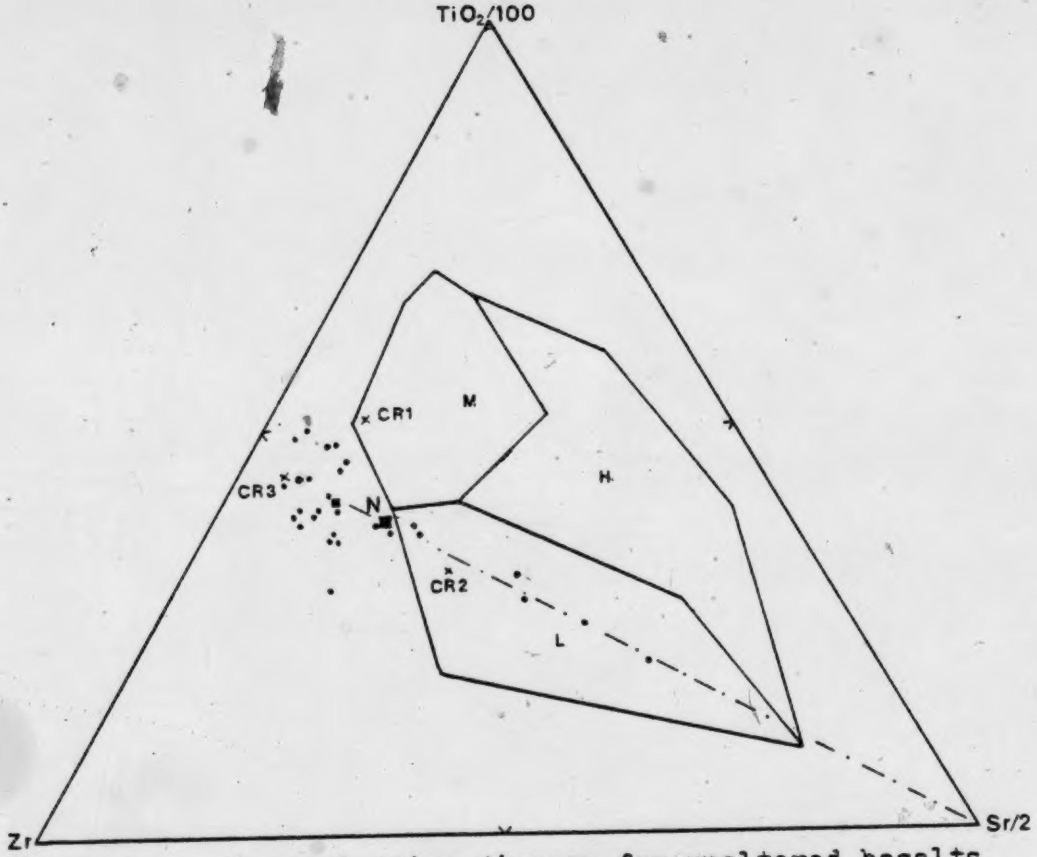

Figure 15: Discrimination diagram for unaltered basalts, (after Pearce and Cann, 1972). Ocean floor values plot in field M; low K tholeiite values in field H; and calc-alkaline basalt values plot in field L. Note the generally low Sr concentrations and the relatively constant TiO_2/Zr ratios in the Northrim samples. Sr redistribution is suggested by the bimodal distribution of Sr concentrations.

elements has created the probably bimodal distribution in sample alkaline element values.

(b) Camsell River Rocks

The three Camsell River basalts described by Badham (1973a) are similar in composition to the Northrim basalts (Table 4). The three basalts were collected within 7 kilometres of the Northrim Mine (Fig. 3). The two samples (2, 3) collected in the Northrim Sequence (Unit 7, Fig. 3) have Al_2O_3, TiO_2, Nb, Y and Zr concentrations similar to those of the Northrim basalts and consequently their values plot with Northrim basalt values in the Harker and other discrimination diagrams (Fig. 6, 7, 10 - 15). The sample collected in the Terra Sequence has a lower Na_2O/K_2O ratio, a lower Al_2O_3 concentration and higher TiO_2, Nb, Y and Zr concentrations than the Northrim Sequence and Mine samples. Consequently their values usually plot separately from the others in the discrimination diagrams. The primary Terra basalt may be considered as a marginally alkaline, non-primitive, ocean floor olivine basalt but the primary Northrim rocks are not alkaline olivine basalts.

Alkaline element concentrations and ratios are also extremely variable for Camsell River andesitic and rhyolitic lavas, tuffs and volcanoclastic sediments

TABLE 4

COMPARISON OF CAMSELL RIVER BASALT COMPOSITION WITH VARIETAL BASALT AVERAGES

	Camsell River 1			Northrim[2]	Spilite[3]	Calcalkaline Basalt[3]	Alkaline Olivine Basalt[3]
	1	2	3	Average (n=29)	Average (n=124)	(n=161)	(n=199)
SiO_2	50.82	48.01	51.19	49.07	48.8	50.16	47.1
Al_2O_3	14.14	17.18	17.23	17.98	15.7	17.61	15.3
FeO	14.62	15.50	19.62	14.19	10.4	9.75	12.6
MgO	7.95	6.13	7.25	7.08	6.1	6.22	7.0
MnO	0.46	0.12	0.15	0.16	0.15	0.17	0.17
TiO_2	2.60	1.03	0.86	0.90	1.3	1.20	2.1
CaO	3.49	5.79	0.42	2.42	7.1	9.99	9.0
Na_2O	2.11	4.33	2.94	4.77	4.4	2.90	3.4
K_2O	3.39	1.61	0.06	2.12	1.0	0.85	1.2
P_2O_5	0.25	0.28	0.28	0.37	0.34	0.21	0.41
S	0.16	0.01	0.00	1.40	-	-	-
Rb	153	85	4	94	-	-	-
Sr	103	177	19	91	-	-	-
Ba	1113	246	34	248	-	-	-
Ni	43	28	53	18	-	-	-
Y	37	16	17	20	-	-	-
Zr	196	124	99	104	-	-	-
Nb	17	8	8	4	-	-	-

Sources: 1. Badham, 1973. 2. This study. 3. Hyndman, 1972. All oxide and S concentrations are expressed as weight percent; all other elements as ppm.

but these concentrations and ratios are less variable in the syenitic and granitic plutons of the area (Badham, 1973a). Na_2O/K_2O ratios in the plutons are generally less than 1 and it appears that the underlying plutonic basement was free of much of the alkaline migration so prevalent in the overlying volcano-sedimentary pile.

The alkaline element migration within the volcano-sedimentary pile almost certainly involved material derived from the pile itself and the Camsell River basalts generally gained Na_2O and SiO_2 but lost CaO, SrO, and Al_2O_3 (?) in the process, at least in the vicinity of the Northrim, Norex and Terra Mines. A similar condition probably exists in the vicinity of the Port Radium Mines.

Metamorphic Conditions

The Northrim basalts are composed of minerals which overgrow primary minerals and textures and which are characteristic of regional greenschist facies metamorphism. The tourmaline, scapolite, andradite, diopside and hornblende found in the metacalcargillites near the Terra Mine (Badham, 1973b) and elsewhere in contact aureoles of the alkaline plutons (Badham and Morton, 1976), are absent at the Northrim Mine. This is to be expected since some of these minerals and idocrase are restricted to granoblastic calcareous tuffs and other rocks within 100 m. of the similar granitic (cf. syenitic--Hoffman et al., 1976) plutons at Echo Bay (Robinson, 1971). Some of the "contact" minerals have been replaced by calcite, actinolite, albite and epidote secondary minerals not only more characteristic of regional metamorphism but also found in rocks further removed from the Great Bear plutons. Contact metamorphism, and especially contact metasomatism has had a limited effect on the development of metamorphic textures and minerals away from the plutons.

The Northrim rocks, situated 2 kilometres south of the Balachey Lake pluton have neither the secondary minerals nor the granoblastic textures associated with contact metamorphism. In this respect they are similar to the majority of other Camsell River rocks subjected to "metasomatism" by Badham (1973a). The Northrim rocks are not considered to be metasomatic since metasomatism produces rocks of uniform and/or gradational composition and texture: the Northrim basalts are heterogenous in both composition and texture. The writer suspects that this condition applies to other rocks of the Great Bear volcano-sedimentary sequence elsewhere in the Camsell River and Port Radium districts.

The porphyritic dykes of the granite-granodiorite suite have also been metamorphosed. Primary minerals and textures have been irregularly replaced by carbonate, quartz, epidote, clinozoisite, biotite, chlorite and sphene, the very same metamorphogenic minerals found in Northrim basalts. If these replacements were contact metasomatic in origin, one would have expected the higher-temperature, volatile-rich assemblages found in the contact aureoles next to major plutons. One would have expected the obliteration of the primary textures so well preserved in these rocks. Similar "retrograde" metamorphogenic minerals replace primary minerals in the syenite-monzonite and granite-granodiorite suites of the Camsell River (Badham, 1973b) and Echo Bay (Robinson, 1972) districts. The distinction between quartz-rich and quartz-poor rocks of the Contact Lake pluton in the Echo Bay district is unclear (J. Casey, pers. comm.) and this writer suggests that some "plutonic" quartz may be of metamorphic origin.

The mineralized veins at Northrim are undoubtedly metamorphogenic features. Mineralized wall rock stringers composed dominantly of dolomite, quartz calcite and albite, terminate in carbonate-rich patches which overgrow primary minerals and textures (Plate V-1). They also terminate in larger vein structures (Plate V-2). Small carbonate-quartz stringers truncate vesicle and breccia carbonate mineralization but in some instances stringer

PLATE V. Wall Rock and Vein Mineralization

V-1. Transmitted light image. Mineralized vein - country rock contact. The dolomite (dt) vein has been truncated by albite and penninite-dominated stringers which also contain quartz, dolomite and calcite. The chloritic and albite wall rocks have been highly metamorphosed but not to any greater intensity than wall rocks further away from this vein. Area: 2.7 x 2.0 mm.

V-2. Transmitted light. Quartz-carbonate vein mineralization truncating and merging with country rock vesicle (?) mineralization. Pyrite (py), actinolite (ac), chloritized biotite (bi), sphene and albite are the abundant metamorphogenic minerals. Area: 2.7 x 2.0 mm.

V-3. Transmitted light: Dolomite (dt) vein - wall rock contact. Quartz, albite and K-feldspar are the minerals which line vein walls. Two wall rock quartz-albite stringers also occur on the image. Area: ~600 x 450µ.

V-4. Transmitted light. Wall rock stringers of dolomite and calcite truncate chlorite-rich stringers and disseminated chlorite mineralization. Chlorite (ch) envelopes a corroded pyrite mass and one carbonate stringer truncates it. The stringers occupy a series of parallel joint fractures. Area: 2.7 x 2.0 mm.

V-5. Transmitted light. Dolomite vein - wall rock contact. The wall rock has been intensely hematized and feldspathized. A opaque oxide (black) coats relict pyroxene (white) phenocrysts. The matrix consists of microcrystalline K-feldspar. Area: 2.7 x 2.0 mm.

V-6. Transmitted light. Dolomite stringers (white) in feldspathized rock. The relict plagioclase and pyroxene crystals (white) have been replaced by a series of undetermined micas, amphiboles and chlorites. The matrix is composed dominantly of an undetermined Na-bearing alkaline feldspar. Hematization has occurred. Area: 2.7 x 2.0 mm.

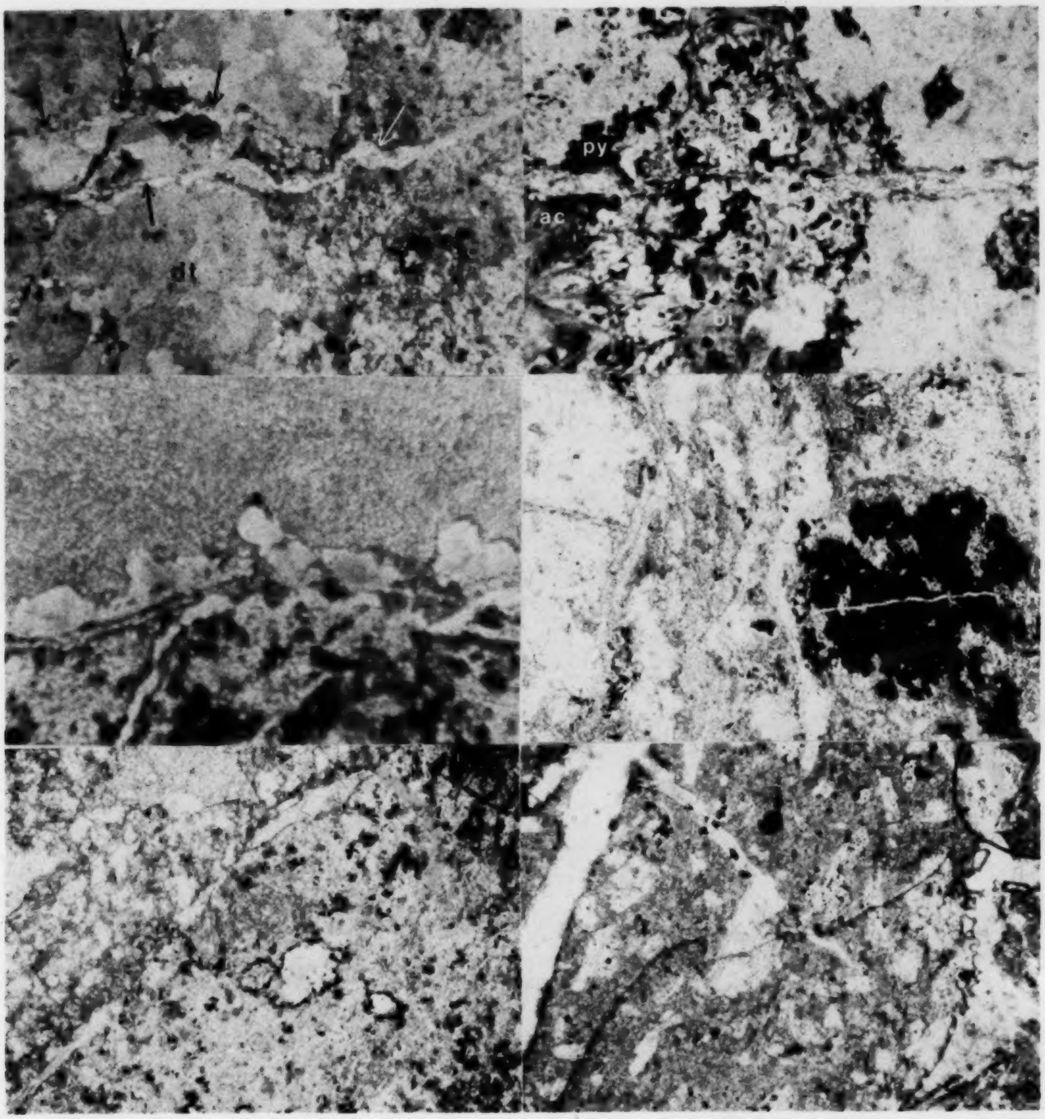

PLATE V

carbonate is visibly indistinguishable from vesicle and breccia carbonate. Wall rock sulfide minerals of varied textures have almost always been truncated by small carbonate-rich stringers but some sulfide-rich stringers truncate some carbonate-rich stringers. Wall rock stringer mineralization occurred synchronously with both wall rock metamorphogenic and major vein mineralization. Carbonate and quartz-dominated mineralization was generally preceded by silicate and sulfide-dominated mineralization in both wall rock stringers (Plate V-3) and in mineralized veins (Plate V-4). Magnetite and epidote are abundant in some stringers.

Regional metamorphism was almost certainly accompanied by subsurface hydrothermal fluids. The subaerial Northrim basalts contain an estimated 1.6 - 5 wt. % H_2O, chiefly in the metamorphic minerals chlorite, biotite, epidote, and various amphiboles. The maximum solubility of H_2O in a basaltic magma at 1100° C. and 1 kilobar is only 2.5 wt. %; magmas extruded at surface pressures would contain even less water (Scarfe, 1973). Hydrothermal fluids would also carry the soluble carbonate necessary for the formation of secondary dolomite and calcite. An estimated 1 - 5 wt. % CO_2 occurs in the Northrim basalts: only a smaller portion of this occurs in mineralized stringers. The hydrothermal brines would have also carried Na and Fe since some secondary amphiboles growing off vesicle walls change from blue to colorless within individual crystals (R. Lambert, pers. comm.). Other vesicle minerals include magnetite, pyrite, pyrrhotite, chalcopyrite, quartz, albite, biotite, chlorite and epidote; the elements found in these minerals were almost certainly contributed by hydrothermal/metamorphic fluids. Hydrous and carbonaceous minerals are concentrated in vesicles and along fractures but are also distributed throughout the wall rocks.

Preliminary primary fluid inclusion studies of vesicle mineralization indicate that the metamorphic fluid was a hot ($T > 320^\circ$ C., $T \sim 350^\circ$ C.), saline (30 - 35 wt. % NaCl equivalent) brine. The carbonate host to these inclusions occur in vesicles far removed (at least 5 m.) from any major mineralized vein structure. Carbonate stringers are rare in these vesicles. An unknown mineral, possibly a zeolite, decrepitated at a temperature of 312° C.--it sent a splash of aqueous vapor across the miscroscopic field of view. The fluid inclusion brine appears to be similar to the one thought responsible for greenschist facies metamorphism and proto-scale ore fluid generation in the Salton Sea geothermal area.

Spilitization, Diagenesis and Metamorphism

Notwithstanding the mineralogical, textural, geochemical and stratigraphical evidence presented above, the calcalkaline Northrim and Camsell River basalts may be considered as spilitic basalts, whatever commonly held definition of the term "spilite" may be preferred, whether mineralogical, textural or geochemical.

The origin of some spilites is controversial but Northrim spilitic assemblages are clearly metamorphogenic. Seawater alteration of basalt would not account for the Northrim spilitic composition and mineral assemblages for several reasons. Firstly, Northrim basalts are non-pillowed and are members, along with Northrim subaerial free-fall pyroclastic breccias, of a volcanic sequence which includes subaerial free fall tuffs, and intercalated fluviatile and lacustrine sediments (Hoffman and McGlynn, 1977). Secondly, seawater-basalt ionic exchange leads to K^+ enrichment in all major alkaline-bearing, basalt minerals (pyroxenes, orthoclases, plagioclases, amphiboles) and Na^+ enrichment in seawater for surficial and diagenetic temperatures and pressures (Dr. J. Gill, pers. comm.). Seawater-basalt exchange of alkaline elements before or during diagenesis thus leads to a composition diametrically opposed to that of the Na-rich and Ca-poor Northrim rocks. Therefore seawater alteration of non-spilitic basalts to form

Northrim spilitic basalts is physically and chemically unlikely, if not impossible, either before or during diagenesis.

The hypothesis that Northrim basalts were originally extruded as hydrous, spilitic rocks may also be rejected. Not one single, hydrous spilitic basalt has been yet observed on the earth's surface during or immediately after extrusion (e.g. Vuagnat in Amstutz, 1974), and the H_2O solubility data of basaltic magmatic mixtures preclude the existence of hydrous, spilitic magmas. Reaction of hydrous vapor within a cooling basalt is precluded by textural evidence: the most vesicular basalts at Northrim are not altered any more intensively than most non-vesicular rocks and vesicle minerals are the same as those in both vesicular and non-vesicular basalt matrices. The absence of regular and rhythmic mineral banding at Northrim also counters protracted mineral readjustment to hydrous vapors during cooling of the basalt. Furthermore, vapors of modern oceanic and continental basaltic magmas are particularly deficient in dissolved solid matter.

The Northrim "spilites" are clearly metamorphogenic.

Summary Statement

Petrological and geochemical evidence are consistent with respect to the calcalkaline affinity of the parent magma, the metamorphogenic composition of the secondary rock and to the contribution of subsurface brine fluids to metamorphism of the Northrim basalts. The geochemical and petrological evidence indicates that secondary Northrim vein and host rock mineralization are both spatially and temporally related with one another; they are almost certainly products of regional metamorphism. Fluid inclusions indicate that metamorphogenic mineralization was accompanied by a hot, saline brine.

The Northrim magmatic, "hydrothermal" and metamorphic conditions appear to be the ones characteristic of the Camsell River and Echo Bay mining camps.

CHAPTER 4

REGIONAL STRUCTURE AND VEIN CONTROL

Structural Features

The Camsell River volcano-sedimentary sequence is broadly folded and fold axes strike 125° but plunge 20° WNW (Fig. 4). NNE-dipping limbs predominate to form a part of the overall homocline of Great Bear volcano-sedimentary rocks against the Wopmay Fault (Hoffman and McGlynn, 1977). Concordant plutonic rocks of the syenite-monzonite suite, such as the monzonite 3 kilometres north of the Northrim Mine, are often exposed in anticlinal zones; volcano-sedimentary roof rocks to the Great Bear Batholith, such as the basalts at the Northrim Mine, are more often exposed in synclinal zones.

Volcanic rocks at the Northrim Mine strike 120° and dip 65° NNE, an orientation similar to that of the regional trend. However, the brick-red porphyritic latite at the north end of the decline (Fig. 3) varies in orientation. Its strike changes from E to N, its dip from N to W all within 200 feet of the strike length. Its position at the north end of the decline may mark the nose of a syncline plunging NW, a syncline parallel with the one interpreted by Badham (1973b). The syncline trend is approximately parallel to the monzonite-andesite contact 3 kilometres north, and hence fold orientation is compatible with origin by folding of the volcano-sedimentary sequence against the concordant Balachey Lake pluton to the north.

Folding is a compressional feature and the major compressional axis must have been aligned NNE by NE-SSW by SW. This orientation is similar to that of NE trending fractures which often form the planar loci of NW side down normal faults, dextral strike-slip faults, some porphyritic granite diorite dykes, some giant quartz veins and a few tholeiitic diabase dykes. The dextral movements which offset fold axes (Fig. 4) and tensional movements which allow dyke and vein emplacement along NE fractures would not have accompanied simple fold compressional stress, however, and the foregoing statement would also apply to tensional and shear motions which created the dilatancies on ENE and ESE fractures, also subsequently filled by dyke and vein mineralization.

N, NE, ENE and ESE trending dilatancies, faults, veins and dykes must postdate the main period of folding since these features are hardly folded themselves. The WNW by NW plunge of fold axes indicates uplift to the SE within the Great Bear Batholith and downdrop to the NW within the Great Bear volcano-sedimentary sequence. This uplift and downdrop may be synchronous with both forceful rise of the granitic plutons of the batholith and corresponding depression of the volcano-sedimentary pile. Hoffman and McGlynn (1977) refer to minor "synvolcanic", NW side down, NE trending dip-slip faults which have been truncated by most plutonic rocks. Displacement across and strike lengths along these faults are less than those of the later but parallel NE dextral strike-slip faults which offset major fold axes. Oblique strike slip is indicated across most major NE faults on the maps of Hoffman et al. (1976).

The writer has measured the orientations of prominent structural fault, dyke and vein features and this information is presented in Figures 16-19. The information was found useful in reconstructing the tectonic regime of the Great Bear Batholith, the regime under which the mineralized veins were emplaced.

Structural Relationships

The tectonic history of the Camsell River district may be deduced not only from fracture, fold and fault orientation but also from the sequence of intrusional events which occupy these fracture, fold and fault systems. Tholeiitic diabase dykes crosscut all other host rock, dyke and vein types and hence are the youngest rocks of the Camsell River and Echo Bay regions. Mineralized quartz-carbonate and giant quartz veins crosscut plutonic basement, volcanic roof and porphyritic dyke rocks (Campbell, 1957; Dollery-Pardy, unpbl.). Porphyritic dykes of the granite-granodiorite suite truncate the volcano-sedimentary sequence including Fe-oxide-apatite±actinolite bodies (Badham, 1973b; Badham and Morton, 1976) and the synvolcanic dioritic and syenitic-monzonitic intrusional suite (Shegelski and Murphy, 1972). Dextral strike-slip faults cross plutonic basement-volcanic roof contacts and displacements of all lithologies except diabase has occurred along them (Mursky, 1972; Shegelski and Murphy, 1972).

Porphyritic dykes, the secondly emplaced dyke rock type in the Camsell River district, strike N, ENE and NNE by NE and dip vertically (Fig. 16). They fill fractures which were most likely the products of the same stress system which folded the volcano-sedimentary rocks: the N and ENE trending dykes occupy the two expected shear fractures and the NNE by NE trending dykes occupy fractures parallel to the maximum fold compression axis of the strain elipsoid which produced the folding[6]. Fracture generation of the latter orientation is not expected from such a stress system but must have been created before and/or during porphyritic

---

[6] The predicted host rock sinistral displacement of the theoretical strain elipsoid occurs along one ENE-trending dyke; the predicted host rock dextral displacement occurs along one N-striking dyke on the map of Shegelski and Murphy (1972).

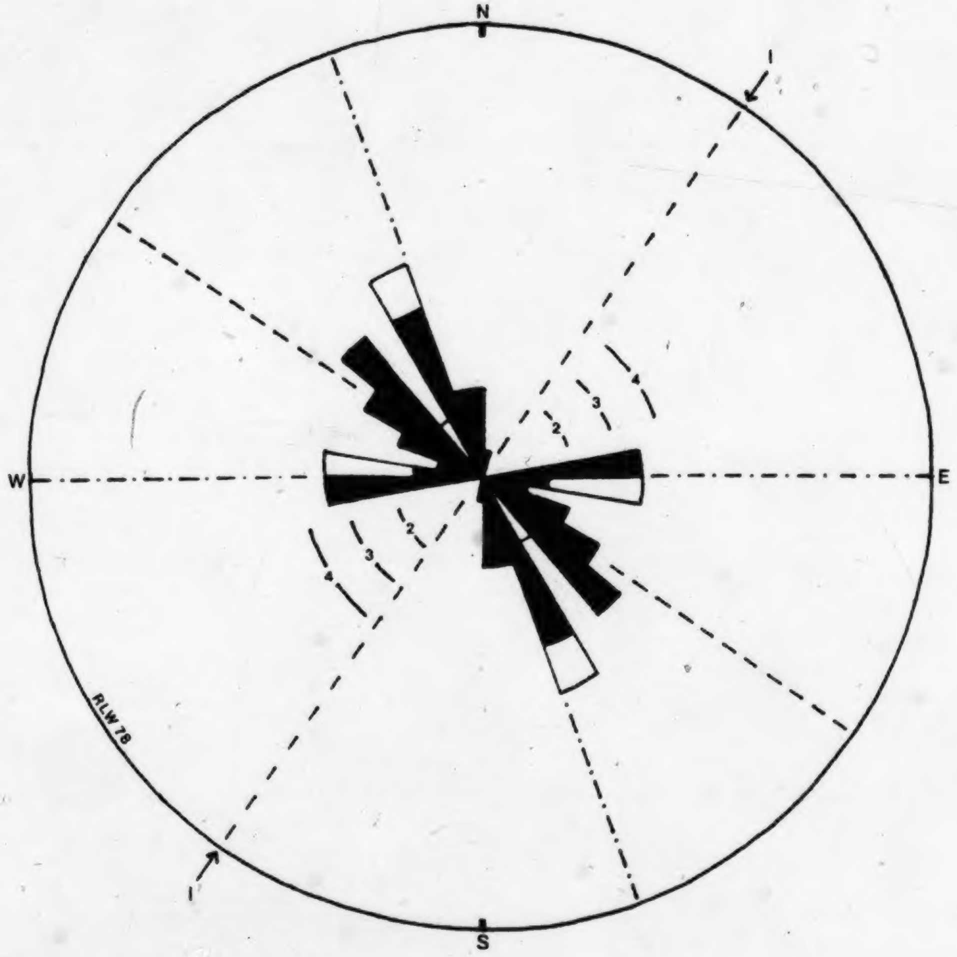

Figure 16: Granitic and dioritic dyke orientation. Compass rosette of stereographic pole strikes. The 23 granitic dyke (black) and 4 dioritic dyke (white) measurements were determined using the map of Shegelski and Murphy (1972). The fold compressional axis (I) and resultant shear plane stereographic axes have also been included on the compass rosette.

dyke emplacement. NE fractures are also the loci of the NW side down faults described above. The Camsell River porphyritic dykes are similar in mineralogy, composition, structure and orientation to the porphyritic granite dykes which preceded synvolcanic granitic intrusions north of Echo Bay (Hoffman and McGlynn, 1977). Previously emplaced, synvolcanic diorite dykes of the Camsell River district have orientations similar to those of the Camsell River porphyry dykes but they may not occupy NE orientations (Fig. 16), the loci of later dip-slip and strike-slip faults. Porphyritic granite dykes were probably emplaced after the onset and dioritic dykes were probably emplaced at the onset of fold compression and dip-slip NE faulting.

NE strike-slip faults and their N to E-striking splays are similar in orientation to those of most porphyritic dykes and almost identical to those of giant quartz veins (Fig. 17, 18, 19). Some NE faults and splays are occupied by giant quartz veins and giant quartz mineralization was contemporaneous with shearing and brecciation induced by dextral strike-slip movement. At least 3 periods of shearing and brecciation, each followed by introduction of more quartz and carbonate have been identified (Kidd, 1932; Furnival, 1935; Badham, 1973b). The abundant, sheared N and ENE fault splays were developed along fractures of orientation parallel

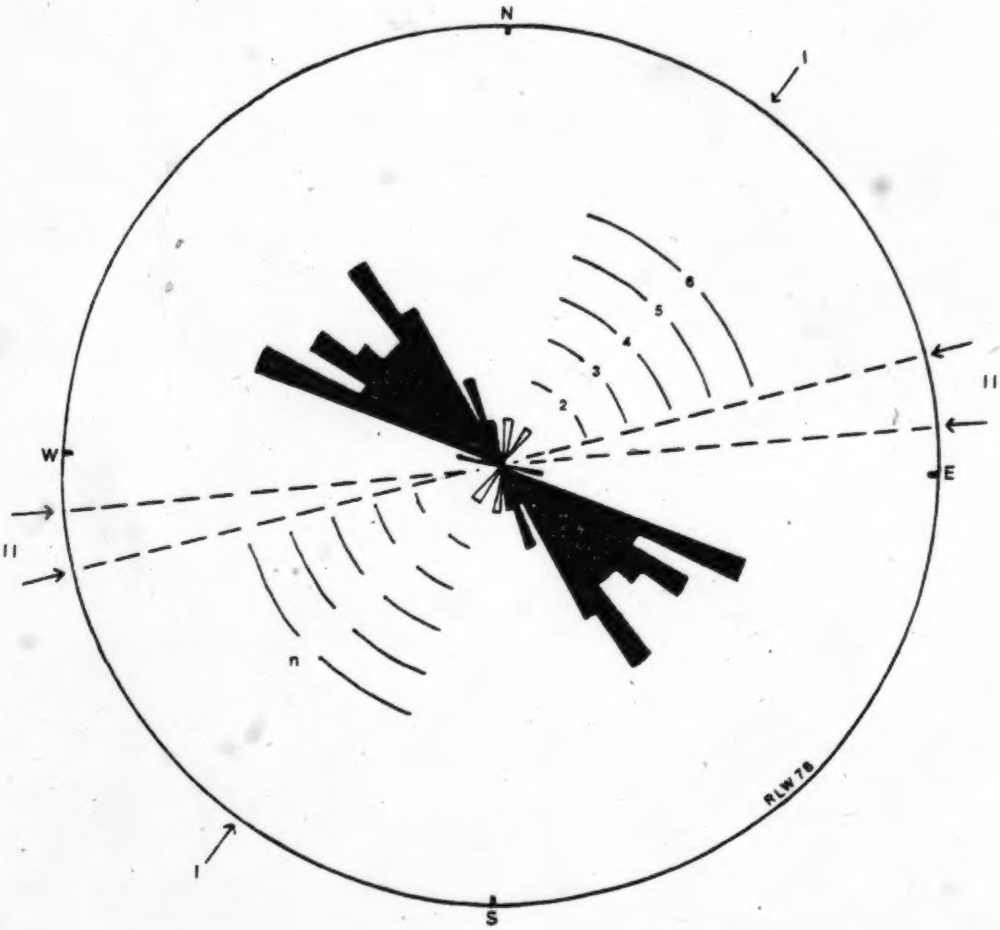

Figure 17: Major strike-slip fault orientation. Compass rosette of stereographic poles. The 40 Camsell River (black) measurements, 28 of them determined on the map of Hoffman et al. (1976) and 12 of them on the Terra Mine map of Badham (1973b), are dextral strike-slip faults; the 2 Echo Bay (white) measurements, determined on the map of Mursky (1972) are sinistral strike-slip faults. A secondary axis of maximum compression (II) is also included on the projection. It may have been produced by interaction between fold compressional axis (I) and the rigid Hepburn block along the N-S Wopmay Fault.

to the previously formed fold compressional shear planes and splay development would have been expedited by the latter's previous existence. Dextral movements offset fold axes for several kilometres along NE faults and splays. The stress system which would account for dextral movement on N, NE and ENE faults would be somewhat different than the one which produced the observed folding and shear fractures. Its maximum compressional stress would not only be oriented to produce dextral movement of the N, NE and ENE faults and splays but also sinistral movement on the two E and ESE splays found in the Echo Bay district on the maps of Mursky (1972) and Hoffman et al. (1976). The axis of maximum compression would be oriented WSW-ENE and would account for all the strike-slip displacements observed along this fault system. This compressional axis orientation would also account for the compensating sinistral strike-slip ESE to SE faults and splays in the Hepburn metamorphic belt east of the Wopmay Fault (Hoffman and McGlynn, 1977).

Mineralized quartz-carbonate stringers and veins, believed to be related to giant quartz veins on the basis of mineralogy, texture and occurrence, also occupy dextral NE faults but they do not occur commonly in N-striking fault splays (Fig. 17, 18). Mineralized veins occupying NE faults and parallel fractures in the Eldorado, Echo Bay, Terra and Contact Lake mines have been repeatedly sheared and brecciated (Campbell, 1957; Robinson, 1971; Badham, 1973b; J. Casey, pers. comm.). The same condition is displayed by the gouged mineralized phases in E to ENE-striking Northrim veins where no major dextral faults have yet been found. The E to ENE veins at Northrim have been more intensely sheared and occupy dilatancies formed from fractures parallel to the expected fold shear plane but the more dilatant, non-gouged Northrim ESE veins do not occupy any fracture plane previously mentioned. The ESE fractures which dip at varying angles both to the north and south may have been first formed upon forceful rise of the synvolcanic Balachey Lake pluton (R. Folinsbee, pers. comm.). A somewhat similar situation exists for the less sheared ESE and more sheared E(NE) fracture systems adjacent to the syenite at Contact Lake (J. Casey, pers. comm.) and reference has been made to gouge-covered, chloritic slip planes in the NE shear zones and the brecciated, highly dilatant E-ESE fracture zones of the Eldorado-Echo Bay vein system near the Glacier Lake pluton (Campbell, 1957). The mineralized veins are post-volcanic, syntectonic features which truncate plutonic-volcano-sedimentary contacts and porphyritic granite dykes and hence the multiple shearing and dilatancy generation during vein mineralization of the Camsell River and Echo Bay districts were not the results of

Figure 18: Mineralized and 'giant quartz' vein orientation. Stereographic projection of poles to mineralized veins and compass rosette inset of 'giant quartz' vein poles. The Camsell River (black) 'giant quartz' measurements, 8 of them determined from the map of Shegelski and Murphy (1972) and 3 from a map of Badham (1973a), and the 6 Echo Bay (white) measurements determined from the map of Mursky (1972) differ in orientation from the contemporaneous (?) mineralized veins. Northrim vein/stringer (small dots), 4 Northrim major structure (big dots), 20 Terra major vein (crosses), 5 Port Radium shear gouge (closed triangle) and 4 Port Radium dilatant fracture (open triangel) measurements indicate the presence of fracture systems different than the ones predicted by compressional axes I and II. A tertiary axis of (III) compression may have been generated during interaction of E-W compression (II) with rigid interfault blocks between strike-slip movements along NE faults. The Terra vein measurements were determined from a map in Badham (1973b) and Port Radium vein measurements from a map in Campbell (1957).

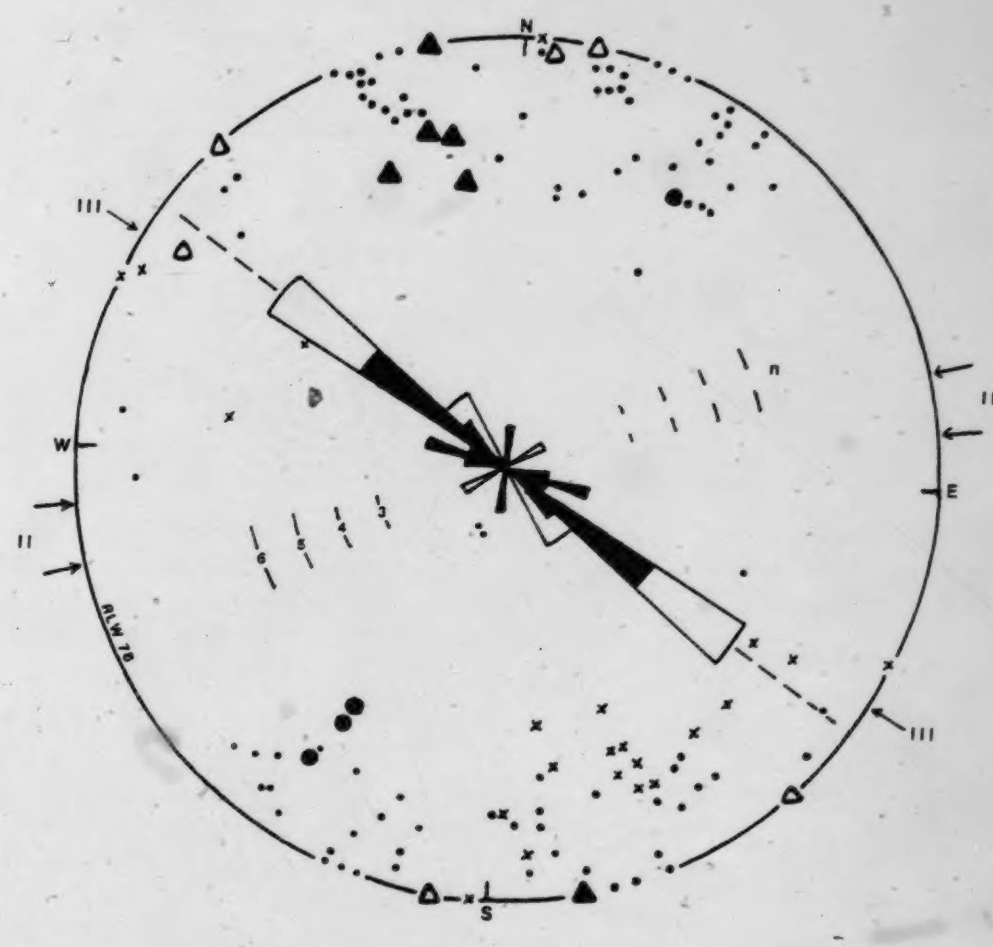
N
III
II
W
E
S
n
3
4
5
6
RLW 78
III
II

a stress system arising from forceful rise of synvolcanic plutons, although such a rise could have first formed some part of the fractures hosting later vein mineralization. The tectonic movements which occurred during vein mineralization may be attributed to secondary ESE-WNW compression and pronounced secondary NNE-SSW tension, perhaps secondary stresses related to the release of ENE-SSW compressional strain built up during inactivity on the major NE fault-splay systems. The pronounced NNE-SSW tensional condition alternated with dextral strike-slip movement on the ENE and NE faults since new phases of mineralization (dilatancy fillers) grow off fault and fracture gouges in the ENE-striking Northrim fracture systems and off the ENE to NE-striking Terra fracture systems. Dilatancies in both the E-ENE and ESE fracture systems at Northrim are filled by the same phases of mineralization. Dilation on the ESE fracture system was quite substantial at Northrim but it is not as pronounced at Terra where major NE and ENE faults and splays predominate (Badham, 1973b; 1975). Shear brecciation does occur along the ESE fracture systems but intensely ground gouge zones do not.

Tholeiitic diabase dykes, the latest epigenetic features, occupy fractures of nearly all orientations but ENE to ESE striking dykes are overwhelmingly predominant (Fig. 19). Displacements of dykes along NE strike-slip faults or displacements of country rocks along ENE-ESE diabase dykes are found neither on the Camsell River maps of Shegelski and Murphy (1973), Badham (1973b) and Hoffman et al. (1976), nor on the Echo Bay map of Mursky (1972). Hence movements on the NE faults preceded diabase emplacement. The orientation maximum of diabase dykes does not coincide with those of the earlier dykes, faults and veins. The greater dyke widths, the lack of shearing and the lack of faulting in the diabase dykes themselves indicate that compressive tectonic stresses similar to the ones responsible for previous dyke and vein emplacement were weak and only tensional conditions could have opened the fractures which were subsequently filled by diabase magma. Similar N-S tension may have also been responsible for the opening of similarily-oriented fractures now occupied by the later phases of mineralized veins but the orientation maximum of the diabase dykes does not coincide with the orientation maxima of mineralized veins (Fig. 18, 19). Some botryoidal arsenide-bearing quartz-carbonate veins occur in diabase south of Contact Lake in the Echo Bay district (Mursky, 1972) and at Gunbarrel Inlet in the Camsell River district (Badham, 1973b; 1975), but the writer cautions the reader that remobilization of quartz-carbonate material (emplacement

7

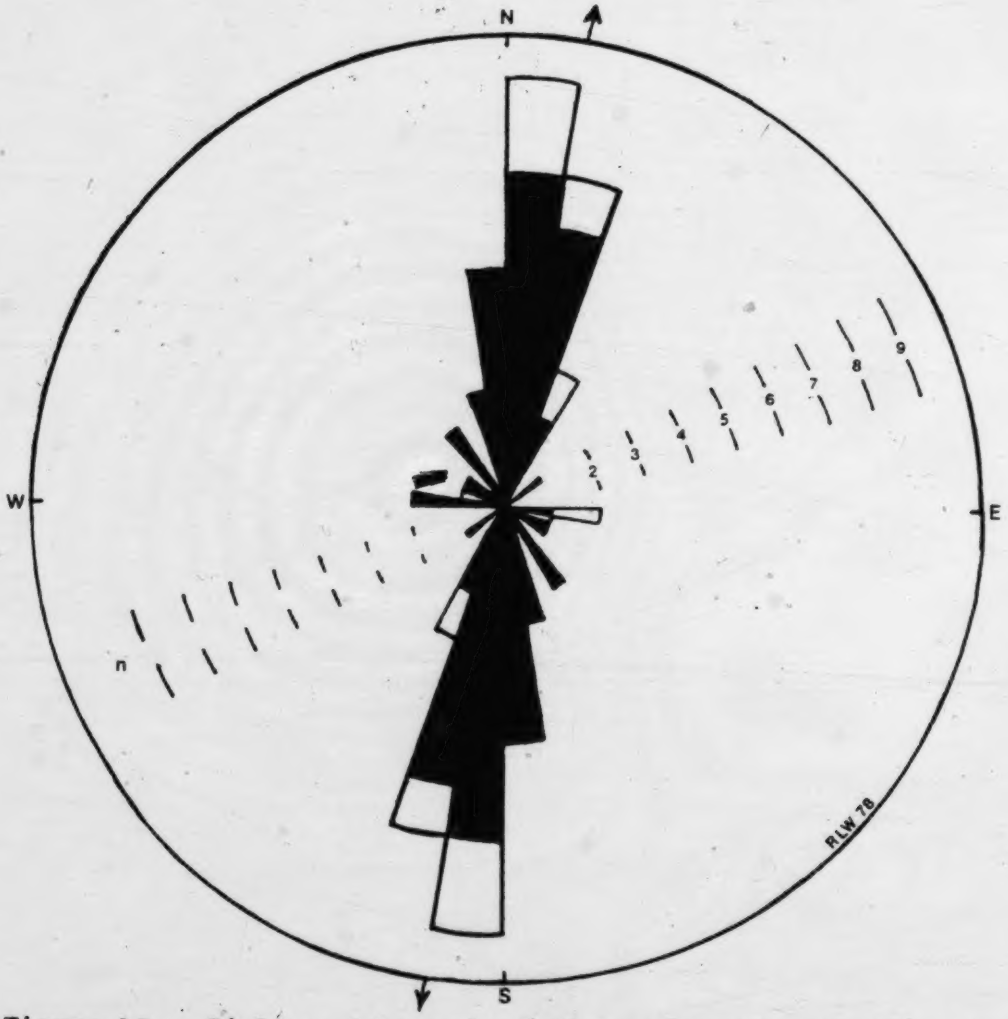

Figure 19: Diabase dyke orientation. Compass rosette of stereographic poles. Camsell River (black) measurements, 27 of them determined from the map of Shegelski and Murphy (197) and 3 of them determined from a map in Badham (1973b), are similar in orientation to the 6 Echo Bay (white) measurements determined from the map of Mursky (1972).

temperature--100 to 350° C.) would be expected upon intrusion of diabase magma (1200-1400° C.) and that precipitation of quartz-carbonate etc. would occur upon cooling of that same magma. This remobilization has been observed in the Cobalt-Gowganda diabases by Jambor (1971b) and in the Blind River diabases by the present writer. Diabase dykes crosscut major vein structures at the Eldorado and Echo Bay Mines near Port Radium (Campbell, 1957; Robinson, 1971) and updating of Pb isotopes in galena from 1625 m.y. to 1450 m.y. has been reported from the Eldorado Mine (Thorpe, 1971; Robinson and Morton, 1972).

The tectonic movements of the Camsell River and Echo Bay belts and the sequence of depositional, intrusional and metamorphic events is given in Figures 20 and 21.

Great Bear Structural Features

The Camsell River and Echo Bay volcano-sedimentary belts have been folded and faulted in the same manner as the overlying belts of the Great Bear Batholith. The ESE by SE fold axial planes, the NW side down NE faults, and the dextral NE fault systems and their dextral ENE and N splays, are present throughout the Great Bear Batholith (Hoffman et al., 1975; 1976; 1977).

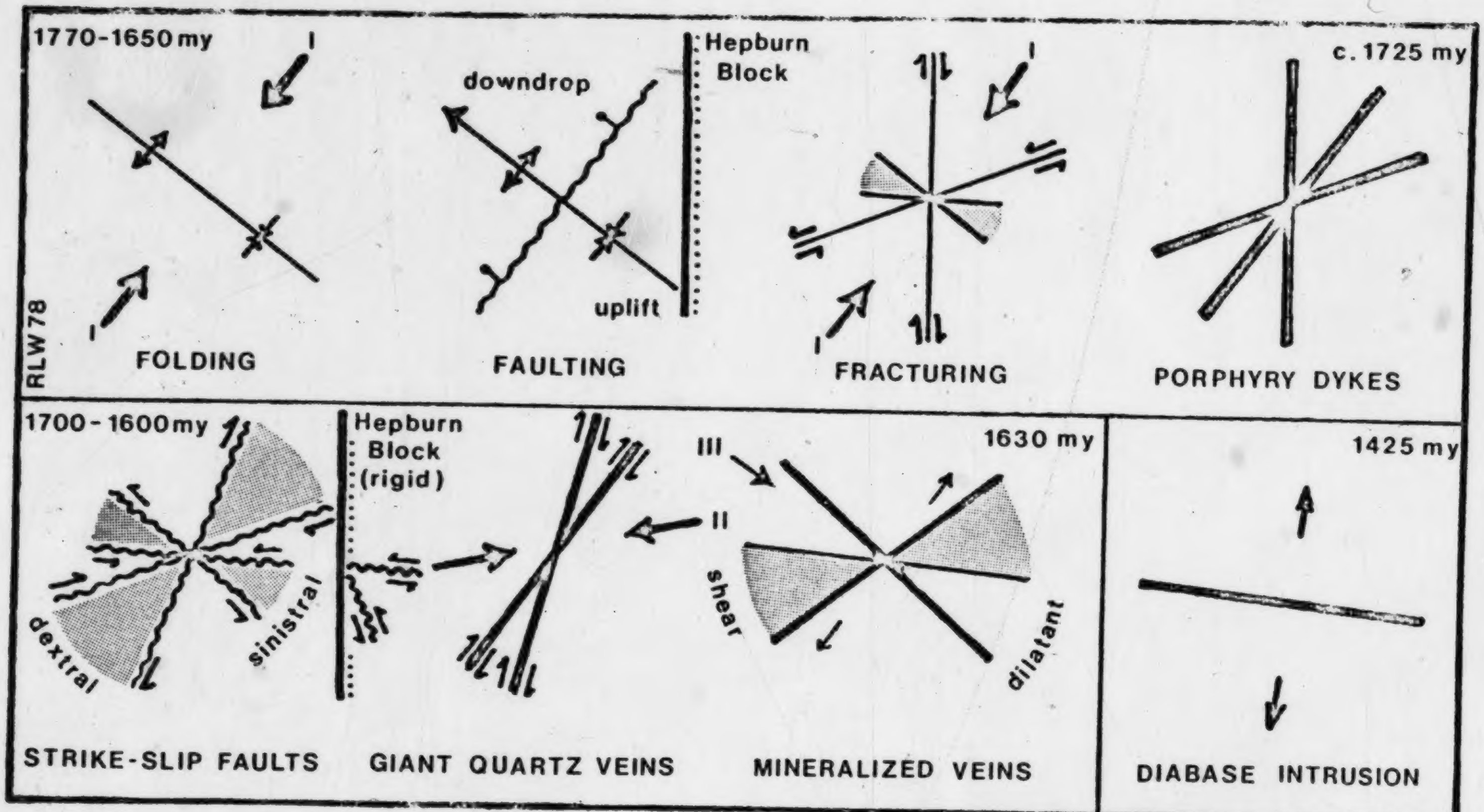

Figure 20: Tectonic elements of the Great Bear Batholith. The tectonic conditions which created the patterns in fold, fracture, fault dyke and vein orientation have been assembled in this diagram. Early-stage orogenic conditions have been illustrated in the top panel, later-stage orogenic conditions have been illustrated in the bottom panel. The dates given have been inferred from radiometric evidence. The generation of the Great Bear volcano-plutonic depression (cf. Hoffman and McGlynn, 1978) is but a simple matter using a migrating plate model and the tectonic elements illustrated above.

Porphyritic granite and tholeiitic diabase dykes exist north of the Echo Bay belt. Hence the same tectonic stresses inferred for the Camsell River and Echo Bay belts above are thought to have determined the present regional structure of the Great Bear Batholith.

Most of the major structural features appear to diminish in intensity towards the Wopmay Fault and the Hepburn Metamorphic Belt to the east. These include the NE dips of the overall homocline, the overall dominance of NE-dipping limbs, the observed dip-slip and strike-slip displacements across NE faults and the overall dominance of NE faults over their ENE and N splays. NE faults also diminish in number and break into splays towards the north and the uppermost members of the north eastern Great Bear volcano-sedimentary pile overstep the Wopmay Fault (Hoffman and McGlynn, 1977). Hence all structural features, and all structurally-controlled dykes and veins, with the exception of the universally distributed diabase dykes, were formed during the accumulation of the upper units of the Great Bear volcano-sedimentary pile, an inference which may also be drawn from evidence presented in the previous section.

The transition from the Camsell River-Echo Bay lavas of the southwest to the overwhelmingly more abundant subaerial tuffs to the northeast may represent a part of the fore-arc to back arc transition within a

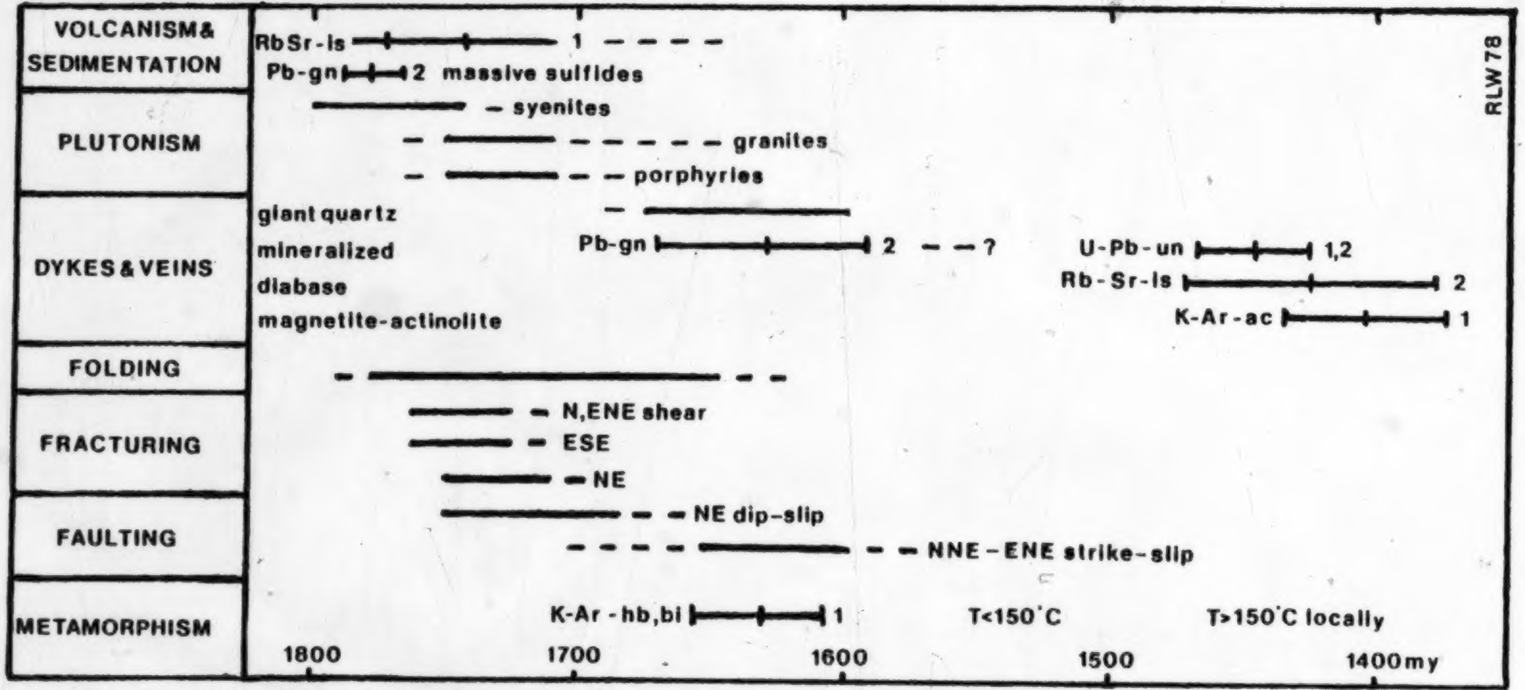

Figure 21: Depositional and tectonic history of the Great Bear Batholith. Radiometric evidence has been borrowed from (1) Robinson (1971); Robinson and Morton (1972); and (2) Thorpe (1974). The metamorphic dates are the K-Ar ones determined on Port Radium volcanic and plutonic rocks and the U-Pb dates are ones determined on Eldorado Mine vein minerals. Note that the mineralized veins were emplaced during regional metamoprhism, and were remobilized locally during diabase intrusion. Abbreviations: is-isochron, gn-galena, un-uraninite, ac-actinolite, hb-hornblende, bi-biotite.

continental margin. This would have been accompanied by a chronological shift of volcanism and perhaps of plutonism, to the northeast (Hoffman et al., 1976). The volcano-plutonic shift, the arc transition, the compressive folding and the calcalkaline Camsell River lavas are highly indicative of subduction-plate tectonic conditions.

Structural Vein Control

Mineralized quartz-carbonate veins and vein structures occupy dilatancies on major NE fault, ENE fracture splays and ESE fracture systems in the Camsell River and Echo Bay districts. These fracture systems may be quite extensive and there are indications that proto-vein fluids were allowed easy passage through some regional fracture systems. Several "giant quartz" veins may be traced for several kilometres along NE faults (Kidd, 1932; Furnival, 1935; Mursky, 1972) and one Camsell River vein has been traced on outcrop for 1 kilometre (Shegelski and Murphy, 1973). A few Northrim mineralized veins have been traced at distances up to 2 kilometres (Dollery-Pardy, unpbl.) and green, laminated, cherty xenoliths, either silicified argillite or banded tuff, both of which have not yet been found in the Northrim Mine, have been found in Northrim veins. They may have been plucked from the argillite and tuff-bearing Terra sequence about 0.5 kilometres below.

Veins at the Northrim Mine and other mines pinch from millimetres and swell to metres in true thickness. This is important for mining widths and quite often mining grades are obtainable only at swells. These swells were dilatancies produced by shearing along curviplanar fracture surfaces, shearing along offset fractures and displacement at fault and/or fracture splay junctions (see Robinson, 1971; Badham, 1973b). However these controls are only local and economic mineralization would have been unlikely without regional-scale access of proto-vein fluids to such dilatanices. Large dilatancies may not have been always required since economic mineralization occurs very often in host rock stringers and hairline fractures. Proto-vein fluid access would be expedited by the numerous fault splays and jointed fractures which vary in orientation, even in individual mines and vein structures (Fig. 18). The access of proto-vein fluids to, and possible fluid derivation from country rocks via fracture systems, are indicated by the presence of quartz-carbonate etc. mineralized fillings even in the smallest of fractures.

Fracturing and dilatancy generation are the obvious vein controls. Mineralized veins occupying fault and fracture systems truncate almost any host rock lithology to be found in the Camsell River and Echo Bay districts. These include volcanic flows and tuffs (Norex, Northrim, Echo Bay, Eldorado, most other occurrences), volcanogenic massive sulfide deposits (Northrim, Terra, Smallwood Lake, Norex, Republic ?), sedimentary rocks (dolomite--Bloom Island; siltstone--south shore of Rainy Lake; mudstone--Terra Mine), syenite plutons (El Bonanza, Contact Lake), granitic plutons (granite-aplite contact near andesite border--Republic property), porphyry granite dykes and upon remobilization diabase dykes (Gunbarrel property; Eldorado and Echo Bay mines in part). The mineralized veins are not restricted to any particular host rock, although they do occur more often in the volcano-sedimentary pile at various distances away from obvious plutons.

Plutons in the Camsell River and Echo Bay districts generally belong to the synvolcanic, syenite-monzonite suite. This suite predates the intruding porphyritic granite dykes which are in turn truncated by mineralized veins. Hence syenitic magma fluids are not those responsible for vein mineralization, although the widespread hematization and feldspathization in their contact aureoles may be attributed to them. The porphyritic granite dykes, the only granitic intrusions present within the Camsell River volcano-sedimentary pile, precede vein mineralization and occupy fracture systems which do not coincide completely with those of mineralized veins (Fig. 16, 18), and they are not spatially related to mineralized veins throughout the Camsell River area. Mineralized fracture systems cross granitic pluton volcanic roof contacts in the Eldorado Mine of the Echo Bay district and in at least one instance, veins occupy a NE fault which offsets the granitic pluton-volcanic roof contact (Campbell, 1957). Thus, granitic intrusions are not likely sources for the proto-vein fluids in both the Camsell River and Echo Bay districts. Diabase dykes truncate the mineralized veins at several locations and they occupy fracture systems which do not coincide with those of the mineralized veins nor any other dyke and vein features. They have not been offset by dextral movement on the syn-veinal NE faults, unlike syenitic and granitic plutons everywhere and hence their magmatic fluids were simply not available at the time of vein formation. Host rock lithology and plutonic magmatism do not appear to be factors in vein fluid formation but they may affect the later fracture and dilatancy generation necessary for vein fluid transportation.

Mineralized veins of the (Ag, Bi, Ni, Co, As) type are restricted to the Camsell River and Echo Bay districts of the Great Bear region. Mineralized veins have not yet been found in the NE faults and ESE fracture systems north of the Echo Bay district and structural conditions will not account for this absence. Granitic plutons and dykes, diabase sheets and dykes, tonalite intrusions and basalts, tuffs and volcano-sedimentary rocks are found in the north (Hoffman et al., 1975; 1976; 1977) but no corresponding reference to (Ag, Bi, Ni, Co, As) veins have been found in the literature. Hence mineralized vein emplacement in the Camsell River and Echo Bay districts must be related to some other regional phenomenum(a) found only throughout the two mining districts. Advanced hydrothermal regional zeolite/greenschist facies metamorphism, coincident upon tectonic fracturing and vein mineralization is the only natural factor restricted to the two districts.

Evidence concerning the spatial and temporal coincidence of hydrothermal greenschist metamorphism, fracture emplacement and vein mineralization, especially at the Northrim Mine, has already been presented. Structural evidence indicates that generation of the hydrothermal brines necessary for vein mineralization was regional in extent.

CHAPTER 5

NORTHRIM MINERALIZED VEINS

Introduction

The mineralized ore shoots of the Northrim Mine occur in multistage, polyphase veins dominated by dolomite, quartz and calcite. The veins occupy several fracture systems and consequently mineralized veins and stringers coalesce and splay to form vein networks; the larger vein networks coalesce to form composite polyphase vein structures. Individual phases of vein mineralization may occupy portions of different vein structures and individual phases of vein mineralization are mineralogically identical to and are spatially continuous with the numerous lightly mineralized dolomite-calcite-quartz stringers of the Northrim wall rocks.

Major composite vein structures of the Northrim Mine include the 000 level, 000 level north, 014 level, 056 level and the 210 level systems. The dominant, widest and most dilatant vein phases of the 000 and 000 north systems, and consequently the 000 and 000 north structures themselves, dip 75-80° N.; the dominant vein phases and structures of the other systems dip 70-85° S. All major vein phases and vein structures strike ESE, except for some parts of the 014 level system which strike ENE. Smaller stringers and veins in the Northrim wall rocks also strike ENE and ESE, they also dip 75-85° N. and S. In general the most dilatant, less brecciated, less sheared phases and structures strike ESE; the less dilatant, more brecciated, most sheared phases and structures strike ENE. Narrow (0.1-10 cm.) ENE-striking gouge zones are particularly abundant in the 014 vein system.

Individual composite vein structures are sinuous and vary from millimetres to metres in true thickness. Component mineralized phases also vary from millimetres to metres in thickness and the wider portions, termed lenses or pods, have been emplaced at fracture and fault junctions, and between parallel offset fractures and faults. Individual mineralized phases, often composed of rhythmically banded carbonates, quartz and other minerals, grow off the vein wall rocks and off one another--they are essentially accretionary structures. Early mineralization fills small, dilatant fractures which have been brecciated by subsequent tectonic movement, and later mineralization envelopes the resultant breccia fragments. Later phases of mineralization generally occupy dilatancies parallel to and next to the dilatancies now occupied by earlier phases of mineralization--the creation of adjacent dilatancies promotes the development of composite polyphase vein structures of conveniently mineable widths.

The wall rocks and vein structures have been repeatedly brecciated and angular fragments (1 mm. - 1 m.) of both wall rock and vein phases occur in the mineralized veins. The wall rocks themselves have been fractured and fragments, termed "xenoliths" in this treatise, are most abundant in mineralized phases and adjacent to vein walls. Wall rock xenoliths are generally larger and more numerous in the earlier phases of mineralization; vein phase xenoliths are generally smaller and more numerous in the later phases of mineralization. Early breccia zones occur in the wall rocks; later breccia zones occur most often within the vein structures. Many wall rock and vein phase xenoliths are coated with rhythmically banded carbonate and quartz--these cockade structures are most common in the lightly sheared, highly dilatant 000 vein ore stope.

Ore and protore are restricted to a few of the larger veins, polyphase vein structures and to some parts of the adjacent wall rocks. Ore and protore most often occur in the wider polyphase vein structures but this relationship is only coincidental. Individual ore minerals and aggregates occur only within specific phases, and often within specific zones, of discontinuous mineralization.

Vein Alteration

Some Northrim veins and stringers are enveloped by feldspathized and hematized alteration zones (Plate V-5, V-6) mineralogically identical to the much more extensively feldspathized lavas described in the previous chapter. Vein alteration zones are only a few centimetres wide and most of them accompany early-stage, lightly mineralized stringers associated with the 010 and 014 vein systems east of the decline. K-feldspar occupies the wall rocks closest to and albite the wall rocks furthest from the veins; hematite dust pervades parts of the potassic and sodic alteration zones. Later, highly-mineralized veins contain hematitic feldspathized wall rock fragments but they are not accompanied by recognizable alteration haloes themselves. They truncate earlier mineralized veins and their attendant alteration zones.

Feldspathized and hematized country rocks also occur at the Eldorado, Echo Bay and Terra Mines (Campbell, 1957; Robinson, 1971; Badham, 1973b, 1975). Robinson (1971) associates these rocks with pitchblende ore shoots but Campbell (1957) does not. At the Northrim Mine, country rocks are neither hematitic nor particularly feldspathic adjacent to any known pitchblende mineralization. The same condition is true of a pitchblende-mineralized specimen from a Terra vein shown to the writer. Reduction of U during pitchblende mineralization or subsequent autoxidation[5] will not account for country rock hematization at the Northrim and Terra, and perhaps the Eldorado and Echo Bay mines.

The feldspathized and hematized country rocks are the only major vein-related features at the Northrim Mine. Other alterations: the argillic (biotitic?), silicic, sulfurous and chloritic ones not related to specific phases of vein mineralization at Port Radium (Campbell, 1957), exist at Northrim but they are most often indistinguishable from secondary wall rock mineralization. The vein alterations at Northrim are considered to be metamorphogenic and their apparent concentration along some early vein systems may be attributed to a regional metamorphic condition, whereby deeper-seated, higher-temperature, metamorphic fluids gain access to shallower levels via fracture systems also exploited by the later derivative fluids which gave rise to vein mineralization.

Characteristic vein minerals, for example the various arsenides, are restricted to quartz-carbonate veins and stringers at the Northrim Mine, unlike the corresponding minerals of the Echo Bay Mine, which may occur in the wall rocks immediately adjacent to some veins.

---

[5] Rusty, hematite-dusted dolomite haloes surround some pitchblende spherules at Northrim. The haloes are almost certainly autoxidation reaction products and they are restricted to vein dolomite.

Paragenesis

The sequence of Northrim mineralization, the paragenesis (Fig. 22), has been resolved into 4 stages, each comprised of several phases of mineralization. A phase is considered here to be a distinct assemblage of vein minerals deposited penecontemporaneously. A mineralized phase may include several distinct bands, layers or fracture fillings if the mineral assemblages are identical and if the mineral aggregates are spatially continuous with one another. Criteria useful in constructing the paragenesis included truncation, banding, crustification and brecciation. Truncation of some mineralized phases by other phases of mineralization was the most useful. The criteria were observed both in specimen and on site.

The first stage of mineralization, the U-Ag-As one, consists of carbonate, quartz, uraninite, native silver, sulfide and Ni-rich arsenide assemblages. It is not an abundant one in the upper levels of the Northrim Mine but it does occur as xenoliths in the later mineralization of the Bi-As-S stage. The Bi-As-S stage, an amalgamation of complex assemblages

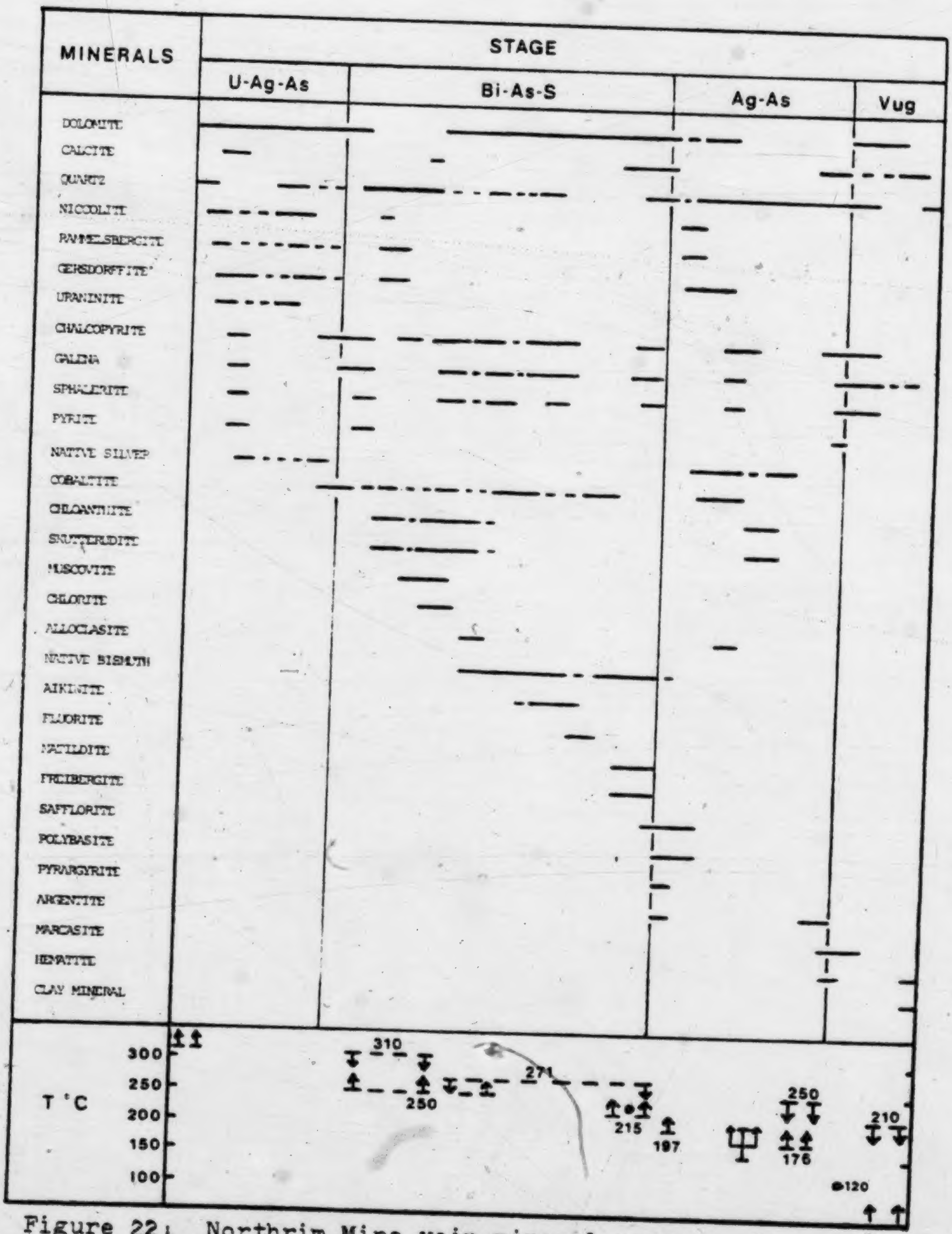

Figure 22: Northrim Mine vein mineral paragenesis. Depositional temperature estimates have also been included. Neptune's trident represents a pressure-uncorrected temperature range indicated by estimated fluid inclusion filling temperatures.

containing sulfarsenide, triarsenide, sulfide, sulfosalt and native bismuth mineralization is well represented at the Northrim Mine: it is the dominant stage of all the vein systems. The following "Ag-As" stage consists of quartz, native silver, triarsenide and acanthite-dominated mineral assemblages. The Ag-As stage assemblages are not abundant and they are succeeded in turn by the carbonate and sulfide-rich "vug" stage assemblages, the latest ones emplaced in the Northrim veins. The maximum intensity of vein brecciation occurred during the early Bi-As-S stage of mineralization but it was preceded by more intensive wall rock brecciation.

Several difficulties were encountered during construction of the paragenesis. Firstly, there are 2 major vein structures. It was impossible to correlate all phases in both structures since many mineralized phases found in one have no counterparts in the other and reference phases were not available for their correlation. This difficulty was circumvented by combining the observations at the intersections of the 000 and 014 structures on the 000 level with inferences based on mineral assemblages of both vein structures. Secondly, some pods of mineralization were sealed off during vein formation and consequently they have a more varied mineral assemblage than their lateral and temporal equivalents. Their assemblages include minerals which may have been formed during later phases of mineralization. This difficulty is not considered crucial with respect to the overall paragenesis since most minerals were deposited in several consecutive phases and some in nearly all the phases of mineralization.

Another difficulty, the position of dendritic structures within the paragenesis, is somewhat perplexing. Dendrites form on pre-existing surfaces but unless they cross banding or some other primary depositional feature, the mineral affording the surface may have been penecontemporaneously deposited with dendrite mineralization. Penecontemporaneous deposition appears to be the rule for arsenide-uraninite dendrites of the U-As stage of mineralization since these dendrites are restricted to individual plugs and bands of carbonate-quartz mineralization. The same condition applies to silver-arsenide dendrites of later U-Ag-As assemblages and to dendritic and inflorescent native bismuth-arsenide intergrowths of the Bi-As-S stage of mineralization. The native bismuth-cobaltite dendrites found with native silver-cobaltite dendrites were probably formed during the Bi-As-S stage of mineralization but the native silver-safflorite dendrites which overgrow carbonate phase contacts adjacent to quartz-rich, silver-arsenide assemblages were probably formed during the later Ag-As stage. The latter dendrites have been included in the Ag-As stage of mineralization on the paragenetic record. A fourth difficulty, incompleteness of the sample and site record, was not considered as important as the third since new information would only demand the insertion of new assemblages into the paragenetic record. It would not demand reorganization of the paragenesis itself.

The paragenetic record for the Northrim Mine is based on observations of the veins down to the 125 level. This record is thought to be nearly complete since samples from the lower levels shown to the writer by Dr. R. Morton are composed of assemblages which fit into the paragenesis presented above. The Northrim paragenesis is remarkably similar to the one of the Great Bear veins by Rojkovic (1973) and to the one of the Terra veins by Badham (1975). The Northrim paragenesis differs from the one of Rojkovic in only two matters: the earliest quartz-hematite phase, common in the Port Radium veins (Robinson, 1971) and the latest Cu-Ag-sulfide phase, a low temperature one (op. cit., 1973) have not yet been identified at Northrim. The Northrim paragenesis of this treatise resembles the Northrim and Norex parageneses by Badham (1973b, 1975) only with respect to the double period of silver-arsenide mineralization. This double period of mineralization may also occur at the Terra Mine.

Mineralogy

The mineralogy of the Northrim veins is complex but over 90% of the vein material occurs as gangue carbonates and quartz. Aluminosilicate gangue minerals include muscovite, chlorite, albite and K-feldspar but these minerals are never abundant and they occur only in pre-Ag-As stages of mineralization. Albite and K-feldspar are never common in vein structures, although they are abundant in the chlorite and carbonate-rich stringers which enter the host rocks. Albite and K-feldspar form layers (< 1 mm.) which accrete directly onto vein walls or onto earlier mineralized phases attached to vein walls. They are accompanied by spherulitic chlorite with Berlin blue interference colors and apatite, minerals which are also found adjacent to carbonate stringers in the host rocks.

The more prominent and economically important minerals are described below.

(a) Carbonates and Quartz

Dolomite, calcite and quartz are the dominant vein minerals at Northrim. Dolomite is the dominant carbonate but calcite is a constant accessory mineral in the early stages of mineralization and the dominant carbonate of the last stage of mineralization. Both dolomite and calcite contain appreciable Mn and Fe. Mn concentrations are higher in the late phases; Fe concentrations are higher in the early stages of vein mineralization. Rhodocrosite and siderite do not occur in the Northrim Mine, although they do occur at the Eldorado Mine (Robinson, 1971).

Early U-Ag-As stage dolomites are finely crystalline, granular in appearance, and yellowish-white in color. They are often rhythmically banded (3-15 mm.) with thin laminations (1-3 mm.) of quartz. This dolomite is the most ferroan of the Northrim dolomites and it is the host of uraninite-arsenide-sulfide±native silver mineralization. These dolomites are most abundant towards the sides of and in the wall rocks adjacent to the 000 vein structure. The ferroan dolomite bands may increase to several centimetres in thickness and in such instances uraninite spherules and colloform masses, botryoidal arsenide aggregates and sulfide grains are abundant. In smaller stringers, individual bands of this mineralization form discrete plug-like bodies. Quartz and calcite grains are intergrown with the dolomite.

Later U-Ag-As stage dolomites resemble the earlier ones but are usually less granular, more crystalline in appearance and are lighter in color. They are also rhythmically banded with quartz, and cockade structures (dia. 2-15 cm.) composed of earlier dolomite and wall-rock breccia fragments, have been enveloped by banded dolomite and quartz. These structures are remarkably abundant in the widely dilatant 000 vein stope on the upper levels. Arsenide-native silver±uraninite dendrites and sulfide grains are found in this dolomite. Early Bi-As-S stage dolomite is identical to that of the late U-Ag-As stage but becomes more granular with increasing calcite and quartz concentration. This dolomite is the host of the later heavy sulfide mineralization, especially abundant as podiform lenses in the upper level 000 vein stope.

Quartz is the dominant mineral of the early phase of Bi-As-S stage mineralization. Rhythmically banded (1-15 mm.) milky and transparent quartz, sometimes alternating with banded diarsenide-triarsenide tubercular growths, form parallel rows of euhedral crystals whose termini jut into tensional dilatancies filled by later mineralization. These comb structures grow off vein walls, elongate wall rock xenoliths, previously emplaced comb structures and shear fracture gouges. Comb structures occupying ENE-striking stringers of the 014 vein system have been repeatedly sheared and brecciated. Shear fracture gouges have been filled by finely-brecciated wall rock and vein mineral fragments and a jet-black triarsenide matrix in the thinner (1-15 mm.), more elongate (up to 10 m.) and more gouged fractures, and by an additional green, micaceous mineral (probably muscovite) in the wider, less elongate, less gouged fractures. Dilatancy generation of a tensional nature was synchronous with pronounced shearing since the bases of comb structures are attached to fracture gouges. Individual gouge zones splay and coalesce; they are only abundant in ENE-striking mineralized phases. The latest bands of the shear-banded sequence are composed of coarsely crystalline dolomite.

Shear-banded quartz mineralization is succeeded by coarsely crystalline, milky, often chalcedonic quartz, then dolomite mineralization: the first quartz-rich phase is associated with native bismuth-skutterudite dendrites and lenses; the second dolomite-rich phase is associated with native bismuth-aikinite-sulfide mineralization. In the 000 vein stope, these phases are wide and have been only mildly brecciated; in the ENE-striking parts of the 014 vein stope and the lower levels of the 000 vein stope, these phases have been sheared in the same manner as the shear-banded quartz phase of the paragraph above. These sheared bands are wider, less elongate and less brecciated than the ones above, and chlorite, instead of muscovite, is the abundant mineral in the fracture gouges. Penecontemporaneously emplaced pegmatitic (to 10 cm.) rhombs of white dolomite with quartz, aikinite-rezbanyite, native bismuth, galena and chalcopyrite occupying interstitial surface and cleavage traces have been observed in the 000 vein system. This pegmatitic phase immediately precedes coarse, crystalline quartz mineralization.

Coarsely crystalline quartz with interstitial silver, arsenide and sulfide mineralization is the last mineral phase of major economic importance yet discovered. It fills dilatancies in fracture systems which occur in the 000 vein structure on the middle levels and in the 014 vein structure on the lower levels (R. Morton, pers. comm.). Coarsely crystalline, barren, zoned quartz crystals--first milky, finally transparent in color, then amethystine and coarsely crystalline white calcite with sulfide and argentite mineralization occupy the same fracture systems. The coarsely crystalline quartz occupies those portions between elongate, individual plug-like pods of silver-arsenide-quartz mineralization and is penecontemporaneous with them. Calcite-argentite-sulfide mineralization follows the milky phase, but precedes the amethystine phase of zoned quartz mineralization. Vugs are common in these fracture systems and vug-filling minerals include quartz, calcite, marcasite, chalcopyrite, galena and hematite. The coarsely crystalline, white dolomite-calcite stringers with scalenohedral calcite, cubo-octahedral galena and a powdery clay mineral are the last vein features to form. They were preceded by highly manganiferous yellow-orange dolomite stringers.

Quantitative electron microprobe analyses were not performed on either the carbonate or quartz but were performed on several samples of the more economically important minerals which follow. The wavelength dispersion method was employed in the quantitative analyses. Qualitative reconnaissance was performed using the energy dispersion method.

(b) Native Elements

Native silver, native bismuth and perhaps native gold are found in the Northrim veins. Native gold has been identified in neither hand nor polished section but one anomalously high assay value (0.78 oz. Au/ton) was determined in one sample from a vein south of the mine workings.

Native silver is never pure, and although it does not contain Cu, Cd, Zn, Pb nor Bi in excess of 0.05 wt. %, the detection limit of the wavelength dispersion method employed; it does contain appreciable Sb (0.3-0.5 wt. %) and Hg (1-14 wt. %). Hg concentration is particularly variable and 13.8 wt. % Hg

PLATE VI. Ag-As Mineralization

VI-1. Backscattered electron image. Ag-As dendrite. Native silver (Ag) is enveloped by an arsenide (as) rim. Polybasite, acanthite and a Ag-Hg amalgam are also present. The gangue minerals are quartz (qz) and dolomite (dt). C3 marks the position of an analytical entry in Table 7.

VI-2. AgLα.100,000 counts. Native silver (Ag) is the major Ag-bearing mineral. Polybasite (pb) and acanthite (ac) also carry the element but in lesser concentrations. ADP (Ammonium dihydrogen phosphate) detector.

VI-3. Sb Lα . 677 second exposure. 30,000 counts. Both native silver and polybasite contain appreciable Sb. The measured concentration in native silver is 0.4 wt. %. Acanthite and the Ag-Hg amalgam do not contain appreciable Sb. EDDT (ethylene diamine dextrotartrate) crystal.

VI-4. HgMα . 15,000 counts. Native silver contains 1.7 wt. % Hg and a thin sliver of a $(Ag_{0.86}\ Hg_{0.14})$ amalgam occupies a small fracture (→) which crosses the less mecuric grain. The concentration of Hg in both minerals has been measured by quantitative wavelength dispersive analysis. Acanthite (ac) and polybasite (pb) do not contain appreciable Hg.EDDT crystal.

VI-5. AsLα . 30,000 counts. Arsenide minerals rim the native silver dendrite. There are at least three arsenide minerals in this assemblage but they are indistinguishable here. TAP (Thallium acid phthalate) crystal.

VI-6. SkαK 30,000 counts. Polybasite acanthite and the arsenide rim but not the innermost arsenide blebs, contain appreciable concentrations of the element. Apparent concentrations in native silver are atomic number effects. ADP crystal.

The white bars of this plate and the ones of succeeding plates represent 50μ sample distance.

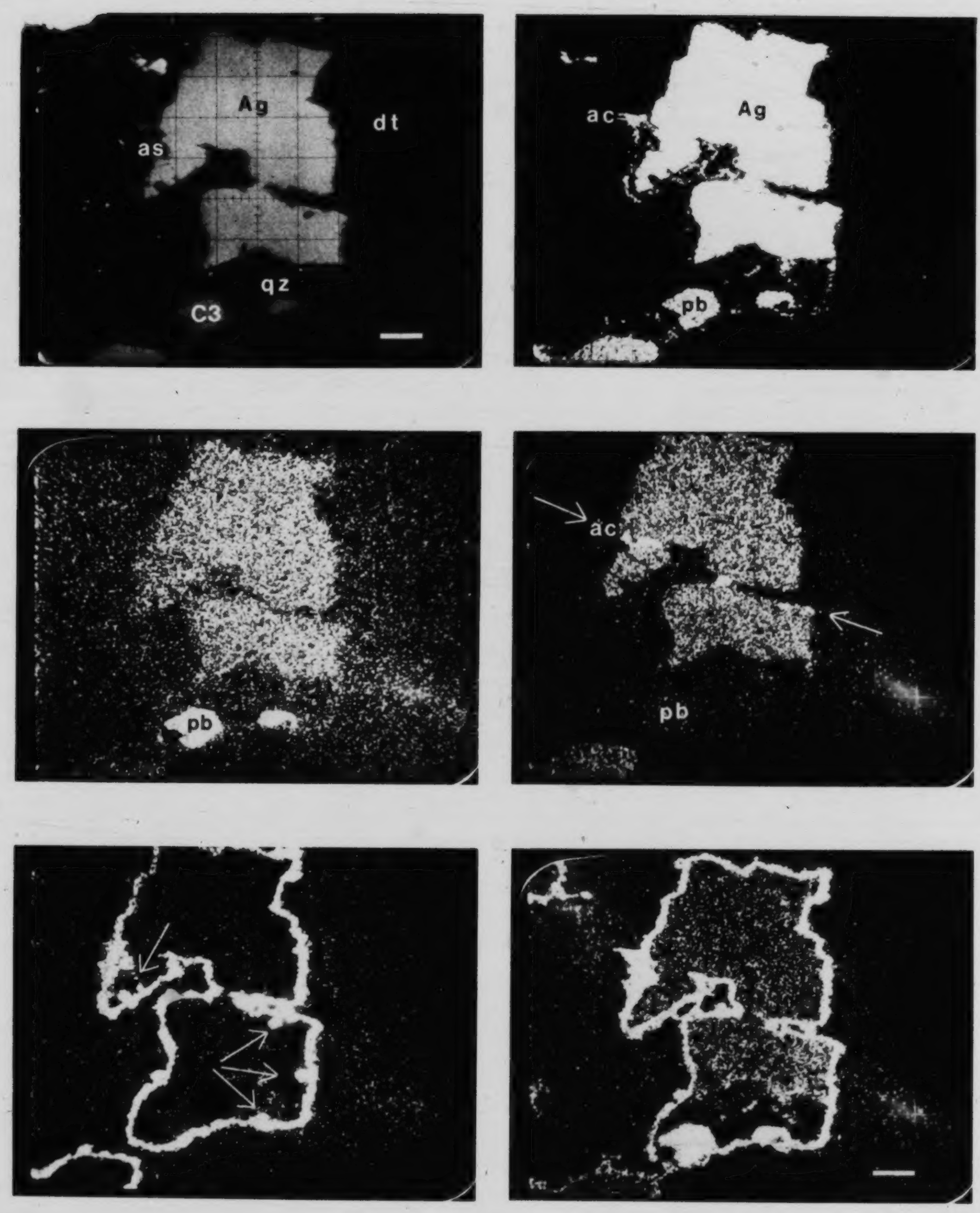

PLATE VI

PLATE VII. Ag-As Mineralization (continued)

VII-1. NiLα image. 15,000 counts. The innermost arsenide blebs are Ni-rich but are Co-poor. They have a composition of 2 wt. % Ni, 2 wt. % Co, 70 wt. % As and 1.6 wt. % S. They are almost certainly rammelsbergites. The safflorite (sf) rim and the outer most arsenide inclusions also contain Ni. LiF (Lithium fluoride) crystal.

VII-2. CoLα image. 40,000 counts. The safflorite rim and outer most arsenide inclusions contain appreciable Co. The outer most inclusions are probably cobaltites. The most prominent cobaltite is marked by an arrow. The apparent concentration of dots within native silver and polybasite is an atomic number effect. Safflorite and cobaltite also contain appreciable Fe but a FeK image was not taken. LiF crystal.

VII-3. Reflected light. Late U-Ag-As stage dendrite. Native silver (white) enveloped by gersdorffite (light gray) in dolomite (dark gray) matrix. Note the rhombic shape of some parts of the native silver dendrite--this may represent pseudomorphic replacement of dolomite. The following images (Plates VI-4, 5, 6; VII-1, 2) were obtained on this dendrite in the area marked "K".

VII-4. AgLα image. 90,000 counts, 319 second exposure. Native silver (Ag) also occurs as small inclusions in gersdorffite (gf). Dolomite (dt) and quartz (qz) are the gangue minerals. ADP crystal.

VII-5. AsLα image. 80,000 counts, 165 seconds. The As is concentrated in gersdorffite (gf).TAP crystal.

VII-6. SKα image. 60,000 counts, 746 seconds. Gersdorffite contains the element. ADP crystal.

The white bars of this plate represent 50 μ sample distance.

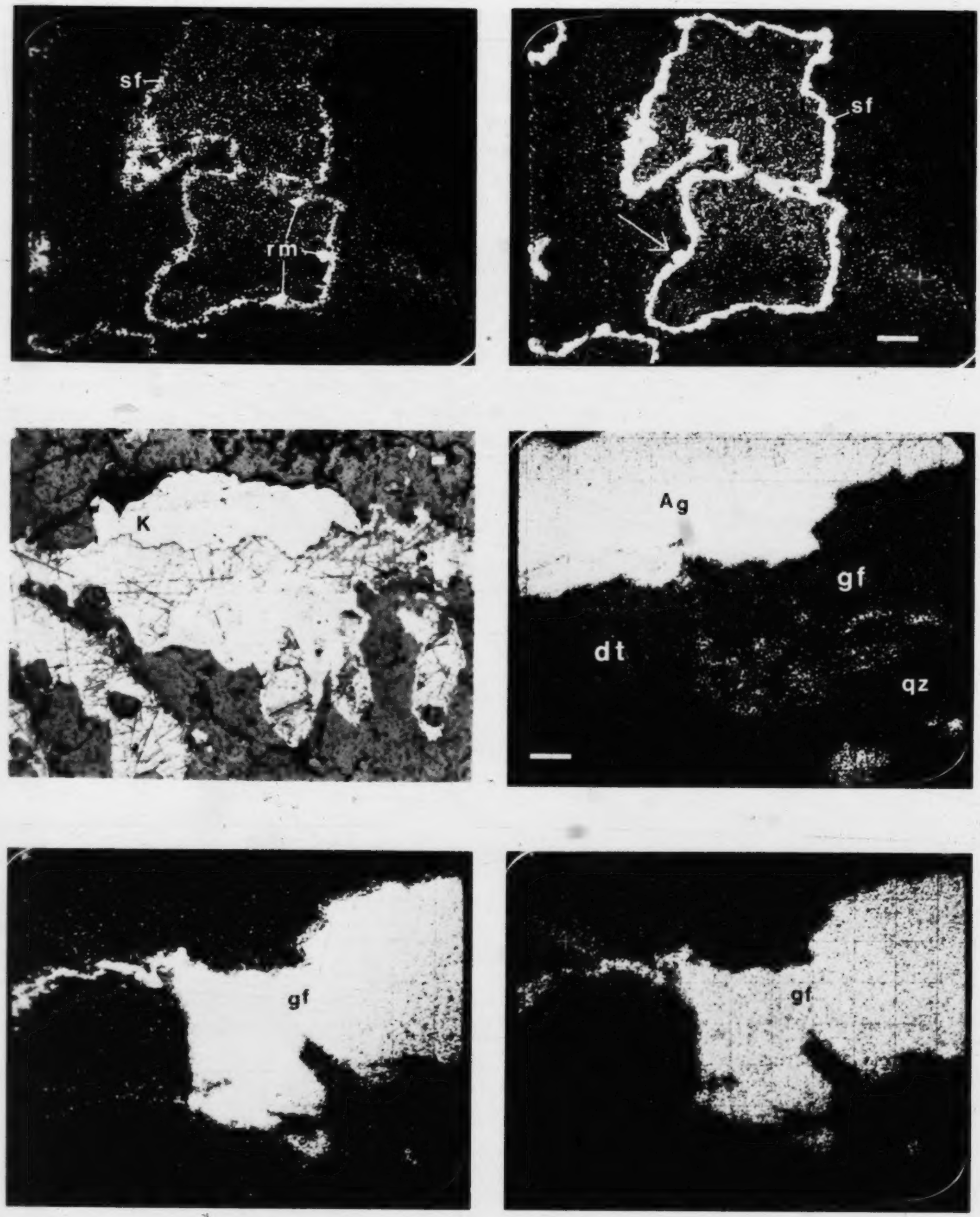

PLATE VII

was found in a thin, optically distinct sliver of native silver lining a hairline fracture which crosses a Ag-As stage native silver dendrite (Plate VI-3). Native silver does not contain more than 100 ppm Au, the maximum concentration possible if all Au in the concentrate assays (Table 1) was assumed to be present in the native silver portion. Native bismuth, unlike native silver, was found to be almost completely free of other elements. Spurious, low concentrations of Ni, Co, Fe and As encountered during microprobe analysis of some small (1-5µ) native bismuth inclusions is attributed to contamination of the enveloping arsenide mass within the excitation sphere of electron beam impact.

Exsolution of native metals in Ag and Bi-bearing sulfosalts was found only in one instance. A few native bismuth droplets (5-25µ) were found in matildite and a few native silver inclusions (1-5µ) were found in associated freibergite of an irregular hybrid assemblage including galena, sphalerite and chalcopyrite (Plates VIII, IX, X). Matildite and freibergite observed in other, more regular phases of Northrim mineralization do not have native metal inclusions. This lack of native metal exsolution phenomena in matildite and freibergite suggest low temperatures of vein mineralization. Native metal exsolution has not been observed in galena or other Ag and Bi-bearing minerals.

Native silver of at least 3 generations occurs at the Northrim Mine. The first generation of native silver occurs as separate grains accompanied by niccolite, rammelsbergite, gersdorffite and pitchblende dendrites and rosettes in isolated, early phase U-Ag-As stage plugs. This generation of native silver is not abundant in the Northrim Mine and unlike the early Echo Bay (Robinson, 1971), Terra (Badham, 1973b, 1975) and Great Bear Lake (Rojkovic, 1973) silvers, known Northrim silver stringers do not truncate pitchblende structures. The second generation, accompanying various arsenide minerals in late U-Ag-As stage dendrites, is much more abundant and this generation may be spatially associated with native bismuth-diarsenide dendrites and masses. Silver-cored, arsenide-rimmed dendrites and rosettes (dia. 1-8 cm.) belong to this generation, which in all respects save the absence of pitchblende, resembles the first. The third generation of native silver, occurring within concentric and oscillatory gersdorffite, cobaltite, safflorite, galena and chalcopyrite intergrowths interstitially emplaced between Ag-As stage "granular" quartz crystals (cf. "salt and pepper" ore) is the most widespread and abundant phase of native silver mineralization known at Northrim.

PLATE VIII. Bi-Ag-As-S Mineralization

VIII-1. NiKα image. 90,000 counts, 525 second exposure. Gersdorffite (gf) is Ni-rich. It contains very little Co since no CoKα image could be obtained. LiF crystal.

VIII-2. FeKα . 20,000 counts, 670 seconds. Only the dolomite (dt) contains significant Fe. LiF crystal.

VIII-3, VIII-4. Backscattered electron images. Different exposure times and different light intensities. Ag-As/Bi-As-S stage combined assemblages. Minerals include sphalerite (sp), galena (gn), matildite (md), freibergite (fb) and native silver (Ag). Inclusions (up to 3μ) of galena, matildite, sphalerite and an unidentified mineral (ud) occur in freibergite to the right of the native silver bleb. Sulfide and sulfosalt minerals were deposited first; native silver last. Such assemblages are disequilibriate and they are found wherever previously emplaced sulfide-bearing carbonates are intruded upon by Ag-sulfosalt and "salt and pepper" native silver-skutterudite phases. The oxidized splotches (x) should be ignored.

VIII-5. SKα .50,000 counts. Only native silver and quartz (qz) do not contain the element. ADP crystal.

VIII-6. AgLα . 50,000 counts. Native silver, freibergite and matildite carry the element. The native silver also contains 1.4 wt. % Hg, an element not detected in the other silver-bearing minerals. ADP crystal.

The white bars of this and succeeding plates represent 50μ sample distance.

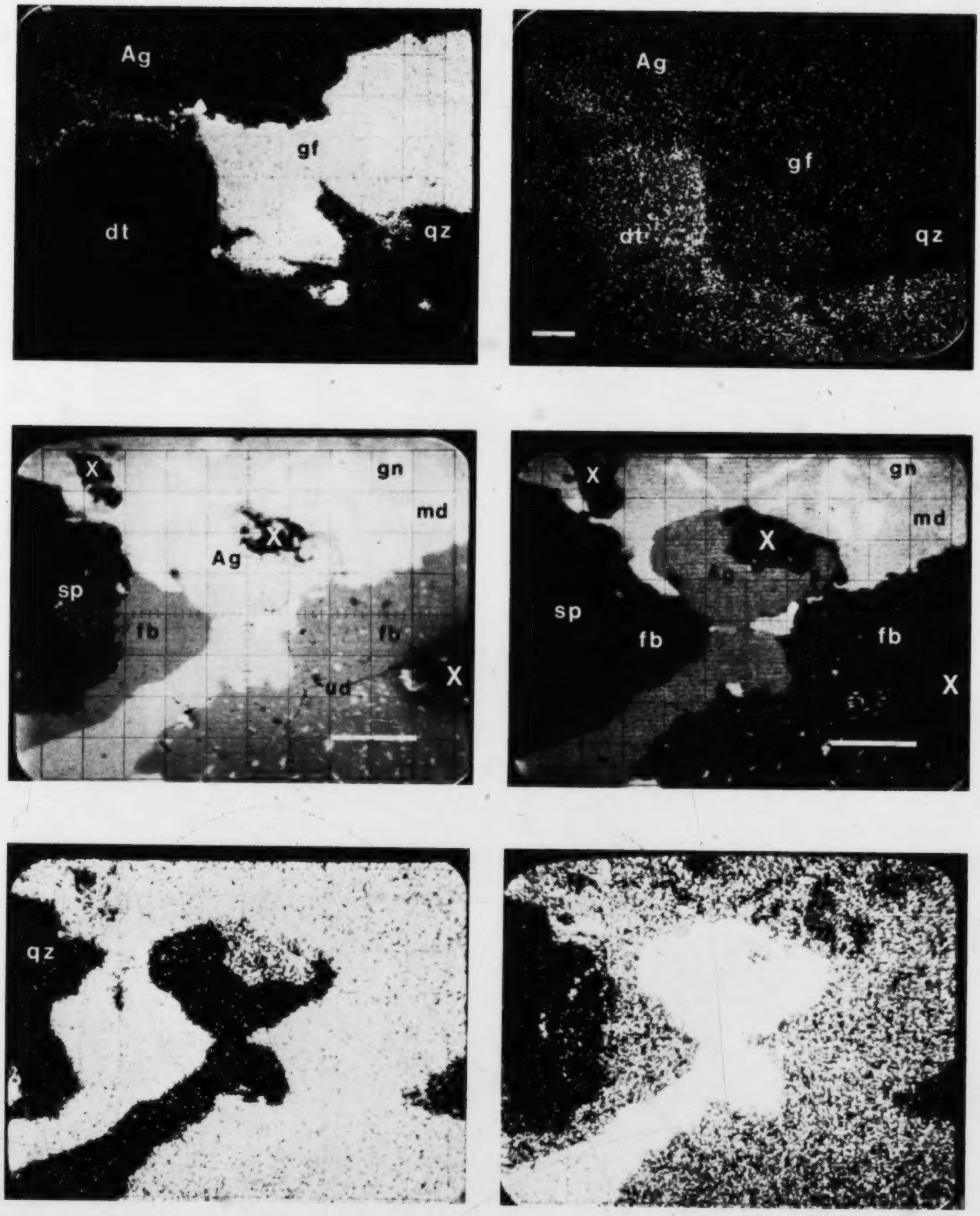
Ag
gf
dt
qz
Ag
gf
dt
qz
X
gn
md
X
Ag
sp
fb
fb
ud
X
X
gn
md
X
Ag
sp
fb
fb
X
qz

PLATE VIII

PLATE IX. Bi-Ag-As-S Mineralization (continued)

IX-1. ZnKα image. 12,000 counts. Sphalerite (sp) is the major Zn-bearing mineral but freibergite (fb) also contains Zn. The sphalerite contains 0.6 wt. % Cd but it was impossible to obtain a clear image because of AgL line interference. LiF crystal.

IX-2. CuKα . 25,000 counts. Freibergite is the host mineral. LiF crystal.

IX-3. FeKα . 20,000 counts. Undetermined inclusions (ud) and freibergite contain the element; sphalerite (sp) may not. LiF crystal.

IX-4. SbLα . 30,000 counts. Freibergite is the major Sb-bearing mineral. Native silver does carry appreciable Sb (0.5 wt. %) but not enough to show on this image. EDDT crystal.

IX-5. AgLα . 30,000 counts. Freibergite contains As but the undetermined inclusions (ud) carry higher concentrations of the element. These inclusions also contain high concentrations of S, Fe and Cu but not Sb, Zn nor Ag. The mineral, most likely a sulfosalt or a sulfarsenide, warrants further study. Apparent As concentrations in other metal-bearing minerals are atomic number effects. RAP (Rubidium acid phthalate) crystal.

IX-6. SnLα . 10,000 counts. Only trace concentrations of Sn may be present in any mineral. Dots on the image represent continuum radiation.

The white bars on the plate represent 50μ sample distance.

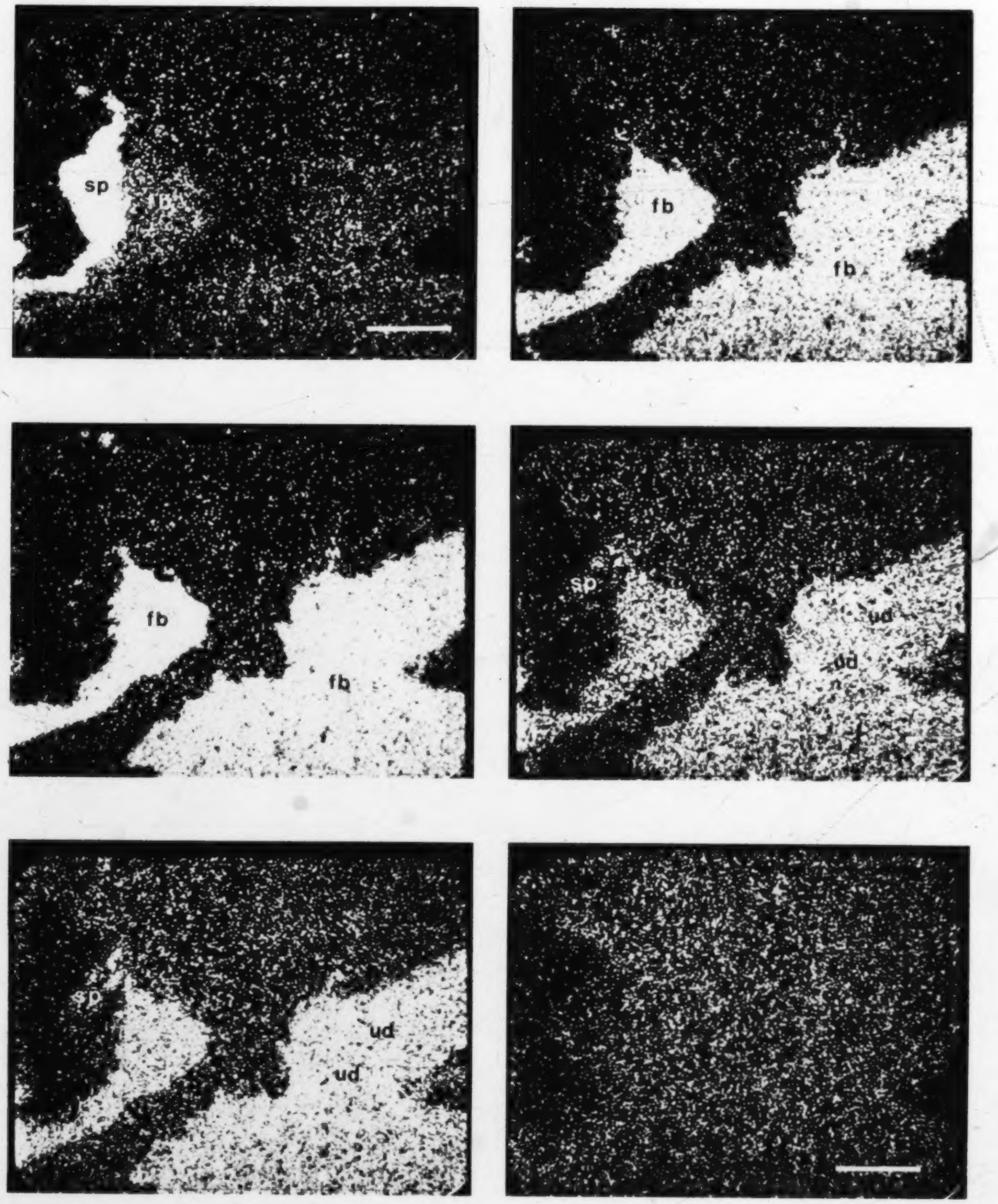

PLATE IX

PLATE X. Bi-Ag-As-S Mineralization (continued)

X-1. BiMα image. 25,000 counts. Matildite is the Bi-bearing mineral. Native bismuth inclusions (exsolution) are found within this mineral a few millimetres away PbM line interference was minimal. ADP crystal.

X-2. PbMα . 20,000 counts. Galena is the Pb-bearing mineral. Note the Widmanstatten-like exsolution of galena in matildite. The PbS-(Ag, Bi)S exsolution is almost complete. LiF crystal.

X-3. Reflected light image. The image includes the area found in Plates VII and VIII. The lettered series indicate locations of corresponding entries in Tables 6 and 7. This image encompasses the area pictured in the previous plates (VII-3 to 6, VIII, IX-1,2).

X-4. Reflected light. Early Bi-As-S stage. Cobaltite (light, low relief) and dolomite (gray) brecciated and replaced by native bismuth (light gray, tarnished). Most of the smaller fractures (→) in the cobaltite may have been created upon native bismuth expansion. Small fractures of this kind, some of which are radial, are restricted to early arsenide-bismuth assemblages. They are absent in later sulfosalt-bismuth assemblages.

X-5. Reflected light image. Late Bi-As-S stage. Native bismuth (Bi, tarnished), galena (gn) and aikinite-rezbanyite (ak) form aggregate structures in dolomite (gray). The Bi-bearing arsenide, most probably a saf-florite, occurs as small ($< 5\mu$) inclusions within aikinite next to native bismuth.

X-6. Reflected light. Early Bi-As-S stage. Banded chloanthite-skutterudite (gray) of oscillatory composition with interstitial bands of quartz (black).

The white bars on the plate represent 50 μ sample distance.

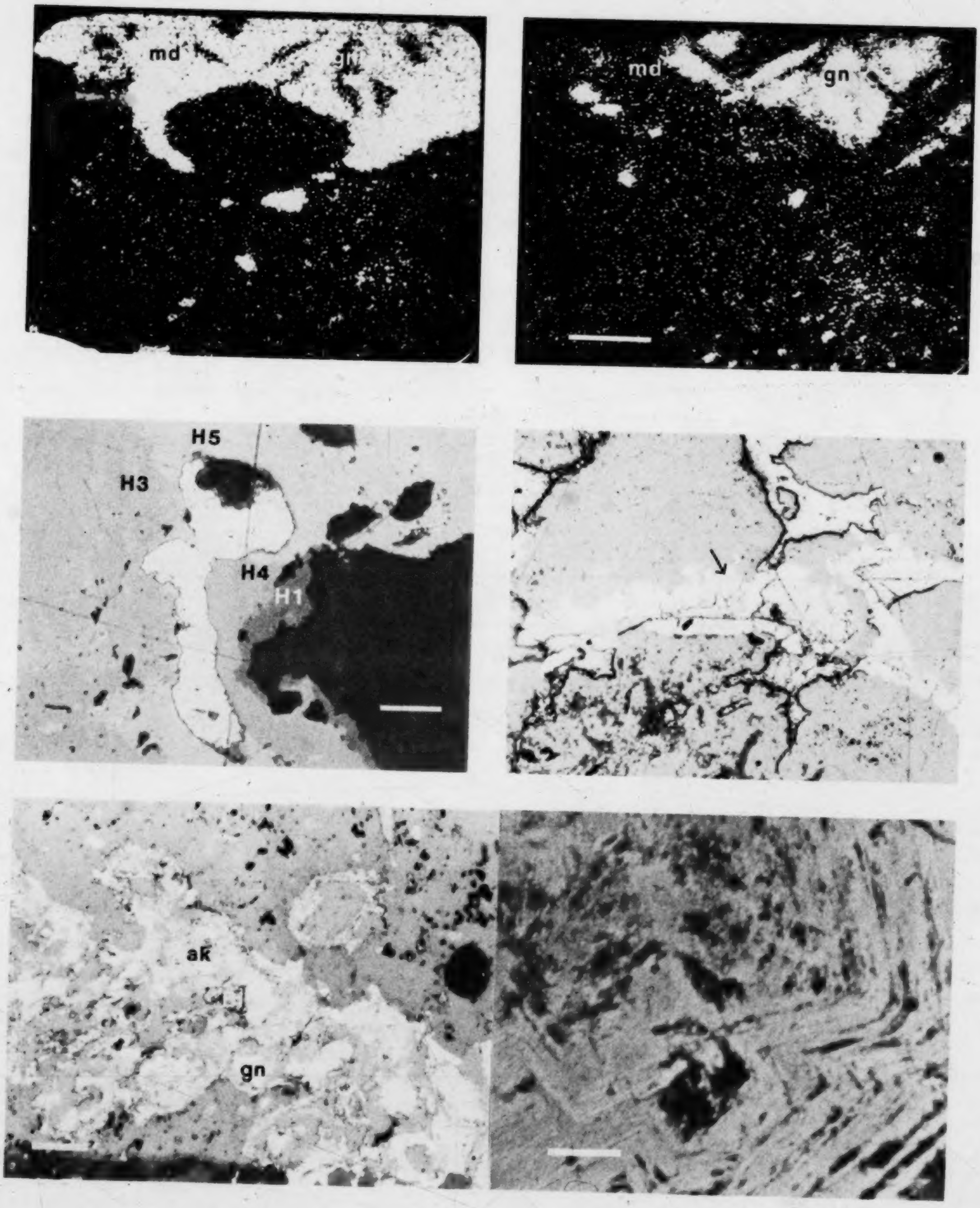

PLATE X

Native silver stringers, dendrites and fracture fillings found with complex assemblages of native bismuth, arsenide and sulfosalt mineralization along fractures truncating Bi-As-S stage banded and massive dolomite within centimetres of the interstitial silver-quartz mineralization were almost certainly introduced with the third generation of silver. Third generation silver has been overgrown by skutterudite grains (1-4 mm. dia.) but a later generation of silver fills hairline fractures which truncate skutterudite crystals. This generation most probably represents a local remobilization of old third generation silver since oscillatory growths of native silver and skutterudite has been observed by the writer. The three or four generations of native silver are always associated with diarsenide, sulfarsenide and quartz mineralization: gersdorffite in the first, gersdorffite and cobaltite in the second; and safflorite, gersdorffite, cobaltite and chloanthite-skutterudite in the third generations. Native silver dendrites and rosettes of the first generation are often cored by quartz and most often rimmed by diarsenide minerals. Native silver most often forms the cores and sulfarsenide minerals the rims of second generation dendrites and rosettes.

Native bismuth appears in at least 5 different situations. It occurs as fracture fillings truncating

U-Ag-As stage diarsenide dendrites, as interstitial fillings between Bi-As-S stage pegmatitic dolomites and quartz, as oscillatory intergrowths with cobaltites in Bi-As-S stage dolomites, as cores of safflorite and skutterudite dendrites and masses, as fracture fillings truncating visibly banded skutterudites and as exsolved blebs in hybrid Bi-As-S/Ag-As stage sulfosalts. Penecontemporaneously formed minerals in native bismuth assemblages include cobaltites, chloanthite-skutterudite, aikinite-rezbanyite, galena, chalcopyrite, sphalerite, matildite, freibergite and tetrahedrite. Native bismuth-arsenide aggregates are nearly as abundant as native silver arsenide aggregates. Native bismuth mineralization of all textures precedes third generation but follows first and second generation native silver mineralization.

Native bismuth, like water, is one of the few substances which expand upon solidification and radial fracturing analagous to frost cracking has been observed for some native bismuth occurrences (Ramdohr, 1969). Radial fracturing has not been observed in minerals enveloping native bismuth but locally pronounced, irregular cracking of skutterudite occurs in some early Bi-As-S stage native bismuth-arsenide-sulfide assemblages (Plate X-4). This cracking may be also attributed to tectonic brecciation but this interpretation is not as probable as the first since fracture extensions into gangue carbonates and quartz are not filled with native bismuth. Later native bismuth-arsenide-sulfosalt assemblages do not have this texture and it may be concluded that depositional temperatures of Northrim mineralization of the late Bi-As-S and later Ag-As assemblages never exceeded 271.5° C., the solidification temperature of native bismuth. Maximum temperatures of Northrim vein mineralization for all late phases would have been somewhat less than 271.5° C. since native bismuth may be expected to expand and shatter the surrounding minerals at temperatures lower than its solidification point. Temperatures of early Bi-As-S stage mineralization would have exceeded 271.5° C.

It should be pointed out that leaf silver, wire silver and hair silver varieties quoted in Robinson (1971) have been found in Northrim veins but no detailed compositional study of them has been made by the present writer. To these textural varieties may be added "tear-drop" silver but precusory study of Robinson's data and electron microprobe analysis and reconnaissance of Northrim silvers have indicated that native silver composition does not change substantially with textural type. A series of plates illustrating the occurrence of silver dendrites, inclusions and masses has been given to indicate the complexity of various mineral assemblages containing native silver. Similar complexity may be found in assemblages containing native bismuth, which is often found in hybrid secondary assemblages containing native silver, even though the two metals never touch one another.

(c) Arsenides and Sulfarsenides

Arsenide minerals identified in Northrim veins (in order of first appearance in the paragenesis) include niccolite, rammelsbergite, gersdorffite, cobaltite, chloanthite-skutterudite, safflorite and glauçodot. Three other arsenides were also found: a Bi-bearing safflorite (?) phase occurring with native bismuth, aikinite-rezbanyite and galena (Plate IX-5), an optically distinct, slightly anisotropic phase intermediate in composition between rammelsbergite and gersdorffite (Plate X), and a previously undescribed arsenide with a formula of PbAs (Plate XI). Arsenide minerals are found in the first three stages of mineralization and there is scarcely a mineralized vein structure at Northrim which does not contain them.

Early U-Ag-As stage arsenide plugs contain niccolite, rammelsbergite and gersdorffite. They occur as plug-like masses tapering into "tails" along

PLATE XI. As-Bi-S Mineralization

XI-1. Backscattered electron image. U-Ag-As stage accretionary structure. Niccolite (nc) occupies the center, rammelsbergite (rm) and gersdorffite (gf) the flanks and cobaltite (cb) the rims of such masses. Rim cobaltite mineralization may have been deposited with native bismuth (Bi) during the early Bi-As-S stage of mineralization. A1-A5 mark the positions of corresponding analytical entries in Table 5.

XI-2. AsLα. 100,000 counts. The arsenide and sulfarsenide minerals are represented. TAP crystal.

XI-3. NiKα. 80,000 counts. All the arsenide and sulfarsenide minerals contain appreciable Ni. LiF crystal.

XI-4. CoKα. 40,000 counts. Only cobaltite (cb) contains appreciable concentrations of the element. The apparent Co concentration in native bismuth is an atomic number effect. LiF crystal.

XI-5. SKα. 75,000 counts. Arsenian gersdorffite (agf), gersdorffite (gf) and cobaltite contain appreciable S. Bismuthinite (bs) specks occur locally with native bismuth along small fractures truncating the arsenide mass. PET crystal.

XI-6. BiMα. 30,000 counts. Native bismuth (Bi) and bismuthinite contain the element. Both replace minerals of the accretionary structure. PET (pentaerythritol) crystal.

The white bars on the plate represent 50μ sample distance.

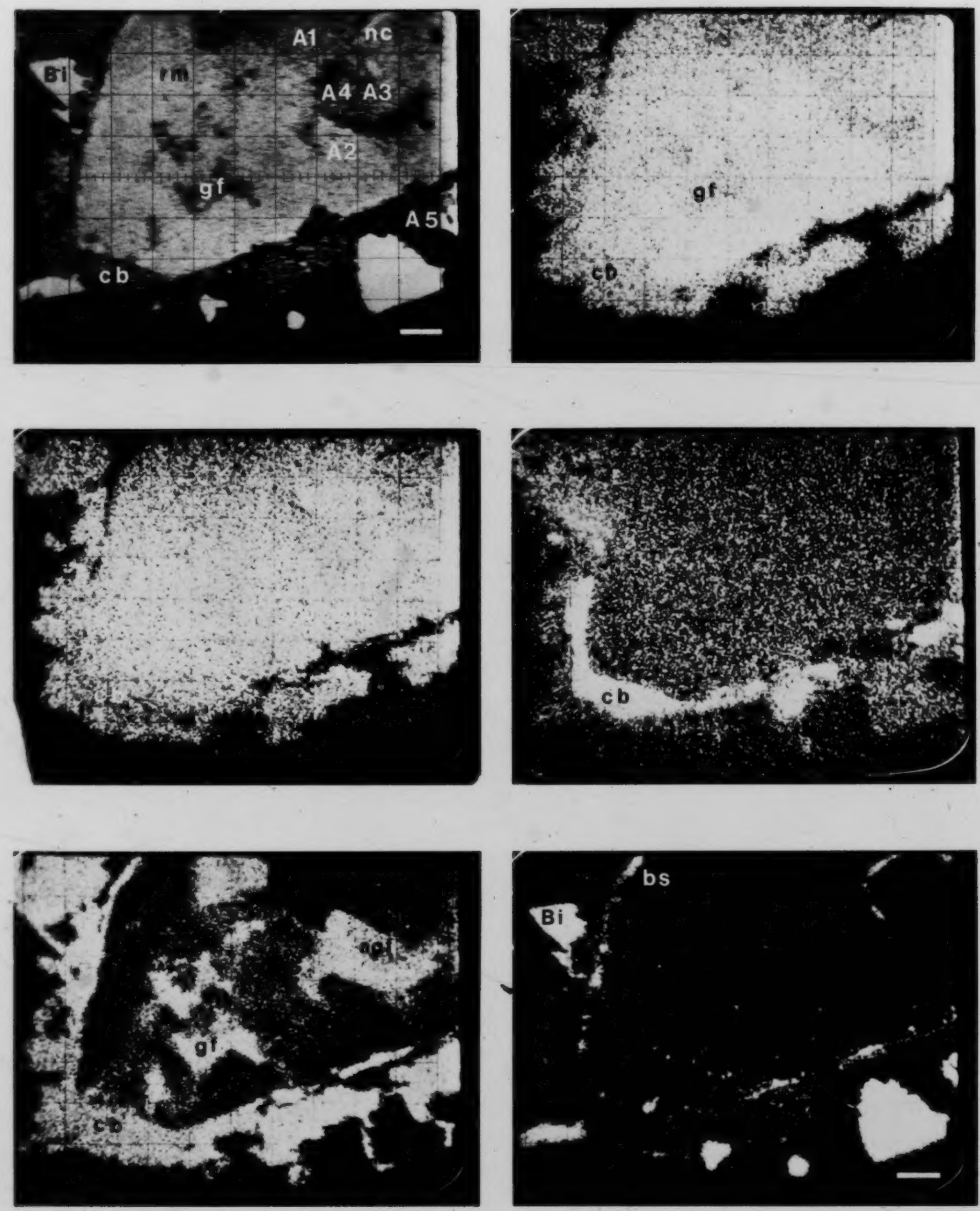

PLATE XI

the sides of veinlet walls. Niccolite occupies the centermost part of the "plug" and the portion of the "tail" closest to the veinlet walls. Niccolite was the first mineral to have been deposited: it was followed by rammelsbergite and then gersdorffite deposition. Skeletal and/or spherulitic rinds of uraninite occur within the three arsenide minerals and uraninite-rammelsbergite and uraninite-gersdorffite dendrites and rosettes (Plates XV-1, 5, 6; XVI) are abundant towards the plug centers.

Later U-Ag-As stage assemblages include the three arsenides of the plugs, cobaltite and an arsenide intermediate in composition between rammelsbergite and gersdorffite (mineral A3, Table 5). This mineral is the arsenian gersdorffite variety found in Cobalt-Gowganda ores (Petruk et al., 1971a). The sequence of arsenide emplacement is identical to that of the previous stage except that arsenian gersdorffite sometimes occurs between gersdorffite, rammelsbergite and niccolite (Plate X). Compositional zonation within individual arsenides was encountered during quantitative electron microprobe analysis but the differences in composition were greater between minerals than within them. The center niccolite (mineral A1) was found to be relatively uniform in composition; the rammelsbergite, arsenian gersdorffite and gersdorffite (minerals

PLATE XII. PbAs Mineralization

XII-1. Reflected light image. Late Bi-As-S stage assemblage. Matildite-galena (md-gn) mass with native silver (Ag) inclusions and one grain of PbAs, a mineral previously unreported in the mineralogical journals scanned by the writer. Its crystallographic features warrant further study. Proposed name: Brederite, after a prominent family of the Netherlands. The image lies a few millimetres away from the images of Plates VII and VIII.

XII-2. Sample current image. Matildite (md), galena (gn), quartz (qz) and "brederite" (PbAs) appear in the image.

XII-3. AsLα. 10,000 counts. 256 second exposure. Brederite alone contains the element. RAP crystal.

XII-4. SKα. 80,000 counts. 126 seconds. Matildite and galena contain the element; brederite does not. ADP crystal.

XII-5. PbMα. 80,000 counts. 256 seconds. "Brederite" and galena contain high concentrations; matildite contains only low concentrations of the element. There is no BiM interference. LiF crystal.

XII-6. BiMα. 80,000 counts. Matildite contains the element; galena may not. Brederite appears to contain some Bi but this may be attributed to PbM line interference. The brederite in the image has the following composition: 90 wt. % Pb, 10 wt. % As. This composition corresponds to a general formula of PbAs and the major mineral is probably amphoteric. No other elements were found in brederite by electronic dispersive analysis, and the elements S, Fe, Co, Ni, Cu, Zn, Ag, Cd, Sb and Hg were undetected in quantitative wavelength dispersion analysis. LiF crystal.

The white bars on the plate represent 50μ sample distance.

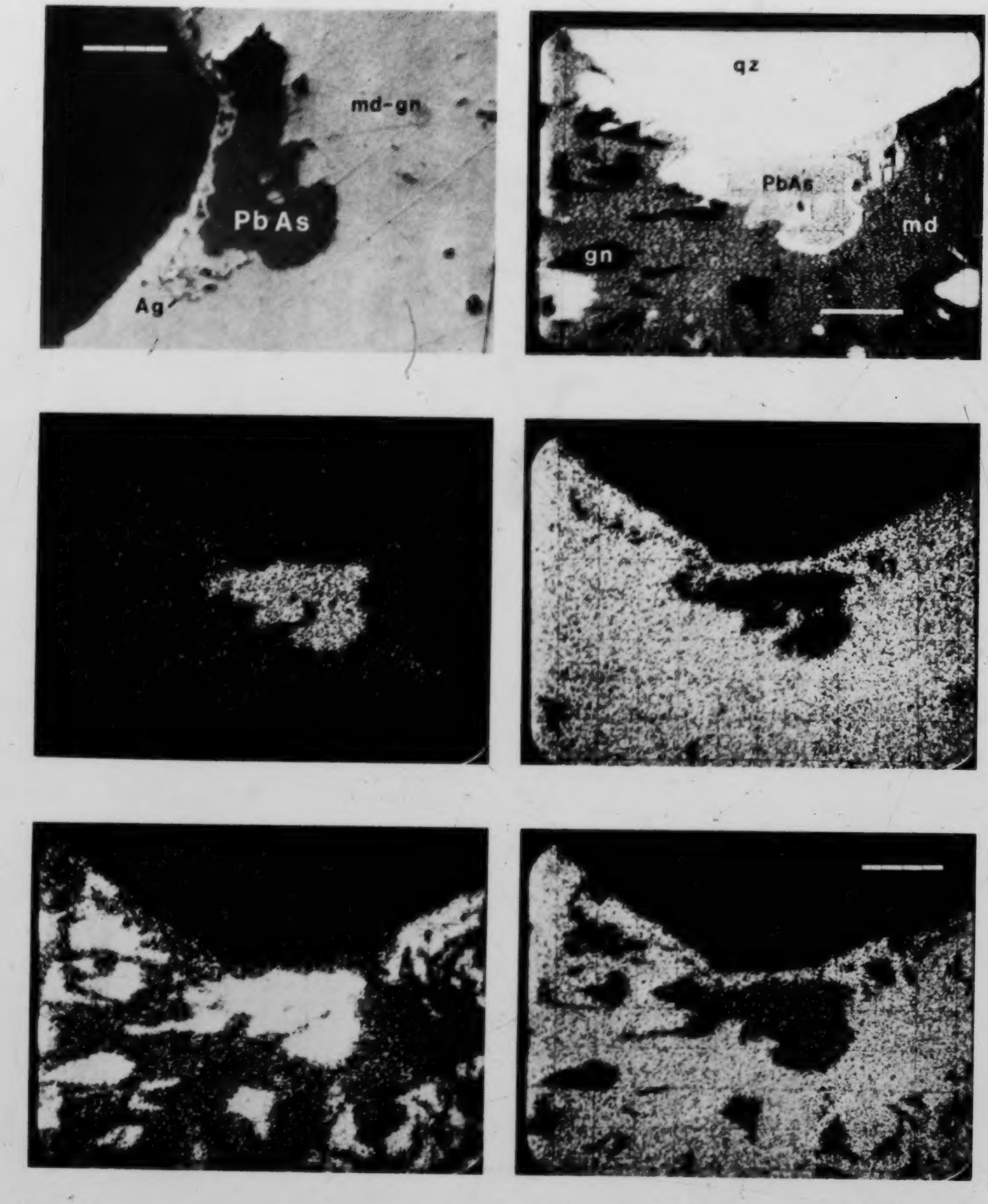

PLATE XII

A2, A3, A4) envelope somewhat more variable in composition and the cobaltite crust (mineral A5) was found to be extremely variable in composition. S concentration was found to be inversely proportional to As concentration in rammelsbergite, a relationship which is not pronounced because of the low S concentration in rammelsbergite; the same relationship is more pronounced for gersdorffite, arsenian gersdorffite and rim cobaltite whose S concentrations are higher than those of rammelsbergite. Ni, Co and Fe concentrations in rim cobaltite vary inversely with one another and similar, less pronounced variations in Ni, Co and Fe (?) concentrations occur in arsenian gersdorffite, gersdorffite and rammelsbergite. The arsenian gersdorffite may be the product of reaction between rammelsbergite and gersdorffite during a minor thermal pulse.

The arsenide mass above is typical of all U-Ag-As stage arsenide accretionary structures observed in the Northrim mine. Niccolite forms the core, rammelsbergite the inner layers, gersdorffite the patches and outer layers, and cobaltite the rind of arsenide masses. In general a Ni-rich but Co, Fe and S-poor niccolite and/or rammelsbergite core of generally uniform composition yields to a Ni-poorer, but S-richer gersdorffite and arsenian gersdorffite envelope of slightly more variable composition, and the latter minerals yield

PLATE XIII. Ag-As Mineralization

XIII-1. AsLα image. 100,000 counts. Early Bi-As-S stage triarsenide assemblage. Oscillatory banded chloanthite-skutterudite similar to that of Plate IX-6. the banding is not obvious in this image since all triarsenides carry similar concentrations of As. Oscillatory-banded triarsenides oxidize and carbonatize very quickly. ADP crystal.

XIII-2. SKα . 77,000 counts. Oscillatory banded zonation in S. The S-rich mineral is cobaltite (cb). ADP crystal.

XIII-3. NiKα . 100,000 counts. Oscillatory zonation in Ni. Ni-rich bands tend to have lower S concentrations. LiF crystal.

XIII-4. CoKα . 100,000 counts. Oscillatory zonation in Co. Co-rich bands tend to have higher S concentrations. Co concentration is always inversely proportional to Ni concentration. The triarsenides also contain minor Fe but the FeKα image was not taken.

XIII-5. Backscattered electron image. Ag-As stage "salt and pepper" assemblage. Native silver (Ag) and gersdorffite inclusions occur in the skutterudite. The gangue is quartz (qz). Note the absence of pronounced oscillatory banding.

XIII-6. AgLα . 20,000 counts. Native silver (Ag) inclusions. ADP crystal.

The white bars on the plate represent 50μ sample distance.

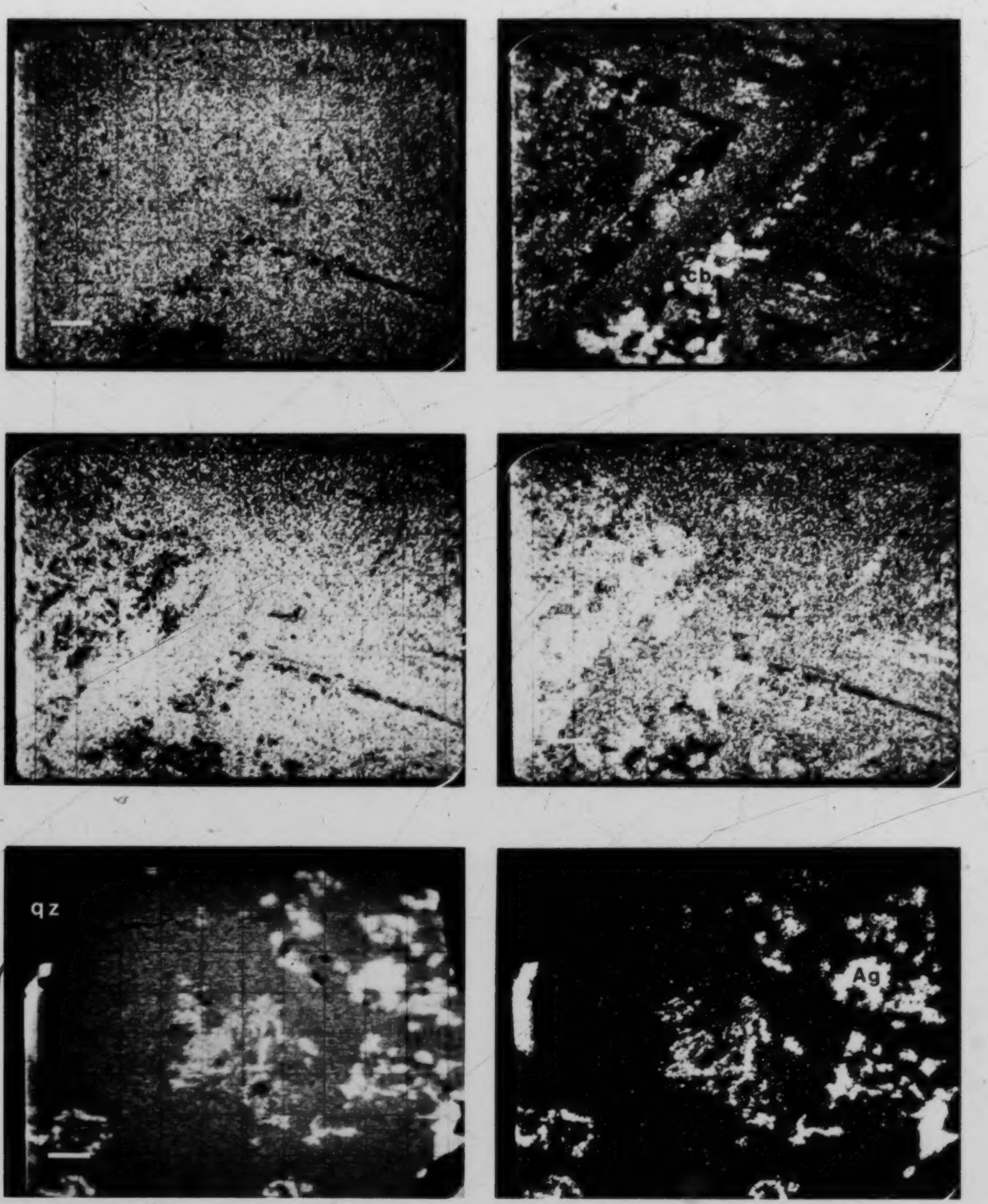

PLATE XIII

to a Ni-poorer but Co and Fe-richer gersdorffite or cobaltite rim of highly variable composition. The greater mass of U-Ag-As stage diarsenide accretions is found as niccolite, rammelsbergite and gersdorffite, and very little mass is found in the compositionally variable cobaltite rims. The compositionally variable rim represents the formation of later Co and Fe-richer arsenide mineralization both from contemporaneous and from later mineralizing fluids. The latter interpretation is favored where the arsenide rim is safflorite or glaucodot and where the rim is separated from the major part of the structure by other minerals, especially those of another phase.

Diarsenide assemblages similar to the ones above but containing less niccolite and rammelsbergite and correspondingly greater gersdorffite and cobaltite, alternate with banded triarsenide sequences of the Bi-As-S stage of mineralization. Triarsenide assemblages of this stage are visibly banded and individual bands consist of chloanthites and skutterudites of oscillatory composition (Plates X-6, XIV). Individual chloanthite bands may contain appreciable Co and minor S and skutterudite bands almost always contain appreciable Ni and minor S. Some chloanthite and skutterudite bands remain fresh; others weather jet black upon exposure to moisture. The cause of

PLATE XIV. Ag-As Mineralization (Con't.)

XIV-1. NiKα image. 240,000 counts. The gersdorffite (gf) inclusions are Ni-rich. The host skutterudite (sk) is also Ni-rich but native silver (Ag) inclusions do not contain the element. LiF crystal.

XIV-2. CoKα. 310,000 counts. Skutterudite but not gersdorffite contains high concentrations of Co. The skutterudite is neither visibly zoned nor banded with respect to Co and Ni in the images. LiF crystal.

XIV-3. FeKα. 60,000 counts. Some parts of the skutterudite contain significant Fe and there may be an Fe-rich rim. The atomic number effect is very pronounced in this image. LiF crystal.

XIV-4. AsLα. 48,000 counts, 45 second exposure. Ag-As stage "salt and pepper" assemblage. Chloanthite (sk) grain in quartz (qz) gangue. There are native silver, gersdorffite and galena inclusions in the grain. TAP crystal.

XIV-5. SKα. 20,000 counts, 836 seconds. Chloanthite contains some S but galena (gn) and gersdorffite (gf) contain higher concentrations. Native silver (Ag) does not contain the element. EDDT crystal.

XIV-6. FeKα. 20,000 counts, 444 seconds. The gersdorffite contains significant and chloanthite minor concentrations of Fe. The apparent concentration in native silver is an atomic number effect. LiF crystal.

The white bars on the plate represent 50μ sample distance.

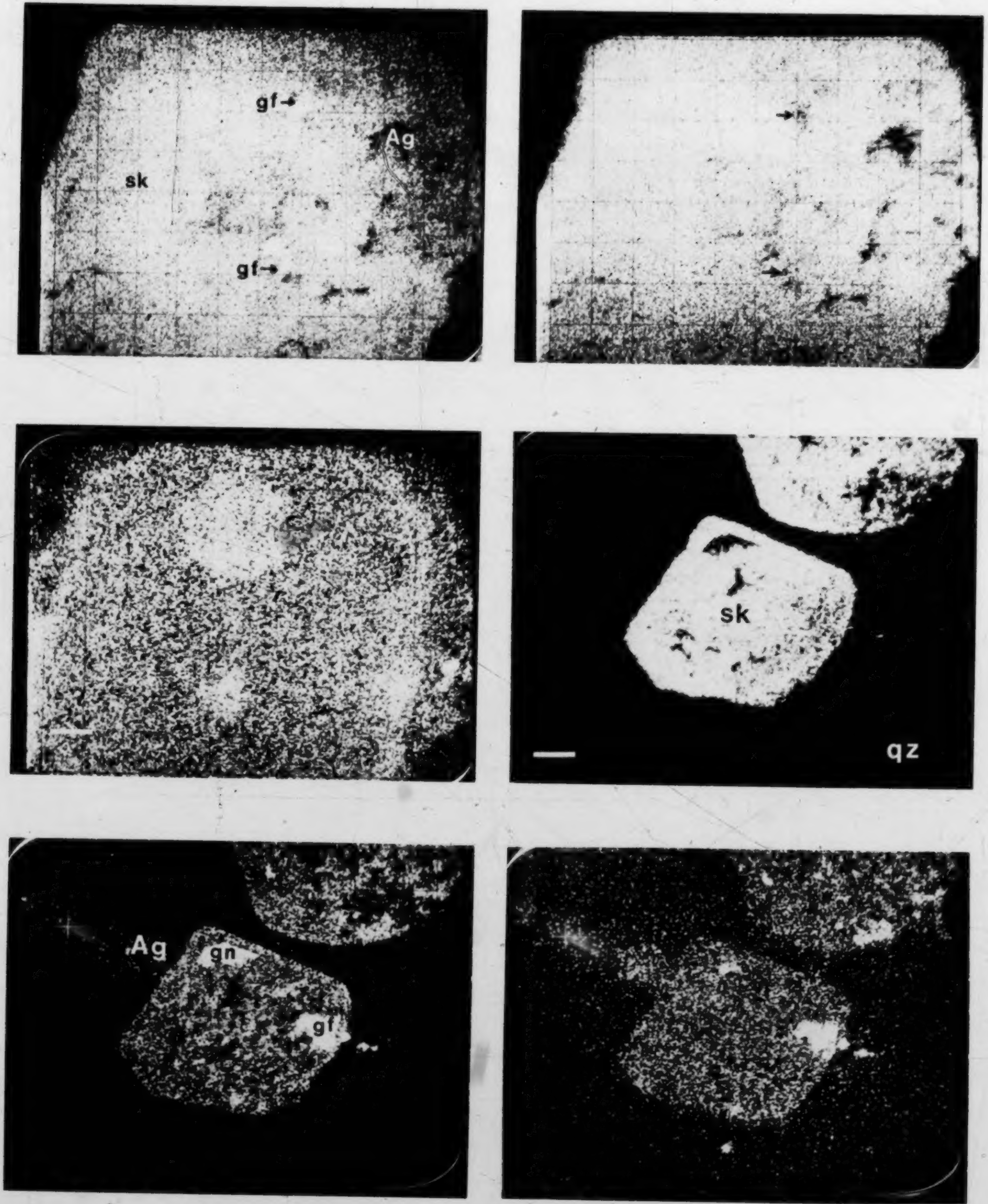

PLATE XIV

this variable weathering is not fully understood but it appears to be related to S concentration. Banded chloanthite-skutterudite structures often include quartz and sometimes carbonate and they are replaced by later native bismuth, cobaltite and safflorite mineralization, especially along fractures. Strongly banded triarsenide sequences are restricted to the early Bi-As-S stage of mineralization and occur previous to the main phase of sulfide mineralization. Banded triarsenide structures are not as abundant as accretionary diarsenide structures and they are more variable in composition. Triarsenide banding is not affected visibly by later fracture mineralization.

Safflorite (minerals C1, C2, Table 5) has not been observed in Northrim diarsenide accretions but it is abundant with native bismuth as fracture fillings in dendritic, florescent, oscillatory and accretionary structures. Safflorite also rims later Ag-As stage dendrites (Plate V). Safflorites are the most variable in composition of all arsenide minerals, both within and between individual grains and structures. The visibly distinct Bi-bearing arsenide observed with native bismuth, aikinite-rezbanyite and galena in one polished section (Plate IX-5) may be a variety of safflorite.

Gersdorffite, cobaltite, safflorite, chloanthite

PLATE XV. Ag-As Mineralization (continued)

XV-1. NiKα . 60,000 counts, 947 second exposure. Both chloanthite (sk) and gersdorffite (gf) are Ni-rich. LiF crystal.

XV-2. CoKα . 10,000 counts, 955 seconds. Unlike the triarsenides of Plates XII and XIII, the ones of this plate contain little, if any, Co. The triarsenides of this plate occur at the edge of a "salt and pepper" veinlet. The image is an atomic number effect. LiF crystal.

XV-3. AgLα . 30,000 counts, 372 seconds. Native silver inclusions and overgrowths are particularly abundant with (in) chloanthite. ADP crystal.

XV-4. Reflected light image. U-Ag-As stage. Gersdorffite accretionary mass (white) alternates with uraninite (gray) in dolomite gangue (dt). Niccolite occupies the centres, rammelsbergite and gersdorffite the flanks of some accretions containing uraninite spherules a few millimetres away.

XV-5. Reflected light. Gersdorffite-uraninite rosette within a few millimetres of the accretionary mass of Plate XIV-4. Such dendritic structures do not carry significant native silver concentrations but sphalerite, galena and chalcopyrite inclusions are abundant. Galena inclusions are abundant in these structures. Quartz (qz) rims most of the structures in the image. Discrete sulfide mineral grains occur outside the dendrite structures.

XV-6. Reflected light. Gersdorffite-quartz dendrites in dolomite gangue. A few drops of native silver (white, Ag) occur on the edges and termini of gersdorffite (white)-rich dendrite branches. Uraninite is absent. Unfortunately, most Northrim arsenide dendrites of this phase do not contain appreciable silver.

The white bars on the plate represent 50μ sample distance.

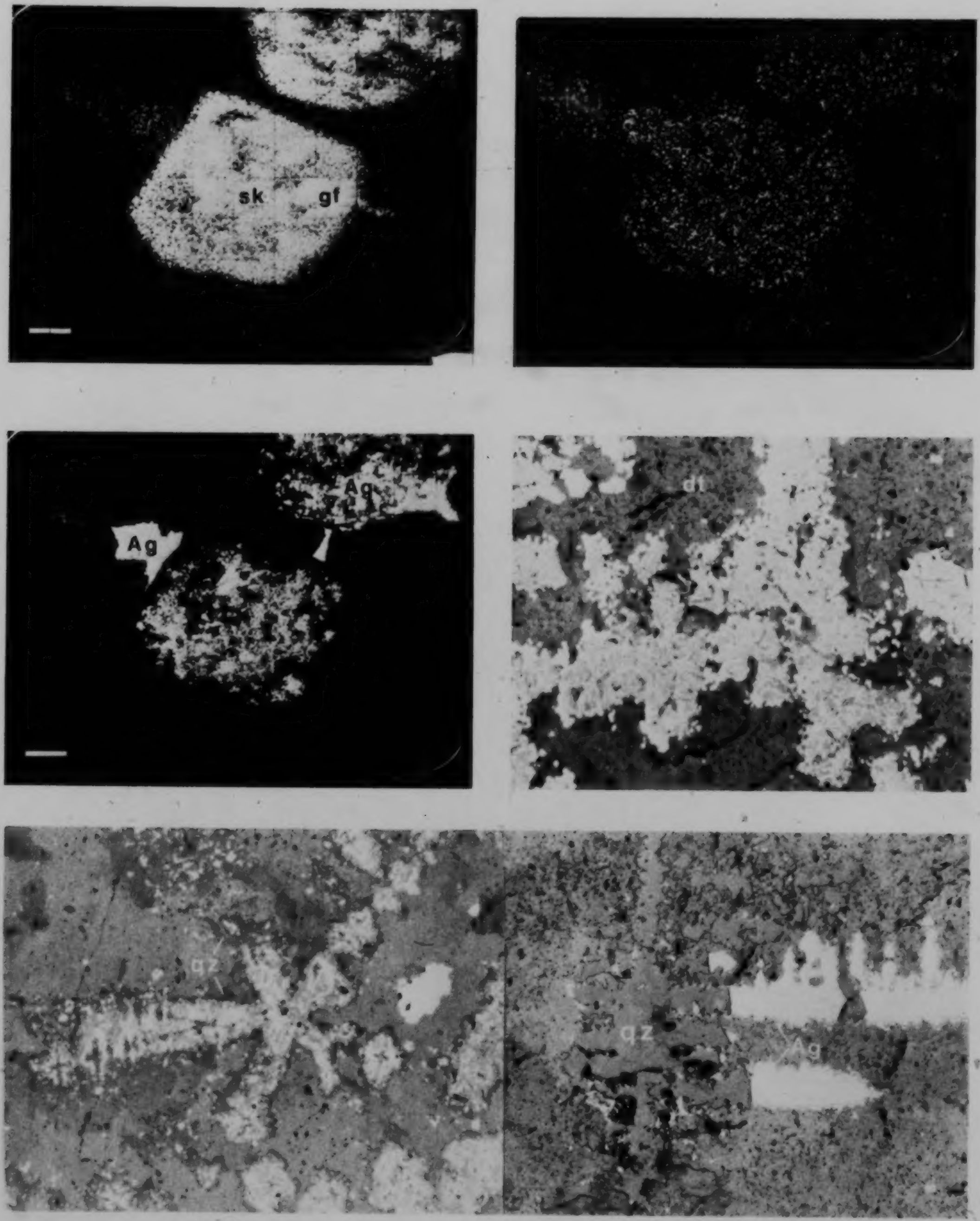

PLATE XV

and skutterudite occur with native silver and "granular" quartz mineralization of the Ag-As stage. The first two arsenides occur as irregular and oscillatory intergrowths with native silver, galena and sphalerite and these intergrowths may be rimmed by skutterudite (mineral D3). These intergrowths occur in turn by large chloanthite and skutterudite grains (1-4 mm.). The resultant texture prompts the mining term "salt and pepper" ore. "Gersdorffite" (mineral D1, Table 5) and cobaltite (mineral D2) vary in composition with respect to Ni, Co, and Fe within individual grains, as well as between them. Large chloanthite (Plate XII) and skutterudite (mineral D4) grains are only weakly zoned in composition within individual grains but extremely variable in composition between them. The compositional variation between grains is a function of mineral location: chloanthite grains occur towards the extremities, particularly the termini of quartz-silver veins, pods and stringers; skutterudite grains occur towards the centers of these structures. In one vein section, niccolite occurs towards the extremities and cobaltite towards the center, but this zonation is not as common as the first. The triarsenides are not optically banded, unlike most triarsenides of the early Bi-As-S stage of mineralization.

The nature of arsenide mineralization is both

TABLE 5

QUANTITATIVE ARSENIDE ANALYSES

	Mineral	Ni	Co	Fe	S	Stage
A1	niccolite	52.3	0.18	n.d.	n.d.	
A2	rammelsbergite	35.2	0.17	n.d.	0.08	
A3	intermediate	37.6	0.29	n.d.	6.6-8.1	U-Ag-As
A4	gersdorffite	39.4	0.11	n.d.	13.9-15.9	
A5	cobaltite	23.7-27.2	10.1-14.3	0.8-1.8	11.2-14.6	
B1	niccolite	51.5	1.2-1.6	n.d.	n.d.	
B2	gersdorffite	39.2	1.3-1.8	n.d.	15.4-16.7	
C1	safflorite	0.09-0.46	4.2-5.5	25.6-27.6	0.46-1.4	Bi-As-S
C2	safflorite	4.5-9.0+	9.4-26.5	2.9-5.4+	1.4-3.6	
D1	"gersdorffite"	25.0-29.3	3.3-6.9	6.1-8.3	13.4-15.9	Ag-As
D2	cobaltite	11.3-14.3	18.3-19.5	6.9-8.0	16.4-17.1	
D3	skutterudite	6.2-8.9	18.2-18.7	0.7	1.3-2.2	
D4	skutterudite	6.4-11.0	14.2-18.5	0.4	0.09-2.5	
	mean	64.68[1]	64.77[2]	61.75[3]	38.25[3]	Run 'A'
	range	±0.2	±0.4	±0.15	±0.15	
	mean	64.68[1]	64.77[2]	61.75[3]	53.46[4]	Run 'B-D'
	range	±0.7	±0.3	±0.1	±0.2	

n.d.--not detected. Standards: [1] NiS (synthetic); [2] CoS (synthetic); [3] FeS (synthetic); [4] Marcasite. All entries are expressed as weight percent. The analyses were performed on an ARL microprobe and the entries above have been corrected only for background. The entries for standard ranges, expressed as weight percent, are the ones of standard values to either side of the standard means obtained during microprobe analyses. Ranges have been given for minerals whose sample compositions vary more than the standard composition over 10μ sample distance. The compositional variation of the skutterudite (D4) which overgrows interstitial native silver mineralization occurs over 30μ sample distance. Sb was not analyzed since no detectable Sb peak was observed on arsenide minerals during microprobe reconnaissance. Sb concentrations up to 0.3 wt. % may be possible but are not likely.

spatially and temporally regular with respect to individual minerals, mineralized phases and mineralized stages throughout the paragenesis. Earliest formed niccolite occupies the cores of accretionary structures, the first linings of vein walls and the first growths of crustiform structures off vein walls in the earliest and later phases of the early U-Ag-As stage. It is compositionally the least variable of the arsenide minerals and it is nearly S-free and Co-poor in its earliest occurrences (mineral A1, Table 5). It is repeatedly the first-emplaced mineral of arsenide structures throughout the paragenesis, although it becomes progressively less abundant within later phases of mineralization. Rammelsbergite, the second arsenide which appears in the paragenesis, is repeatedly the second-emplaced mineral of U-Ag-As arsenide structures where niccolite is present and the first-emplaced mineral in some later-stage structures where niccolite does not occur. Rammeslbergite contains minor S and is only slightly heterogenous in composition. Like niccolite, rammelsbergite becomes progressively less abundant within later phases of mineralization. Gersdorffite, the third arsenide mineral which appears in the paragenesis, is repeatedly the third mineral emplaced in early polyarsenide growth structures. Compositionally it is somewhat more variable than niccolite

PLATE XVI. U-As-S Mineralization

XVI-1. Backscattered electron image. Early U-Ag-As stage assemblage. Uraninite (u) mass with primary gersdorffite and galena inclusions in dolomite, calcite and quartz gangue.

XVI-2. CaKα . 100,000 counts. Dolomite (dt) is the major Ca-bearing mineral. Calcite (cc) rims the uraninite. The decrease of dot intensity on the upper right corner is only a defocussing effect. LiF crystal.

XVI-3. UMα . 100,000 counts. Uraninite is responsible for the image. Like all other Northrim uraninites, no Th was detected in this sample. There may be minor concentrations of U in the dolomite, although Mg satellite lines may be responsible for the effect. PET crystal.

XVI-4. PbMα . 50,000 counts. Galena (gn) inclusions within dolomite and uraninite are particularly striking but Pb is disseminated with S within the uraninite. The dolomite-hosted galena is almost certainly primary; the disseminated Pb in uraninite almost certainly radiogenic. In one bleb (→), a primary galena rim envelopes gersdorffite. PET crystal.

XVI-5. SKα . 52,000 counts. Slightly offset from the other 5 images. Both gersdorffite and galena carry the element. S is present within uraninite next to gersdorffite inclusions; its distribution in the mineral coincides with that of radiogenic Pb. EDDT crystal.

XVI-6. NiKα . 50,000 counts. Gersdorffite is common both as minute inclusions and fracture fillings in uraninite. LiF crystal.

The white bars represent 50μ distances, just as they do in Plates III through XV.

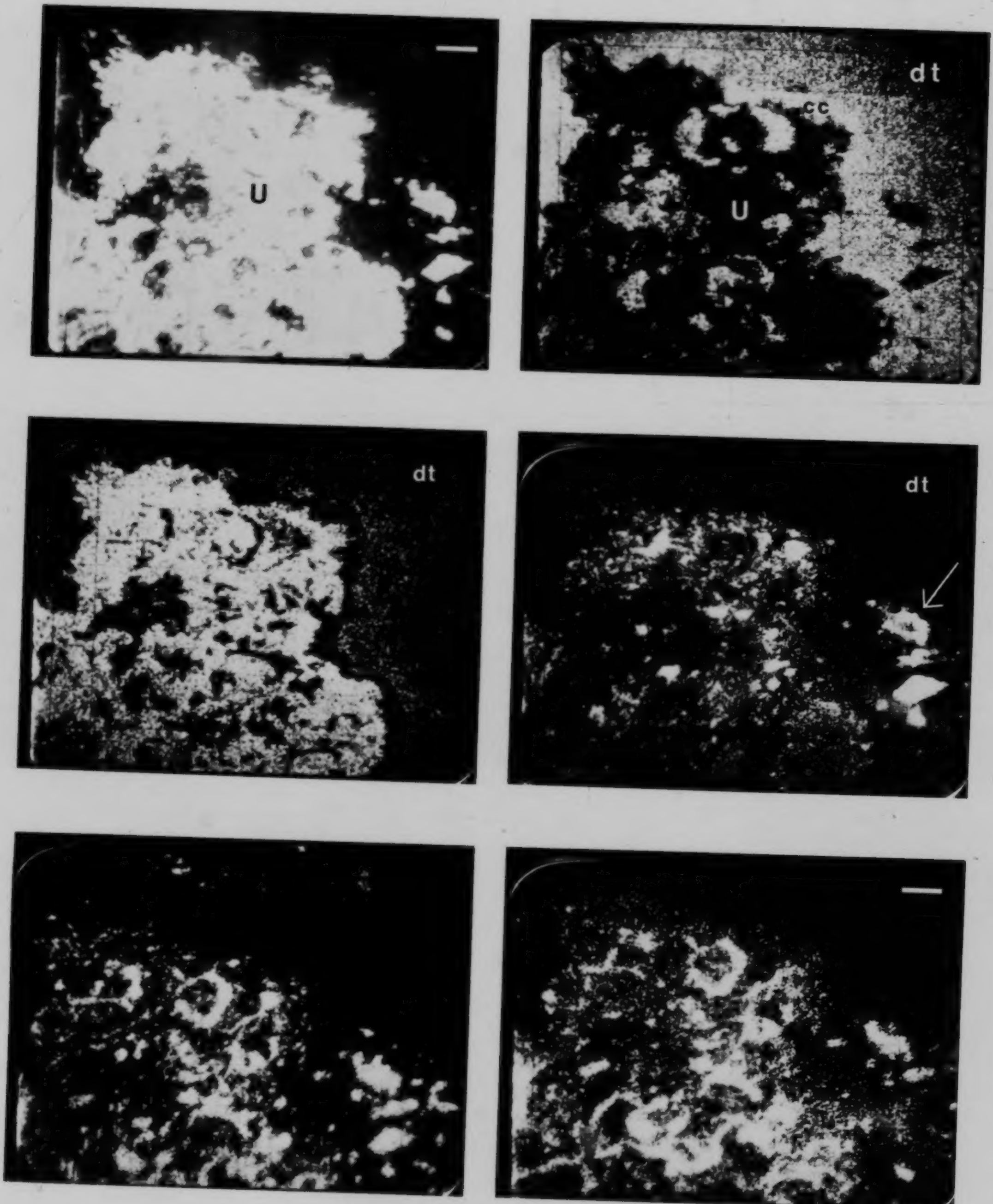

PLATE XVI

and rammelsbergite, but not in the earlier phases (e.g. mineral A4, Table 5). Gersdorffite is usually the first arsenide mineral emplaced in the later Bi-As-S and Ag-As stages of mineralization due to the absence of niccolite and rammelsbergite in most, but not all, later assemblages. Gersdorffite of the later phases of mineralization is extremely variable in composition and its place in arsenide structures is occupied by cobaltite. At Northrim, Bi-As-S and Ag-As stage gersdorffite and cobaltite form a continuous compositional series, and sulfarsenides of almost all possible Co/Ni ratios have been observed. Arsenian gersdorffite has only been observed in rammelsbergite and gersdorffite-dominated accretionary structures of the U-Ag-As stage but it may appear with the same minerals in the later stages.

Cobaltite first appears as irregular rims on early stage arsenide structures but it is not abundant until the early Bi-As-S stage where it occurs in oscillatory diarsenide and triarsenide structures. Cobaltite is very heterogenous in composition and it forms a continuous compositional series with alloclasite in Bi-As-S stage and early Ag-As assemblages. Co/Fe ratios range from 1 to 10 in cobaltites and alloclasites of these assemblages but Ni/Fe variation corresponding to compositions intermediate between gersdorffite and glaucodot is not pronounced. Arsenopyrite, the Fe end member of the glaucodot-arsenopyrite compositional and structural series has not yet been observed in the Northrim veins but it is abundant, like glaucodot, in wall rocks adjacent to the 000 vein structures on the 100 level. Their deposition in wall rock bands and stringers predates vein mineralization, at least the early native bismuth-aikinite-sulfide phases of the Bi-As-S stage and deposition may precede all mineralized vein phases now preserved in the Northrim Mine. Wall rock glaucodot and arsenopyrite are spatially and texturally similar to flow banded, wall rock sulfide mineralization, in terms of texture, fabric and distribution.

Safflorite occurs with native bismuth and native silver assemblages. It is the most heterogenous mineral in composition and the writer had to direct the electron microprobe beam onto small areas (20μ x 20μ; 5μ x 3μ) in order to obtain the heterogenous compositions of the safflorites in Table 5. Loellingite, the Fe end member of the safflorite-loellingite compositional series, has not yet been found at the Northrim Mine, but some safflorites are remarkably close to it in composition (e.g. mineral C2). Individual safflorites are zoned with respect to Ni, Co, Fe and S: Ni is generally most common towards the centers, Co in the middles and Fe is generally most common towards the rims of safflorite structures. S zonation is not so regular and oscillating concentrations of all these elements are especially common in Ag-As stage safflorites.

There are two sequences of triarsenide mineralization: the first, an oscillatory-banded sequence preceding sulfide, sulfosalt and bismuth mineralization of the Bi-As-S stage; the second, an oscillatory-banded sequence surrounding native bismuth cores in dendrites; and the third, a non-banded phase of the Ag-As stage of mineralization. Composition and zonation is most pronounced in the first sequence and the last phase of triarsenide mineralization.

In summary, the following general conditions apply to Northrim arsenide mineralization:

1. Early-emplaced monarsenide (niccolite) diarsenide (rammelsbergite) and sulfarsenide (gersdorffite, Ni-rich cobaltite, arsenian gersdorffite) mineralization occur with silver mineralization in phases of both the U-Ag-As and Ag-As stages.
2. Later triarsenide (chloanthite, skutterudite) mineralization both precede and follow bismuth, sulfosalt and sulfide mineralization in phases of the Bi-As-S stage.
3. The last emplaced diarsenide (safflorite)

and the last emplaced sulfarsenides (Co-rich cobaltite, glaucodot) in the paragenesis accompany bismuth mineralization of the Bi-As-S stage and silver mineralization of the early Ag-As stage.

4. Compositional zonation is limited in early-formed minerals and is more pronounced in later-formed minerals. This statement applies to minerals in individual growth structures, between separate phases and throughout the paragenesis. One exception to this condition (6) will appear below.
5. Compositional zonation is more pronounced in Fe-rich than in Co-rich arsenides and sulfarsenides which in turn, have more pronounced zonation than in Ni-rich arsenides.
6. Compositional zonation of triarsenide minerals of the late Ag-As stage is less pronounced than that of the early Bi-As-S stage.
7. The mineralogical succession niccolite, rammelsbergite, arsenian gersdorffite, gersdorffite, nickelian cobaltite, chloanthite-skutterudite, cobaltite, glaucodot, safflorite and the corresponding compositional succession NiAs, $NiAs_2$, Ni_2As_3S, NiAsS, (Ni,

Co) AsS, (Ni, Co, Fe_{1+x})As_{3-x}, (Co, Ni, Fe) AsS, (Co, Fe)AsS, (Co, Ni, Fe)As_2 represent the order of mineral crystallization and the arrangement of components within individual arsenide structures, individual mineral phases and throughout the period of Northrim vein mineralization. There is one qualification (9) and it is listed below.

8. There are two successions of arsenide mineralization, just as there are two general depositional periods of native silver mineralization. Safflorite appears to be the first mineral formed during the second period.
9. Ag-As stage chloanthite-skutterudite follows cobaltian cobaltite mineralization instead of preceding it.

(d) Oxides

Uraninite (pitchblende) and hematite are the two common oxides of the Northrim veins but the two rarely occur together. Rusty-red haloes of dusty hematite surround uraninite spherules and masses of the Ag-As stage but this dusty hematite is thought to be an autoxidation product of the host Fe-rich dolomite created upon U decay in the uraninite. No discrete hematite blebs were present. Brick-red, hematitic wall rocks adjacent to mineralized veins are not associated with uraninite mineralization at Northrim, just as they are not associated with pitchblende mineralization at the Terra Mine and in the Port Radium area (Campbell, 1957).

Uraninite occurs as spherules, dendrites, rinds, and colloform masses with rammelsbergite and more often gersdorffite in U-Ag-As stage plugs (Plates XIV, XV). The uraninite may have been deposited originally as colloidal pitchblende since "shrinkage" cracks--now filled by rammelsbergite, gersdorffite, dolomite, calcite and quartz have been found in the spherulitic rinds and colloform masses. Galena, sphalerite, chalcopyrite and pyrite inclusions have not only been found in uraninite dendrites and masses but also in the gangue minerals immediately surrounding it. Therefore not all Pb in the galenas associated with uraninite mineralization was necessarily radiogenic. These uraninite-gersdorffite dendrites and rosettes are common and it has been concluded on textural and structural evidence that early U-Ag-As stage uraninite, sulfide, arsenide, carbonate and silica mineralization was cogenetic. Uraninite of later U-Ag-As stage phases has a similar composition, similar textures and the same mineral associates but its dolomitic host is more highly ferroan. No Th was detected in electron microprobe reconnaissance of any Northrim uraninite. No silver mineralization has been observed as veinlets within the uraninite at the Northrim Mine but separate native silver grains do occur within the plugs and native silver occurs in arsenide dendrites of the same stage of mineralization.

Hematite occurs in cavernous, granular quartz-carbonate-sulfide pods of the early Bi-As-S stage as a pronounced red, dusty stain on carbonate and quartz. It is never an abundant vein mineral and the writer has always observed it as a red-brown weathering powder coating crystal surfaces in any phase of mineralization with unfilled fractures and cavities. The writer has never observed discernible hematite crystals in any phase of vein mineralization, except for a few crystals on some open vug surfaces. It is common as microscopic inclusions and smears on some vug-stage quartz crystal, calcite cleavage and calcite crystal surfaces. Hematite's most interesting occurrence is in late Ag-As stage vein quartz. This quartz occupies the same fracture systems as "salt and pepper" ore mineralization and grades from a milky, coarsely crystalline to an amethystine, coarsely crystalline quartz and finally to a clear, euhedral quartz whose termini do not quite fill open vug space. Hematite not only accounts for the amethystine color of the intermediate quartz but also coats surfaces between the 3 thin (1-3 mm.) outer-most quartz layers deposited on the termini of some euhedral quartz crystals. Modern, bright red, ferroan, bacterial slimes (thiobacilli) exist in open vug spaces in Northrim veins, especially the ones near the surface and in one drill hole where surface and ground waters percolate through them. When dry, the resultant smear appears as a drab red, dusty coating which gives the brick red hematite streak. By analogy the thin outer layers of some vug quartz crystals and the hematite coatings between the quartz layers and on quartz crystal surfaces have almost certainly been formed by surface to ground water inflow. This interpretation is also confirmed by the paucity of vug sulfide mineralization on layered vug quartz, mineralization so abundant coating non-layered quartz surfaces without hematite smears. The same conditions occur in other minerals of sealed assemblages, including scalenohedral calcite.

Magnetite crystals have been found in early dolomite and quartz but are not abundant nor widespread in the Northrim veins. Its occurrence, compared with that of hematite in later amethystine quartz mineralization, suggest that mineralizing fluid oxygen fugacity was low. Magnetite has only been observed in small carbonate stringers of the early Bi-As-S stage of mineralization adjacent to magnetite-rich wall rocks.

Quartz, the most abundant oxide, has been described with the gangue minerals. It is the dominant vein mineral of some early and most latter phases of mineralization.

(e) Sulfides

Chalcopyrite is the most abundant sulfide and the most abundant economic mineral of the Northrim veins. It occurs in all phases of mineralization and it is particularly abundant with other sulfide minerals. Vein chalcopyrites, unlike some host rock chalcopyrites, are generally free of sphalerite and other inclusions. Chalcopyrite inclusions have been observed in freibergite of the hybrid late Bi-As-S/early Ag-As stage of mineralization, but most chalcopyrite occurs as isolated blebs and masses intergrown with granular carbonate, quartz, galena and various sulfides of the early Bi-As-S stage, and as blebs intergrown with carbonate, quartz, aikinite, safflorite and various sulfides of the middle Bi-As-S stage. The wide distribution and great abundance of chalcopyrite within all vein systems and most vein phases indicate that the proto-vein fluids were saturated with respect to the proto-$CuFeS_2$ molecule(s) throughout vein mineralization. Chalcopyrite is a major constituent of the Northrim wall rocks.

Galena is the second most abundant sulfide and the second most abundant economic mineral. It is the near-constant associate of chalcopyrite. Vein galenas, like host rock galenas contain minor concentrations of Ag (0.1 wt. %) and it appears that the galena itself and not submicroscopic (< 1μ) inclusions are responsible for the Ag concentrations observed since Ag concentration is gradationally variable within single galena crystals. Vein galenas also carry Bi but only those crystals associated with matildite and freibergite of the late Bi-As-S stage contain appreciable amounts (0.6 wt. %) of the element. It is thought that Bi and Ag concentration of galena varies with the phase of mineralization and the low concentrations of both elements coupled with the absence of matildite exsolution in galena suggest low temperatures of galena formation.

Vein galena crystals are cubo-octahedral especially for galenas of the lattermost phase of mineralization where octahedral faces have been extremely well developed. The lattermost cubo-octahedral galenas of the vug stage have planar faces and cleavages but nearly all faces and cleavages on earlier cubo-octahedral galenas are curviplanar. Deformation twinning of most earlier Bi-As-S stage galena masses have formed parallel "tails of lead" structures (cf. Ramdohr, 1969) and it is concluded that the last major period of tectonic deformation occured before the lattermost stage of vein mineralization. The same conclusion may be derived from observation of fractures: early mineralized phase structures are often displaced a few centimetres along fractures; late phase structures are hardly displaced, let alone fractured at all.

Sphalerite is a common but not abundant sulfide in most phases of vein mineralization, particularly the ones of the Bi-As-S stage. Vein sphalerites are almost always free of minute chalcopyrite inclusions, unlike some host rock sphalerites, but intergrown aikinite-pyrite-sphalerite masses are common in Northrim veins. Sphalerite composition can be highly variable since the sphalerite structure may accommodate Cu, Fe and Mn at higher temperatures (Ramdohr, 1969) but Northrim vein sphalerites contain only low concentrations (<0.1 wt. %) of these elements. Host rock sphalerites also have low concentrations of Cu and Mn but somewhat higher concentrations of Fe (Table 6). The vein sphalerites may have been formed under temperatures lower than the ones of host rock sphalerite formation.

Preliminary electron microprobe reconnaissance and quantitative analysis indicate that Northrim sphalerites vary systematically in Fe and Zn concentrations. Host rock sphalerite (mineral E1, Table 6), coexisting

TABLE 6

QUANTITATIVE SPHALERITE ANALYSES

	Zn	Fe	Cd	S	Total	
E1	60.4-62.5	5.39-6.10	0.12	31.72	99.8	primary
F1	58.6-65.6	1.42-4.99	0.05	31.53	99.7	primary
G1	64.0-65.8	1.94-2.38	0.10	31.72	99.6	primary(?)
G2	64.1-65.3	2.00-2.29	0.10	31.72	99.1	primary(?)
F2	64.1-67.2	0.46-1.77	0.07	31.50	99.2	primary
G3	65.8-67.4	0.36-0.66	0.10	31.70	99.5	secondary
H1	57.6(65.3)	0.01	1.02(1.15)	29.8 (33.6)	88.4 (100)	Bi-As-S vein
H2	57.8(65.7)	0.01	0.58(0.65)	29.7 (33.6)	88.0 (100)	Bi-As-S vein
	67.1[1]	61.75[2]	100[3]	38.25[2]	mean	Run 'E-G'
	66.2-68.0	61.5-62.0	98.0-102.0	38.0-38.4	range	
	100[5]	61.75[2]	100[3]	53.46	mean	Run 'H'
	98.9-101	61.3-62.2	97.9-101.7	53.1-53.6	range	

Standards: [1] ZnS (synthetic); [2] FeS (synthetic); [3] Cd metal (synthetic); [4] Marcasite FeS ; [5] Zn metal (synthetic). All entries are expressed as weight percentages after background corrections were made. Excellent results were obtained for the 'E-G' run; poor results for the H run. Concentrations in brackets have been normalized to 100 wt. % and the Cd concentrations despite contamination problems, were found to be real. The high variability of Zn and Fe in samples H1 and H2 is also real.

with marcasite in sulfide bodies of the 100 level contains the highest Fe and the lowest Zn concentrations of any sphalerite analyzed quantitatively by the electron microprobe. Primary sphalerite (mineral F1) with minute chalcopyrite inclusions along intercrystalline boundaries (Plate III-5) contains more Fe and less Zn than sphalerite (mineral F2) intergrown with chalcopyrite in flow bands (Plate III-4). Both "primary" and "flow band" sphalerites may contain Cu near chalcopyrite boundaries and both form relict pyroclasts in breccia described in Chapter 2. Host rock brown sphalerites (minerals G1, G2) intergrown with chalcopyrite and quartz contain more Fe and less Zn than the black sphalerite (mineral G3) which occurs in veinlets truncating brown sphalerite-chalcopyrite intergrowths of sulfide-rich wall rocks near the 000 vein structure on the 100 level (Plate IV-6). The vein sphalerites (minerals H1, H2) are distinctively different than all host rock sphalerites: they contain substantially greater Cd and lesser Fe concentrations.

Host rock "primary", "flow band" and "stringer" sphalerites and mineralized vein sphalerites are compositionally distinct. Sphalerites of the sulfide pyroclastic breccias, whether they are primary pyroclasts or flow-banded pyroclasts, may be distinguished from each other by Fe concentration but not by Cd concentration. They cannot be distinguished from "primary" sphalerites of the 100 level by Fe concentration, although their Cd concentrations are significantly different. "Stringer" sphalerites may be distinguished from their parent sphalerites by lower Fe and high Zn but not lower Cd concentrations. The wall rock-vein transition between primary, secondary host rock and mineralized vein sphalerites seems to be marked by a sharp increase of Cd and a slight decrease of Fe concentration in vein sphalerites. Chemical evidence is compatible with textural evidence in showing that the formation of secondary host rock sphalerite, and by inference the formation of coexisting chalcopyrite, pyrite, marcasite and galena, is the result of pre-vein/syn-vein mineralization by wall rock hydrothermal/metamorphic and not vein fluids. The chemical evidence is compatible with the writer's contention that greenschist facies metamorphism of host rock sulfides involved primary sulfide material and that secondary host rock and vein sulfides in general, and sphalerite specifically, were derived from hydrothermal/metamorphic wall rock fluids which selectively mobilized Pb, Cd, Zn and Cu from sulfides and other primary minerals in the host rocks.

Pyrite and marcasite are found only as accessory vein minerals. Vein pyrite is common only in early U-Ag-As stage plug and in early Bi-As-S stage sulfide assemblages; vein marcasite is found only in the vug stages of sulfide-rich mineralization. Alternating layers of pyrite and marcasite crystals have been deposited along vein walls of the late vug-stage yellow calcite and marcasite is the Fe-sulfide deposited on prismatic quartz and scalenohedral calcite crystals in vug cavities. Marcasite formation is favored by lower temperatures and pH and the writer concludes that temperature rather than pH, dropped substantially during late vein mineralization since the carbonates were deposited at the end of Northrim mineralization as they had been before. Wall rock marcasite may have formed at lower pH and/or higher temperatures than vein marcasite--the wall rock fluids responsible for secondary carbonate mineralization in the wall rocks did not deposit the amounts of carbonate found in the mineralized veins and would not have had the carbonate pH buffer sustained during Northrim vein mineralization. Marcasite and pyrite are far more abundant in the host rocks than in the veins. The pyrite is slightly anisotropic.

Argentite, now inverted to acanthite is restricted to sulfosalt-rich assemblages of the hybrid Bi-As-S/Ag-As assemblages and to sulfide-rich assemblages of the late Ag-As stage. All minerals with the formula Ag_2S observed in hand specimen were deposited as argentite since all crystal outlines are composed of cubic and octahedral faces. Thus the lowest temperature of the late Ag-As stage exceeded 176.3° C., the lowest recorded temperature of argentite-acanthite inversion when native silver is present (Skinner, 1966). Argentite occurs with polybasite and pyrargyrite as a hybrid assemblage which replaces chalcopyrite and other sulfide minerals in Bi-As-S stage assemblages intruded by Ag-As stage "salt and pepper" mineralization. Pyrargyrite and argentite are only stable together above 197° C. and this indicates that the depositional temperature of the early Ag-As stage of mineralization exceeded 197° C. (ibid., 1966). Argentite also occurs with chalcopyrite and unidentified sulfides in post "salt and pepper" mineralization assemblages. Pressure-uncorrected fluid inclusion filling temperatures of the Ag-As stage of mineralization at Northrim were estimated at 175° C. Argentite replaces interstitial native silver mineralization along fractures and one grain of argentite was seen in one fracture which truncated a native silver dendrite. Replacement of previously emplaced Bi-As-S stage minerals by argentite, polybasite and freibergite is particularly common adjacent to "salt and pepper" mineralized phases.

Bismuthinite is an uncommon mineral in the Northrim veins. It occurs as a replacement of native bismuth and associated arsenide minerals along fractures (Plate X-6). Minor sulfide minerals expected but not observed in the Northrim veins were bornite Cu_5FeS_4, Chalcocite Cu_2S, stromeyerite $Cu_{1+x}Ag_{1-x}S$ and mckinstryite $Cu_{0.8+x}Ag_{1.2-x}S$. All but the first were expected to be found in the vug stage of mineralization; the first was expected in earlier sulfide assemblages and it has not been positively identified. If these minerals are truly supergene as stated in Rojkovic (1973), then the "supergene" stage found in vein systems in other deposits of the Camsell River and Port Radium regions is an insubstantial, if not an absent, stage of mineralization at the Northrim Mine. Only the vug-stage clay powder, hematite powder and quartz overgrowth mineralization is considered "supergene" by the writer since late Cu-Ag(?)-S-bearing quartz and carbonate phases occupy unfilled continuations of the "salt and pepper" ore mineralization.

Vein sulfides, unlike some wall rock sulfides and some vein sulfosalts are remarkably free of mineral inclusions.

(f) Sulfosalts

Sulfosalt minerals identified in Northrim veins include a member of the aikinite-rezbanyite group $(PbBi, Cu)S_3$, freibergite $(Ag, Cu, Fe, Zn)_{12}(Sb, As)_4S_{13}$, matildite-schapbachite $AgBiS_2$-PbS and polybasite $Ag_{16}Sb_2S_{11}$.

Semi-quantitative analytical results of the last three minerals are given in Table 7.

The aikinite-rezbanyite member occurs with native bismuth, galena, chalcopyrite and sphalerite. It is the most abundant sulfosalt of the Bi-As-S stage of mineralization and the most abundant ore mineral of the sulfosalt group. It often envelopes native bismuth mineralization in small fractures within strongly sheared dolomite, quartz and calcite. It is the dominant economic mineral of sulfide assemblages containing native bismuth. Aikinite-rezbanyite, galena, chalcopyrite and native bismuth occupy interstitial spaces, cleavage planes and fracture surfaces in the pegmatitic dolomite rhomb mineralized phase. Chalcopyrite and galena occur as small, (0.1-0.3 mm.) widely distributed but separated patches in aikinite-rezbanyite but these patches are not exsolution products which exploit mineral and structural planes of weakness. The exact composition of aikinite-rezbanyite has not been determined but the mineral appears to be compositionally unzoned and free of Ag and elements other than those of the general formula, $PbCuBiS_3$.

Freibergite occurs with matildite in stringers and masses which truncate previous arsenide, sulfide, aikinite-rezbanyite and native bismuth mineralization of the Bi-As-S stage. Northrim freibergite contains

TABLE 7

SEMI-QUANTITATIVE SULFOSALT ANALYSES

	Freibergite			Matildite	Polybasite	Error
	H3	H4	J1	H5	C3	
Cu	19.3	19.6	17.7	0.3	n.d.	±0.3
Pb	n.d.	n.d.	0.3	0.8	0.4	±0.1
Zn	3.2	3.4	2.0	n.d.	n.d.	±0.1
Ag	23.2	49	27.0	24.7	69.6	±3.6
Sb	25.3		23.7	n.d.	11.2	±2.1
As	0.6	1.6	0.4	n.d.	0.5	±0.1
Fe	3.9	3.0	4.9	n.d.	n.d.	±0.1
Bi	n.d.	n.d.	n.d.	54.6	0.4	±0.7
S	24.5	22.4	24.0	19.6	17.7	±0.3

All analyses were performed on an ARL electron microprobe. All results were corrected for background and normalized to 100 wt. % but atomic number, fluorescence and absorption corrections were not made. The error stated is the analytical accuracy for 2 standard deviations. J1 and 2 contained numerous small chalcopyrite, sphalerite and galena inclusions; matildite J3 contained numerous galena inclusions; the inclusions in polybasite are unknown. All sulfosalts analyzed were nevertheless homogenous in composition over 1 millimetre.

extremely high Ag concentrations but Ag and other base metal concentrations are comparable to those of other freibergites from other Great Bear Lake veins (Rojkovic, 1973). Most freibergites are free of chalcopyrite, sphalerite and galena inclusions but one freibergite (mineral H4, Table 7) contains many of them (Plates VII, VIII, IX). The inclusions in the freibergite to the right of the silver are considered to be relicts of previous sulfide mineralization. The mineral assemblage in the plates is definitely one of disequilibrium and such hybrid assemblages involving freibergite, matildite, "brederite" (PbAs) and native metals are common only in banded dolomite adjacent to mineralized veins of the "salt and pepper" variety.

Matildite (mineral H5, Table 7) contains minor Cu and Pb and in one instance was found to contain native bismuth, native silver, galena and PbAs inclusions (Plates VII-IX, XI). The native bismuth inclusions are almost certainly exsolution phenomena and the galena inclusions form a somewhat regular pattern within the host matildite. Adjacent sections of the matildite contain Pb and it is thought that this pattern represents exsolution of PbS from $AgBiS_2$. Widmanstatten-like structures of galena (taenite equivalent) and matildite (kamacite equivalent) have been reported for matildites from several deposits throughout the world and it is thought that such exsolution features can only be formed upon cooling of PbS-$AsBiS_2$ mixtures which have previously crystallized above 215° C., the temperature at which matildite or $\beta AgBiS_2$ assumes the α-$AgBiS_2$ or galena structure (Ramdohr, 1969). Thus formational temperatures of this matildite-galena mass of the Northrim Mine would be greater than 215° C., unless galena and α-$AgBiS_2$ were somehow able to crystallize together. Native bismuth mineralization without cracking textures both precede and succeed matildite crystallization and hence matildite formational temperatures could not have exceeded 271.5° C., the melting point of bismuth. Most matildites, like most of the freibergites they are associated with, are relatively free of galena and other inclusions.

Northrim polybasite (mineral C3, Table 7), a common mineral of hybrid Bi-As-S/Ag-As stage assemblages, is remarkably Cu-free and As-poor and must have been formed at a time when Cu and As were less available for mineral formation. Pb and Bi appear to be present in the mineral analysed (Table 7) but these elements may be attributed to galena and bismuthinite inclusions since concentrations of these elements were pronounced to one corner of the grain analyzed. Polybasite, pyrargyrite and argentite replace sulfide minerals along the edges of native silver-skutterudite-quartz mineralization of the Ag-As stage. Numerous relict native bismuth, galena, sphalerite and chalcopyrite inclusions occur in most instances. Pearceite, the As end member of the polybasite-pearceite series was not observed in Northrim ores.

Sulfosalt minerals sought but not found in the Northrim veins were stephanite Ag_5SbS_4, emplectite $CuBiS_2$, proustite Ag_3AsS_3 and pavonite $AgBi_3S_5$. Stephanite was expected in late Ag-As stage assemblages; pavonite in vug-stage; emplectite in Bi-As-S stage assemblages. These minerals, if present at Northrim, would be rather uncommon since major sulfosalt assemblages containing the same elements, but in different proportions, have already been identified at Northrim.

(g) Other Minerals

A green, micaceous mineral, tentatively identified as muscovite and probably a phengitic variety reported by Badham (1973b, 1975) in veins of the Terra Mine, fills fractures which brecciated shear-banded quartz and carbonate mineralization of the 014 vein structure at Northrim. It was not an abundant mineral and it is thought to be coeval with jet black triarsenide breccia fillings and chalcopyrite blebs of the early Bi-As-S stage.

Chlorite also occurs in shear-banded carbonate and quartz of the 014 vein structure as smears between the bands. Pale green fluorite occurs with some arsenide dendrites of the late Bi-As-S stage. A clay mineral of undetermined structure and composition covers scalenohedral calcite in the lattermost phase of mineralization.

Some weathering products of the underground mine workings include acanthite Ag_2S, malachite $Cu_2(CO_3)(OH)_2$, annabergite $(Ni, Co)_3(AsO_4)_2 \cdot 8H_2O$, erythrite $(Co, Ni)_3(AsO_4)_2 \cdot 8H_2O$, hydrozincite $Zn_2(CO_3)_2(OH)_6$, limonite $2Fe_2O_3 \cdot 3H_2O$ and wad $MnO_2 \cdot nH_2O$. These minerals form on wet vein surfaces in a few months or a few years upon exposure to the atmosphere. Vug marcasite, exposed for one year in a laboratory at the University of Alberta, developed thin (1-3 mm.) colloform rinds, possibly limonite.

Depositional Conditions

The Northrim mineralized veins are the products of hydrothermal brine fluids which carried at least the following elements: the alkaline metals H, Na, K, Rb; the alkaline earths Mg, Ca, Sr, Ba; the transition elements Mn, Fe, Co, Ni, Cu, Zn, Mo, Ag, Cd, Au, Hg; the metallic and/or amphoteric elements, B, C, Al, Si, P, As, Sb, Pb, Bi; and the non-metallic elements O, S, F and Cl. All of these elements occur in vein minerals and fluid inclusions at the Northrim Mine; other elements, especially alkaline metals and halides, may be present in trace amounts. Some of the elements may occur only in trace amounts within the Northrim veins but this does not imply that they were insignificant components of the parent ore fluid--some elements (e.g. Na, K, Cl) have hardly been concentrated in vein mineral assemblages, but have been retained by the brines entrapped within vein fluid inclusions.

The Northrim veins are not only complex in composition but also complex in mineralogy. Mineral assemblages change throughout the paragenesis (Fig. 22) but most of their major constituent elements were available for vein mineral formation throughout the paragenesis. This is undoubtedly true of C, O, H, Si, Ca, Mg, Mn, Fe, S, Cu, Zn, Cd and Pb; other elements such as Hg, As, Ni, Co, Ag, Sb and Bi are likely trace constituents of many vein minerals other than the hosts detected by microprobe reconnaissance. The distribution of some elements throughout the paragenesis is shown in Figure 23 but it should be stressed that the present element distribution like the present mineral deposition, is dependant on the vein fluid complexes actually precipitated, and not on the availability of elements in the solution. The Northrim veins, then, are almost certainly the products of one hydrothermal fluid regime; a regime dominated by one fluid of complex but relatively constant composition. The discovery of the late stage stromeyerite, mckinstryite and pavonite assemblages, so common in the other Great Bear veins (Robinson and Ohmoto, 1973; Rojkovic, 1973; Badham, 1975) would also support this conclusion for the Northrim veins.

Temperatures of vein mineralization are generally low. There is limited native metal and sulfide component exsolution in sulfosalt (e.g. matildite, most freibergites) and sulfide (chalcopyrite, sphalerite, galena) vein minerals known to accommodate various components at high temperatures. The highest possible temperature accompanying vein mineralization is 590° C., the lower stability limit of pararammelsbergite (Yund, 1961), a mineral not yet found in any Great Bear vein. The presence of K-feldspar in mineralized carbonate stringers indicates a minimum temperature of about 310° C. for this phase of mineralization (Fig. 22); the presence of chlorite and muscovite in the early Bi-As-S stage indicates a temperature range of 250-310° C. for this stage of mineralization (Fig. 22).

Temperatures of Northrim vein deposition have been inferred from mineral assemblages, isotope data and fluid inclusions. The temperature estimates from

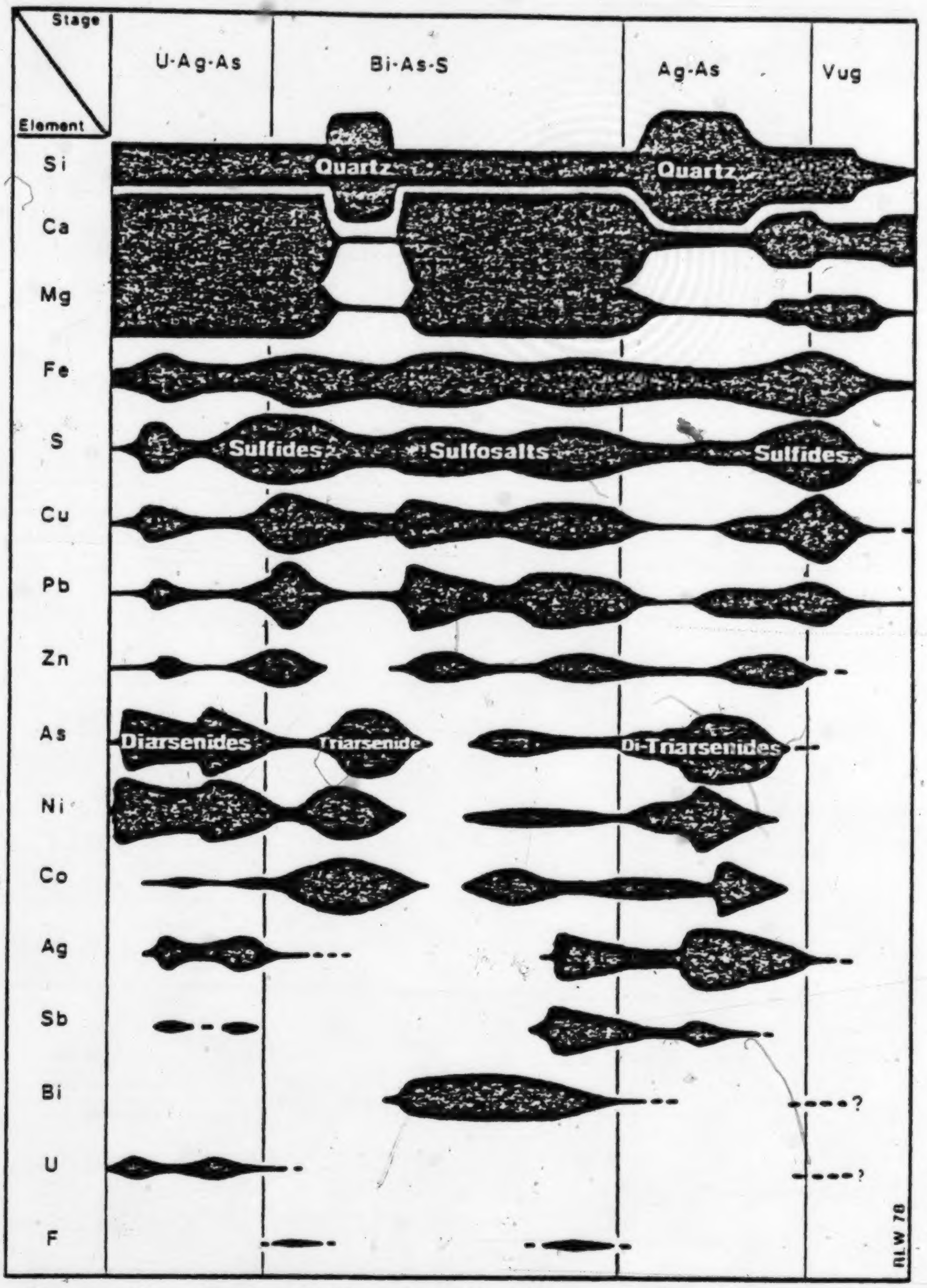

Figure 23: Paragenetic distributions of elements characteristic of Northrim mineralized veins. The widths of the bars are proportional to the relative concentrations of the elements incorporated in vein minerals throughout the paragenesis but no detailed comparison of relative concentration can be made between bar widths representing different elements.

all three sources were found to be consistent. Temperatures of the middle Bi-As-S stage and ensuing assemblages did not exceed 271.5° C., the melting point of native bismuth since there has been no evidence for native bismuth recrystallization. Depositional temperatures of the earlier bismuth-cobaltite dendrites were probably near 271.5° C. since cracking of cobaltite rims may have been caused by bismuth core expansion. Exsolution of galena in matildite of later Bi-As-S assemblages implies deposition of a mixed $AgBiS_2$-PbS phase, "schapbachite" (cf. Ramdohr, 1969), above 215° C. The assemblage argentite-pyrargyrite (-polybasite), one which replaces sulfide mineralization adjacent to the granular quartz-silver-skutterudite phase, is stable above 197° C. (Keighin and Honea, 1969); the cubic morphology of all acanthites, even the ones of the late Ag-As stage, indicates the deposition of argentite, a phase stable above 176° C. (Skinner, 1966). Primary fluid inclusion filling temperatures for Ag-As stage quartz were estimated to be 150-200° C. and if one applies a correction factor equivalent to 0.9 kb. maximum pressure, filling temperatures of 190-250° C. are obtained. S isotope fractionation between sulfide pairs yield temperatures of 255° C.(cp-gn), 230° C. (cp-py) and 120° C. (cp-gn), upon employment of the calibration curves of Kajiwara and Krouse (1971). These temperatures were estimated by Badham (1973b) and this writer has been able to fit the second and the third temperature estimates onto the paragenesis on the basis of Badham's phase descriptions. The presence of clay in the lattermost assemblage of the vug stage indicates a depositional temperature maximum of about 210° C., the maximum stability temperature of any clay in the boreholes of the Salton Sea geothermal system.

A generally steady decrease of mineralization temperatures is indicated by the evidence above. The same conclusion may be derived from the following textural and geometrical evidence. Minerals of heterogenous composition, especially the arsenides and sulfarsenides, are compositionally zoned in a regular manner. They generally have not reacted to form intermediate phases of uniform or gradational composition, a reaction favored by temperature increase. The one possible exception, the formation of arsenian gersdorffite, has already been mentioned. Vein minerals, layers, crusts and accretions have hardly been embayed or otherwise affected by the passage of hydrothermal fluids responsible for later mineralization. Any mineralogical and textural changes in earlier vein mineralization have occurred within millimetres, and most often with fractions of a millimetre, removed from later vein mineralization. The preservation of heterogenous U-Ag-As stage assemblages

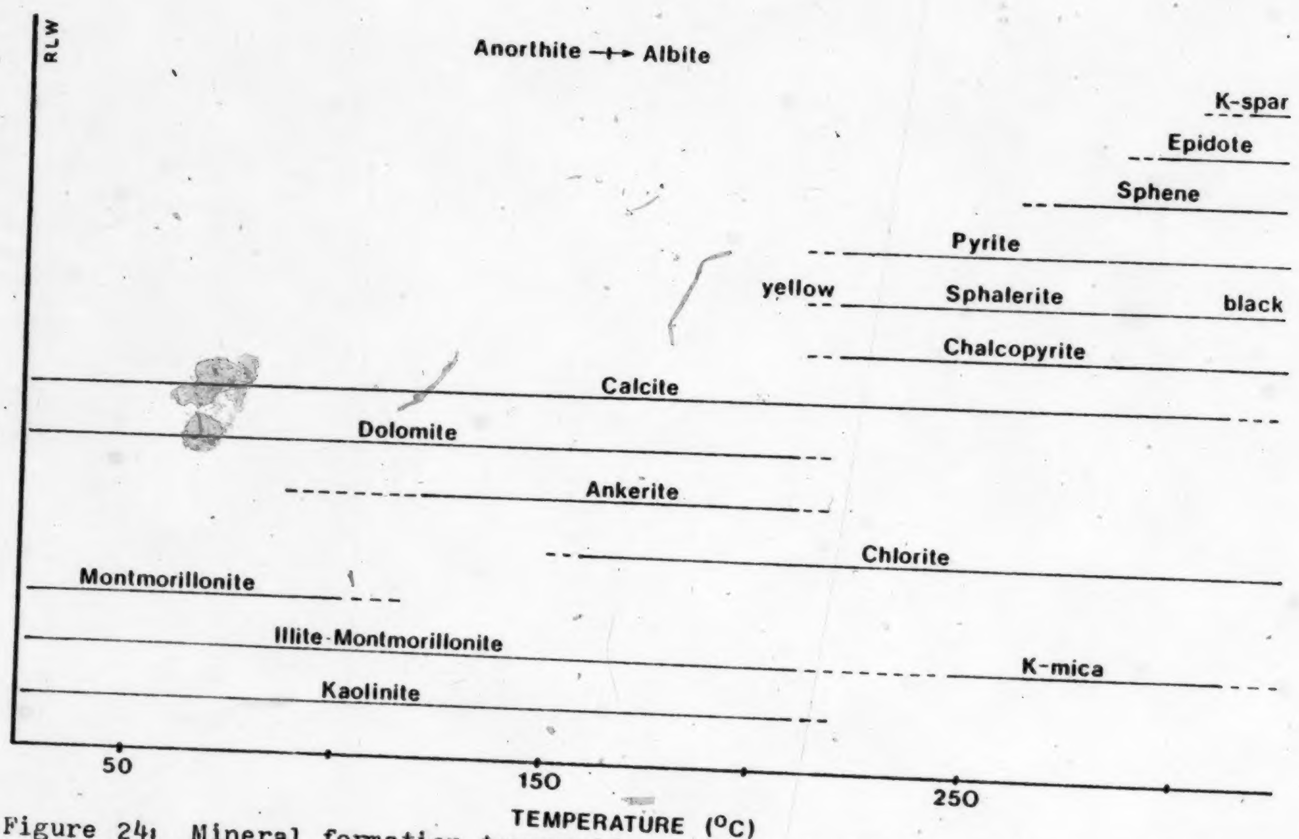

Figure 24: Mineral formation temperatures of the Salton Sea geothermal system (modified after Muffler and White, 1969). Temperatures remain constant over the estimated pressure range of 0.3-1.0 kilobar. Formation temperatures have been inferred directly from bore hole temperature and mineral assemblage determinations from the IID1 and Sportsman No. 1 geothermal wells. Actinolite (not included) occurs with K-spar, epidote and sulfides in high-temperature Salton Sea assemblages. The temperature data is thought to be applicable to similar host rock and vein mineralization of the Northrim etc. veins, at least in relative terms of comparison between similar mineral assemblages.

indicates that temperature decrease may have accompanied mineralization throughout vein deposition.

Temperature decrease may not have been completely steady. Oscillatory banding of chloanthite-skutterudite, cobaltite and safflorite composition may be attributed to fluctuating temperature. The alternation of diarsenide and triarsenide bands in the early Bi-As-S stage would have been related to temperature fluctuation as would the development of hybrid sulfosalt and sulfide assemblages next to granular quartz-silver-skutterudite mineralization. Such hybrid assemblages, oscillatory compositions, and oscillatory banding are insignificant when compared to major assemblages, gradational mineral compositions and simple mineral banding with respect to magnitude, abundance and distribution. They are considered by the writer as small-scale products of hot, deeper-seated brine fluids which were permitted entry to mineralization sites upon tectonically-induced fracture and dilatancy generation. Such entry would also account for the formation of "tear-drops", dendrites and rosettes, features which are formed from quick-cooling supersaturated fluids deposited onto cooler surfaces.

Another major vein control, fracture and dilatancy generation, determined the sites available for mineralization. Fracture and dilatancy generation coincided with vein formation: all phases of vein mineralization, except the lattermost, have been repeatedly fractured, brecciated and split by tensional and shear movements; any openings have been subsequently mineralized. During the first stages of fracture generation, mineral formation did not keep pace with dilatancy creation. The results of this lag were the development of multiple plug-like pods of carbonate, quartz, pitchblende, silver and arsenide mineralization within single stringers and the development of wide dilatancies on the 000 and 014 vein systems which were often filled by single phases of later mineralization. In the middle stages of vein formation, mineral precipitation outstripped dilatancy creation, and successive bands of similar mineralogy, sometimes of rhythmic and oscillatory composition, developed in the smaller vein systems. This continued until the lattermost stages of mineralization and dilatancy generation, when first, mineral precipitation and then brecciation diminished and finally ceased in intensity. The products were sealed, lightly mineralized, open-space vugs, which act as conduits of modern ground and surface waters, after they have been connected by small, non-mineralized fractures.

Pressure conditions during vein formation are not known as precisely as temperature conditions but they must have been very low. Vesicles, comprising up to 35 volume per cent in the center of one basalt, are still recognizable. Closed vuggy cavities, up to 15 centimetres in thickness, exist in the later phases of vein mineralization. Vug assemblage temperatures of formation were less than 176° C., a temperature attained within 5 kilometres depth assuming a normal modern temperature gradient of 3° C./100 metres. The lithostatic pressure would be 1400 bars (rock density ~2.8 g./cc.); the hydrostatic pressure 550-1400 bars (fluid denisty ~1.1 g./cc.). These pressures may be considered as maxima since the geothermal gradient of the ancient continental margin region may have been much greater. The hydrostatic pressure would have been the effective pressure of vein formation since dilatant fracture systems are the hosts of vein mineralization. The pressure probably remained relatively constant throughout vein mineralization since all vapor, all liquid, etc. fluid inclusion mixtures, symptomatic of effervescence induced upon pressure release, have not been observed at the Northrim Mine.

The mineralizing fluid was a saturated brine with 30-35 wt. % NaCl equivalent, a brine like the one responsible for host rock vesicle mineralization. At elevated temperatures and pressures, the mineralizing fluid was probably the carrier of the elements now concentrated into the various vein minerals. The vein minerals would form as various components became saturated in the brine fluid upon temperature decrease. The double period of quartz, arsenide, silver and sulfide deposition may not involve the influx of new mineral components or new hydrothermal fluids since a whole series of molecular/polymeric brine components could have been responsible for the earlier, high temperature periods and a whole series of ionic brine components would have been responsible for the later, lower temperature periods of mineralization. Ionization increases in concentrated solvent-solute fluid systems and polymerization decreases in similar systems under decreasing temperature conditions (Fyfe and Henley, 1973). Temperatures similar to the ones responsible for greenschist facies metamorphism would be accompanied by polymeric and molecular fluids (ibid., 1973). The bulk of the components now present in the veins would have been concentrated in the brine fluids during the higher-temperature greenschist facies conditions and would have been deposited in lower temperature conditions. A similar condition would apply to secondary wall rock mineralization.

Vein fluid migration, expedited by the opening of fracture systems, now the sites of vein mineralization, would have been accompanied by vein fluid migration in the wall rocks, even the relatively impenetrable ores at Northrim. Evidence for this assertion includes the continuity of vein mineralization with secondary host rock mineralization and the presence of the As geochemical halo. Vein fluid migration may have been upwards in the former fracture systems since vein xenoliths, similar in lithology to the wall rocks at Northrim, occur throughout the veins. Vein fluid migration may not have been substantial--the wall rock xenoliths could have been suspended by volatile fluid component migration or another buoyancy mechanism. Fluid components would be expected to migrate from wall rock to vein during fluid formation and from vein to wall rock during vein mineralization. This suggestion is compatible with the highly variable Na, K, As, S and Cu, Pb, Zn concentrations measured in the wall rocks immediately adjacent to the 000 vein structure. (Fig. 8, 9).

The complex geochemistry; the complex mineralogy; the paragenetic sequence of vein mineral and structural events; the tectonically-banded, accretionary dendrite and other textures; the tectonic control of vein formation (cf. telescoping); depositional temperatures of vein mineralization are common to Northrim and other Great Bear veins. The Great Bear veins may be considered as the products of one or two ancient regional geothermal system(s), a system(s) which resembles the modern Salton Sea system in many respects.

CHAPTER 6

THE NORTHRIM, GREAT BEAR AND COBALT-GOWGANDA VEINS

The Cobalt-Gowganda (Ag, Bi, Ni, Co, As) veins are remarkably similar to the mineralized veins of the Northrim Mine. They have been studied much more intensively than the veins of the Great Bear region and a comparative study of the Northrim, Great Bear and Cobalt-Gowganda veins has been undertaken to identify genetic conditions common to these veins of the (Ag, Bi, Ni, Co, As) type.

Mineralization

The multiphase, mineralized veins of the Cobalt-Gowganda mining camp occupy subvertical fractures, joints and faults. The veins are dominated by quartz, calcite and chlorite but subordinate albite, K-feldspar, actinolite, sphene, epidote, hematite, magnetite, anatase and various ore minerals are sometimes present (Jambor, 1971a). The vein minerals fill dilatant fractures which have been repeatedly brecciated during vein mineralization and miarolitic cavities filled with carbonate (Sampson and Hriskevich, 1957) may be found.

The dominant dolomite, calcite, chlorite and quartz gangue of the Cobalt-Gowganda ores is remarkably similar in composition, texture, habit and distribution to the gangue at the Great Bear mines (Halls and Stumpfl, 1969; Jambor, 1971a; Petruk, 1971ac). The identity extends to the economic minerals identified in Cobalt-Gowganda mineralized veins listed on Table 8.. Of the 53 Cobalt-Gowganda minerals, 27 of the commonest have already been identified in the mineralized veins and adjacent wall rocks at the Northrim Mine (this study) and 39 have already been identified in at least one mineralized vein in the Camsell River or Port Radium area (Robinson, 1971; Rojkovic, 1973; Badham, 1973b, 1975). Of all the economic minerals described or implied to be abundant, common or widespread in the Cobalt-Gowganda veins (Petruk, et al., 1971a,b,c), only pararammelsbergite, breithauptite and three-phase silver have not yet been identified in the Great Bear region. These three minerals occur together in a high-temperature assemblage not found in the Great Bear deposits.

The Cobalt-Gowganda minerals are not only similar in details of relative abundance, composition, texture and habit but also occur in assemblages paragenetically similar to the ones of the Northrim Mine and Great Bear region. Early arsenide-dominated assemblages associated with native silver in rosettes, dendrites and masses are followed by sulfosalt- and sulfide-dominated assemblages also accompanied by native silver (Halls and Stumpfl, 1969; Petruk, 1971a,c). Individual mineral grains,

TABLE 8

COBALT-GOWGANDA AND GREAT BEAR ORE MINERALS

Mineral	Formula	Cobalt-Gowganda (1)	Great Bear (2)	Northrim (3)
acanthite	Ag_2S	+ +	+	
aikinite-rezbanyite	$(PbCuBi)S_3$			++
allargentum	(Ag, Sb, Hg)	+		
argentite	Ag_2S	++	++	++
arsenopyrite	$FeAsS$	++	++	++
bismuth	Bi	+	++	++
bismuthinite	Bi_2S_3	+	+	+
bornite	$Cu_{8-9}Fe_{2-1}S_9$	++	++	+
bravoite	$(Fe, Ni, Co)S_2$	+		
brederite	PbAs			+
breithauptite	NiSb	+		
chalcocite	Cu_2S	++	++	
chalcopyrite	$CuFeS_2$	++	++	++
clinosafflorite	$CoAs_2$	+		
cobaltite	(Co, Ni, Fe)AsS	++	++	++
covellite	CuS	+	+	
dyscrasite	Ag_6Sb	+		
emplectite	$CuBiS_2$		+	
freibergite	$(Ag, Cu, Zn, Fe)_{12}(Sb, As)_4S_{13}$	++	++	++
galena	PbS	++	++	++
galenobismutite	$PbBi_2S_4$	+	+	
gersdorffite	NiAsS	+	++	++

TABLE 8 (continued)

gersdorffite (arsenian)	$NiAs_{1.5}S_{0.5}$	+		+
hematite	Fe_2O_3	++	++	++
hessite	Ag_2Te		+	
langisite	$Co_{0.8}Ni_{0.2}As$	+		
loellingite	$FeAs_2$	+	+	+
marcasite	FeS_2	++	++	++
matildite	$AgBiS_2$	+	+	++
maucherite	Ni_7As_6	+	+	
mckinstryite	$Cu_{0.8+x}Ag_{1.2+x}S$	+	+	
millerite	NiS		+	
molybdenite	MoS_2	+	+	
niccolite	NiAs	++	++	++
pararammelsbergite	$NiAs_2$	++		
parkerite	$Ni_3Bi_2S_4$	+		
pavonite	$AgBi_3S_5$	+	+	
pearceite	$Ag_{16}Sb_2S_{11}$		+	
pentlandite	$(Fe, Ni)_9S_8$		+	
pentlandite (cobaltian)	Co_9S_8	+		
polybasite	$Ag_{16}As_2S_{11}$	++	++	+
proustite	Ag_3AsS_3	+	+	
pyrargyrite	Ag_3SbS_3	+	+	+
pyrite	FeS_2	++	++	++
pyrrhotite	$Fe_{1-x}S$	+	+	+
rammelsbergite	$NiAs_2$	++	++	++
safflorite	$(Fe, Co, Ni)As_2$	++	++	++

TABLE 8 (continued)

samsonite	$Ag_4MnSb_2S_6$	+		
siegenite	$(Co, Ni)_3S_4$	+		
silver	Ag	++	++	++
skutterudite	$(Co, Ni, Fe)As_3$	++	++	++
smythite	Fe_3S_4	+		
sphalerite	$(Zn, Fe, Cd)S$	++	++	++
stephanite	Ag_5SbS_4	++	++	
stibnite	Sb_2S_3		+	
stromeyerite	$Cu_{1+x}Ag_{1-x}S$	+	+	
tetrahedrite	$(Cu, Ag, Zn, Fe)_{.2}(Sb, As)_4S_{13}$	++	++	++
ullmannite	$NiSbS$	+		
uraninite	UO_2-UO_3		++	++
violarite	$(Ni, Fe)_3S_4$	+		
wittichenite	Cu_3BiS_2	+	+	
xanthoconite	Ag_3AsS_3	+		

Sources: (1) Halls and Stumpfl (1969); Petruk et al. (1971a, b, c). (2) Bastin (1939); Robinson (1971); Badham (1973b; 1975); Rojkovic (1973). (3) Badham (1973b, 1975); this study.

++ abundant, common and/or widespread.
+ uncommon or rare

Known weathering products have not been listed.

dendrites, rosettes, layers and masses are compositionally and mineralogically zoned: Ni-rich centers are succeeded by Co-rich flanks and finally by Fe-rich rims (Petruk et al., 1971a). Ni-As, Ni-Co-As, Co-As, Co-Fe-As and Fe-As assemblages succeed one another in the paragenesis (ibid., 1971a). Sulfide assemblages include the earlier, higher temperature native silver-pyrargyrite-argentite and the later, lower temperature chalcocite-stromeyerite (Petruk et al., 1971c). The pyrargyrite-stephanite-polybasite assemblages may have been secondary (cf. hybrid) phases of mineralization (Halls and Stumpfl, 1969).

Depositional Conditions

Crustiform, layered, dendritic, botryoidal and compositionally zoned minerals and mineral structures in the Cobalt-Gowganda, Northrim and Great Bear veins indicate that the mineralized veins were products of solutional and not magmatic conditions. Fluid inclusions at Northrim, Echo Bay and Cobalt consist of an aqueous vapor bubble, salt solution and a salt crystal(s) but the foremost and lattermost constituents may be absent in some Cobalt-Gowganda and Northrim fluid inclusions. The solutions were concentrated brines with approximately 30 wt. % NaCl equivalent at all locations (op. cit., 1971; 1973; this study). Pressure-uncorrected filling temperatures (Scott and O'Connor, 1971) of primary fluid inclusions in Silverfields Mine (Cobalt) quartz (T. = 125-275°C.) and late-stage Silverfields Mine cross-veins (T. = 40-120°C.) are similar both to the ones in Echo Bay dolomite and quartz (Robinson and Ohmoto, 1973) and to the ones in Northrim quartz (this study).

Temperatures of Cobalt-Gowganda vein deposition have also been inferred by mineral and mineral assemblage stabilities from successive phases of mineralization (Petruk, 1971a,c). The maximum temperature of vein deposition was 690° C., the upper stability limit for chlorite at 1 kb. (Fawcett and Yoder, 1966); the minimum temperature was less than 93° C., the upper stability limit for stromeyerite (Skinner, 1966). Early high-temperature arsenide assemblages with pararammelsbergite, breithauptite and three-phase silver are succeeded by assemblages composed of minerals characteristic of successively lower temperatures of formation (op. cit., 1971a). The succession of lower temperature assemblages also occurs in the Terra (Badham, 1973b; 1975) and the Northrim (this study) veins. A sharp initial increase in temperature is suggested by Mg enrichment towards the outer edges of chlorite, especially prominent in the earliest stage of vein mineralization (Jambor, 1971c) and by replacement of earlier safflorite and skutterudite assemblages by later pararammelsbergite-bearing assemblages (Hall and Stumpfl, 1969).

Fluid inclusion composition and filling temperatures indicate that the mineralizing fluids of all three vein groups were concentrated brine fluids which were entrapped in vein minerals under similar temperature conditions. Minerals and mineral assemblages diagnostic of formational temperature conditions are similar for all vein groups with one exception: three-phase silver, breithauptite and pararammelsbergite have been found in some early Cobalt-Gowganda assemblages. Inferred temperatures of vein deposition dropped steadily after an initial rise in all vein groups. Inferred lithostatic pressure conditions were probably low since all three vein groups contain vuggy cavities.

It can only be concluded that the Cobalt-Gowganda, Northrim and Great Bear Lake veins were formed from remarkably similar mineralizing brines under similar temperatures and pressures and furthermore, brine composition was remarkably alike throughout the depositional history of the veins of all three groups. Brine compositions would be nearly identical to the ones responsible for (Ag, Bi, Ni, Co, As) type scale formation (Skinner et al., 1967; White, 1968) and regional greenschist metamorphism (Muffler and White, 1969) in the Salton Sea geothermal system.

Cobalt-Gowganda Regional Metamorphism

Mineralized veins of the Cobalt-Gowganda mining camp occur in the Archaean "Keewatin" volcanosedimentary basement, the Helikian "Huronian" sedimentary cover and the intruding "Nipissing" diabase sheets (Table 9). Unlike the Great Bear veins which occur throughout the Camsell River and Echo Bay districts, Cobalt-Gowganda veins are restricted to fractures within Nipissing diabase sheets or in neighboring rocks within 250 metres of diabase contacts. Ni-As, Ni-Co-As, Co-As, Co-Fe-As and Fe-As assemblages generally succeed one another within veins leading away from centers of diabase sheets, both above and below diabase centers (Petruk, 1971c). Inferred diabase wall rock temperatures, based on paleomagnetic evidence, did not exceed $500 \pm 75^\circ$ C. at the bottom of a slate (i.e. argillite) 20-25 feet below the diabase contact in the Silverfields Mine (Symons, 1967; 1970) although wall rock temperatures would have been higher above this level, and fracture temperatures would have been higher below this level during diabase intrusion and subsequent cooling. Paleomagnetic evidence indicates that only the diabase sheet would have heated any mineralizing fluids occupying nearby fractures to temperatures sufficiently high for pararammelsbergite and three-phase silver formation. The relationship between diabase sheets and mineralized veins appears to be both a spatial and a genetic one.

TABLE 9

COBALT-GOWGANDA PRECAMBRIAN

GEOLOGICAL COLUMN

PROTEROZOIC	MINERALIZED VEINS (recrystallized)	
	fractures	
	Keewanawan Diabase Dykes	Elsonian 1370 m.y.
	intrusive contacts	
	MINERALIZED VEINS	
	fractures	
HELIKIAN	"aplites" or "red rock"*	
	alteration contacts	Penokean 2155 m.y.
	Nipissing Diabase Sheets*	
	intrusive contact	
	Huronian Sediments	
	- - - - - - - - - - unconformity - - - - - - - - - - - - - -	
	Matachewan Diabase Dykes	Kenoran 2490 m.y.
	intrusive contact	
	Algoman Granite/Granodiorite Plutons	
ARCHAEAN	intrusive contact	
	Haileyburian Lamprophyre Dikes	
	intrusive contact	
	Timiskaming Sedimentary Sequence	
	- - - - - - - - - - unconformity - - - - - - - - - - - - - -	
	Keewatin Volcanosedimentary Sequence*	

Modified after Jambor (1971b). *Known hosts of mineralized veins.

The Huronian sedimentary and neighboring rocks have undergone regional zeolite/greenschist facies metamorphism. Post-depositional albitization of detrital plagioclase and post-depositional replacement of coarse detritus have been reported by Pettijohn and Bastron (1959). Sporadic patches of carbonate have replaced other minerals in Gowganda Formation sediments (Young, 1969). Tillite matrices are composed of chlorite and albite but no clinopyroxene nor amphiboles have been found in thin sections studied by Young (1969). Some vesicles of prehnite occur in Keewatin volcanic rocks of Casey and Harris Townships, a few miles northeast of Cobalt (Thomson, 1966). Prehnite, pumpellyite, epidote and sphene are found in Nipissing diabase associated with metamorphosed argillites in Henwood Township, east of Elk Lake and north of Cobalt (Jambor, 1971d). Clearly all of the prehnite, pumpellyite and epidote, and much of the albite, chlorite, sphene and carbonate are metamorphogenic and have replaced many detrital minerals once present in rock matrices.

Metamorphic mineralization has been accompanied by changes in rock composition, especially in the Huronian Gowganda Formation (Table 10). Tillite matrices have anomalously high Na_2O and H_2O concentrations but anomalously low K_2O and CaO concentrations. Laminated argillites have similar Na_2O, CaO and H_2O concentrations

TABLE 10

GOWGANDA FORMATION ALKALINE AND WATER ANALYSES

Lithology	Location	Number of Samples	Na_2O	K_2O	CaO	H_2O	Source
laminated argillite	Blind River to Cobalt	9	3.15±0.73	3.36±0.83	1.22±0.69	3.19±0.22	(1)
laminated argillite	Henwood Township	2	1.41, 2.74	2.63, 2.74	-	-	(2)
laminated argillite	Iron Bridge; Cobalt	2	3.99, 4.03	2.62, 1.60	0.53, 0.76		(3)
tillite	Blind River to Espanola	7	5.07±0.57	1.51±0.60	0.62±0.29	2.30±0.35	(1)
tillite	Cobalt to Gowganda	9	4.07±0.42	1.77±0.39	2.15±0.88	3.02±0.64	(1)
tillite ("graywacke")	Silverfields Mine		4.5 - 6.0	0.1 - 0.2	-	-	(2)
arkose	Leith Township	1?	6.47	0.28	-	-	(2)
shales	worldwide	-	1.30	3.24	3.11	5.00	(3)
slates	worldwide	-	1.19	3.69	1.54	4.13	(3)
various rocks*	Canadian Shield	-	3.68	2.82	4.07	1.78	(3)

Sources: (1) Young (1969); (2) Jambor (1971b); (3) Pettijohn and Bastron (1959)

* weighted to include 70% batholithic rocks, 17% volcanic rocks and 13% sedimentary rocks.

and they generally have higher K_2O concentrations except for two argillites collected from Iron Bridge and Cobalt. K_2O concentrations are particularly variable and they are extremely low in tillites from the Silverfields Mine. The only arkose analysed has the lowest K_2O and the highest Na_2O concentrations of any table entry.

Na_2O concentrations and Na_2O/K_2O ratios are higher and CaO concentrations lower than estimated averages of worldwide shales, worldwide slates, worldwide pelites, Precambrian slates, New Zealand argillites, Norwegian varved clays, Canadian Shield rocks and Eastern Canada igneous rocks quoted in Pettijohn and Bastron (1959). The high Na_2O concentrations and Na_2O/K_2O ratios are considered unusual for the two argillites from Iron Bridge and Cobalt since most modern natural muds are composed of clays richer in K than in Na. The high Na_2O concentrations and Na_2O/K_2O ratios coupled with low CaO concentrations found in some argillites are difficult to explain by weathering or by elemental exchange with seawater. The same statement applies to similar concentrations in tillites: "if it is truly a glacial flour, the low CaO content is difficult to explain; if it is a normal sediment, leached of its CaO, then the Na_2O content is an anomaly."[9]

---

[9] Pettijohn and Bastron (1959).

The regionally anomalous Na_2O, K_2O, CaO and H_2O concentrations and the regionally dominant albite-chlorite±carbonate assemblages are most characteristic of Gowganda (Huronian) rocks. Net gains of Na_2O and H_2O and net losses of K_2O and CaO occur in various rocks of the Gowganda Formation, particularly the very units which would have been most permeable (i.e. arkoses, tillites, graywackes) to any hydrothermal fluid which would have mobilized alkaline and other elements involved in mineral-fluid exchange reactions. Such hydrous fluids would be similar to brines which are responsible for greenschist facies mineral formation in the Salton Sea geothermal area where albitization and decalcification of calcic plagioclase is accomplished above 160° C., chloritization of various silicate minerals above the range 125° C. to 180° C. and carbonatization within the range 25° to 290° C. (Schoen and White, 1965; Muffler and White, 1969). Such hydrous fluids could have produced the chill zone aplitic and mineralized vein alterations found in the Nipissing diabase and the alteration zones beside the mineralized veins in the diabase country rocks, probably the mineralized veins themselves.

Nipissing "Contact" Metamorphism

Metamorphism near the contacts of the Nipissing diabase appears quite limited. Contact alteration of country rocks is restricted to an erratic, narrow (2 m.) zone with secondary biotite, muscovite and/or hematite on the country rock side and an erratic, narrow (1 m.) but more intensely altered zone with sericite, albite, chlorite and carbonate on the diabase side of the contacts (Hriskevich, 1968; Jambor, 1971c). Primary (?) diabase chill zone minerals have been replaced by secondary minerals in a regular fashion: labradorite has been replaced first by sericite and then by albite, augite has been replaced by chlorite and all minerals have been overgrown by carbonate towards the country rocks, although labradorite and augite may persist to the very edge of the diabase (op. cit., 1968; 1971c). The erratic nature of contact alteration zones and their characteristic secondary minerals indicate that the diabase magma did not heat nearby rocks to temperatures any higher than the ones associated with greenschist facies metamorphism. The centimetre-wide altered chill zones of the diabase occur next to hectometres upon hectometres of albitized, chloritized and carbonatized wall rocks of the regionally metamorphosed Huronian and Keewatin sequence.

Alteration sequences similar to the ones above also occur in "aplites" (Bastin, 1935) and beside mineralized quartz-carbonate veins. The alterations are particularly prominent in Nipissing diabase hosts and are barely discernible in Huronian and Keewatin hosts since hosts of the latter two designations are composed of secondary minerals identical to the ones of the aplitic and vein alterations themselves (Jambor, 1971c). Quartz and carbonate generally overgrow other secondary minerals, especially in sections adjacent to mineralized veins (Bastin, 1935; op. cit., 1971e).

"Contact" metamorphism in the country rocks of the Nipissing diabase does not seem to result from metasomatic processes. Porphyroblasts and intergrowths (0.5-3.0 cm.) dominated by secondary chlorite, sphene and apatite (cf. spotted alteration), are surrounded by lighter-colored, mafic mineral-deficient "aureoles" (0.1-2 cm.) and this indicates that source material was obtained within a few centimetres of the porphyroblasts (Jambor, 1971d), a conclusion reached for similar chlorite-rich patches at Northrim. Chlorite spot distribution is controlled partly by lamination, grain size and unconformities (i.e. permeability) within the Huronian sediments and in at least one instance chloritic alteration proceeds from the boundary of coarser-grained laminae into finer-grained laminae of a banded argillite (Hall and Stumpfl, 1969). The writer considers the chlorite etc. porphyroblasts products formed from regionally-distributed wall rock fluids upon cooling of the Nipissing diabase. Prophyroblasts have been truncated by vein mineralization (op. cit., 1971d).

Contact metamorphism associated with the Nipissing diabase is much less intensive and much less extensive than regional metamorphism of the country rocks. "Contact" effects are identical to "regional" effects in every respect but the following: spatial association with Nipissing diabase sheets; the development of higher-temperature secondary assemblages containing biotite and amphibole; and the development of large porphyroblasts. All of these "contact" features could have been formed upon regional fluid influx during cooling of the Nipissing magma(s).

The association of (Ag, Bi, Ni, Co, As) vein deposits with regional greenschist facies metamorphism in the Cobalt-Gowganda camp is a constant one. The spatial aspects of the vein-metamorphic association are more consistent than the spatial aspects of the Nipissing diabase-mineralized vein association: mineralized (Ag, Bi, Ni, Co, As) type vein deposits at the Bruce Mines southwest of the Cobalt-Gowganda camp, are spatially associated with a granite, not a diabase, but regional greenschist facies metamorphism occurred at Bruce Mines (Bastin, 1939) just as it did in the Cobalt-Gowganda district. The (Ag, Bi, Ni, Co, As) deposit-greenschist metamorphism association also occurs in the Great Bear mining camp (this study) and the Salton Sea geothermal system (Skinner et al., 1967; Muffler and White, 1969).

Temporal Relationships

Cobalt-Gowganda field relationships have been summarized in Table 9 and Cobalt-Gowganda radiometric dates have been listed in Table 11.

Cross-cutting field relationships indicate that (Ag, Bi, Ni, Co, As) mineralization occurred after the formation of vein alteration zones, "aplitic" alteration zones and Nipissing diabase emplacement. Mineralized veins abut the Cobalt Lake Fault which has displaced one Nipissing diabase sill some 250 feet (Thomson, 1967). The mineralized veins occupy fractures and their attendant alterations in host diabase form zones of regular geometrical form just as similar alterations form aplitic "dykes" (Bastin, 1935). Thus, the mineralized veins, aplitic "dykes" and their adjacent carbonate-impregnated and chloritized diabase alteration zones were not only emplaced after the diabase sill had crystallized but after a minimum 30 metres of fault displacement had occurred along the Cobalt Lake Fault. One can only conclude that late-stage diabasic magma fluids were unlikely to have been the fluids responsible for vein mineralization and vein-related alteration of host

TABLE 11

RADIOMETRIC DATES OF HURONIAN UNITS

Lithology	Unit	Location	Method	Minerals	Age	Event	Source
olivine diabase	Keweenawan	Spragge	Rb-Sr isochron	fd, bi, wr	1205±50 m.y.	Elsonian	(1)
actinolite vein	Keweenawan	Gowganda	K-Ar	?	1465±168 m.y.	Elsonian	(2)
diabase	Keweenawan	Gowganda	K-Ar	?	1400±116 m.y.	Elsonian	(2)
granite	Keweenawan	Eagle Island	Rb-Sr isochron	fd, bi, ms, wr	1475±50 m.y.	Elsonian	(1)
granite	Cutler	Spragge	K-Ar	bi	1300 m.y.	Elsonian (o)	(1)
pegmatite	Cutler	Spragge	Rb-Sr isochron	fd, bi, wr	1750±50 m.y.	Hudsonian	(1)
acidic "dykelet"	Nipissing	Blind River area	Rb-Sr	fd, wr	1700±135±55 m.y.	Hudsonian	(1)
"granophyre"	Nipissing	Blind River area	Rb-Sr	fd	1775, 1805 m.y.	Hudsonian (o)	(1)
"granophyre"	Nipissing	Blind River area	Rb-Sr isochron	wr	2185±50 m.y.	Penokean	(1)
diabase	Nipissing	Espanola to Sault Ste. Marie	K-Ar, Rb-Sr	bi	2095, 2180 m.y.	Penokean	(1)
diabase	Nipissing	Gowganda	Rb-Sr isochron	wr	2162±27 m.y.	Penokean	(1)
diabase	Nipissing	Espanola to Sault Ste. Marie	Rb-Sr isochron	fd, bi, wr	2155±80 m.y.	Penokean	(1)
rhyolite	Huronian	Thessalon	Rb-Sr	wr	1915, 1940, 2065 m.y.	Hudsonian (o)	(1)
sediments, volcanics	Huronian	Sudbury to Espanola	Rb-Sr isochron	wr	1950±100 m.y.	Hudsonian (o)	(3)
sediments	Huronian	Gowganda	Rb-Sr isochron	wr	2288±87 m.y.	Penokean (o)	(3)
gneisses	Algoman	various	K-Ar, Rb-Sr	fd, ms, bi	1715-2155 m.y.	Hudsonian (o)	(1)
pegmatites	Algoman	various	K-Ar, Rb-Sr	fd, ms, bi	2155-2400 m.y.	Penokean (o)	(1)
granites	Algoman	various	K-Ar, Rb-Sr	fd, ms, bi	2400-2700 m.y.	Kenoran	(1)
granite	Algoman	South Lorrain	K-Ar	bi	2525±72 m.y.	Kenoran	(2)
granite	Algoman	Round Lake	Rb-Sr, K-Ar	bi	2550, 2570 m.y.	Kenoran	(4)

Sources: (1) Von Schmus (1965); (2) Jambor (1971b); (3) Fairbairn et al. (1969); (4) Aldrich and Wetherill (1960).
o--metamorphic overprint; fd--feldspar; ms--muscovite; bi--biotite; wr-whole rock.

diabase. No such geological constraints exist for mineralizing fluids present during regional country rock metamorphism.

The relative age relationships inferred from radiometric evidence are consistent with the ones established by field criteria. Kenoran events include the intrusion and subsequent metamorphism of Algoman felsic plutons; Penokean events the intrusion of Nipissing diabase sills and metamorphism of Huronian sediments; Hudsonian events, intrusion of Cutler granites and metamorphism of Nipissing and Huronian sedimentary rocks in the Sudbury-Sault Ste. Marie region and Elsonian events include intrusion of two generations of Keewanawan diabase (Table 11). In the Cobalt-Gowganda region, Penokean radiometric dates predominate and the two generations of granite emplacement, Algoman and Cutler, are not Penokean in radiometric age. The latter generation of granites are absent in the Cobalt-Gowganda region.

Mineralized veins have been dated radiometrically using vein galenas. Model Pb ages for ordinary galenas in mineralized veins average 2280 m.y. and this indicates that the veins were emplaced about the same time as the Nipissing diabase (Thorpe, 1974) and about the same time as Penokean regional metamorphism (this study). Ordinary galenas in sulfide-rich Keewatin and Huronian sediments have similar radiometric ages but one Keewatin galena has been dated at 2805 m.y. (ibid., 1974). Thorpe suggests that the Pb was not leached from the country rocks and favors the diabase as the source of the Pb. This writer favors the Keewatin and Huronian sulfides as the Pb source since country rock metamorphism is both intensive and extensive (this study) and S isotope ratios of both country rock and vein sulfides are quite similar, except for some late stage sulfides with slightly higher ^{34}S values (Petruk, 1971d). The Nipissing diabase itself is not known for its high sulfide content nor do known hydrothermal fluids carry high concentrations of S.

The radiometric evidence indicates that vein mineralization, regional metamorphism and Nipissing diabase emplacement occurred during the Penokean orogeny. Huronian sedimentation occurred before this orogeny and the 20° arc change in paleomagnetic pole directions between Huronian and Nipissing poles indicate that sedimentation would have preceded the orogeny by 10^7 to 10^8 y. if the modern rate of magnetic pole wandering is applicable to Precambrian conditions (Symons, 1967). Radiometric evidence also indicates that the rocks of the Cobalt-Gowganda mining camp were not affected by the Hudsonian nor Elsonian orogenies and their consequent metamorphic regimes. The Hudsonian and Elsonian orogenies occurred in the Sault Ste. Marie-Sudbury part of the

Southern Province but the Grenvillian orogeny did not affect radiometric dates anywhere in the Southern Province. The radiometric evidence supports the writer's contention that vein mineralization, Nipissing diabase intrusion and country rock metamorphism were synchronous events in the Cobalt-Gowganda mining camp. The lack of radiometric isotope reequilibration in the veins and rocks of the Cobalt-Gowganda mining camp indicate that the veins and rocks have not been subjected to temperatures in excess of 150 to 200° C. since the Penokean, except for some veins and rocks truncated by later Keewanawan dykes.

A similar coincidence of regional metamorphism, plutonic emplacement and (As, Bi, Ni, Co, As) mineralization occurs in the Great Bear mining camp. Veins of the Port Radium district have also been truncated by later diabase dykes.

Genesis

The Cobalt-Gowganda vein and wall rock mineral assemblages are the common products of wall rock formational fluids which promoted regional zeolite and greenschist facies metamorphism during the intrusion and subsequent cooling of the Nipissing diabase. The Nipissing diabase magma would have heated these fluids to temperatures somewhat higher than the ones they would have attained under normal geothermal gradients and subsequent cooling of the diabase would have indirectly controlled mineral formation in the adjacent veins and wall rocks.

Fluid inclusion studies indicate that the mineralizing fluids were similar to brines involved in the metamorphism of Salton Sea sediments. The albite, chlorite, K-feldspar and carbonates characteristic of Cobalt-Gowganda wall rock metamorphism are the minerals which constitute the bulk of the gangue in the mineralized veins. Sphene, epidote, actinolite, apatite and prehnite are other metamorphogenic minerals found in the veins but some of these and other minerals mentioned (e.g. garnet, stilpnomelane, allanite) in Jambor (1971a) may have been physically introduced from the host rocks during vein emplacement subsequent to tectonic brecciation, just as similar host rock minerals were introduced to the mineralized veins at Northrim. The albite, K-feldspar and chlorite of the earlier stages and the carbonate of the later stages of vein mineralization are some of the most abundant wall rock minerals. Vein minerals of economic importance are abundant in the wall rocks adjacent to mineralized veins. Thus both wall rock and vein mineral assemblages could have formed simultaneously from the same hydrothermal fluid, almost certainly a brine which had been formed by interaction of formational waters with coexisting wall rock minerals, under temperatures and pressures corresponding to those of zeolite and greenschist facies metamorphism. Evaporitic and seawater sources, usually invoked as a source of alkaline, halide and other elements in ore solutions, are not necessary for Cobalt-Gowganda metamorphic/vein fluid formation, and indeed, evaporites and seawater would be implausible, if not impossible, constituents of the subaerial, periglacial, fluviatile Gowganda Formation and its highly fractured Keewatin volcanic basement.

Metamorphism was not confined to the Keewatin basement and Huronian etc. wall rocks. The Nipissing diabase itself contains characteristically metamorphic minerals. These include carbonate, pumpellyite and prehnite in the ones from Henwood Township and albite, sphene, chlorite and sericite in the ones from the Cobalt and Gowganda areas. These minerals are the metamorphogenic minerals of the Keewatin and Huronian wall rocks but in most diabase sheets, these minerals are confined to the borders, cavities and fractures open to host rock fluid penetration. There are fewer restrictions to metamorphic mineralization in the Huronian and Keewatin country rocks: the Keewatin basement was intensely fractured during the Kenoran orogeny, and the Huronian cover may have been only partially lithified before the generation of metamorphogenic vein fluids.

Only two metamorphogenic mineral structures of the diabase host rocks may be termed "contact" features. These are the narrow, biotitic, hematitic aureoles and the secondary porphyroblasts. The non-metasomatic nature of the latter and the sporadic distribution of the former features indicate that Nipissing diabase intrusion contributed little, if any, material to the parent metamorphic/vein fluid. The Nipissing diabase would merely heat nearby metamorphogenic fluids to temperatures sufficiently high for modification of the geothermal gradient.

Mineralized vein formation was certainly controlled by the Nipissing diabase thermal aureole. Temperatures sufficiently high for formation of the pararammelsbergite-three phase silver-breithauptite assemblage were generally attained only within 25 feet of the Nipissing diabase. Later mineral assemblages of succeedingly lower temperatures of formation would have been deposited upon further cooling of the diabase and surrounding wall rocks. The highest inferred temperature of vein mineralization (690° C.) is less than the estimated crystallization temperature of the Nipissing diabase magma (1200° C.) and hence the diabase had crystallized before the onset of vein mineralization. This conclusion is supported by field evidence: mineralized veins occupy fractures which truncate diabase-wall rock contacts, just as they truncate chlorite porphyroblasts and "aplitic" alteration boundaries.

The Nipissing diabase intrusion would have had time to contract to form the cylindrical and polygonal jointing attributed to cooling during and/or before the onset of vein mineralization.

The intrusion of the Nipissing diabase was a key factor in the genesis of the Cobalt-Gowganda ores but there is other evidence that the Nipissing diabase magma did not introduce the chalcophile and other elements so characteristic of the wall rocks and mineralized veins. Pb isotope studies by Thrope (1974) indicate that remobilization of ordinary Archaean and addition of wall rock radiogenic Pb will account for the Pb isotope ratios observed in ordinary country rock and vein galenas. The similarities in S isotope ratios observed by Petruk (1971d) indicate that early vein sulfides may have been formed simultaneously with wall rock sulfides from the same hydrothermal fluid and that vein S would have been derived from pre-vein wall rock sulfides. The Nipissing diabase itself contains low concentrations of the chalcophile elements so characteristic of the mineralized veins but sulfide-rich Keewatin interflow sediments and andesitic lavas contain appreciable concentrations of these elements (Boyle and Dass, 1971). Some sulfide structures of both the Keewatin and Huronian wall rocks are demonstrably synvolcanic and syndepositional (Hall and Stumpfl, 1969)--hence sulfides were present before intrusion of the

Nipissing diabase. Small carbonate and sulfide stringers analogous to the ones of the Salton Sea and Great Bear Lake regions are locally abundant in the Huronian and Keewatin wall rocks of the Cobalt-Gowganda ores.

The formation of Cobalt-Gowganda, Great Bear and Salton Sea ores are identical in details of process but not always in details of geometrical form. The ancient Cobalt-Gowganda geothermal system differs from the other two geothermal systems (one ancient, one modern) only in the modification of the normal geothermal gradient by horizontally-emplaced diabase magmas.

CHAPTER 7

CONCLUSIONS

Mineralogical Summary

The deposits of the Northrim mine are multi-stage, polyphase veins which occupy dilatancies generated along ENE and ESE fracture systems during the Aphebian (1600-1675 m.y.). The veins are composed dominantly of dolomite, quartz and calcite but various minerals of economic significance are present in variable concentrations. The sulfide minerals chalcopyrite, galena and sphalerite are the most abundant and they occur in all phases of vein mineralization. Silver-bearing phases include native silver, freibergite, matildite, argentite and significant concentrations of Ag (up to 0.4 wt. %) occur in some vein galenas. Ni- and Co-bearing minerals include niccolite, rammelsbergite, safflorite, chloanthite-skutterudite but gersdorffite and cobaltite are also abundant. Bi-bearing phases include matildite, native bismuth and aikinite-rezbanyite (Pb, Bi, Cu)S_3. Uraninite is an uncommon constituent. A rare compound, termed "brederite" in this study, may be a mineral previously undiscovered. The Northrim vein mineralogy resembles the ones of other Camsell River and Echo Bay deposits in details of composition, texture and morphology.

There are two distinct periods of native silver and arsenide mineralization but only one period of sulfosalt and native bismuth mineralization. This also occurs in the Norex veins (Badham, 1973b; 1975). Estimated temperatures of mineralization are 310- 590° C. for the early U-Ag-As stage, 215-271° C. for the late Bi-As-S stage, 176-250° C. for the late Ag-As stage and 210° C. for the vug stage assemblages. Useful criteria for temperature estimation included mineral assemblages, fluid inclusion and sulfur isotope data. The vein temperatures are generally higher than the ones estimated for the Camsell River deposits by Badham (1973b; 1975) and for the Echo Bay deposits by Robinson and Ohmoto (1973). An upwards revision of depositional temperatures may be necessary.

Wall rock metamorphic assemblages include albite, actinolite, biotite, chlorite, sphene, K-spar, epidote, magnetite, hematitem pyrite, chalcopyrite, sphalerite, marcasite, pyrrhotite, galena, quartz, dolomite and calcite. Inferred temperatures of formation are identical to the ones of vein mineralization. The metamorphic mineral assemblages of the Northrim Mine are identical to the ones common throughout the Camsell River and Echo Bay districts. They are also characteristic of greenschist facies metamorphic conditions. Some wall rock primary minerals, still preserved, include some rutile, ilmenite, magnetite, pyrite and calcic plagioclase.

The common volcanic rocks hosting the Northrim veins are labradorite- and pyroxene-porphyritic basalts, lithic lapilli pyroclastic breccias, magmato-pyroclastic flow breccias and poorly-graded lapilli tuffs. The rocks were emplaced under a high-energy, subaerial regime within 1 kilometre of (a) major volcanic vent(s). Syenite and monzonite pyroclasts, especially common in the pyroclastic breccias, were derived from the synvolcanic Rainy Lake pluton at the bottom of (a) magma chamber(s) some 1-2 kilometres stratigraphically below the Northrim datum. Pyroclasts of magnetite and magnetite-rich basalt indicate that magnetite-rich bodies may have been emplaced simultaneously with plutons of the synvolcanic syenite-monzonite suite, a conclusion reached by Badham and Morton (1976) regarding the numerous magnetite-apatite±actinolite lenses of the Camsell River district. The lithological and stratigraphical evidence presented in Chapter 2 supports the conclusions reached by Hoffman et al. (1975, 1976, 1977) concerning the Northrim sequence in specific and the Camsell River volcano-sedimentary pile in general.

The Northrim volcanic rocks may be termed calc-alkaline in every respect but in total alkaline element concentration. Their geochemical composition resembles that of basalts associated with active modern continental margins which overlie subduction zones. Two basalts of the Northrim sequence, also calcalkaline in all respects but in alkaline element concentrations, resemble the ones at the Northrim Mine. The Northrim basalts form a part of the calcalkaline (Badham, 1973a) Camsell River volcano-sedimentary sequence. Basalts at the Terra Mine may have been derived from magmas of alkaline affinity.

The Northrim, Camsell River and Echo Bay rocks have been metamorphosed under advanced greenschist facies conditions to rocks dominated by the metamorphogenic minerals albite, actinolite, biotite, chlorite, K-feldspar, magnetite and sphene. This regional metamorphism was expedited by the influx of heated brine solutions, the products of surficial water influx and of remarkably high geothermal gradients. Such brine solutions were available throughout the ancient Camsell River and Echo Bay districts, and even the predictably impermeable plutonic rocks, have been altered by their passage. Solutional textures (vesicle mineral transitions, mottling, fracture fillings, alteration zones) involving minerals most characteristic of greenschist facies metamorphism are abundant in the volcanic rocks within and are locally common in the plutonic rocks near the Northrim Mine.

The metamorphogenic mineral assemblages and some of their textures are identical to the ones of the Salton Sea geothermal system, a system bathed by brine solutions of surficial and sedimentary provenance, and heated by high geothermal gradients at an unstable continental margin. The terms "hydrothermal", "geothermal" and "metamorphic" are interchangeable with respect to the solutions and minerals of the ancient Echo Bay - Camsell River geothermal system as they are interchangeable in the ancient Salton Sea geothermal system (Muffler and White, 1969).

The exchange (cf. scavenging when transfer is made to the solution), transportation and depositional power of metamorphic brines must have been great. The Northrim sequence "basalts" despite the preservation of most primary textural and compositional features, are no longer the rocks they once were. They probably have lost much of the Ca and Sr they had once contained and they probably have gained more Na, Si, H_2O and CO_2 than they had during their formation. They are dominated by metamorphogenic mineral assemblages. They satisfy all the criteria deemed necessary for the dubious term "spilite". The volcanogenic massive sulfide deposits of the Camsell River (and Echo Bay ?) districts have been so metamorphosed that their primary textures are barely recognizable. The term "fahlbands" may be applied to them since they generally remain conformable with their host rocks despite their metamorphosed appearance. They are not the skarn deposits as suggested by Badham (1975). The Cu- and Fe-rich volcanogenic massive sulfide deposits are probably relicts of much more extensive and varied deposits.

Metamorphogenic mineralization in the volcano-sedimentary rocks almost certainly occurred simultaneously with (Ag, Bi, Ni, Co, As) vein mineralization. Mineralized quartz-carbonate, sulfide-, and metamorphogenic silicate-dominated stringers truncate one another. Metamorphogenic silicate minerals occur in various phases of (Ag, Bi, Ni, Co, As) vein mineralization. Radiometric dates of vein sulfides and metamorphogenic silicates also indicate that mineralized veins were formed during regional metamorphism. The spatial and temporal coincidence is thought to be no accident: the Northrim, Camsell River and Echo Bay veins and wall rock minerals are almost certainly the common products of regional geothermal brine-aquifer mineral exchange activity. The concentration of residual carbonate, quartz and "exotic" minerals in (Ag, Bi, Ni, Co, As) veins is not unusual--they have been observed to precipitate from brine fluids in the Salton Sea geothermal system. The vein mineralization represents the fracture-filled portion of host rock metamorphogenic assemblages.

Geothermal-Metamorphic Model of (Ag, Bi, Ni, Co, As) Vein Formation

The major aspects of the model have been summarized in Figure 25 and have been described in detail within the previous chapters. The model incorporates various geological features and interpretations common to the modern Salton Sea geothermal system and the proposed ancient Great Bear and Cobalt-Gowganda geothermal systems.

Deposits of the (Ag, Bi, Ni, Co, As) association and secondary mineral assemblages of the country rocks are the common products of regional and/or contact zeolite and greenschist facies metamorphism accomplished through host rock mineral interaction with geothermal brines. The brines may act both as catalysts and reactants in reactions leading to the formation of metamorphogenic mineral assemblages and in so doing become saturated with the very elements now concentrated in (Ag, Bi, Ni, Co, As) deposits. Most host rock and deposit mineralization would have occurred during cooling of the goethermal brine system, the so-called retrograde phase of metamorphism.

Certain geological conditions are considered to be necessary for (Ag, Bi, Ni, Co, As) deposit formation. The influx of surficial waters bearing CO_2 appears to be one requirement. H_2O and CO_2 are needed for brine formation and both compounds are substantial components of country rock and deposit mineralization. The incorporation of non-magmatic, surficial water and carbonate are supported by C and O isotopic evidence pertaining to Great Bear carbonate mineralization, by D/H and O isotopic evidence pertaining to Salton Sea brine formation and by H_2O and CO_2 analyses pertaining to Cobalt-Gowganda country rock mineralization. Surficial water influx is characteristic of all modern brine systems: meteoric waters are involved in subaerial and seawaters are involved in submarine systems, even in areas where shallow-seated magmas are thought to be present (White, 1968). Other brine carbonate sources almost certainly include wall rock carbonates but potential sedimentary sources of carbonate were probably absent in the subaerial, periglacial Huronian sediments and the volcano-sedimentary basement of the Cobalt-Gowganda district.

A substantially high geothermal gradient is considered to be another requirement for (Ag, Bi, Ni, Co, As) deposit formation. The geothermal gradient of the modern Salton Sea system is particularly high and the geothermal gradient of the ancient Echo Bay - Camsell River (Great Bear) system must have been similarly anomalous since intense greenschist facies metamorphism appears to be restricted to the Echo Bay and Camsell River districts of the Great Bear region[10]. The geothermal gradient associated with Cobalt-Gowganda metamorphism was modified by diabase magma intrusion and the result-and thermal gradient must have been quite high. High geothermal gradients are thought to be necessary since they will facilitate the formation of concentrated brines at high temperatures and at depths sufficiently shallow to coincide with appreciable surface water inflow. Shallow depths of regional metamorphism and vein mineralization in the Cobalt-Gowganda, Great Bear and Salton Sea environments, are well supported by geological evidence, most notably the occurrence of miarolitic cavities and the preservation of wall rock vesicles.

---

[10] Sub-greenschist facies metamorphism is charac-

Geothermal gradients are generally highest where magmas are closest to surface. The generation of magmas close to surface is directly related to high subsurface temperatures and one may argue whether high geothermal gradients determine the manner and emplacement of magmatic bodies or the rise of magma bodies determine high geothermal gradients. The former argument applies to the ancient Great Bear system since higher temperature mineralized vein assemblages occur with lower temperature vein assemblages in most deposits throughout the Great Bear districts, irregardless of distance from

---

teristic of the Great Bear Batholith region (Hoffman et al., 1975; 1976; 1977) but advanced greenschist facies metamorphism occurs in the Echo Bay and Camsell River districts (this study).

obvious felsic plutons. The mineralized veins of the Cobalt-Gowganda region are restricted to distances within 1000 feet of the Nipissing diabase sheets and higher-temperature vein phases occur in vein sections closer to the Nipissing diabase. Determination of thermal gradient by magma heat is more applicable to the Cobalt-Gowganda situation.

Another requirement for (Ag, Bi, Ni, Co, As) deposit formation is the eventual decline of geothermal temperatures. Such declines occurred in the Great Bear and Cobalt-Gowganda systems since both metamorphogenic wall rock and vein mineralizations were formed at temperatures higher than the ones now present in both regions. (Ag, Bi, Ni, Co, As) pipe scale formation in the Salton Sea system did not occur until drilling altered (lowered) the temperatures in sectors adjacent to precipitation sites within the drill holes. Continuously decreasing temperature conditions occurred in the Northrim, Great Bear and Cobalt-Gowganda sequences of vein mineralization. Retrograde amphibole-biotite-chlorite successions occur in at least the Northrim wall rock assemblages.

Confined or partially confined aquifer systems are also considered necessary for (Ag, Bi, Ni, Co, As) deposit formation. The confinement is thought to be necessary since substantial leakage of thermally-heated fluids through hot springs would ultimately "drain" the geothermal system of many elements necessary for deposit formation. The Salton Sea sand(stone?) aquifer system is partially confined by muddy silt(stone) horizons and appreciable pressure build-ups of CO_2 gas have occurred within the Imperial CO_2 field (White, 1968). Similar conditions are most likely to have occurred in the Great Bear region of the late Aphebian (~1630 m.y.) and in the Cobalt-Gowganda region of the late Archaean (~2200 m.y.). The permeable tuffs, volcanoclastic sediments and pyroclastic breccias intercalated with the more impermeable volcanic lavas and mudstones of the folded Great Bear "homocline", would have made ideal confined aquifer systems. The permeable "graywackes", tillites and conglomerates intercalated with the more impermeable argillites of the Gowganda Formation, would also have made ideal aquifer systems. Permeable rock units were certainly exploited by geothermal fluids in the Salton Sea, Great Bear and Cobalt-Gowganda regions since solutional phenomena involving metamorphogenic carbonate, amphibole, albite, chlorite, biotite, oxide and sulfide mineralization have been identified in all regions (Chapters 2, 3, 5, 6).

Other geological factors, including subarid/arid paleoclimates and subaerial environments, may be necessary for (Ag, Bi, Ni, Co, As) deposit generation. These relate to the formation and preservation of saturated brine fluids. Humid climates would tend to add greater quantities of fresh, meteoric water to aquifer systems and seawater addition to aquifer systems under submarine conditions would tend to be too high in volume. The Cobalt-Gowganda, Great Bear and Salton Sea country rocks were generally deposited in subaerial environments and subaerial conditions seem to have predominated after deposition.

The formation of saturated geothermal brines may not involve rock types of extreme composition in all instances. Neither the periglacial, terrestrial Huronian sedimentary cover nor the highly fractured Keewatin basement rocks of the Cobalt-Gowganda region were likely hosts of bedded carbonate and evaporite deposits. Similar statements concerning evaporites apply to the Great Bear and Salton Sea country rocks. The alkaline and halide elements in the three regions would have been provided by brine fluid interaction with various common silicates and apatite. Connate seawater is another possible source for some alkalies and halides. Decarbonation reactions of limestones during the formation of calcsilicate skarns is a most probable source of some CO_2 in the Salton Sea system but decarbonation reactions of carbonate traces in other rocks may provide that part of the CO_2 not supplied by meteoric water influx.

Primary concentrations of sulfide mineralization, ones existing previous to geothermal brine fluid formation, may be instrumental in the formation of (Ag, Bi, Ni, Co, As) ores. Syngenetic sulfide horizons within the Keewatin basement and basement-derived sulfide clasts exist in the Huronian cover adjacent to the Nipissing diabase. Numerous relict sulfide textures have been reported by Halls and Stumpfl (1969) and high background concentrations of many chalcophilic elements have been reported for sulfide-rich Keewatin basement rocks by Boyle and Dass (1971). These writers conclude that the Keewatin sulfide horizons are the major sources of hydrothermal mineralization concentrated in the mineralized veins, but this writer suggests, on the basis of the predictably greater permeability of the Huronian cover rocks (then sediments ?) and consequently greater susceptibility to passing fluids of any kind, that the Huronian rocks, despite their present, generally chalcophilic element-depleted condition (the most logical conclusion of effective hydrothermal scavenging!) are the major sources of most of the elements now present in the Cobalt-Gowganda mineralized veins.

Volcanogenic massive sulfides exist throughout the Camsell River district and all major (Ag, Bi, Ni, Co, As) veins discovered in the district are hosted in part, by them. These conformable deposits, certainly the stratabound ones at the Northrim, Norex and Terra

Mines, are not the magmatic skarns interpreted by Badham (1973b, 1975) but they have certainly been metamorphosed under tectonic and hydrothermal conditions The dominance of Cu and Fe-bearing sulfides preserved in the volcanogenic deposits are attributed to selective dissolution of the Zn, Cd, Pb, Ag and/or Bi (?)-bearing sphalerite and galena etc. by the metamorphogenic brines ultimately responsible for adjacent (Ag, Bi, Ni, Co, As) vein mineralization. The wall rock Fe-sulfides pyrite (primary and secondary) and marcasite (primary? and secondary) generally retain their crystalline outlines but wall rock chalcopyrite, sphalerite and galena crystal boundaries have been obliterated. Cu, Pb and Zn-bearing sulfides and sulfosalts are far more abundant than pyrite and marcasite in the mineralized veins at the Northrim Mine and the mineralized veins of the Camsell River district contain high concentrations of Cu, Ag, Bi, Co, Sb, As and S, elements hardly concentrated in Salton Sea geothermal brine solutions but elements most highly concentrated in Salton Sea pipe scales! Geochemical evidence is compatible with textural evidence as to the derivation of vein components from sulfide-rich country rocks in the Camsell River district though the action of a heated, wall rock-hosted (cf. geothermal) brine system. Similar "diagenetic" sulfide-rich wall rocks (Robinson, 1971) and sulfide "gossans" exist in the Echo Bay district.

The formation of geothermal brines saturated with respect to chalcophilic elements may not require primary sulfide concentrations. Metamorphic reactions involving silicate minerals "bathed" by geothermal brines, for example the ones of the Salton Sea (Muffler and White, 1969), would be expected to yield various incompatible trace elements during the active stages of reaction. At least the high concentrations of Pb and Zn in Salton Sea brines may be attributed to such reactions.

The composition of plutonic bodies proximally or distally associated with (Ag, Bi, Ni, Co, As) mineralization is irrelevant except, perhaps, with respect to Sn, W and Mo mineralization discussed below. The veins of the Cobalt-Gowganda and the Great Bear mining camps are nearly identical in terms of morphology, mineralogy, composition and paragenesis even though the vein systems of one may be synchronous with diabase intrusions in the former and the other synchronous with felsic intrusion in the other. The composition of the Salton Sea pipe scales are nearly identical with the ones of both vein systems and yet diabase and other mafic magmas are unknown in the Salton Sea Trough. The obvious conclusion: magmas do not generally contribute significant quantities of material to the non-magmatic hydrothermal fluids responsible for vein mineralization but they may act as heat sources which promote brine fluid-mineral element exchange. Even the Nipissing diabase magma may not have contributed appreciable material to the Cobalt-Gowganda veins since vein mineralization formed after diabase crystallization and some vein mineralization formed after movement along the Cobalt Lake Fault had displaced the Nipissing diabase-Huronian host contact some 200 feet. The writer has suggested that metamorphogenic wall rock fluids entered the cooling, post-magmatic Nipissing diabase via fracture systems and along chilled diabase margins and if this did indeed occur, then the deposits of the Cobalt-Gowganda region are composed of material almost completely derived from volcanic and sedimentary country rock material. A hot, mafic magma may have been required to create the thermal conditions suitable for advanced zeolite and greenschist facies metamorphism and concentrated brine formation in the region which was a stable continental hinterland during the Archaean (~2200 m.y.). The Salton Sea and Great Bear deposits occur in continental margin environments which may be related to subduction zone plate activity, a point aptly made by Badham (1976) concerning several (Ag, Bi, Ni, Co, As) deposits.

The role of volcanic and sedimentary country rocks appears to be quite important in deposit formation. The average, primary composition of volcanic and/or sedimentary successors does not seem to determine the existence of (Ag, Bi, Ni, Co, As) vein formation or the existence of regional greenschist facies metamorphism but it seems to influence the relative abundances of the elements and their host minerals ultimately present in the veins and wall rocks, through interaction with the intermediary brine fluids. Low concentrations of Ni in Salton Sea brines and pipe scales is attributable to low concentrations of mafic mineral detritus in the Salton Sea sediments. U, an element abundant in Great Bear veins, is attributable to brine interaction with felsic tuffs and volcanoclastic sediments. An intermediate but varied country rock composition equivalent to that of an andesitic lava or of a shale, may be required for (Ag, Bi, Ni, Co, As) deposit formation but this criterion may not be too discriminating for natural systems, because most volcanic and/or sedimentary rock sequences are of intermediate composition. Plutonic rocks may also contribute material through brine fluid-mineral interaction but this contribution is not as substantial since most plutons are generally more massive, less porous, less permeable and less fractured than volcanic and sedimentary cover rocks.

Another requirement, not thought to be necessary for (Ag, Bi, Ni, Co, As) deposit formation but for vein formation, is the coincidence of waning geothermal activity with tectonic fracture generation. Tectonic stress is necessary to create the fracture sites of vein formation and waning geothermal activity is required to encourage precipitation of various components in concentrated brine fluids. Fracture generation will also provide channel ways permitting deeper-seated, more concentrated brines to rise to levels sufficiently cool enough for vein mineral precipitation. The Salton Sea pipe scales in particular, formed because the natural geothermal gradient was disturbed along the drill holes and hotter, deeper-seated, more concentrated brine components rose in the open holes to the cooler sites of present pipe scale mineralization. Wall rock metamorphic/hydrothermal fluids, sometimes termed formational waters, are often confined at pressures equalling or exceeding load pressures and such fluids would generate their own dilatancies even if "split" or "pull apart" tensional stress systems were not operating during brine cooling. The lack of tectonically-imposed weaknesses would preclude the development of veins but not of disseminated deposits containing the elements characteristic of the (Ag, Bi, Ni, Co, As) association. Disseminated deposits of this association would tend to be of lower grade than vein deposits since brine fluid flow would not be confined to one set of planar fractures but higher grade deposits may occur wherever primary concentrations of these elements had existed before the development of secondary fluid systems. The Hg haloes commonly surrounding sulfide deposits are probably the lower temperature phases of such secondary deposits. Similar meta-hydrothermal origins have been proposed for small satellite (Ag, Bi, Ni, Co, As) veins associated with massive sulfide deposits at Broken Hill, Australia and 'fahlbands' at Kongsberg, Norway (Halls and Stumpfl, 1972).

The model developed and described above seems to be consistent with all the mineralogical, geochemical, textural, paragenetic, radiometric, stratigraphic and structural evidence concerning the genesis of the Northrim, Great Bear, Salton Sea and Cobalt-Gowganda (Ag, Bi, Ni, Co, As) veins. It incorporates many of the ideas and interpretations common to many researchers but many of these ideas and interpretations have never been applied systematically to studies of the genesis of the (Ag, Bi, Ni, Co, As) veins. The model appears to be a reasonable but crude first approximation of the events leading to vein formation in the deposits studied within the thesis, but there may be some deposits which do not fit the model. The Hercynian (Ag, Bi, Ni, Co, As) deposits, ones not studied in great detail within the thesis, will be considered briefly.

The Hercynian Cornwall and Erzegebirge (Bohemian) deposits have substantial Sn, W and Mo concentrations not found in the Great Bear, Cobalt-Gowganda and Salton Sea deposits. The polyphase Cornwall Sn, W and Mo mineralization is present at depth and estimated temperatures of formation (500-575° C.) exceed the ones (< 150-500° C.) of native silver, arsenide, sulfide and fluorite mineralization present at shallower depths (Stanton, 1972). Erzegebirge Sn-W, Au-quartz and Mo mineralized phases are the earliest ones to be formed: they are succeeded in turn by quartz-base metal, pitchblende-quartz-calcite, and Ag-Sb-carbonate assemblages which occupy Hercynian fracture systems; the later succession of base metal sulfide-quartz-barite-fluorite, arsenide-native metal and Ag-Hg-carbonate-sulfosalt assemblages occupy the later Saxonic fracture systems (Badham, 1976). All the Erzegebirge and Cornwall mineralized phases are considered by most authorities to be the products of either mafic or felsic magmas but Halls and Stumpfl (1969) consider all single sources of vein mineralization suspect since the emplacement of the structurally and temporally distinct polyphase assemblages of both regions spans the period from the late Carboniferous to the late Tertiary. This writer suspects that all assemblages but the ones containing Sn-W and Mo-bearing minerals were derived from metamorphogenic fluids of vein provenance since the "all but one" group of assemblages present in the Cornwall and Erzegebirge regions are remarkably similar to the ones studied in great detail within the thesis. The geothermal-metamorphic genetic model is also supported by the occurrence of regional low pressure, high temperature (greenschist facies) metamorphism in rocks of the Hercynian orogen (op. cit., 1976). It is most significant that spilitic basalts and keratophyric andesites of Devonian age, including the ones hosting mineralized veins in Cornwall and Devonshire, are characteristic of the Hercynian orogenic belt(s) (Juteau et Rocci en Amstutz, 1974). The geothermal/metamorphic model of brine formation and vein deposition appears to be applicable to the genesis of the Hercynian deposits.

The proposed genetic model (Fig. 25) may apply to almost all (Ag, Bi, Ni, Co, As) vein systems. The collection or "scavenging" phase involves the conversion of meteoric to formational and ultimately to saturated brine fluids through interaction with aquifer minerals under shallow-seated prograde (increasing) and retrograde (decreasing) temperature conditions. The later deposition or "mineralization" phase involves the formation of metamorphogenic minerals under prograde conditions and the formation of metamorphogenic mineralization in both permeable wall rocks and fracture systems under retrograde conditions. The opening of fracture systems would

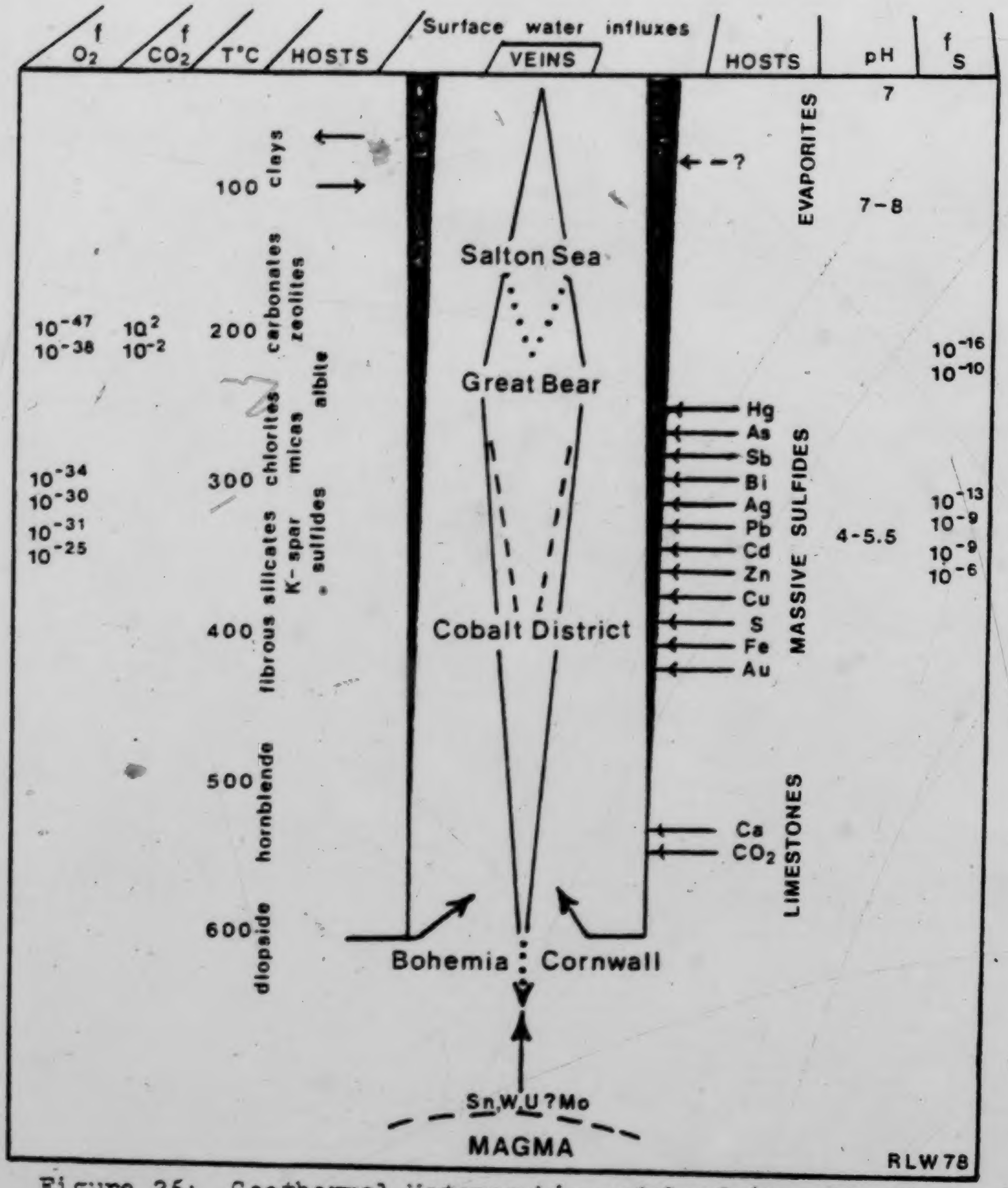

Figure 25: Geothermal-Metamorphic model of (Ag, Bi, Ni, Co, As) vein formation (rough sketch). Many of the major physical and chemical conditions of greenschist etc. metamorphism are indicated on the diagram. Metamorphogenic mineral products are included under the host column to the left of and rock types of extreme composition under the host column to the right of the vein column. Much of the discussion included in Chapters and pertains to the model. The writer expects that better and more complete models will be presented by more experienced researchers in the near future.

accompany upwards movement of volatile brine components and continued brine component flow would concentrate specific mineralized phases at specific levels.

Summary Statement

A general-case geothermal/metamorphic genetic model seems to apply to all the (Ag, Bi, Ni, Co, As) deposits studied by the writer. Some ideas incorporated within the model, most notably the ones concerning lateral secretion, have been applied to the Cobalt-Gowganda (e.g. Halls and Stumpfl, 1969) and to the Great Bear (Robinson, 1971) deposits but little reference has been made to the crucial studies of researchers involved with the Salton Sea geothermal system, e.g. Muffler and White (1969) and consequently the role of intense, regional/contact greenschist facies metamorphism associated with most, if not all, (Ag, Bi, Ni, Co, As) veins has been virtually ignored.

Present misconceptions concerning the genesis of the (Ag, Bi, Ni, Co, As) vein deposits are attributable to the lack of knowledge concerning and the consequent underestimation of the contribution of meteoric and other surface waters to zeolite and greenschist facies metamorphism, the scavenging potential of such waters with respect to the components which are concentrated within resultant geothermal brines and the tendency of all brine solutions to lose various components at various rates upon temperature decrease with subsequent lowering of the geothermal gradient. The invocation of hypothetical, special or mythical magmatic conditions to cover gaps and inconsistencies in our knowledge concerning these deposits adds little to a proper evaluation or to our understanding of the genesis(es). The role of magmatic fluids in the formation of (Ag, Bi, Ni, Co, As) deposits appears to be negligible except, perhaps, with respect to Sn, W, Mo, and some U-bearing mineralization of high-temperature phases which are spatially and temporally related to felsic plutons but which are either rare or absent in rocks adjacent to mafic plutons. The geneses of the (Ag, Ni, Bi, Co, As) deposits considered here are remarkably similar to one another in terms of process but not necessarily in terms of geometrical form.

The model presented above suffers from numerous defects due to the complexity of the metamorphic processes indicated by various lines of evidence and to the inexperience of the writer as a researcher. Nevertheless, the writer considers the model as a crude but necessary approximation of the natural conditions truly responsible for deposit formation of the (Ag, Bi, Ni, Co, As) association. Perhaps the model will indicate more appropriate directions of research not apparent to the writer.

APPENDIX I

MAJOR OXIDE AND TRACE ELEMENT ANALYSES

All X-ray fluorescence analyses were performed in the laboratories of Dr. J. G. Holland of the University of Durham, England. Corrections of analytical values were made using the procedures of Holland and Brindle (1966). Analytical values quoted in the tables were well in excess of the lower detection limits for the procedure employed on a Phillips 1212 X-ray fluorescence spectrometer.

The analytical values were normalized on a CO_2- and H_2O-free basis and fed into a computer program, "Normcal", developed by Dr. R. C. O. Gill. The various petrochemical functions were calculated using the X-ray fluorescence data.

The detection limit of As was 5 ppm; many samples had lower concentrations of this element. Sample distribution of concentrations in some elements appeared to be bimodal and averages were computed from the element concentrations closest to the value of the major peak.

TABLE A-1

TABLE OF VOLCANIC ROCK ANALYSES: MAJOR OXIDES AND SULFUR

Sample	SiO_2	Al_2O_3	Fe_2O_5	FeO	MgO	MnO	TiO_2	CaO	Na_2O	K_2O	P_2O_5	S
1	52.02	15.06	2.79	7.69	7.55	0.35	0.99	7.90	2.62	2.66	0.30	0.07
2	53.69	18.25	3.11	8.58	4.07	0.30	0.95	2.20	7.02	0.57	0.43	0.81
3	42.75	19.52	4.81	13.17	9.16	0.14	0.87	1.46	3.77	3.15	0.42	0.75
4	52.90	18.53	3.26	8.98	4.45	0.17	0.90	1.17	6.62	1.31	0.39	1.28
5	53.94	17.65	3.58	9.82	2.98	0.07	0.80	0.57	6.96	0.66	0.35	2.51
6	49.31	18.72	4.34	11.92	6.06	0.15	0.94	0.85	5.14	0.63	0.45	1.43
7	44.24	20.63	4.35	11.92	11.03	0.12	0.82	1.71	4.27	0.44	0.40	0.08
8	42.07	17.62	4.88	13.35	12.11	0.15	0.98	1.01	2.60	4.83	0.29	0.10
9	47.08	18.08	4.35	11.96	7.10	0.19	0.83	0.53	5.87	1.07	0.37	2.48
10	43.98	20.13	4.57	12.53	10.86	0.18	0.96	1.22	3.99	0.80	0.41	0.37
11	39.78	16.44	4.98	13.60	13.86	0.29	0.92	1.65	1.65	6.48	0.24	0.10
12	50.13	17.96	3.42	9.41	7.62	0.05	0.85	1.10	5.68	2.87	0.39	0.52
13	51.47	16.66	3.73	10.25	5.20	0.12	0.69	4.12	5.98	0.35	0.38	1.02
14	47.64	19.44	4.08	11.19	8.49	0.11	0.86	1.86	5.46	0.37	0.44	0.07
15	56.15	16.89	2.47	6.82	4.61	0.10	0.85	4.19	7.07	0.26	0.47	0.11
16	52.65	17.78	1.89	5.22	5.66	0.43	1.09	4.30	0.21	10.04	0.43	0.30
17	45.18	18.57	4.34	11.90	8.41	0.08	1.17	1.11	4.24	3.88	0.36	0.74
18	52.73	17.23	3.52	9.66	3.69	0.17	0.94	2.80	6.31	1.14	0.35	1.41
19	55.65	17.38	2.39	6.59	4.67	0.19	0.87	3.94	6.83	0.94	0.44	0.12
20	47.74	19.01	3.89	10.67	8.09	0.09	0.89	1.38	5.12	2.64	0.41	0.07
21	49.20	19.09	3.39	9.33	9.70	0.17	0.84	2.18	3.79	1.74	0.41	0.15
22	39.58	21.82	5.14	14.05	13.24	0.13	0.98	0.66	2.62	1.10	0.39	0.28
23	49.62	17.56	4.85	13.27	4.50	0.13	0.80	1.13	4.73	1.14	0.34	1.85
24	51.31	18.57	3.47	9.54	6.73	0.13	1.09	2.15	3.77	2.72	0.43	0.09
25	51.26	17.36	4.42	12.10	3.15	0.05	0.72	0.45	6.30	0.56	0.31	3.17
26	53.85	17.29	3.30	9.06	4.24	0.09	0.67	2.69	7.00	1.03	0.36	0.43
A1	49.05	17.04	4.21	11.55	6.30	0.06	1.01	0.97	5.18	4.26	0.30	0.07
A2	48.84	14.68	3.89	10.67	6.75	0.15	0.95	9.23	3.35	1.08	0.31	0.09
A3	49.46	16.64	3.65	10.06	5.08	0.20	1.01	5.79	4.22	2.77	0.28	0.83

Analyst: Dr. Grenville Holland, University of Durham.

All entries are weight percentages. The calculations were performed on a CO_2- and H_2O-free basis and the sums of all oxide weight percentages for any given sample has not been normalized to 100 weight percent. Underlined entries have been discarded in the calculation of a revised average composition in Table 2.

TABLE A-2

TABLE OF VOLCANIC ROCK ANALYSES:

MINOR ELEMENTS

Sample	Rb	Sr	Ba	Cr	Ni	Cu	Zn	Pb	ΣCuZnPb	As	Y	Zr	Nb	Nb/Y	Zr/P_2O_5
1	135	512	1146	152	25	19	280	8	297	5	21	114	6	0.28	.038
2	19	59	58	101	5	256	8004	1305	9565	37	22	109	5	0.23	.025
3	135	102	470	87	22	408	168	19	595	246	14	93	2	.14	.022
4	51	94	172	85	24	710	7765	1196	9671	425	18	104	7	.39	.027
5	14	36	48	81	18	1960	232	591	2783	290	16	102	0	0	.029
6	16	48	82	124	13	259	11452	101	11812	218	20	106	4	.2	.024
7	29	70	76	134	5	8	244	11	263	5	15	114	7	.47	.029
8	271	31	315	81	11	58	251	26	335	23	15	89	6	.4	.031
9	29	25	57	81	39	1320	58000	2474	61794	328	16	91	6	.38	.025
10	30	38	127	170	8	432	214	35	681	12	22	95	5	.23	.023
11	366	20	339	74	8	43	211	66	320	5	20	83	4	.2	.035
12	177	50	163	119	4	611	109	7	727	5	14	103	4	.28	.026
13	220	53	38	130	10	3210	153	35	3398	5	21	94	4	.15	.025
14	23	48	48	163	15	31	80	4	115	5	20	120	1	.05	.027
15	11	66	40	194	16	10	62	4	76	5	25	117	5	.2	.025
16	211	20	303	191	14	2480	298	5	2783	5	23	106	6	.26	.025
17	227	54	316	191	19	209	82	38	329	5	20	110	2	.10	.031
18	28	28	69	231	9	1310	5554	2550	9414	5	27	103	4	.15	.029
19	19	47	55	207	8	244	127	27	398	5	18	109	7	.39	.025
20	163	81	211	145	19	30	101	3	134	5	16	102	4	.25	.025
21	34	24	53	153	13	121	343	6	470	5	16	101	4	.25	.025
22	36	42	155	163	32	10	204	13	227	246	10	113	2	.2	.029
23	23	28	114	70	23	664	615	272	1551	5	19	86	4	.21	.025
24	111	239	1235	94	17	20	79	3	102	5	23	107	6	.26	.025
25	13	34	62	88	78	8100	79	59	8233	261	14	96	0	0	.031
26	55	78	83	112	7	199	93	12	304	5	37	119	6	.16	.033
A1	334	122	248	129	15	6	146	2	154	5	15	108	5	.33	.036
A2	53	341	299	131	16	27	108	2	137	5	22	103	5	.23	.033
A3	100	246	800	155	25	150	249	244	643	72	22	108	3	.14	.038

Analyst: Dr. Grenville Holland, University of Durham.

All entries are parts per million (ppm). In addition several other elements were analyzed but were not detected in any sample. These elements were U (detection limit 2 ppm), Th (4 ppm), and Bi (detection limit 4 ppm). Co was not analyzed for the atomic absorption method yields inaccurate results at the Co levels expected. (Dr. Roger Morton, personal communication.)

Underlined entries are those discarded in the revised trace element compositions of Table 4.

TABLE A-3

PETROCHEMICAL FUNCTIONS OF VOLCANIC HOST ROCKS

Sample	$Na^+ + K^+ / Al^{+3}$	$Na^+ / Na^+ + K^+$	MgO/ MgO + FeO	Qz + Ab + Or	Cpx + Ol + Opx + Mt + Il + Ap	Olivine		Ortho-pyroxene		Clinopyroxene			Feldspar		
						Fo	Fa	En	Fs	Wo	En	Fs	Or	Ab	An
N1	0.48	0.60	0.70	37.8	40.45	61.70	38.30	63.47	36.53	51.42	31.08	17.50	26.46	37.30	36.24
2	0.67	0.95	0.58	62.2	23.58	49.11	50.89	51.44	48.56	-	-	-	4.76	83.79	11.46
3	0.49	0.64	0.64	46.4	38.16	55.44	44.56	-	-	-	-	-	39.89	50.44	9.68
4	0.66	0.88	0.63	63.0	24.11	54.15	45.85	56.57	43.43	-	-	-	11.55	83.60	4.85
5	0.69	0.94	0.63	64.8	20.32	-	-	56.02	43.98	-	-	-	6.18	92.99	0.83
6	0.49	0.93	0.61	48.3	36.18	-	-	54.82	45.18	-	-	-	7.66	89.70	2.64
7	0.36	0.94	0.68	38.7	44.22	59.51	40.49	61.88	38.12	-	-	-	5.79	81.02	13.19
8	0.54	0.45	0.68	44.3	45.22	59.26	40.74	-	-	-	-	-	71.02	21.16	7.82
9	0.60	0.89	0.71	54.7	29.06	62.94	37.06	65.32	34.68	-	-	-	11.26	88.41	0.33
10	0.37	0.88	0.68	38.3	45.51	59.37	40.63	61.72	38.28	-	-	-	11.23	80.63	8.14
11	0.59	0.28	0.70	40.0	48.76	61.58	38.42	-	-	-	-	-	62.97	0.00	37.03
12	0.69	0.75	0.68	61.3	29.49	60.01	39.99	-	-	-	-	-	28.05	67.11	4.84
13	0.61	0.96	0.60	52.2	26.66	50.41	49.59	52.71	47.29	48.50	24.25	24.25	2.92	72.06	25.05
14	0.48	0.96	0.64	48.3	37.31	54.98	45.02	57.35	42.65	-	-	-	3.95	54.43	11.63
15	0.71	0.98	0.63	61.3	24.74	53.92	46.08	56.42	43.58	50.84	27.62	21.54	2.07	79.80	18.13
16	0.63	0.03	0.75	60.4	20.64	67.83	32.17	-	-	51.07	34.04	14.85	76.21	0.78	23.01
17	0.60	0.62	0.66	53.2	34.68	57.42	42.58	-	-	-	-	-	45.34	48.35	6.30
18	0.67	0.89	0.57	59.3	22.70	47.93	52.07	50.36	49.64	-	-	-	9.38	74.43	16.19
19	0.71	0.92	0.64	63.2	22.36	54.91	45.09	-	-	50.93	28.24	20.83	7.18	74.73	18.09
20	0.59	0.75	0.64	55.5	33.84	55.26	44.74	-	-	-	-	-	27.94	64.64	7.52
21	0.43	0.77	0.71	42.3	41.03	63.20	36.80	65.40	34.60	-	-	-	20.38	63.47	16.15
22	0.25	0.78	0.69	28.6	53.57	60.82	39.18	63.01	36.99	-	-	-	22.11	75.32	2.57
23	0.51	0.86	0.52	49.4	33.33	-	-	45.63	54.37	-	-	-	13.42	79.86	6.72
24	0.49	0.68	0.63	47.9	37.34	53.85	46.15	56.65	43.35	-	-	-	28.83	57.08	14.10
25	0.63	0.94	0.59	59.2	22.96	-	-	51.80	48.20	-	-	-	5.88	93.80	0.32
26	0.73	0.91	0.54	63.7	23.13	45.24	54.76	-	-	-	-	-	8.26	76.71	15.03
A1	0.77	0.65	0.56	62.0	32.01	47.14	52.86	-	-	-	-	--	44.46	50.52	5.02
A2	0.45	0.83	0.60	34.6	43.18	50.77	49.33	53.38	46.62	50.66	26.23	23.11	11.24	50.11	38.65
A3	0.60	0.70	0.59	48.9	29.90	49.97	50.03	-	-	50.63	25.91	23.46	25.41	46.13	28.46

The first three columns are ratios comparing components in molecular proportions, the next two columns are sums of normative minerals in weight percentages, the following two columns are resolved components of normative olivine in weight proportions, the next two columns are resolved components of normative orthopyroxene in weight proportions, the next three columns are resolved compositions of normative clinopyroxene in weight proportions and the last three columns are resolved compositions of normative feldspar. The $Na^+ + K^+/Al^{+3}$ ratio is also known as the peralkalinity index, the (Qz + Ab + Or) sum may be termed the differentiation index and the (Ol + Cpx + Opx + Mt + Il + Ap) sum is the color index for these analyses.

Figures underlined are discarded in calculating the revised averages of Table A-4.

TABLE A-4

NORMATIVE MINERALS AND PETROCHEMICAL FUNCTIONS

OF VOLCANIC HOST ROCKS

Mineral	Mean	Standard Deviation	Mean	Standard Deviation	Rejection Level	No. of Analyses
Qz	0.5	1.1	0.5	1.2	-	29
Cd	5.0	4.0	5.3	4.1	-	29
Or	11.6	11.5	10.3	7.2	> 5% K_2O	27
Ab	37.0	16.6	42.0	13.8	< 5.0	27
An	7.7	6.5	4.8	3.3	> 12.0	22
Lc	0.7	3.8	0	0	> 0	28
Ne	1.6	2.6	1.5	2.5	< 2% Na_2O	27
Cpx	1.5	4.0	1.6	4.0	-	29
Opx	8.3	9.2	8.8	9.3	-	29
Ol	15.3	10.4	16.2	10.4	-	29
Mt	5.5	1.1	5.8	1.1	-	29
Il	1.7	0.2	1.8	0.2	-	29
Ap	0.8	0.1	0.9	0.1	-	29
Py	2.7	3.0	0.4	0.1	> 1.0	12
TOTAL	100.0		100.0			
$Na^+ + K^+/Al^{+3}$	0.57	0.12	0.57	0.12	-	29
$Na^+/Na^+ + K^+$	0.77	0.21	0.81	0.14	< 0.40	27
MgO/MgO + FeO	0.63	0.06	0.63	0.06	-	29
DI	49.7	13.7	49.7	13.7	-	29
CI	33.3	9.2	33.3	9.2	-	29

Program: Normcal by Dr. R. C. O. Gill.

All normative mineral entries are weight percentages. D.I. refers to the differentiation index, in this instance the normative (Qz + Ab + Or); C.I. refers to the color index, in this instance the normative (Cpx + Opx + Ol + Mt + Il + Ap). Average values refers to the average of individual normative values for the 29 samples collected. Revised average values pertains to the same samples but anomalous values have been discarded in the manner stated in the text.

BIBLIOGRAPHY

AHRENS, L. H. and ERLANK, A. J., 1972. Bismuth. In Wedepohl, K. H. (ed.). Handbook of geochemistry, Springer Verlag, Heidelberg.

AMSTUTZ, G. C. and PATWARDHAN, A. M., 1974. A reappraisal of the textures and the composition of the spilites in the Permo-Carboniferous Verrucano of Glarus, Switzerland. In: Amstutz, G. C. (ed.). Spilites and spilitic rocks, Springer Verlag, Heidelberg, 484 pp.

BAADSGAARD, H., 1965. Geochronology. Medds. fra Dansk. Geol. Foren. 16, 1-48.

BADHAM, J. P. N., 1972. The Camsell River - Conjuror Bay area, Great Bear Lake, N. W. T. Can. Jour. Earth Sci. 9, 1460-1468.

——————, 1973a. Calcalkaline volcanism and plutonism from the Great Bear Batholith, N. W. T. Can. Jour. Earth Sci. 10, 1319-1328.

——————, 1973b. Volcanogenesis, orogenesis and metallogenesis, Camsell River area, N. W. T. Unpubl. Ph. D. Thesis, University of Alberta, 334 pp.

——————, 1975. Mineralogy, paragenesis and origin of the Ag-Ni, Co arsenide mineralisation, Camsell River, N. W. T. Miner. Dep. 10, 153-175.

——————, 1976. Orogenesis and metallogenesis with reference to the silver-nickel-cobalt arsenide ore association. In: Strong, D. F. (ed.) Metallogeny and plate tectonics. Geol. Assoc. Cda. Spec. Pap. 14, 559-571.

——————, ROBINSON, B. W. and MORTON, R. D., 1972. Geology and genesis of the Great Bear Lake silver deposits. 24th Intern. Geol. Congr., Montreal, Sect. 4, 541-547.

——————, and MORTON, R. D., 1976. Magnetite-apatite intrusions and calcalkaline magmatism, Camsell River, N. W. T., Can. Jour. Earth Sci, 13, 348-354.

BASTIN, E. S., 1935. "Aplites" of hydrothermal origin associated with Canadian cobalt-silver ores. Econ. Geol. 30, 715-734.

__________, 1939. The nickel-cobalt-native silver ore-type. Econ. Geol. 34, 1-40.

BATTEY, M. H., 1974. Spilites as weakly metamorphosed tholeiites. In Amstutz, G. C. (ed.). Spilites and spilitic rocks, Springer-Verlag, Heidelberg, 484 pp.

BELL, J. M., 1900. Topography and geology of Great Bear Lake. Geol. Surv. Canada, Ann. Rept. XIIIC, 5-28.

BILLINGS, G. K., HITCHON, B. and SHAW, D. R., 1969. Geochemistry and origin of formation waters in the Western Canada sedimentary basin, 2. Alkalimetals. Chem. Geol. 4, 211-223.

BOYLE, R. W., 1968a. Fahlbands, sulfide schists and ore deposition. Econ. Geol. 63, 835-840.

__________, 1968b. The geochemistry of silver and its deposits. Geol. Surv. Cda. Bull. 160, 264 pp.

__________, and DASS, A. S., 1971. Origin of the native silver veins at Cobalt, Ontario. Can. Mineral. 11, 414-417.

CAMPBELL, D. D., 1957. Port Radium Mine. In: Structural geology of Canadian ore deposits (Vol. II), 6th Commwlth. Min. Metall. Congr., 177-189.

CHAYES, F., 1966. Alkaline and subalkaline basalts. Amer. Jour. Sci. 264, 128-145.

CLAYTON, R. N. and EPSTEIN, S., 1958. The relationship between O_{16}/O_{18} in co-existing carbonates and iron oxides from various geological deposits. Jour. Geol. 66, 352-373.

__________, MUFFLER, L. J. P. and WHITE, D. E., 1968. Oxygen isotope study of calcite and silicates of the River Ranch well, Salton Sea geothermal area, California. Amer. Jour. Sci. 266, 968-979.

CRAIG, H., 1957. Isotopic standards for carbon and oxygen and correction factors for mass spectrographic analysis of carbon dioxide. Geochim. Cosmochim. Acta. 12, 133.

__________, 1966. Isotopic composition and origin of the Red Sea and Salton Sea geothermal brines. Sci. 154, 1544-1548.

CRAIG, J. R., 1967. Phase relations and mineral assemblages in the Ag-Pb-Bi-S system. Mineral. Dep. 1, 278-306.

COOMBS, D. S., 1974. On the mineral facies of spilitic rocks and their genesis. In: Amstutz, G. C. (ed.). Spilites and spilitic rocks, Springer Verlag, Heidelberg, 484pp.

DOE, B. R., HEDGE, C. E. and WHITE, D. E., 1966. Preliminary investigation of the source of lead and strontium in deep geothermal brines underlying the Salton Sea geothermal area. Econ. Geol. 61, 462-483.

FAIRBAIRN, H. W., HURLEY, P. M., CARD, K. D. and KNIGHT, C. S., 1969. Correlation of radiometric ages of Nipissing diabase and Huronian metasediments with Proterozoic orogenic events in Ontario. Can. Jour. Earth Sci. 6, 489-497.

FAWCETT, J. J. and YODER, H. S., 1966. Phase relationships of chlorites in the system $MgO-Al_2O_3-SiO_2-H_2O$. Amer. Mineral. 51, 353-380.

FENIAK, M., 1947. The geology of the Dowdell Peninsula, Great Bear Lake, N. W. T. Geol. Surv. Cda. Spec. Rep., 14p.

FLOYD, P. A. and WINCHESTER, J. A., 1975. Magma type and tectonic setting discrimination using immobile elements. Earth Planet. Sci. Letters 27, 211-218.

FRASER, J. A., HOFFMAN, P., IRVINE, T. N. and MURSKY, G., 1972. The Bear Province. In: Douglas R. S. W. and Price, R. A. (eds.). Variations in tectonic styles in Canada. Geol. Assoc. Cda. Spec. Pap. 11, 454-503.

FURNIVAL, G. M., 1935. The large quartz veins of Great Bear Lake. Econ. Geol. 30, 843-850.

__________, 1939. A silver-pitchblende deposit at Contact Lake, Great Bear Lake area, Canada. Econ. Geol. 34, 739-776.

FYFE, W. S. and HENLEY, R. W., 1973. Some thoughts on chemical transport processes with particular reference to gold. Miner. Sci. Engng. 5, 295-303.

GAMMON, J. B., 1966. Fahlbands in the Precambrian of southern Norway. Econ. Geol. 61, 174-188.

GANDHI, S. S., 1978. Geological observations and exploration guides to uranium in the Bear and Slave structural provinces and the Nonacho Basin, District of Mackenzie. Geol. Surv. Cda. Pap. 78-1B, 141-150.

HALL, C. and STUMPFL, E. F., 1969. Geology and ore deposition, western Kerr Lake Arch, Cobalt, Ontario. 9th Common. Min. and Met. Congr. Pap. 18, 44pp.

__________, and __________, 1972. The five element (Ag-Bi-Co-Ni-As) association--a critical appraisal of the geological environments in which it occurs and of the theories affecting its origin. 24th Intern. Geol. Congr., Montreal, Sect. 4, 540.

HART, S. R., DAVIS, G. L., STEIGER, R. H. and TILTON, G. R., 1968. A comparison of the isotopic mineral age variations and petrologic changes induced by contact metamorphism. In: Hamilton and Farquhar (eds.). Radiometric dating for geologists. Interscience Publications, New York, 73410.

HEIER, K. S. and BILLINGS, G. K., 1972. Rubidium. In: Wedepohl, K. H. (ed.). Handbook of geochemistry, Springer-Verlag, Heidelberg.

HOFFMAN, P. F. and BELL, I., 1975. Volcanism and plutonism, Sloan River map-area (86-K), Great Bear Lake, District of Mackenzie. Geol. Surv. Cda. Pap. 75-IA, 331-337.

__________, __________, and TIRRUL, R., 1976. Sloan River map-area (86K), Great Bear Lake, District of Mackenzie. Geol. Surv. Cda. Pap. 76-IA, 352-357.

__________, and McGLYNN, J. C., 1977. Great Bear Batholith: a volcano-plutonic depression. In: Strong, D. F. (ed.). Volcanic regimes of Canada. Geol. Assoc. Cda. Spec. Pap. 16, 169-192.

HOLLAND, J. G. and BRINDLE, D. W., 1966. A self-consistent mass absorption correction for silicate analysis by X-ray fluorescence. Spectrochim. Acta. 22, 2083-2093.

HRISKEVICH, M. E., 1968. Petrology of the Nipissing Diabase sill of the Cobalt area, Ontario, Canada. Geol. Soc. Amer. Bull. 79, 1387-1404.

HYNDMAN, D., 1972. Petrology of igneous and metamorphic rocks. McGraw Hill, New York, 553p.

IRVINE, T. N. and BARAGAR, W. R. A., 1971. A guide to the chemical classification of the common volcanic rocks. Can. Jour. Earth Sci. 8, 523-548.

JAMBOR, J. L., 1971a. Gangue mineralogy. Can. Mineral. 11, 232-262.

__________, 1971b. General geology. Can. Mineral. 11, 12-32.

__________, 1971c. The Nipissing diabase. Can. Mineral. 11, 33-75.

__________, 1971d. Spotted chloritic alteration. Can. Mineral. 11, 305-357.

__________, 1971e. Wall rock alteration. Can. Mineral. 11, 272-304.

JOLLIFFE, A. W., 1948. The northwest part of the Canadian Shield. Intern. Geol. Congr., Sess. 18, Pt. 8, 141-149.

KEIGHIN, A. and HONEA, J., 1969. The system Ag-Sb-S from 600° C. to 200° C. Mineral. Dep. 4, 123.

KIDD, D. F., 1932. A pitchblende-silver deposit, Great Bear Lake, Canada. Econ. Geol. 27, 145-159.

__________, 1936. From Rae to Great Bear Lake, Mackenzie District, N. W. T. Geol. Surv. Canada Mem. 187.

__________, and HAYCOCK, M. H., 1934. Mineragraphy of the ores of Great Bear Lake. Geol. Surv. Amer. Bull. 46, 879-960.

LINDSEY, D. A., 1969. Glacial sedimentology of the Precambrian Gowganda Formation, Ontario, Canada. Geol. Soc. Amer. Bull. 80, 1685-1702.

LOWDON, J. A., 1961. Age determinations by the Geological Survey of Canada, Report No. 1 Isotopic Ages. Geol. Surv. Cda. Pap. 61-17.

MOORBATH, S., 1970. Dating by radioisotopes. F. Hodgson, Guernsey.

MUFFLER, L. J. P. and DOE, B. R., 1968. Composition and mean age of detritus of the Colorado River delta in the Salton Trough, southeastern California. Jour. Sed. Petrology 38, 384-399.

__________, and WHITE, D. E., 1968. Active metamorphism of Upper Cenozoic sediments in the Salton Sea geothermal field and the Salton Trough, southeastern California. Geol. Soc. Amer., Bull. 80, 157-182.

ONISHI, H., 1972a. Antimony. In: Wedepohl (ed.). Handbook of geochemistry, Springer Verlag, Heidelberg.

__________, 1972b. Arsenic. In: Wedepohl (ed.). Handbook of geochemistry, Sprinver Verlag, Heidelberg.

PEARCE, J. A., 1975. Basalt geochemistry used to investigate past tectonic environments on Cyprus. Tectonophys. 25, 41-67.

__________, and CANN, J. R., 1973. Tectonic setting of basic volcanic rocks determined using trace element analyses. Earth Planet. Sci. Letters 19, 290-300.

PETRUK, W., 1971a. Depositional history of the ore minerals. Can. Mineral. 11, 396-401.

__________, 1971b. General characteristics of the deposits. Can. Mineral. 11, 76-107.

__________, 1971c. Mineralogical characteristics of the deposits and textures of the ore minerals. Can. Mineral. 11, 108-139.

__________, 1971d. S isotope ratios of the sulfides in the Cobalt-Gowganda ores. Can. Mineral. 11, 305-319.

__________, HARRIS, D. C. and STEWART, J. M., 1971a. Characteristics of the arsenides, sulfarsenides and antimonides. Can. Mineral. 11, 150-186.

__________, __________, __________, and CABRI, L. J., 1971b. Characteristics of the Ag-Sb minerals. Can. Mineral. 11, 187-195.

__________, and others, 1971c. Characteristics of the sulfides. Can. Mineral. 11, 196-231.

PETTIJOHN, F. J. and BASTRON, H., 1959. Chemical composition of argillites of the Cobalt Series (Precambrian) and the problem of Na-rich sediments. Geol. Soc. Amer. Bull. 70, 593-600.

RAMDOHR, P., 1969. The ore minerals and their intergrowths. Pergamon Press, Oxford, 1174pp.

REX, R. W., 1966. Heat flow in the Imperial Valley of California. Amer. Geophys. Union Trans. 47, p. 181.

ROBINSON, B. W., 1971. Studies on the Echo Bay silver deposit, N. W. T. Unpubl. Ph. D. Thesis, University of Alberta, 256pp.

__________, and MORTON, R. D., 1972. The geology and geochronology of the Echo Bay area, N. W. T., Canada. Can. Jour. Earth Sci. 9, 158-172.

__________, and OHMOTO, H., 1973. Mineralogy, fluid inclusions, and stable isotopes of the Echo Bay U-Ni-Ag-Cu deposits, N. W. T., Canada. Econ. Geol. 73, 635-656.

__________, and BADHAM, J. P. N., 1974. Stable isotope geochemistry and the origin of the Great Bear Lake silver deposits, N. W. T. Can. Jour. Earth Sci. 11, 698-711.

ROBINSON, H. S., 1933. Notes on the Echo Bay District, Great Bear Lake, N. W. T., Canada. Can. Inst. Min. Metall. 26, 609-629.

ROJKOVIC, I., 1973. Silver mineralization at Great Bear Lake, Canada. Geol. Zborn. Slov. 24, 325-338.

SAMPSON, E. and HRISKEVICH, M. E., 1957. Cobalt-arsenic minerals associated with aplites at Cobalt, Ontario. Econ. Geol. 52, 60-75.

SCARFE, C. M., 1973. Viscosity of Basic Magmas at Varying Pressures. Nature (London) 241, 101-104.

SCHOEN, R. and WHITE, D. E., 1965. Hydrothermal alteration in GS-3 and GS-4 drill holes, Main Terrace, Steamboat Springs, Nevada. Econ. Geol. 60, 1411-1421.

SCOTT, S. D. and O'CONNOR, T. P., 1971. Fluid inclusions in vein quartz, Silverfields Mine, Cobalt, Ontario. Can. Mineral. 11, 263-271.

SHEGELSKI, R. S. and MURPHY, J. D., 1972. The Camsell River silver district, Great Bear Lake area. Dept. Ind. Aff. and N. Dev. Open File Rept. 135.

__________, and SCOTT, S. D., 1975. Geology and mineralogy of the silver-uranium-arsenide veins of the Camsell River district, Great Bear Lake, N. W. T. Geol. Surv. Amer. Abst.

SKINNER, B. J., 1966. The system Cu-Ag-S. Econ. Geol. 61, 1-26.

__________, WHITE, D. E., ROSE, H. J. and MAYS, R.E., 1967. Sulfides associated with the Salton Sea geothermal brine. Econ. Geol. 62, 316-330.

STANTON, R. L., 1972. Ore Petrology. McGraw-Hill, New York, 713 pp.

THOMSON, R., 1965. Casey and Harris Townships. Ont. Dept. Mines Geol. Rep. 36,

__________, 1967. Cobalt and district. Can. Inst. Min. Met., C.I.M.M. Field Excursion, Northwestern Quebec - Northern Ontario, 136-143.

THORPE, R. I., 1974. Lead isotope evidence on the genesis of the silver-arsenide vein deposits of the Cobalt and Great Bear Lake areas, Canada. Econ. Geol. 69, 771-791.

VAN SCHMUS, R., 1965. The geochronology of the Blind River - Bruce Mines area, Ontario, Canada. Jour. Geol., 73, 755-780.

VINCENT, E. A., 1972. Silver. In: Wedepohl, K.H. (ed.). Handbook of geochemistry, Springer Verlag, Heidelberg.

VON HERZEN, R. P., 1963. Geothermal heat flow in the gulfs of California and Aden. Sci. 140, 1207-1208.

VUAGNAT, M., 1974. A new appraisal of alpine spilites. In: Amstutz, G. C. (ed.), Spilites and Spilitic Rocks.

WEDEPOHL, K. H., 1972. Lead. In Handbook of geochemistry, Springer Verlag, Heidelberg.

WHITE, D. E., 1968. Environments of generation of some base-metal ore deposits. Econ. Geol. 63, 301-335.

WINCHESTER, J. A. and FLOYD, P. A., 1977. Geochemical discrimination of different magma series and their differentiation products using immobile elements. Chem. Geol. 20, 325-343.

YOUNG, G. M., 1968. Sedimentary structures in Huronian rocks of Ontario. Paleogeog., Paleoclimatol., Paleoecol. 4, 125-153.

__________, 1969. Geochemistry of Early Proterozoic tillites and argillites of the Gowganda Formation, Ontario, Canada. Geochim. Cosmochim. Acta 33, 483-492.

YPMA, P. J. M., 1972. The multi-stage emplacement of the Chalanches (France) Ni-Co-Bi-As-Sb-Ag deposits and the nature of the mineralising solutions. 24th Intern. Geol. Congr., Montreal, Sect. 4, 525.

YUND, R. A., 1961. Phase relations in the system NiAs. Econ. Geol. 56, 1273-1296.

JUTEAU, T., and ROCCI, G., 1974. Vers une meilleure connaissance du probleme des spilites a partir de donnees nouvelles sur le cartege spilito-keratophyrique Hercynotype. In: Amstutz, G. C. (ed.). Spilites and spilitic rocks, Springer Verlag, Heidelberg, 484 pp.